

DISSERTATION

**DEVELOPMENT AND APPLICATION OF FUNCTIONAL GENE PROFILING AND
QUANTIFICATION OF MICROBIAL COMMUNITIES REMEDIATING MINE
DRAINAGE**

Submitted by

Luciana Paula Pereyra

Civil and Environmental Engineering Department

In partial fulfillment of the requirements

For the Degree of Doctor of Philosophy

Colorado State University

Fort Collins, Colorado

Summer 2009

UMI Number: 3385123

All rights reserved

INFORMATION TO ALL USERS

The quality of this reproduction is dependent upon the quality of the copy submitted.

In the unlikely event that the author did not send a complete manuscript and there are missing pages, these will be noted. Also, if material had to be removed, a note will indicate the deletion.



UMI 3385123

Copyright 2009 by ProQuest LLC.

All rights reserved. This edition of the work is protected against unauthorized copying under Title 17, United States Code.



ProQuest LLC
789 East Eisenhower Parkway
P.O. Box 1346
Ann Arbor, MI 48106-1346

COLORADO STATE UNIVERSITY

December 12, 2008

WE HEREBY RECOMMEND THAT THE DISSERTATION PREPARED UNDER OUR SUPERVISION BY LUCIANA PAULA PEREYRA ENTITLED "DEVELOPMENT AND APPLICATION OF FUNCTIONAL GENE PROFILING AND QUANTIFICATION OF MICROBIAL COMMUNITIES REMEDIATING MINE DRAINAGE " BE ACCEPTED AS FULFILLING, IN PART, REQUIREMENTS FOR THE DEGREE OF DOCTOR OF PHILOSOPHY.

Committee on Graduate Work

Charles D. Shackelford
Dr. Charles Shackelford

Sybil Sharvelle
Dr. Sybil Sharvelle

Kenneth F. Reardon
Co-Advisor: Dr. Kenneth F. Reardon

Amy Pruden
Advisor: Dr. Amy Pruden

Luis García
Department Head: Dr. Luis García

ABSTRACT OF DISSERTATION

DEVELOPMENT AND APPLICATION OF FUNCTIONAL GENE PROFILING AND QUANTIFICATION OF MICROBIAL COMMUNITIES REMEDIATING MINE DRAINAGE

Mine drainage (MD) is the product of the oxidation of sulfide minerals. It is characterized by elevated concentrations of heavy metals and sulfate and acidic to near-neutral pH. MD has serious effects on the environment and exposed biota. Sulfate-reducing permeable reactive zones (SR-PRZs) represent a common passive treatment approach for MD. In these systems, a lignocellulose-based substrate supports a complex microbial community that is responsible for remediation. Sulfate-reducing bacteria (SRB) produce sulfides that precipitate the metals as metal sulfides. Microbial reactions also consume sulfate and produce alkalinity, which increases the pH. Although SR-PRZs are microbially catalyzed, little is known about their microbiology and ecology. In this research, several aspects of the SR-PRZ microbial community were explored at laboratory and pilot scales with established as well as newly developed biomolecular methods.

A study using microcosm column experiments demonstrated that the type of inoculum plays an important role in the bioremediation of MD. Biomolecular analyses targeting the bacterial 16S rRNA gene revealed that the microbial communities in SR-PRZs were phylogenetically and functionally diverse and contained cellulose-degrading

bacteria, fermenters, and sulfate-reducing bacteria. The concerted action of these three microbial groups is essential for successful remediation, as cellulose degraders and fermenters convert the lignocellulosic material into carbon and energy sources for the SRB through hydrolytic and fermentative reactions, respectively. Interestingly, quantitative polymerase chain reaction (Q-PCR) assays revealed that SRB were a small fraction of the microbial community.

The effect of the type of substrate on the microbial community was also investigated in pilot-scale SR-PRZs treating the MD from the National Tunnel site in Black Hawk, CO. Lignocellulose-based SR-PRZs contained a more diverse microbial community and higher bacterial density than ethanol-fed SR-PRZs, as determined by 16S rRNA gene cloning and Q-PCR. In addition, the ethanol-fed SR-PRZs were highly enriched in SRB, most of which can directly utilize ethanol as a carbon and energy source. Methanogens, which can compete with SRB for carbon and energy sources, were quantified targeting the methyl-coenzyme M reductase gene. Higher numbers of these genes were detected in the lignocellulose-based SR-PRZs than in those fed ethanol.

The microcosm and pilot-scale studies provided significant insight into the SR-PRZ microbial community. However, they also revealed the limitations of the 16S rRNA-based approach to study phylogenetically diverse microbial communities and to quantify microbial groups that were a small fraction of the microbial community, such as SRB. This motivated the development of a new biomolecular approach targeting genetic markers (also known as functional genes) of the functions of interest: cellulose degradation, fermentation, sulfate reduction, and methanogenesis. PCR primers targeting the genes encoding cellulases of the Family 5 and 48 of cellulose degraders, the iron

hydrogenases of fermenters, the dissimilatory sulfite reductase of SRB, and the methyl-coenzyme M reductase of methanogens were designed and validated. This approach provides a more efficient and direct means of studying microbial functions and is applicable to study these functions not only in SR-PRZs but in any other anaerobic natural or engineered system such as rumen, sulfate-reducing reactors, sediments, and wetlands.

The functional gene-based approach was adapted to denaturing gradient gel electrophoresis and Q-PCR and applied to study the microbial communities in laboratory columns simulating SR-PRZs during the initial and pseudo-steady-state operation. The columns received different inocula and supplemental carbon sources. The new biomolecular approach was used successfully to monitor the changes of the microbial communities in the columns at the whole community level as well as at the functional level. Although the microbial communities in the different treatments were different during pseudo-steady-state operation, performance of the columns was comparable in terms of sulfate and metal removal and pH neutralization. This suggests that various microbial compositions can lead to successful MD remediation.

The studies presented in this dissertation have provided significant insights in the microbial communities involved in MD remediation at laboratory and pilot scale. In addition, a variety of biomolecular methods are presented that can be applied to explore different aspects of the microbial community such as diversity, structure, function, and relative abundance of specific microbial groups not only in SR-PRZs and but also in other systems with complex microbial communities. Integration of biomolecular and

performance data will provide a more complete understanding of SR-PRZ function that could be used to improve SR-PRZ performance and reliability.

Luciana Paula Pereyra
Civil and Environmental Engineering Department
Colorado State University
Fort Collins, CO 80523
Summer 2009

ACKNOWLEDGEMENTS

I would like to thank my advisor, Dr. Amy Pruden and my co-advisor, Dr. Ken Reardon for their invaluable guidance, support and commitment throughout these years and for helping me develop independent thinking and research skills. They have been incredible mentors for my professional and personal development and I am honored to have met them and worked with them. I would also like to acknowledge Dr. Sybil Sharvelle and Dr. Charles Shackelford for their time and expertise to better my work.

I am extremely grateful to all the members of the Pruden lab for all their help, friendship, and generosity. I would also like to thank Sage Hiibel for all the enthusiasm, expertise, and commitment that he brought into our project and all the past and present members of the mine drainage remediation project.

I would like to thank the financial support of the Rocky Mountain Hazardous Substance Research Center, the National Science Foundation, and the U.S. EPA Engineering Technical Support Center.

My sincere gratitude goes to my family and my extended family (the Brizuelas) for all their support and encouragement. I would also like to thank my friends from Argentina and the new and many friends that I made here in Fort Collins.

Finally, I would like to thank Fernando Brizuela, my life partner and best friend for his patience and help and for being there every step of this journey helping me keep my life in perspective and balance.

Table of Contents

Chapter 1 Biological Treatment of Mining-Influenced Waters	1
1.1. Introduction	1
1.1.1. Mining-Influenced Waters	1
1.1.2. Abiotic AMD Treatment	4
1.1.3. Passive Biological MIW Treatment	5
1.1.4. Focus of this Review	6
1.2. Microbial Ecology of SR-PRZs.....	8
1.2.1. Community Structure	8
1.2.2. Cellulose and other Polysaccharides Degraders	9
1.2.3. Fermenters.....	13
1.2.4. Acetogens.....	14
1.2.5. Sulfate-Reducing Bacteria	15
1.2.6. Methanogens.....	18
1.2.7. Interactions.....	19
1.2.7.1. Synergism.....	21
1.2.7.2. Competition	22
1.2.7.3. Factors Influencing Microbial Interactions.....	24
1.3. Sulfate-Reducing Treatment Systems	25
1.3.1. General Aspects	25
1.3.2. SR-PRZ Configurations	26
1.3.3. Factors Impacting Performance	28
1.3.3.1. Startup	30
1.3.3.2. Longevity	31
1.3.3.3. Performance in Cold Weather	33
1.3.3.4. Failures	33
1.4. Future Research	34
1.5. References	36
Chapter 2 Research Approach and Dissertation Overview.....	53
2.1. Research Approach	53
2.2. Research Objectives	54
2.3. Dissertation Overview.....	55
Chapter 3 The Effect of Inoculum on the Performance of Sulfate-Reducing Columns Treating Heavy Metal Contaminated Water	58
3.1. Abstract	58
3.2. Introduction	59
3.3. Materials and Methods	61
3.3.1. Column Specifications and Packing	61
3.3.2. Inocula	62
3.3.3. Influent Composition	62
3.3.4. Column and Effluent Sampling	63
3.3.5. Analytical Methods	63
3.3.6. DNA Extraction	64
3.3.7. PCR Amplification of 16S rDNA	65
3.3.8. Denaturing Gradient Gel Electrophoresis (DGGE).....	65

3.3.9. DNA Sequence Analysis	66
3.9.10. Cloning.....	66
3.9.11. Real Time Q-PCR.....	67
3.9.12. Statistical and Mathematical Analyses	68
3.4. Results	69
 3.4.1. Qualitative Observations	69
 3.4.2. Cumulative Sulfate Removal	69
 3.4.3. pH	70
 3.4.4. Cumulative Metal Removal	71
 3.4.5. Distribution of Metals within the Columns	72
 3.4.6. DGGE of Columns Microbial Communities	74
 3.4.7. Q-PCR	77
3.5. Discussion	78
 3.5.1. Effect of Inoculum on Column Performance	78
 3.5.2. Spatial Distribution of Metal Removal	80
 3.5.3. Microbial Community Composition and Dynamics.....	80
3.6. Conclusions	83
3.7. Acknowledgements.....	83
3.8. References	84
Chapter 4 Comparison of Microbial Community Composition and Activity in Sulfate-Reducing Batch Systems Remediating Mine Drainage	91
4.1. Abstract	91
4.2. Introduction	92
4.3. Materials and Methods	94
 4.3.1. Inocula	94
 4.3.2. Batch Tests Setup	95
 4.3.3. Analytical Methods	96
 4.3.4. DNA Extraction.....	96
 4.3.5. PCR Amplification	97
 4.3.6. Denaturing Gradient Gel Electrophoresis (DGGE).....	97
 4.3.7. DNA Sequence Analysis	98
 4.3.8. Quantitative PCR (Q-PCR)	99
 4.3.9. Statistical Analyses	100
4.4. Results	100
 4.4.1. Effect of Inoculum on Performance.....	100
 4.4.1.1. Sulfate Removal.....	100
 4.4.1.2. Metal Removal.....	102
 4.4.1.3. pH.....	103
 4.4.2. Microbial Community Composition.....	103
 4.4.2.1. Microbial Diversity.....	103
 4.4.2.2. Microbial Composition of the Cultures	104
 4.4.2.3. Analysis of Microbial Community Differences and Temporal Changes	106
 4.4.2.4. Quantification of Total Bacteria and SRB.....	107
4.5. Discussion	110
 4.5.1. Effect of Inoculum on Performance.....	110

4.5.2. Microbial Community Composition and Performance	111
4.5.3. Potential Indicators of Inoculum Suitability for MD Remediation.....	112
4.5.3.1. Inoculum Source.....	112
4.5.3.2. Overall Biomass and Diversity.....	113
4.5.3.3. Presence of Key Functional Groups.....	113
4.5.3.3.1. Cellulose and other Polysaccharide Degraders.....	114
4.5.3.3.2. Fermenters	115
4.5.3.3.3. Sulfate Reducers	116
4.6. Conclusions	116
4.7. Acknowledgements.....	117
4.8. References	117
Chapter 5 Effect of Organic Substrate on the Microbial Community Structure of Pilot-Scale Sulfate-Reducing Permeable Reactive Zones Treating Mine Drainage	124
5.1. Abstract	124
5.2. Introduction	125
5.3. Materials and methods.....	128
5.3.1. Sample Site and Collection	128
5.3.2. DNA Extraction.....	129
5.3.3. 16S rDNA and <i>apsA</i> PCR Amplification and Cloning.....	129
5.3.4. Sequence Analyses.....	130
5.3.5. Q-PCR	131
5.3.6. Statistical Analyses	132
5.4. Results	133
5.4.1. SR-PRZ Performance	133
5.4.2. Microbial Community Diversity and Composition.....	133
5.4.3. Quantification of Total Bacteria, SRB, and Methanogens	136
5.5. Discussion	138
5.5.1. Effect of Type of Substrate on Community Composition	138
5.5.2. Microbial Composition and Operational Problems	140
5.5.3. Implications for Response to an Environmental Stress	140
5.6. Conclusions	141
5.7. Acknowledgements.....	142
5.8. References	142
Chapter 6 Development of PCR Primers Targeting Functional Genes for the Detection and Quantification of Cellulose-Degrading, Fermentative, and Sulfate-Reducing Bacteria, and Methanogenic Archaea	148
6.1. Abstract	148
6.2. Introduction	149
6.3. Materials and Methods	152
6.3.1. Primer Design	152
6.3.2. Environmental Samples	155
6.3.3. DNA Extraction.....	156
6.3.4. Optimization of PCR Conditions.....	156
6.3.5. Cloning.....	156
6.3.6. Selection of Restriction Enzymes	157

6.3.7. Restriction Enzyme Digestion and DNA Sequencing.....	157
6.2.8. Q-PCR	158
6.4. Results	160
6.4.1. Primers Design	160
6.4.2. PCR Optimization	163
6.4.3. Validation of Specificity	164
6.4.4. Adaptation and Validation of Q-PCR	165
6.5. Discussion	168
6.5.1. Advantages of the Functional Gene –Based Approach.....	168
6.5.2. Quantification of Genetic Markers for Cellulose Degradation	170
6.5.3. Quantification of Genetic Markers for Fermentation	172
6.5.4. Quantification of Genetic Markers for Sulfate Reduction.....	173
6.5.5. Quantification of Genetic Markers for Methanogenesis.....	174
6.6. Conclusions	175
6.7. References	176
Chapter 7 Application of Functional-Gene Profiling and Quantification for the Characterization of the Initial and Pseudo-Steady State Operation of Sulfate-Reducing Columns Treating Mine Drainage.....	183
7.1. Abstract	183
7.2. Introduction	185
7.3. Materials and Methods	188
7.3.1. Column Specifications.....	188
7.3.2. Influent Composition	189
7.3.3. Inocula	190
7.3.4. Effluent Sampling.....	192
7.3.5. Column Substrate Sampling	192
7.3.6. Analytical Methods	193
7.3.7. Biomolecular Analyses	194
7.3.7.1. DNA Extraction and Purification	194
7.3.7.2. DGGE PCR.....	194
7.3.7.3. DGGE.....	195
7.3.7.4. Analysis of DGGE gels	196
7.3.7.5. Quantitative PCR.	197
7.3.8. Statistical Analyses	198
7.4. Results	198
7.4.1. Column Performance	198
7.4.1.1. Sulfate Removal and Column Startup.....	198
7.4.1.2. Metal Removal.....	199
7.4.1.3. pH.....	200
7.4.2. Functional Gene Characterization	201
7.4.2.1. DGGE Profiling of Functional and 16S rRNA genes	201
7.4.2.2. Quantification of Microbial Functional Groups.....	205
7.5. Discussion	207
7.5.1. Effect of Inoculum on Pseudo-Steady-State Community.....	207
7.5.2. Effect of Inoculum on Performance.....	207
7.5.3. Qualitative Changes in Microbial Community	208

7.5.4. Quantitative Changes in Microbial Community	211
7.6. Conclusions	214
7.8. Acknowledgements.....	214
7.8. References	215
Chapter 8 Conclusions and Future Work	222
8.1. Conclusions	222
8.2. Future Work	224
Appendix A PCR Efficiency	227
A.1. The Concept of PCR Efficiency	227
A.2. Quantitative PCR (Q-PCR) and Absolute Quantification.....	228
A.3. PCR Efficiency and Q-PCR.....	230
A.4. Methods to Estimate Amplification Efficiency.....	232
A.5. Correction for Difference in Efficiency between Samples and Standards	236
A.6. References.....	240
Appendix B Primer Design	243
B.1. Design of <i>cel48</i> primers	243
B.2. Design of <i>cel5</i> primers	248
B.3. Design of <i>hydA</i> primers	251
B.4. Design of <i>dsrA</i> primers	256
Appendix C Chapter 7 – Supplementary Material	260
C.1. Tracer Test	260
C.2. Gelcompar Analysis	262
Appendix D Detailed Protocols and Methods.....	278
D.1. DNA Extraction.....	278
D.1.1.PowerMax™ Soil DNA Isolation Kit (MoBio cat # 12988-10).....	278
D.1.2. UltraClean™ Soil DNA Isolation Kit (MoBio cat#12800-50 or 12800-100)	280
D.1.3. UltraClean™ Microbial DNA Isolation Kit (MoBio cat # 12224-50 or 12224-250)	282
D.2. Purification of DNA Extracts.....	284
D.2.1.Important Considerations before Use.....	284
D.2.2. Purification of DNA from Solutions	284
D.3. Cloning	286
D.3.1. Preparation pf LB Agar Plates	286
D.3.2. Cloning.....	286
D.3.3. M13 PCR	288
D.4. Preparation of Samples for DNA Sequencing.....	289
D.4.1. Preparing a 96-well Plate	289
D.4.2. Placing Sequencing Requests	292
D.5. Denaturing Gradient Gel Electrophoresis (DGGE).....	294
D.5.1.Setting up the Glass Plates	294
D.5.2. Preparing the Stacking Gel	294
D.5.3. Mixing the Gel Solutions	295
D.5.4. Preparing the Second Stacking Gel	296
D.5.5. Running the Gel.....	297
D.5.6. Preparing the Gel Stain.....	298

D.5.7. Imaging the DGGE Gel	298
D.6. Setting up a Quantitative-PCR Run	299
D.6.1.Creating a Plate Document	299
D.6.2. Preparation of Master Mix and 96-well Plate	300
D.7. Ion Chromatography	301
D.7.1. Startup Procedure	301
D.7.2. Starting up a Sample Queue	303
D.7.3. Preparation of Standards	304
D.7.4. Processing the Data	304
D.7.5. Purging the IC	306
D.8. Microwave Digestion for Inductively Coupled Plasma Atomic Emission Spectroscopy (from EPA method SW-3015)	307

List of Figures

Figure 1. 1: Distribution of cellulases of anaerobic bacteria into glycoside hydrolases families. Thermophilic microorganisms are indicated in bold. The chart was constructed using information from the Carbohydrate Active enzymes database (CAZy, http://www.cazy.org/index.html).	11
Figure 1. 2: Proposed framework of the SR-PRZ microbial community with interactions among microbial groups indicated.	20
Figure 1. 3: Different SR-PRZs configurations. (A) vertical flow (Hiibel et al. 2008), (B) horizontal flow, (C) successive alkalinity producing system (SAPS) which combines lignocellulose-based anaerobic treatment of AMD with limestone neutralization (Younger et al. 2003).	27
Figure 3. 1: Cumulative sulfate removal in duplicate SR-PRZ columns that were uninoculated (U) or inoculated with an acclimated culture (SRC) or with bovine dairy manure (DM). Cubic splines were fit to the effluent sulfate concentrations and flow rate data and then interpolated for direct comparison with the discrete influent data using a residence time of 4d. The negative cumulative removal values for the DM and U columns during the first 30d can be attributed to variable influent concentrations at the beginning of the experiment and to the propagation of error associated with the mathematical treatment of the minimal sulfate removal during this time.	70
Figure 3. 2: Cumulative zinc (a) and cadmium (b) removal in the uninoculated columns (U) and columns inoculated with an acclimated inoculum (SRC) or with bovine dairy manure. Cubic splines were fit to effluent metal concentrations and flow rate data and then interpolated for direct comparison with the discrete influent data using a residence time of 4d.	72
Figure 3. 3: Distribution of (a) cadmium and (b) zinc in the columns determined by ICP-AES analysis of digested column material collected from the top, middle, and bottom sections of each column after 170d of operation. The influent entered the columns from the bottom. Results for only one uninoculated column are shown because the second was used for tracer test. Error bars represent standard deviation of the means of five replicates.	73
Figure 3. 4: DGGE gel image of nested I341F and I533R PCR products of DNA extracted from (a) column SRC1 and (b) columns DM1 during the first 6 wk. Lane numbers correspond to the sampling week. 'std' is the positive control. Twenty-three of the labeled bands were sequenced and their identities are indicated in Table 3.1.	75
Figure 3. 5: Quantification of <i>Desulfobacterium</i> with time by Q-PCR for SRC, DM, and U columns (a) normalized to mass of sample used for DNA extraction and (b) normalized to total bacteria. Error bars represent standard deviation of the means of two to six replicates.	78
Figure 4. 1: Sulfate concentration in the liquid phase of the bottles. Data points represent the average of technical triplicates and biological duplicates, and error bars correspond to the pooled standard error. Since ACC and ADS bottles were not significantly different, one curve is shown to represent the trend observed in both types of inocula.	101

Figure 4. 2: Sulfate removal observed at Weeks 2 and 9 of the experiment. Column heights are the average of biological duplicates, and the error bars are the corresponding pooled standard error.....	101
Figure 4. 3: Concentration of soluble zinc in the bottles determined by ICP-AES analysis of digested liquid-phase material. Data points represent the average of technical triplicates and biological duplicates, and error bars correspond to the pooled standard error. PJK data could not be obtained due to technical difficulties with the acid digestion.....	102
Figure 4. 4: pH in the liquid phase of the bottles. Data points represent the means of biological duplicates, and error bars correspond to the pooled standard error. Since ACC and ADS bottles were not significantly different one curve is shown to represent the trend observed in both types of inocula.....	103
Figure 4. 5: Principal coordinates analysis of the microbial communities in the bottles. Bottles inoculated with different materials, overall comparison (a), and at Weeks 0 (solid symbols) and 14 (open symbols) (b), and LUTR (c), DM (d), PJK (e), ACC (f), and ADS (g) bottles over time.....	108
Figure 4. 6: Quantification of total bacteria, and the SRB of the genus <i>Desulfovibrio</i> with time by Q-PCR. Total bacterial 16S rRNA gene copies normalized to mass of substrate (a), and total <i>Desulfovibrio</i> 16S rRNA gene copies normalized to total bacteria (b). Data points are the average of technical triplicates and biological duplicates. Error bars represent pooled standard error.....	109
Figure 5. 1: Relative diversity of the ETOH 2, HYWD 3, and CSWD 5 SR-PRZs determined by cloning of the 16S rRNA gene. Shannon diversity indices for each SR-PRZ are indicated in parenthesis and were calculated based on the frequency of each clone in the clone library.....	134
Figure 5. 2: Distribution of microbial functions in each SR-PRZ based on the identity of the microorganisms identified through 16S rRNA gene cloning and DNA sequencing.	134
Figure 5. 3: Identity and percentages of <i>apsA</i> -containing microorganisms in ETOH, HYWD, and CSWD SR-PRZs.....	135
Figure 5. 4: Principal coordinates analyses (PCoA) of the (A) total bacterial community based on 16S rRNA gene sequences and the (B) <i>apsA</i> gene-containing community based on <i>apsA</i> gene sequences.....	136
Figure 5. 5: Quantification of total bacteria, the SRB of the genus <i>Desulfovibrio</i> , and methanogenic microorganisms for the ETOH, HYWD, and CSWD SR-PRZs by Q-PCR. Total bacteria 16S rRNA gene copies normalized to mass of substrate (A), total <i>Desulfovibrio</i> spp. 16S rRNA gene copies normalized to total bacteria (B), and <i>mcrA</i> genes normalized to total bacteria (C). Bars with the same letter are not significantly different at the 0.05 level. NA – not analyzed.	137
Figure 6. 1: CODEHOP primer design strategy (A) Block of conserved sequence in a multiple protein sequence alignment of seven glycoside hydrolases of the Family 48 identified with the Blockmaker program (B) Consensus amino acid sequence as determined by the CODEHOP algorithm (in bold and boxed). The other amino acids	

found at each position are aligned vertically above the consensus amino acid. Two primers (A and B) are indicated with the 5'consensus clamp in upper case and the 3'degenerate region in lower case (C) DNA alignment of the <i>cel48_490F</i> primer with reference sequences used for its design. The primer sequence was modified (boxed sequence) to adjust for differences in the degeneracy of the primer and the different nucleotides present in the DNA alignment of the reference sequences at a particular position.....	161
Figure 6. 2: Number of <i>cel5</i> , <i>cel48</i> , <i>hydA</i> , <i>dsrA</i> , and <i>mcrA</i> copies in the lignocellulose-based bioreactor with respect to the ethanol-fed bioreactor as determined by Q-PCR.....	168
Figure 6. 3: Schematic of the cellulosome of anaerobic bacteria.....	171
Figure 6. 4: Distribution of cellulases of anaerobic bacteria into glycoside hydrolases families. Thermophilic microorganisms are indicated in bold. The chart was constructed using on information from the Carbohydrate Active enzymes database (CAZy, http://www.cazy.org/index.html).	172
Figure 7. 1: Column feed and effluent sulfate concentrations determined by ion chromatography. Feed data were adjusted by 4 days to adjust for the hydraulic residence time. Data points represent the average of two biological replicates. Error bars represent the standard deviation of independently prepared technical replicates	199
Figure 7. 2: Feed and effluent concentrations of (A) cadmium and (B) zinc as determined by ICP-AES. The error bars represent the standard deviation of independently prepared technical replicates	200
Figure 7. 3: Column feed and effluent pH. Data points represent the average of biological replicates and the error bars represent the average deviation of the biological replicates.	200
Figure 7. 4: Cluster analysis of DGGE fingerprints of GChydA_1290F/hydA_1538R PCR products of DNA extracted from the columns at the beginning of the experiment (-i), and during the pseudo-steady state (-1) for the columns inoculated with dairy manure only (DM), dairy manure and an enrichment of SRB (SRB), dairy manure and an enrichment of cellulose degraders (CD), inoculated with dairy manure alone and supplemented with carboxymethyl cellulose (CMC) or ethanol (EtOH). 1 and 2 indicate the replicate number. Samples with a '#' in their label were used as reference to compare different gels.....	204
Figure 7. 5: Number of (A) 16S rRNA genes, (B) <i>cel5</i> genes, (C) <i>cel48</i> genes, (D) <i>hydA</i> genes, (E) <i>dsrA</i> genes, and (F) <i>mcrA</i> genes in the columns in the initial inoculated substrate and during the pseudo-steady state normalized to the mass of substrate as determined by Q-PCR. * indicates samples that were below the quantification limit.	206
Figure A. 1: Absolute quantification using Q-PCR. (A) Amplification curve. The end of the exponential phase of amplification is indicated with a double arrow (B) Logarithmic plot of the amplification curve. The threshold value used to determine the Ct value is indicated with a dashed line (C) Calibration curve constructed using serial dilutions of a standard. The y-intercept is the logarithm of the threshold value and the slope is the negative logarithm of the average amplification efficiency of the standards.	230

Figure B. 1: Multiple protein alignment of seven glycoside hydrolases of the family 48 and the blocks of conserved protein sequence (indicated with green boxes) identified by the Blocksmaker program. The alignment was constructed using ClustalX.	243
Figure B. 2: Multiple DNA alignment of the reference glycoside hydrolase genes of the family 48 and the primers selected for their amplification. The alignment was constructed with ClustalX.	248
Figure B. 3: Multiple protein alignment of six glycoside hydrolases of the family 5 and the blocks of conserved protein sequence (indicated with green boxes) identified by the Blocksmaker program. The alignment was constructed using ClustalX.	248
Figure B. 4: Multiple DNA alignment of the reference glycoside hydrolase genes of the family 5 and the primers selected for their amplification. Other family 5 glycoside hydrolase genes that were not used for the primer design were also included in the alignment. The alignment was constructed with ClustalX.	250
Figure B. 5: Multiple protein alignment of seven glycoside iron hydrogenase sequences and the blocks of conserved protein sequence (indicated with clear boxes) identified by the Blocksmaker program. The signature sequence of the H cluster of iron hydrogenases is indicated with orange boxes. The alignment was constructed using ClustalX.	251
Figure B. 6: Multiple DNA alignment of the reference iron hydrogenase genes and the primers selected for their amplification. The alignment was constructed with ClustalX.	255
Figure B. 7: Multiple protein alignment of dissimilatory sulfite reductase genes and the blocks of conserved protein sequence (indicated with green boxes) identified by the Blocksmaker program. The alignment was constructed using ClustalX.	256
Figure B. 8: Multiple DNA alignment of the reference dissimilatory sulfite reductase genes and the primers selected for their amplification. The alignment was constructed with ClustalX.	259
Figure C. 1: Conductivity in the effluent of two replicate columns after the feed was switched from DI water to a 10 g/L NaBr solution.	260
Figure C. 2: Cluster analysis of DGGE fingerprints of I341F/I533R PCR products of DNA extracted from the columns at the beginning of the experiment (-i), and during the pseudo-steady state (-1) for the columns inoculated with dairy manure only (DM), dairy manure and an enrichment of SRB (SRB), dairy manure and an enrichment of cellulose degraders (CD), inoculated with dairy manure alone and supplemented with carboxymethyl cellulose (CMC) or ethanol (EtOH). 1 and 2 after the column name indicate the replicate number.	262
Figure C. 3: Cluster analysis of DGGE fingerprints of I341F/I533R PCR products of DNA extracted from the columns during the pseudo-steady state (-1) for the columns inoculated with dairy manure only (DM), dairy manure and an enrichment of SRB (SRB), inoculated with dairy manure alone and supplemented with carboxymethyl cellulose (CMC) or ethanol (EtOH). 1 and 2 after the column name indicate the replicate number.	264

- Figure C. 4: Cluster analysis of DGGE fingerprints of GC*cel48_490F/cel48_920R* PCR products of DNA extracted from the columns at the beginning of the experiment (-i), and during the pseudo-steady state (-1) for the columns inoculated with dairy manure only (DM), dairy manure and an enrichment of SRB (SRB), dairy manure and an enrichment of cellulose degraders (CD), inoculated with dairy manure alone and supplemented with carboxymethyl cellulose (CMC) or ethanol (EtOH). 1 and 2 indicate the replicate number. Samples with a '#' in their label were used as reference to compare different gels.....266
- Figure C. 5: Cluster analysis of DGGE fingerprints of GC*cel5_392F/cel5_754R* PCR products of DNA extracted from the columns at the beginning of the experiment (-i), and during the pseudo-steady state (-1) for the columns inoculated with dairy manure only (DM), dairy manure and an enrichment of SRB (SRB), dairy manure and an enrichment of cellulose degraders (CD), inoculated with dairy manure alone and supplemented with carboxymethyl cellulose (CMC) or ethanol (EtOH). 1 and 2 indicate the replicate number. Samples with a '#' in their label were used as reference to compare different gels.....268
- Figure C. 6: Cluster analysis of DGGE fingerprints of GC*dsrA_290F/dsrA_660R* PCR products of DNA extracted from the columns at the beginning of the experiment (-i), and during the pseudo-steady state (-1) for the columns inoculated with dairy manure only (DM), dairy manure and an enrichment of SRB (SRB), dairy manure and an enrichment of cellulose degraders (CD), inoculated with dairy manure alone and supplemented with carboxymethyl cellulose (CMC) or ethanol (EtOH). 1 and 2 indicate the replicate number. Samples with a '#' in their label were used as reference to compare different gels.....271
- Figure C. 7: Cluster analysis of DGGE fingerprints of GC*mcrA_1035F/mcrA_1530R* PCR products of DNA extracted from the columns at the beginning of the experiment (-i), and during pseudo-steady state (-1) for the columns inoculated with dairy manure only (DM), dairy manure and an enrichment of SRB (SRB), dairy manure and an enrichment of cellulose degraders (CD), inoculated with dairy manure alone and supplemented with carboxymethyl cellulose (CMC) or ethanol (EtOH). 1 and 2 indicate the replicate number. Samples with a '#' in their label were used as reference to compare different gels.....273
- Figure C. 8: Microbial community evenness (E), species richness (S), and Shannon diversity index (H) based on DGGE patterns of PCR products obtained with the I341F/I533R and GC*cel5_392F/cel5_754R* primers on the substrate samples collected at the beginning of the experiment and during the pseudo-steady state from the columns inoculated with dairy manure only (DM), dairy manure and an enrichment of SRB (SRB), dairy manure and an enrichment of cellulose degraders (CD), inoculated with dairy manure alone and supplemented with carboxymethyl cellulose (CMC) or ethanol (EtOH).275
- Figure C. 9: Microbial community evenness (E), species richness (S), and Shannon diversity index (H) based on DGGE patterns of PCR products obtained with the GC*cel48_490F/cel48_920R* and GChydA_1290F/hydA_1538R primers on the substrate samples collected at the beginning of the experiment and during the pseudo-steady state

from the columns inoculated with dairy manure only (DM), dairy manure and an enrichment of SRB (SRB), dairy manure and an enrichment of cellulose degraders (CD), inoculated with dairy manure alone and supplemented with carboxymethyl cellulose (CMC) or ethanol (EtOH).....276

Figure C. 10: Microbial community evenness (E), species richness (S), and Shannon diversity index (H) based on DGGE patterns of PCR products obtained with the GC_{dsrA_290F/dsrA_660R} and GC_{mcrA_1035F/mcrA_1530R} primers on the substrate samples collected at the beginning of the experiment and during the pseudo-steady state from the columns inoculated with dairy manure only (DM), dairy manure and an enrichment of SRB (SRB), dairy manure and an enrichment of cellulose degraders (CD), inoculated with dairy manure alone and supplemented with carboxymethyl cellulose (CMC) or ethanol (EtOH).....277

List of Tables

Table 3. 1: Characterization of microorganisms represented by DGGE bands. Band numbers correspond to numbering on Figure 3.4. A: cellulose degradation; B: fermentation of polysaccharides; C: fermentation of monosaccharides (and/or disaccharides); D: sulfate reduction. Where more than one sequence had the same similarity with the DGGE sequence, all the results corresponding to the highest match are presented. When the DGGE band sequence corresponded to an uncultured bacterium the function of the microorganisms was assigned based on the functions of the closest known relative.	76
Table 4. 1: Characterization of major constituents of the microbial communities in the cultures represented by DGGE bands.....	105
Table 5. 1: Proportion of solid substrate components in the HYWD and CSWD SR-PRZs	129
Table 6. 1: Sequences used for the design of the <i>cel5</i> , <i>cel48</i> , <i>hydA</i> , <i>dsrA</i> , and <i>mcrA</i> primer sets.	154
Table 6. 2: Temperature programs used for PCR amplification of <i>cel5</i> , <i>cel48</i> , <i>hydA</i> , <i>dsrA</i> , and <i>mcrA</i> genes using the primer sets selected after specificity validation.....	159
Table 6. 3: Primer combinations designed by the CODEHOP strategy and selected for further validation PCR. The primers mcrA_1035F/1530R were designed by Luton and others (2002) and the primer RH3-dsr_R' is a modified version of the primer RH3-dsr-R designed by Ben-Dov and others (2007).Primer sets that were selected after specificity validation are indicated in bold.	162
Table 6. 4: Optimized PCR master mix for <i>cel5</i> , <i>cel48</i> , <i>hydA</i> , <i>dsrA</i> , and <i>mcrA</i> primer sets selected after specificity validation.	164
Table 6. 5: DNA sequencing results of clones of PCR product obtained with the <i>cel5</i> , <i>cel48</i> , <i>hydA</i> , <i>dsrA</i> , and <i>mcrA</i> primer sets on a sample from a lignocellulose-based sulfate-reducing bioreactor. Clone sequences were compared to those in the NCBI database	.

using the BLASTX tool that searches the protein database using a translated nucleotide query	166
Table A 1: Example of how differences in amplification efficiency between samples and standards can impair absolute quantification in Q-PCR. In this example, the amplification efficiency is 95% for the standards and 90% for the samples and all Ct values are calculated at the same threshold value. The calibration curve (Eq. A5) was used to calculate the number of copies of target DNA in the sample (N_0 's) and compared to the actual number of copies in the sample ($N_{0,s}$)	231
Table A 2: Methods used to calculate PCR amplification efficiency.	232
Table A 3: Number of copies (N_0 's _{S,corr}) in the samples of the example in Table A1 calculated using Equation A16 to correct for different amplification efficiencies between samples and standards.....	238
Table A 4: Table 6 from Jørgensen and Leser (2007). The table summarizes the results of the quantification of <i>Bacillus licheniformis</i> CH200 and <i>Bacillus subtilis</i> CH201 spores in animal feed samples by multiplex Q-PCR.....	239
Table A 5: Number of copies (N_0 's _{S,Eq.A18}) in the samples of the example in Table A1 calculated using Equation A18 to correct for different amplification efficiencies between samples and standards.....	240
Table C. 1: Similarity matrix constructed from using the Dice coefficient for pairwise comparisons for the DGGE fingerprints of I341F/I533R PCR products of DNA extracted from the columns at the beginning of the experiment (-i), and during the pseudo-steady state (-1) for the columns inoculated with dairy manure only (DM), dairy manure and an enrichment of SRB (SRB), dairy manure and an enrichment of cellulose degraders (CD), inoculated with dairy manure alone and supplemented with carboxymethyl cellulose (CMC) or ethanol (EtOH). 1 and 2 after the column name indicate the replicate number.	263
Table C. 2: Similarity matrix constructed from using the Dice coefficient for pairwise comparisons for the DGGE fingerprints of I341F/I533R PCR products of DNA extracted from the columns during the pseudo-steady state (-1) for the columns inoculated with dairy manure only (DM), dairy manure and an enrichment of SRB (SRB), inoculated with dairy manure alone and supplemented with carboxymethyl cellulose (CMC) or ethanol (EtOH). 1 and 2 after the column name indicate the replicate number.....	265
Table C. 3: Similarity matrix constructed from using the Dice coefficient for pairwise comparisons for the DGGE fingerprints of GCcel48_490F/cel48_920R PCR products of DNA extracted from the columns at the beginning of the experiment (-i), and during the pseudo-steady state (-1) for the columns inoculated with dairy manure only (DM), dairy manure and an enrichment of SRB (SRB), dairy manure and an enrichment of cellulose degraders (CD), inoculated with dairy manure alone and supplemented with carboxymethyl cellulose (CMC) or ethanol (EtOH). 1 and 2 indicate the replicate number. Samples with a '#' in their label were used as reference to compare different gels.....	267
Table C. 4: Similarity matrix constructed from using the Dice coefficient for pairwise comparisons for the DGGE fingerprints of GCcel5_392F/cel5_754R PCR products of	

DNA extracted from the columns at the beginning of the experiment (-i), and during the pseudo-steady state (-1) for the columns inoculated with dairy manure only (DM), dairy manure and an enrichment of SRB (SRB), dairy manure and an enrichment of cellulose degraders (CD), inoculated with dairy manure alone and supplemented with carboxymethyl cellulose (CMC) or ethanol (EtOH). 1 and 2 indicate the replicate number. Samples with a '#' in their label were used as reference to compare different gels.....	269
Table C. 5: Similarity matrix constructed from using the Dice coefficient for pairwise comparisons for the DGGE fingerprints of <i>GChydA_1290F/hydA_1538R</i> PCR products of DNA extracted from the columns at the beginning of the experiment (-i), and during the pseudo-steady state (-1) for the columns inoculated with dairy manure only (DM), dairy manure and an enrichment of SRB (SRB), dairy manure and an enrichment of cellulose degraders (CD), inoculated with dairy manure alone and supplemented with carboxymethyl cellulose (CMC) or ethanol (EtOH). 1 and 2 indicate the replicate number. Samples with a '#' in their label were used as reference to compare different gels.....	270
Table C. 6: Similarity matrix constructed from using the Dice coefficient for pairwise comparisons for the DGGE fingerprints of <i>GCdsrA_290F/dsrA_660R</i> PCR products of DNA extracted from the columns at the beginning of the experiment (-i), and during the pseudo-steady state (-1) for the columns inoculated with dairy manure only (DM), dairy manure and an enrichment of SRB (SRB), dairy manure and an enrichment of cellulose degraders (CD), inoculated with dairy manure alone and supplemented with carboxymethyl cellulose (CMC) or ethanol (EtOH). 1 and 2 indicate the replicate number. Samples with a '#' in their label were used as reference to compare different gels.....	272
Table C. 7: Similarity matrix constructed from using the Dice coefficient for pairwise comparisons for the DGGE fingerprints of <i>GCmcrA_1035F/mcrA_1530R</i> PCR products of DNA extracted from the columns at the beginning of the experiment (-i), and during pseudo-steady state (-1) for the columns inoculated with dairy manure only (DM), dairy manure and an enrichment of SRB (SRB), dairy manure and an enrichment of cellulose degraders (CD), inoculated with dairy manure alone and supplemented with carboxymethyl cellulose (CMC) or ethanol (EtOH). 1 and 2 indicate the replicate number. Samples with a '#' in their label were used as reference to compare different gels.....	274

Chapter 1 Biological Treatment of Mining-Influenced Waters

Pereyra, L.P., Hiibel, Reardon, K.F., and A. Pruden

(invited review paper in preparation for submission to Biotechnology and Bioengineering)

Approximate contributions of each author are as follows:

L.P. Pereyra performed 90% of the literature review, and 90% of the manuscript preparation.

S.R. Hiibel performed 10% of the literature review and 10% of the manuscript preparation.

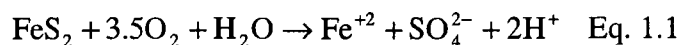
K.F. Reardon and A. Pruden assisted with manuscript preparation

1.1. Introduction

1.1.1. Mining-Influenced Waters

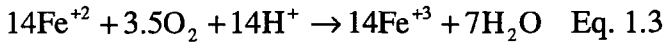
Pyrite-rich deposits are mined for Au, Ag, Cu, Zn, Pb, and other metals that are usually found as impurities or occur as sulfide minerals (Baker and Banfield 2003). Mining exposes these minerals to water and air causing weathering of the rocks and producing a solution with high concentrations of heavy metals and sulfate referred to as acid mine drainage (AMD), when acidic in pH, or mining-influenced water (MIW) or mine drainage (MD) as more general terms recognizing that some mine drainage is near neutral or even alkaline in pH. The composition and pH of the MIW depend on the geochemistry of the site, climate, and mining engineering constraints (Johnson and Hallberg 2003).

Biological and abiotic reactions are responsible for the generation of AMD. Pyrite can be oxidized by oxygen (Eq. 1.1) or ferric iron (Eq. 1.2):





In addition, oxygen can oxidize ferrous iron to ferric iron, which then oxidizes pyrite to produce more AMD (Eq. 1.3). This is the key reaction in promoting the continuous oxidation of the minerals.



At pH<4, the oxidation of sulfide minerals is mainly catalyzed by microorganisms whereas at pH>4 both the biological and chemical oxidation may occur (Johnson and Hallberg 2003).

The reactions that produce AMD are highly exothermic (Baker and Banfield 2003). Despite its acidity, heat, and toxicity, AMD is not sterile. Because of the limited number of energy-deriving reactions available in AMD and the low concentration of organic matter (<20 mg/L), the microbial diversity in AMD is low and dominated by oligotrophic bacteria and archaea (Baker and Banfield 2003; Johnson and Hallberg 2003). These microorganisms play a very important role in the formation of AMD and account for most of the AMD generated given that the rate of bacterial oxidation of ferrous iron can be 10^6 greater than under abiotic conditions (Singer and Stumm 1970). Mineral-oxidizing acidophiles include iron oxidizers such as *Lestospirillum ferrooxidans* and *Thiobacillus ferrooxidans* and sulfur oxidizers such as *Acidithiobacillus thiooxidans* and *Sulfolobus* spp. In addition, non-mineral-oxidizing acidophiles such as *Acidocella* spp., *Thermoplasma* spp., and *Alicyclobacillus* spp. are also found. Interestingly, anaerobic iron- and sulfate-reducing bacteria have also been isolated from AMD sites (Fortin et al. 2000). A thorough review of the microbiology of AMD can be found in Johnson and Hallberg (Johnson and Hallberg 2003).

One of the most extreme cases of AMD in the U.S. is the Richmond Mine at Iron Mountain. The Iron Mountain region in California was in operation from the 1860s to 1962 to mine Au, Ag, Cu, Fe, Zn, and pyrite (Druschel et al. 2004). In some areas of the mine the pH is as low as -4 (Nordstrom and Alpers 1999) and the concentration of sulfate, zinc, and iron can be as high as 108,000 mg/L, 2,600 mg/L, and 1900 mg/L, respectively (Johnson and Hallberg 2003). The chemistry of mine waters in the U.S. and around the world has been extensively covered in other publications (Banks et al. 1997; Carrillo-Chavez et al. 2003; de Mello et al. 2006; Desbarats and Dirom 2007; Espana et al. 2005; Hudson-Edwards et al. 1999; Johnson 1993; Seal et al. 2008; Vaughan and Jambor 2006).

It is estimated that in the U.S. alone, more than two million acres of land are affected by AMD from abandoned mines and this contributes to the pollution of more than 8,600 miles of surface streams (Office of Inspector General 1991). Mining activities have been identified as the second largest source of nonpoint pollution to the country's surface waters (Environmental Protection Agency 1992). AMD has serious effects on the environment and the life that comes in direct contact with it. In addition to the toxicity caused by the heavy metals and acidity, there are other quality problems associated with AMD. Some of these problems are the contamination of fresh water or groundwater with chloride from high-salinity AMD, with nitrates from nitrogen-based explosives used during mining, or with organic compounds derived from coal (Banks et al. 1997).

1.1.2. Abiotic AMD Treatment

Johnson and Hallberg (Johnson and Hallberg 2005) classified the treatment options for AMD into biological and abiotic methods. Each of these groups contains active and passive alternatives, which differ in whether they require continuous energy input.

The most widely used abiotic active technology is limestone addition. The dissolution of limestone increases the pH and causes the precipitation of metals as hydroxides and carbonates. Other neutralizing agents such as CaO or Ca(OH)₂ can also be used instead of limestone (Kuyucak 1998). This type of treatment can be highly effective but has high operational costs. For example, a preliminary study estimated that the acid neutralization of AMD in the State of Minas Gerais, Brazil with commercial limestone would cost between 7.8 and 25.9 million U.S. dollars (de Mello et al. 2006). In addition, acid neutralization with limestone or other agents generates voluminous, water-rich sludges with 1% to 30% solids depending on the metal concentration of the AMD and the sophistication of the process (Kuyucak 1998).

A passive version of limestone addition is the use of anoxic limestone drains (ALD) (Turner and McCoy 1990). In these systems, the AMD flows through a limestone channel held within an air- and water-proof drain. This prevents the oxidation of ferrous iron to ferric iron which can precipitate and cause armouring of the limestone. ALDs can be used alone (Cravotta 2003) or in combination with other treatment technologies (Barton and Karathanasis 1999).

Removal of heavy metals from AMD can also be achieved with chemicals other than neutralizing agents. For example, 1,3-benzenediamidoethanethiol was found to remove more than 90% of metals from AMD collected from an abandoned mine in

Pikeville, Kentucky (Matlock et al. 2002). Recently, the applicability of different low-cost adsorbents for heavy metal removal from contaminated water has been reviewed (Babel and Kurniawan 2003). Chitosan, zeolites, waste slurry, and lignin were considered to be materials with the highest adsorption capacity. Mohan and Chander (2006) evaluated the feasibility of lignite as a low-cost sorbent for the treatment of AMD. They concluded that it could be used for the removal of Fe(II), Fe (III), and Mn(II). Banfalvi (2006) proposed a new approach to remove heavy metals from water by precipitating them as metal sulfides with sodium sulfide and adsorbing them on the surface of bentonite.

Other technologies such as ion exchange, solvent extraction, and membrane processes can be used for the treatment of AMD but only in specific situations because of their cost and specialized requirements (Kuyucak 1998).

1.1.3. Passive Biological MIW Treatment

Aerobic treatment of AMD in the form of wetlands is usually applied to treat alkaline MIW (Johnson and Hallberg 2005). This is because the main reaction that occurs in these systems is the oxidation of ferrous iron to ferric iron and the precipitation of ferric hydroxides. The alkalinity in the AMD helps neutralize the acidity produced in the oxidation and precipitation of iron and prevents an important reduction in pH (Johnson and Hallberg 2005).

Anaerobic treatment of AMD is implemented in wetlands, permeable reactive barriers, etc. collectively referred to here as sulfate-reducing permeable reactive zones (SR-PRZs). It involves microbial reactions that produce alkalinity and sulfides which form metal sulfides with the heavy metals in the AMD. The solubility of most metal

sulfides is extremely low (Kotrba and Ruml 2000) so they precipitate out of the AMD. The carbon and energy source for the microbial reactions is provided by a substrate that consists of a mixture of lignocellulosic materials (e.g., wood chips, straw) and more biodegradable materials (e.g., compost). Because of its recalcitrance, the substrate provides a long-term reservoir of energy compounds for the microbial community.

SR-PRZs offer the potential of treating AMD in a cost-effective way and using natural biological processes. In addition, they can be applied *in situ*, require low maintenance, and, compared to limestone treatment, they do not produce bulky sludges (Johnson and Hallberg 2002). On the downside, their performance and lifetime is relatively unpredictable. However, there are several success stories. The most renowned ones are the systems installed at Nickel Rim site in Ontario and at the Wheal Jane Mine in the U.K. (Whitehead and Prior 2005).

1.1.4. Focus of this Review

The performance of different technologies for the treatment of AMD has been extensively studied (Benner et al. 1997; Hammack et al. 1994; Matlock et al. 2002; Skinner and Schutte 2006; Tsukamoto et al. 2004; Tyrrell et al. 1997; Waybrant et al. 2002; Wilkin and McNeil 2003) and reviewed (Babel and Kurniawan 2003; Blowes et al. 2000; Cohen 2006; Gibert et al. 2002; Johnson and Hallberg 2002; Johnson and Hallberg 2005; Kalin et al. 2006). Passive biological technologies have attracted much attention because of their potential for AMD remediation at a low cost and with minimal maintenance. In particular, anaerobic systems offer the possibility of remediating acidic, metal-rich AMD (Johnson and Hallberg 2005). The key components of the systems are the substrate and the microbial community that is supported by it. The effect of different

substrates on the remediation performance of SR-PRZs was covered in several studies (Bechard et al. 1994; Gibert et al. 2004; Waybrant et al. 1998; Zagury et al. 2006) and was recently review by Neculita (2007). Recently, several studies have focused on investigating the composition and role of the microbial community in SR-PRZ performance in laboratory, pilot-scale, and field SR-PRZs (Benner et al. 2000; Geets et al. 2005; Hiibel et al. 2008; Johnson and Hallberg 2005; Johnson and Hallberg 2005; Logan et al. 2005; Pereyra et al. 2008; Pruden et al. 2007). These studies provided some of the first insights into the SR-PRZ microbial community and also highlight their complex microbial ecology. Considering that they are microbiologically catalyzed, understanding the microbial ecology is a critical frontier in advancing SR-PRZ design and operation. Thus, this review aims to achieve the following:

- describe the microbial groups that are relevant for AMD remediation
- discuss probable interactions between the different members of the microbial community
- integrate the state-of-knowledge with respect to microbial ecology of SR-PRZs
- develop a framework for understanding the SR-PRZ microbial community and its interactions.
- discuss possibilities for improving SR-PRZ design and performance from a microbiological perspective.
- suggest future research avenues

1.2. Microbial Ecology of SR-PRZs.

1.2.1. Community Structure

Upon conception, SR-PRZs were generally treated as ‘black boxes’ without a clear understanding of the processes governing these systems. This resulted in limited control over their performance, which was observed to be highly variable among different systems. Research revealed that, although there are several physico-chemical processes responsible for the remediation, microbially-mediated reactions are the main sink of metals in SR-PRZs. The source of microorganisms or inoculum used in SR-PRZs is highly variable. Dairy manure is a commonly used inoculum (Johnson and Hallberg 2005) because it is inexpensive, readily available, and has a high concentration of microorganisms. Material from contaminated sites, SR-PRZs (Pereyra et al. 2008), or enrichment cultures (Elliott et al. 1998) from these sites are also used.

Culturing techniques such as most probable number and bimolecular methods have been applied to study the microbial composition and dynamics of SR-PRZs. Laboratory and field studies of SR-PRZs have revealed an enormous microbial diversity in terms of phylogeny and function (Hiibel et al. 2008; Labrenz and Banfield 2004; Morales et al. 2005; Pereyra et al. 2008; Pruden et al. 2007). This diversity arises from the complexity of the carbon source in the substrate which requires the coordinated activity of several trophic groups of microorganisms for its degradation. Microorganisms that can hydrolyze cellulose and other polysaccharides reside at the top of the carbon flow. Hydrolysis products include oligomers (e.g., cellobextrins) and monomers (e.g., glucose), which are fermented by cellulose degraders or saccharolytic fermenters to organic acids, alcohols, hydrogen, and carbon dioxide. These simpler organic molecules

and hydrogen serve as energy source for sulfate-reducing bacteria (SRB). SRB play a crucial role in AMD remediation as they produce hydrogen sulfide through dissimilatory sulfate reduction (Eq. 1.4). Their activity also releases bicarbonate, which results in an increase in alkalinity and pH (Waybrant et al. 2002).



Removal of metals occurs through their precipitation as metal sulfides with biogenically produced sulfide (Eq. 1.5):



where Me^{2+} denotes a divalent metal.

In addition, methanogenic archaea might also be present in the microbial community and compete with SRB for energy sources.

The following sub-sections describe the central microbial groups found in SR-PRZ microbial communities, their interactions, and their relevance to AMD remediation.

1.2.2. Cellulose and other Polysaccharides Degraders

Usually, the substrate used in SR-PRZs is a lignocellulosic material. Cellulose is a polymer of glucose (the building unit is cellobiose) and constitutes up to 40% of the plant cell wall (Bayer et al. 2000). In plants, cellulose is embedded in a matrix of hemicellulose and lignin (Beguin and Aubert 1994). Hemicellulose comprises up to 30% of the plant cell wall (Sylvia et al. 2005) and contains a mixture of polymers of hexoses, pentoses, and uronic acids such as xyloglucans, glucuronomannans, and xylans (Hespell and Whitehead 1990). Pectins are chains of esterified galacturonic acid that are also present in the cell wall. Pectin constitutes 10% to 20% of the total carbohydrate complex found in

grasses and alfalfa, respectively (Lagowski et al. 1958; Waite and Gorrod 1959). Lignin is not a polysaccharide. Its decomposition rate is very slow compared to that of cellulose and hemicellulose and it interferes with the access of enzymes to the cellulose component (Bayer et al. 2000).

The diversity of plant polysaccharides is reflected in the variety of enzymes found in polysaccharide degraders. These enzymes, known as glycoside hydrolases (EC 3.2.1.-), include cellulases, xylanases, and mannosases, to name a few (Henrissat and Davies 1997). They are classified into different families based on their amino acid sequence similarity (Henrissat and Bairoch 1993). Even though cellulose has a simple chemical formula, its three dimensional structure is more complex and includes parts of tightly packed cellulose chains (crystalline cellulose) and amorphous parts of ‘unorganized’ chains. Given the complexity and structural diversity of cellulose, microorganisms have evolved a variety of enzymes (called cellulases) to hydrolyze it. Cellulases differ in their specificities, endo/exo mode of action, activity towards amorphous or crystalline cellulose, and preference of substrates of different chain length (Beguin and Aubert 1994). Of the more than eighty glycoside hydrolase families (Henrissat 1991; Rabinovich et al. 2002), cellulases are found in fifteen families (Families 5, 6, 7, 8, 9, 10, 11, 12, 26, 44, 45, 48, 51, 60, and 61) (Figure 1.1).

Since SR-PRZs are anaerobic systems our interest focuses on microorganisms that degrade polysaccharides (cellulose in particular) anaerobically. Anaerobic cellulose-degrading bacteria are also referred to as primary fermenters (Schink 1994) because they convert cellulose into oligomers and monomers (e.g., sugars, amino acids, and glycerol) that they then ferment to fatty acids, succinate, lactate, alcohols, etc. In general, they are

slow growers. Most cellulolytic microorganisms also ferment different hemicellulose components such as xylan and pentoses (Leschine 1995). The majority of the anaerobic cellulose degraders possess a highly efficient extracellular enzymatic complex to degrade cellulose known as the cellulosome (Bayer et al. 2004). This complex allows the microorganisms to attach to the substrate minimizing the distance over which the cellulose hydrolysis product must diffuse and, thus, facilitating efficient uptake of these oligosaccharides by the host cell (Lynd et al. 2002). The cellulosome is made of several components that include the catalytic subunits and carbohydrate-binding domains that attach to a scaffolding subunit through interactions between dockerin and cohesin domains. The most well studied cellulosome is the one of *C. thermocellum* (Bayer et al. 1998).

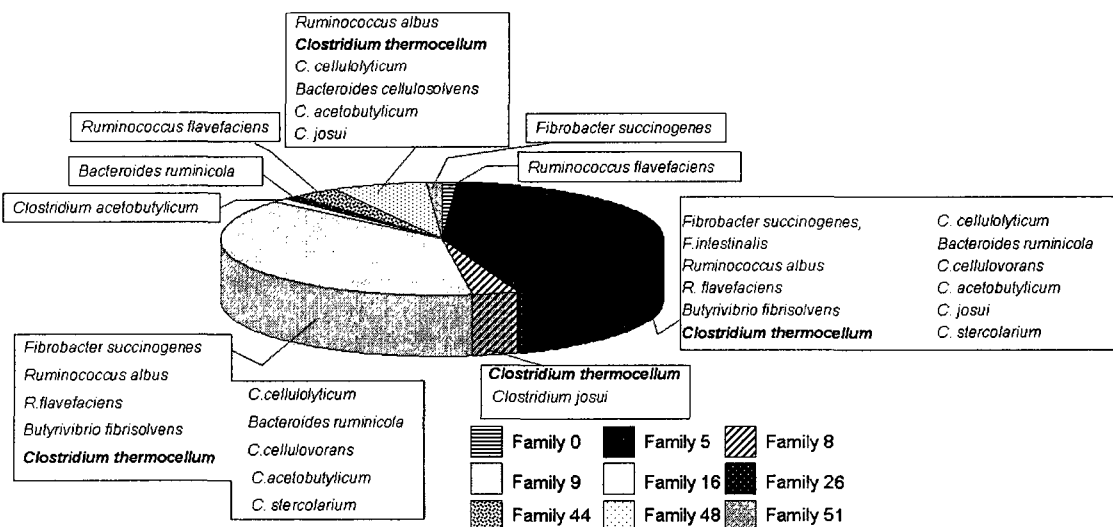


Figure 1. 1: Distribution of cellulases of anaerobic bacteria into glycoside hydrolases families. Thermophilic microorganisms are indicated in bold. The chart was constructed using information from the Carbohydrate Active enzymes database (CAZy, <http://www.cazy.org/index.html>).

The ability to hydrolyze cellulose under anaerobic conditions is widely distributed among many genera of the domain Bacteria. There is considerable concentration of

cellulolytic capabilities in the anaerobic order *Clostridiales* (phylum *Firmicutes*) (Lynd et al. 2002). Examples of mesophilic cellulose degraders found in the genus *Clostridium* include *C. papyrosolvans*, *C. cellulovorans*, *C. cellulolyticum*, *C. josui*, *C. celerecrescens*, *C. longisporum*, and *C. populeti* (Leschine 1995). *Fibrobacter succinogenes*, *Ruminococcus albus*, and *R. flavefaciens* are the most actively cellulolytic of all mesophilic organisms described from any habitat (Weimer 1996). The genus *Bacteroides* contains a variety of polysaccharide degraders. Starch is digested by several *Bacteroides* spp. such as *B. fragilis*, *B. thetaiotamicron*, *B. ovatus*, *B. vulgatus*, *B. distasonis*, *B. amylophilus*, and *B. ruminicola* (Macy and Probst 1979). *B. succinogenes* is an efficient cellulose degrader and is one of the most efficient cellulolytic microorganisms known in rumen. It also degrades some components of hemicellulose. *B. succinogenes* and *B. ruminicola* can also degrade some pectins. Some species able to ferment pectin are *Butyrivibrio fibrisolvens*, *Lachnospira multiparus*, and *Bacteroides rumunicola* (Dehority 1969). *Prevotella* spp. play a role in the utilization of polysaccharides of plant origin, including pectins, xylans, and starch (Avgustin et al. 1997).

The phylogenetic diversity of cellulose degraders is striking. This diversity is evident even for members of the same genus. For example, Rainey and Stackebrandt (1993) compared the 16S rRNA genes of 13 mesophilic cellulolytic species of the genus *Clostridium* with 36 representative thermophilic and mesophilic clostridia. They concluded that the phenotype-based classification has no phylogenetic basis as thermophilic and mesophilic, and proteolytic and saccharolytic species were intermixed.

The 16S rRNA gene-based analysis of laboratory and field SR-PRZs revealed the presence of known cellulose and other polysaccharide degraders in the microbial

community (Hallberg et al. 2004; Hiibel et al. 2008; Pereyra et al. 2008; Pruden et al. 2007). The microorganisms most commonly found are members of *Clostridium*, *Bacteroides*, and *Prevotella*. Polymerase chain reaction (PCR) primers targeting the genes encoding for the cellulases of the Families 5 and 48 were recently developed to detect cellulolytic microorganisms and were applied in laboratory and pilot-scale SR-PRZs (Chapters 6 and 7).

1.2.3. Fermenters

Fermentative bacteria can be divided into two different groups: primary fermenters (i.e., polysaccharide degraders) and secondary fermenters (Schink 1994). Secondary fermenters utilize fermentation products such as fatty acids longer than two carbon atoms, alcohols longer than one carbon atom, and branched-chain and aromatic fatty acids and convert them to acetate, CO₂, H₂, and formate. The end products of this process depend on the microbial species and the environmental conditions. Fermenters play a key role in SR-PRZs because they provide a link between polysaccharide degradation and sulfate reduction and methanogenesis.

Fermentation is supported by a variety of microorganisms such as *Clostridium*, *Acetivibrio*, *Bacteroides*, *Fibrobacter*, *Ruminococcus*, *Eubacterium*, *Aeromonas*, *Lactobacillus*, *Pasteurella*, *Bifidobacteria*, *Propionobacterium*, and *Citrobacter* spp. Many of these species have been found in SR-PRZs.

Because of the phylogenetic diversity of fermenters, biomolecular studies are usually directed at functional genes and not the 16S rRNA gene. Probes targeting the iron hydrogenase genes of fermenters have been used to detect clostridia in anaerobic biohydrogen fermentation systems (Chang et al. 2006; Xing et al. 2008) and the diversity

of H₂-producing bacteria in acidophilic ethanol-H₂-coproducing system (Xing et al. 2008). Primers for quantitative PCR (Q-PCR) have also been developed study the fermentative microorganisms in remediation systems (Chapter 6).

1.2.4. Acetogens

Acetogens catalyze the reductive synthesis of acetate from CO₂ through the acetyl-CoA pathway and this sets them apart from microorganisms that synthesize acetate through other metabolic processes such as fermentation (Drake 1994). Acetogenesis contributes an estimated 10% of the approximately 1,013 Kg of acetate produced annually in anaerobic environments (Wood and Ljungdahl 1991).

Acetogens are arguably the most metabolically diverse group of obligate anaerobes characterized to date. Besides H₂, other electron donors utilized by acetogens (depending on the species) include sugars, C1 compounds, primary alcohols, organic acids, and chloromethanes (Schink 1994). In addition, they can also use electron acceptors other than CO₂ (e.g., fumarate, nitrate, nitrite, pyruvate, thiosulfate, etc). Because of this enormous metabolic versatility, acetogens are virtually ubiquitous and, although they are considered anaerobes, they have been observed to tolerate exposure to oxygen. Several strains of acetogens can reduce oxygen using H₂ as an electron donor and tolerate toxic O₂-reduction products (Boga and Brune 2003). This enables them not only to survive temporary exposure to oxygen but also to actively reestablish conditions favorable for growth.

Nearly one hundred acetogenic microorganisms are found in twenty different genera of the domain Bacteria. Seventeen genera belong to the phylum Gram-positive bacteria with low GC content. Within this phylum, acetogens are found in eight out

nineteen clostridium clusters. Two genera (*Treponema* and *Halophaga*) belong to the phyla Spirochetes and *Halophaga/Acidobacterium*.

The metabolic activity of acetogens is difficult to assess *in situ* because acetate is produced by a variety of processes and can be rapidly consumed by numerous microbes. In addition, their phylogenetic diversity also makes them difficult targets for 16S rRNA gene-based methods. Lovell and Leaphart (2005) used a functional gene-based approach targeting the gene encoding for formyltetrahydrofolate synthetase (FTHDS) to study acetogen diversity and ecology. FTHDS is an enzyme of the acetyl-CoA pathway that is highly conserved in acetogens (Drake et al. 2002). They amplified FTHDS sequences from acetogens, SRB, and nonacetogenic bacteria but all the acetogen FTHDS sequences clustered together, indicating that this is a suitable gene for differentiating acetogens.

Although 16S rRNA gene-based studies of microbial communities in SR-PRZs have detected acetogens, generally this group has not been given special attention. However, it is known that in anoxic environments, acetogens are involved in the degradation of organic matter (McInerney and Bryant 1981) and corresponding production of acetate, and thus, they may have an important role in SR-PRZs.

1.2.5. Sulfate-Reducing Bacteria

The reduction of sulfate can occur either via assimilatory or dissimilatory processes. Assimilatory sulfate reduction is a widespread biochemical capacity in prokaryotes and plants because it generates reduced sulfur for biosynthesis (e.g., cysteine). As a consequence, assimilatory sulfate reduction does not lead to the excretion of sulfide (Rabus et al. 2000) and is not relevant to AMD remediation.

Dissimilatory SRB are ultimately responsible for the remediation of AMD in SR-PRZs. They use the sulfate in the AMD as electron acceptor and, depending on the species, a variety of simple organic compounds such as acetate, ethanol, propionate, lactate (Rabus et al. 2000) can serve as electron donors. Some SRB species can also grow autotrophically from CO₂ and H₂ as carbon and energy sources, respectively (Schauder et al. 1987).

Based on their rRNA sequence and general characteristics, SRB are divided into four groups: Gram-negative mesophilic SRB, Gram-positive spore-forming SRB, thermophilic bacterial SRB, and thermophilic archaeal SRB (Castro et al. 2000). Most of the known SRB genera are found in the Gram-negative mesophilic group and they include *Desulfobulbus*, *Desulfomicrobium*, *Desulfomonas*, *Desulfovibrio*, *Desulfobacter*, *Desulfobacterium*, *Desulfococcus*, *Desulfomonile*, *Desulfonema*, and *Desulfosarcina*. *Desulfotomaculum* is the only genus in the Gram-positive spore-forming group.

Traditionally, SRB were considered anaerobic microorganisms restricted to anoxic environments. In the past two decades several studies have demonstrated that many SRB are tolerant to oxygen and some are even able to utilize it. Different groups and strains of SRB display different adaptations and tolerances to oxygen (Baumgartner et al. 2006). There are three main mechanisms that have been proposed to explain their tolerance to oxygen. One of the mechanisms is aerotaxis and was observed in motile SRB species (Krekeler et al. 1998). By this mechanism, SRB can move to areas where they can tolerate the concentration of oxygen and continue their metabolism. Another mechanism is the formation of clusters or flocs to create anoxic microenvironments (Sigalevich et al. 2000). The third mechanism is the production of enzymes such as

superoxide dismutase to destroy cell-damaging superoxides which could cause damage to the cell. This was observed in *Desulfovibrio* spp. These physical and biochemical mechanisms are linked to oxygen-sensing systems that alert the cell of the presence of oxygen (Voordouw 1995).

SRB are probably the most well-studied microorganisms in SR-PRZs. Benner and others (Benner et al. 2000) used culture-based methods to study the microbial populations associated with the generation and treatment of AMD in the Nickel Rim mine in Ontario, Canada. They found that the numbers of SRB were four orders of magnitude higher than in the aquifer. Interestingly, the populations of sulfur-oxidizing bacteria (SOB) were also elevated in the barrier compared to the aquifer. The coexistence of SRB and SOB could be explained by the existence of redox microenvironments. Benner hypothesized a syntrophic relationship between these two groups where SOB metabolize the reduced sulfur species produced by SRB while SRB benefited from the presence of oxygen-consuming SOB. Other studies have used molecular techniques to study SRB. Geets and others (2005) used 16S- and *dsrB*-based denaturing gradient gel electrophoresis (DGGE) to study the microbial community dynamics in batch laboratory systems for the treatment of AMD. The *dsrB* gene encodes for the beta subunit of the dissimilatory sulfite reductase and is considered a genetic marker for SRB. They found that the *dsrB*-based DGGE community profiles, when compared to the 16S-based analyses, revealed much more diversity between the different treatments. This suggests the *dsrB* gene provided a better reflection of the SRB community composition. Q-PCR targeting the 16S rRNA gene of different SRB genera was also applied to quantify SRB and it revealed that SRB are actually only a small fraction of the SR-PRZ community (Pereyra et al. 2008). Hiibel

(Hiibel et al. 2008) did a comparison of adenosine 5'-phosphosulfate reductase (*apsA*) genes in the Luttrell and Peerless Jenny King SR-PRZs in the Ten Mile Creek superfund site in Helena, Montana. The Luttrell bioreactor was dominated by uncultured SRB most closely related to *Desulfovibrio* spp., while the Peerless Jenny King site was dominated by *Thiobacillus* spp which, interestingly, are SOB.

SRB are sensitive to low pH and this could pose a problem to treat highly acidic waters. In many cases, a pre-treatment in the form of an anoxic limestone drain is used to increase the pH of the AMD before it enters the biological treatment. Nevertheless, sulfate-reducing activity has been observed in laboratory experiments at pH as low as 3.25 (Elliott et al. 1998) and also in acidic environments (Gyure et al. 1990; Herlihy and Mills 1985).

1.2.6. Methanogens

Methanogens are strict anaerobes that produce methane from a variety of organic compounds such as acetate, formate, and ethanol or autotrophically from H₂ and CO₂ (Garcia et al. 2000).

Methanogenic microorganisms belong to the domain Archaea and therefore are not detectable by standard methods targeting bacterial rRNA genes. Because of this, they tend to be overlooked in SR-PRZ studies. Methanogens are phylogenetically diverse microorganisms. Based on their 16S rRNA gene sequences, they are classified into five orders, which consist of ten families, twenty-six genera, and seventy-four validated species (Garcia et al. 2000). Recently, Q-PCR targeting the methyl-coenzyme M reductase gene detected methanogens in samples from a pilot-scale SR-PRZ that treats

the AMD from the National Tunnel in Black Hawk, CO, indicating that methanogens were more prevalent in an ethanol-fed than in a lignocelluloses-based reactor (Chapter 5).

1.2.7. Interactions

Various ecological interactions occur in SR-PRZs depending on the composition of the microbial community and spatial and environmental factors. Based on the following discussion, a framework of the SR-PRZ microbial community with its various microbial groups and their interactions is proposed in Figure 1.2. The interactions of microorganisms in SR-PRZs are likely highly complex based on the kinds and quantities of microorganisms that have been detected. While SR-PRZs in particular have not been studied extensively, what is known about the interactions in similar systems can be used to infer the probable relationships that might occur in SR-PRZs.

The degree of mutual dependence among the different bacterial groups varies considerably. The members at the bottom of the food chain (e.g., SRB and methanogens) always depend on the ones at the top for their energy sources. However, they may also exert significant influence on the upstream members by removing inhibitory metabolic by-products (Schink 1997). Probably, the most important interactions that occur in the SR-PRZ microbial community are inter-species hydrogen transfer and cross-feeding of fermentation products and monomers derived from polymer degradation. Fermentation products such as lactate, ethanol, and hydrogen are major intermediates in the degradation of the lignocellulosic substrate in SR-PRZs. They are produced by cellulose degrading-bacteria and secondary fermenters and can be consumed by SRB, methanogens, and acetogens (Schink 1994). In addition to inter-guild interactions, within

each microbial guild, intra-guild interactions may occur. The network of interactions can become very complex and their outcome depends on several factors.

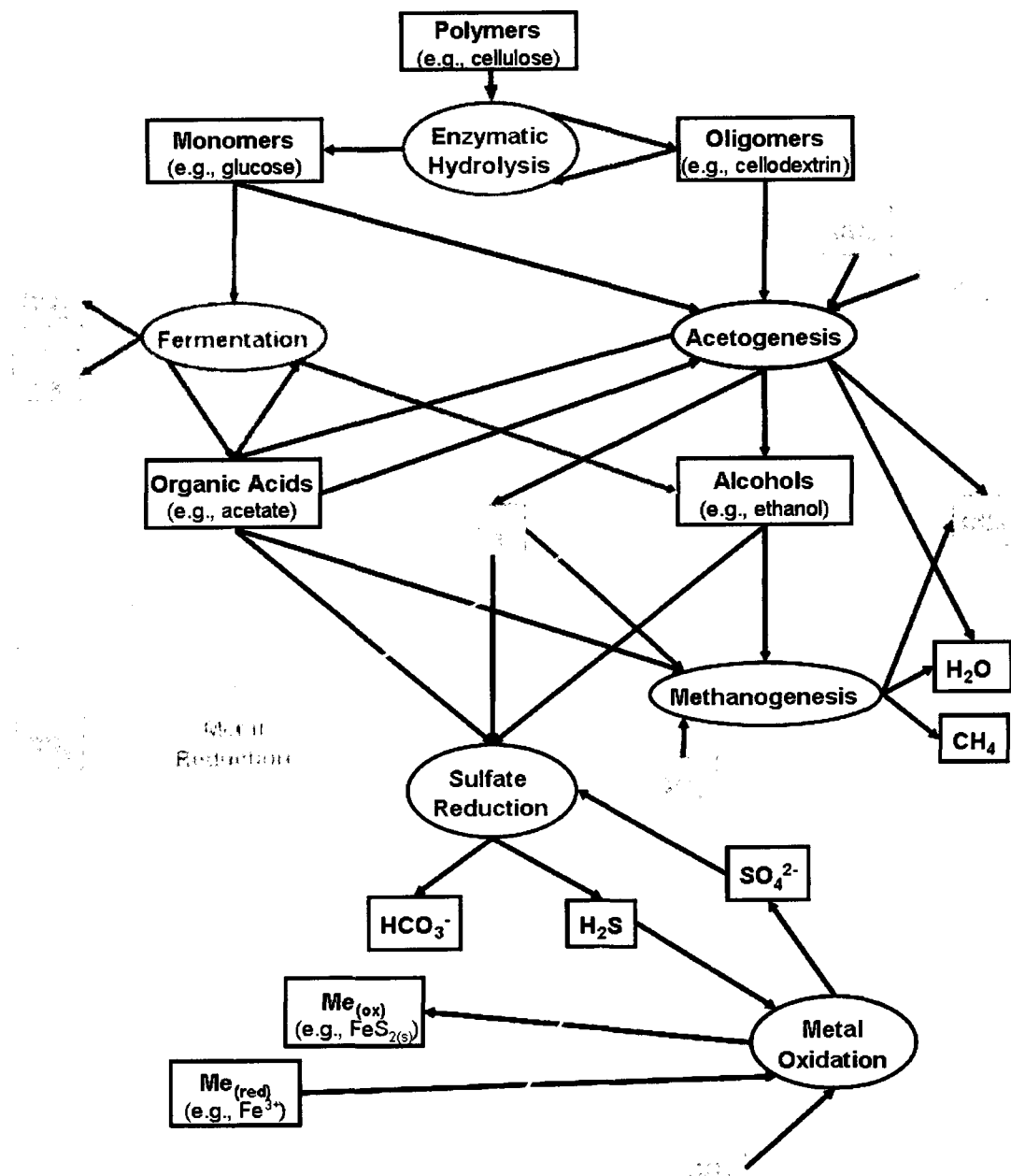


Figure 1. 2: Proposed framework of the SR-PRZ microbial community with interactions among microbial groups indicated.

1.2.7.1. Synergism

Lignocellulose degradation is considered the rate-limiting step in the carbon and energy flow in the degradation of complex organic matter (Hu et al. 2007; Logan et al. 2005). Cellulolytic enzymes are commonly repressed or inhibited by moderate to high concentrations of the hydrolytic or fermentation products (Weimer 1992). There is evidence that certain microbial interactions play an important role in minimizing or eliminating this inhibitory effect. Cellulose degradation is enhanced in co-cultures of cellulose-degrading and cellobiose-fermenting microorganisms because the latter keep cellobiose levels low (Leschine 1995). This effect was observed, for example, in a co-culture of the cellulose-degrading bacterium *C. thermocellum* and the spirochete *Spirochaeta calcaria* (Pohlschroeder et al. 1994). Enhanced cellulose degradation has also been observed in co-cultures of a cellulose degrader and a noncellulolytic saccharolytic microorganism. Interactions of cellulose degraders with acetogens, SRB, and/or methanogens are believed to enhance cellulose degradation by the removal of the hydrogen produced by cellulose degraders during fermentation. For example, the presence of H₂-utilizing acetogens led to an increase in the cellulose breakdown by *R. flavefaciens* strain 007 and *R. albus* strain 7 (Morvan et al. 1996). Laube and Martin (1981) reported enhanced conversion of cellulose to methane and CO₂ by a triculture of *Acetivibrio cellulolyticus*, *Desulfovibrio* sp., and *Methanosarcina barkeri*. In addition, the presence of the hydrogen-utilizing SRB and methanogen caused a shift in fermentation to H₂ production and away from ethanol. Chassard and Bernalier-Donadille (2006) investigated the interrelationships between H₂ and butyrate-producing xylanolytic species *Roseburia intestinalis* and the H₂-utilizing acetogen *Ruminococcus hydrogenotrophicus*.

during xylan fermentation. The H₂ produced by *R. intestinales* during the fermentation of xylan was used as an electron donor by the acetogen to produce acetate, which, in turn, was used by the xylanolytic microorganism to produce butyrate.

Cellulose degraders and noncellulolytic polysaccharide degraders are usually found in close association and this appears to have a positive effect on the degradation of cellulose. For example, the colonization of cellulose by noncellulolytic *Treponema* spp. and the cellulose-degrading *Bacteroides succinogenes* helped enhance cellulose degradation by this microorganism (Kudo et al. 1987). *Prevotella* spp. have also been observed to act in concert with cellulolytic microorganisms (Dehority 1991). Noncellulolytic microorganisms able to digest hemicellulose and pectins have been proposed to aid the cellulolytics by rendering the cellulose more accessible (Weimer 1992).

1.2.7.2. Competition

Sulfate reducers can compete with each other for the available sulfate. Iggen and Harrison (2006) used fluorescent *in situ* hybridization to study the structure of a mixed culture of SRB maintained in anaerobic continuous reactors before and after the addition of sulfate to the influent. They found that the *Desulfococcus* group was more dominant when the feed contained excess amounts of sulfate and that *Desulfobacterium*, *Desulfobacteriaceae*, and *Desulfobacter* were more competitive in environments with less sulfate. In addition, high concentrations of sulfate were toxic for *Desulfobacterium* and *Desulfobulbus*.

Thermodynamically, acetogenesis is less favorable than methanogenesis and sulfate reduction is more favorable than methanogenesis (Stams et al. 2005). However,

the outcome of the competition is different depending on the strains involved and the environmental conditions (e.g., tolerance of various ranges of temperature, pH, dissolved oxygen, substrate and inhibitor concentrations).

In sulfate-rich systems such as SR-PRZs and marine systems, the final products of the degradation of cellulose are H₂S and CO₂ because SRB outcompete methanogens for H₂. In systems where there is no sulfate, the mineralization of cellulose produces CO₂ and methane (Leschine 1995). Whether SRB or methanogens prevail depends on factors such as feedback inhibition of H₂S on SRB, the type of inoculum, biokinetics, and thermodynamics. For example, in a high-rate anaerobic reactor, SRB were outcompeted by methanogens (Isa et al. 1986). SRB compete most efficiently at low substrate levels and the high substrate concentration in the reactor together with the preferential colonization of the matrix by methanogens prevented the SRB from outcompeting methanogens.

Low pH or low temperature seem to improve *in situ* competitiveness of acetogens in lake water environments, flooded rice paddy soils, and tundra wetland soils (Conrad and Babel 1989). In general, acetogens cannot outcompete methanogens for H₂ because they have a higher H₂ threshold. However, this limitation can be overcome in a spatially heterogeneous system if acetogens are closer to H₂-producing cells (Drake et al. 2002). Braunman and others (Brauman et al. 1992) found that acetogenesis outprocessed methanogenesis as the primary sink of H₂ in wood feeding termites but not in soil-feeding and fungus-cultivating termites.

In general, acetogens appear to be inferior to their respective specialists. Their success in anoxic environments appears to be based on their metabolic versatility which

allows them to utilize various substrates or use them simultaneously (mixotrophy) (Drake et al. 1997).

Other microorganisms that might be present in the community are Fe(III) reducers (Lovley and Coates 2000). Fe(III)-reducing bacteria are able to outcompete SRB and methanogens for organic substrates and H₂ in Fe(III)-rich sediments (Lovley 1993; Lovley and Phillips 1987) and are generally only limited by the solubility of Fe(III) oxides.

The SR-PRZ microorganisms might also co-exist with AMD-generating microorganisms. For example, van den Ende and others (1997) reported the syntrophic growth of a mixed culture of the SRB *Desulfovibrio desulfuricans* PA 2805 and the sulfur bacterium *Thiobacillus thioparus* T5 supplied with limiting amounts of lactate and oxygen while sulfate was present in excess. The *Desulfovibrio* spp. grew on lactate using sulfate as an electron acceptor to produce sulfide. The *Thiobacillus* spp. enabled SRB growth by consuming oxygen. The SRB, in turn, provided the electron donor (sulfide) to *T. thioparus* which oxidized it to zero-valent sulfur and sulfate, which were both used as electron acceptors by the *Desulfovibrio* species. In SR-PRZs, this interaction is likely to occur in the oxygen-sulfide interface that might be present in the systems during seasons of low flow.

1.2.7.3. Factors Influencing Microbial Interactions

An important factor that influences the interactions between different microbial groups is their physical proximity. The closer the two associated microbes are, the more efficient the metabolic transfer. This is generally favored by the formation of aggregates or flocs (Schink 1997). Optimal cooperation is secured when the associated

microorganisms are randomly mixed to near homogeneity instead of forming pockets of identical subpopulations. However, as the microorganisms reproduce, each individual bacterium will be surrounded by offsprings of its own, and the metabolic transfer will be less efficient.

Scanning electron microscopy imaging of the cellulose-hydrolyzing and methanogenic populations during anaerobic digestion of cellulose revealed that the microbial community exists in a biofilm that is attached to the cellulose substrate (Song et al. 2005). The hydrolyzing bacteria oriented themselves in relation to the cellulose structure and methanogenic microorganisms resided within the biofilm as clusters.

1.3. Sulfate-Reducing Treatment Systems

1.3.1. General Aspects

In general, SR-PRZs are implemented as below-ground systems. They are constructed by excavating a trench that intercepts the contaminated groundwater. The trench is filled with the substrate and inoculum, and landscaped. Precipitation of metals as metals sulfides with biogenically produced sulfide is believed to be the main mechanism of metal removal in SR-PRZs (Cohen 2006; Jong and Parry 2003). Abiotic mechanisms such as precipitation as (oxy)hydroxides and carbonates, co-precipitation with hydroxides, and adsorption to the substrate surface could also be responsible for metal removal. Another mechanism of metal removal in SR-PRZs is adsorption of heavy metals to bacterially produced metal sulfides. Jong and Parry (2004) found that sulfide minerals have adsorptive properties and can form strong complexes with a variety of heavy metals.

Gibert and others (2005) reported that abiotic mechanisms rather than metal sulfide precipitation were the major sink of metals in upflow compost-based columns treating AMD. However, in this study no removal of sulfate was observed suggesting that there was minimal or no biological activity in the systems. It is generally accepted that sorption onto the substrate is the main mechanism of removal during startup and once the microbial community has established metal sulfide precipitation dominates (Zagury et al. 2006).

If the remediated water discharges into State waters, the EPA might require a National Pollutant Discharge Elimination System permit (Ford 2003). Discharge limits might be based on water quality standards (usually highly stringent) or from experience with similar technologies. Best Practical Technology effluent limitations published by the EPA for copper, zinc, lead, and mercury are 0.15 mg/L, 0.75 mg/L, 0.3 mg/L, and 0.001 mg/L, respectively and pH is required to be between 6 and 9.

1.3.2. SR-PRZ Configurations

SR-PRZs can be implemented as vertical-flow or horizontal-flow systems (Figure 1.3). The Luttrell SR-PRZ in the Ten Mile Creek Superfund site is a single-cell, vertical-flow bioreactor with an impermeable geomembrane liner (Hiibel et al. 2008). Flow is from top to bottom through approximately 1 m of organic substrate covered with a layer of ca. 3 cm rocks. Effluent exits the bioreactor through a series of perforated pipes at the bottom of the substrate. The Peerless Jenny King SR-PRZ located at a neighboring site consists of four gravel-lined, horizontal-flow bioreactor cells in series, with organic substrate depth varying from 0.7 – 1.0 m (Hiibel et al. 2008).

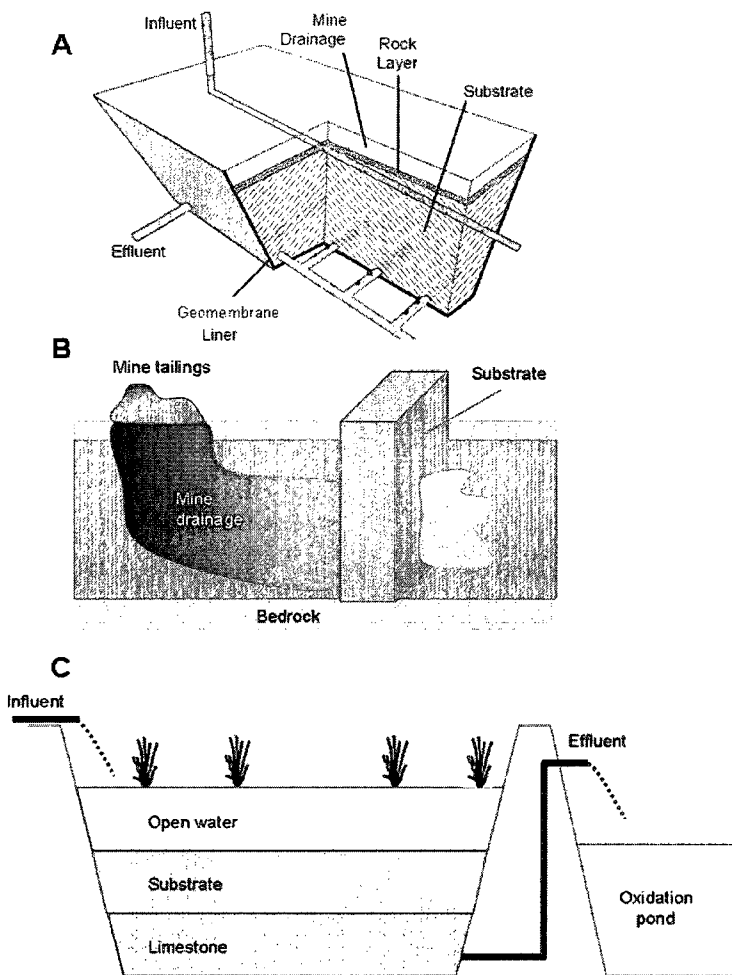


Figure 1.3: Different SR-PRZs configurations. (A) vertical flow (Hiibel et al. 2008), (B) horizontal flow, (C) successive alkalinity producing system (SAPS) which combines lignocellulose-based anaerobic treatment of AMD with limestone neutralization (Younger et al. 2003).

SR-PRZs are commonly applied together with other treatment technologies. For example, reducing and alkalinity producing systems (RAPS) (Younger et al. 2003) or successive alkalinity producing systems (SAPS) combine compost-based anaerobic treatment of AMD with limestone neutralization (Figure 1.3). The water flows through a layer of compost where oxygen consumption and sulfate reduction occur and then through a limestone gravel bed to add alkalinity.

SR-PRZs are also used in combination with aerobic treatment. For example, in the ‘Acid reduction using microbiology (ARUM) system’ (Kalin et al. 1991) iron is oxidized and precipitated in aerobic wetlands and then the AMD flows through ARUM cells where alkalinity and sulfides are produced.

1.3.3. Factors Impacting Performance

The performance of SR-PRZs is usually evaluated in terms of sulfate and metal removal and pH neutralization. To assess the performance of an SR-PRZ, it is also important to consider the startup time and activity retention (i.e., the period over which a rate of sulfate removal is maintained).

Laboratory column and batch experiments demonstrated that the type of inoculum influences performance (Pereyra et al. 2008; Pruden et al. 2007). Dairy manure is a common source of inoculum. However, its microbial composition is variable and, as a consequence, dairy manure-inoculated systems do not always perform well. Before using an inoculum in a large-scale operation, it is advisable to test it in pilot-scale systems. The substrate from the pilot-scale system might even be used as inoculum for the large-scale SR-PRZ. This also has the benefit of using as inoculum microorganisms that are already acclimated.

Factors that affect the microbial community such as exposure to air, sub-freezing temperatures, or increased acidity of the AMD have the potential to cause a decline in performance. Although SR-PRZs are anaerobic systems, there is evidence that some of the microorganisms in the microbial community are tolerant to oxygen. However, the response and recovery of the SR-PRZ microbial community to oxygen has not been studied. The metal sulfides formed during the remediation process might also have an

adverse effect on the microbial activity. Utgikar and others (2003) reported that unsoluble metal sulfides had a inhibitory effect on SRB by forming a ‘shield’ in the vicinity of the microorganisms that prevented access of the sulfate and energy sources to the enzymes.

The hydraulic residence time has a great effect on the efficiency of metal and sulfate removal in SR-PRZs (Bechard et al. 1994). For example, the sulfide concentration in the effluent of compost-based pilot-scale SR-PRZs decreased 99% when the residence time was reduced from 17 to 7 days (Dvorak et al. 1992). Bechard and others (1994) reported that increasing the retention time of alfalfa-based reactors resulted in better metal removal and pH neutralization. Using a retention time of 3.5 and 7 days, long-term stability was not achieved and only a 35 –day retention time produced effluents that met the environmental guidelines. While a short residence time might not allow sufficient contact between the microorganisms and the AMD, a long residence time may lead to rapid depletion of the substrate (Dvorak et al. 1992).

Another factor that is crucial for good performance of field systems is the hydraulic conductivity. This is determined by the substrate used in the SR-PRZ. In general, it is accepted that the hydraulic conductivity of the SR-PRZ should be one order of magnitude higher than that of the adjacent aquifer for good flow distribution (Benner et al. 1997). In addition to hydraulic conductivity, the substrate has to provide enough surface area for microbial attachment (Lyew and Sheppard 1997).

Clogging by metal sulfides may cause a decline in performance and this sometimes discourages the selection of the SR-PRZ technology as a treatment option. However, Benner and others (1997) anticipate that metal sulfides should cause very little clogging as their precipitation is accompanied by conversion of the organic material to

HCO_3^- resulting in the replacement of the organic material with solid sulfides, which have a higher specific gravity.

The type of organic substrate also influences SR-PRZ performance. In general, the quality of an organic substrate is determined based on its biodegradability (Gibert 2004, Bechard 1994, Prasad 1999) and, from this perspective, less lignified substrates are considered better. However, a higher biodegradability might lead to a shorter lifetime of the SR-PRZs defeating the whole purpose of these systems as long-term treatment alternatives. In this sense, a mixture of relatively recalcitrant and biodegradable materials might provide an acceptable compromise between performance and lifetime.

1.3.3.1. Startup

In this review startup time is defined as the time required until sulfate reduction is observed. Since sulfate removal in SR-PRZs is mainly associated with sulfate reduction by SRB, factors that have an impact on SRB or on microorganisms that interact with them will have an effect on startup time. The most critical factors that affect startup time are pH, reducing conditions, flow rate, AMD composition, nutrients, and temperature (Kuyucak and St-Germain 1994).

There is evidence that pre-acclimation of the microorganisms might reduce startup time. For example, microbial populations pre-exposed to *p*-nitrophenol and methyl parathion started degrading these compounds sooner and to a higher extent than populations that had not been pre-exposed (Spain et al. 1980). In an SR-PRZ column experiment, the startup time was immediate for acclimated inoculum but was approximately four weeks for dairy manure and uninoculated columns (Pruden et al. 2007).

Selection of an appropriate inoculum might help not only to ensure continued remediation but also reduce the startup time. For many xenobiotics, suitable microbial cultures are often derived from polluted sites. The method selected for the acclimation of the inoculum appears to have an effect on the resulting microbial composition. Bastos and others (2002) compared batch and continuous methods for the enrichment of microbial cultures for the degradation of 1,3-dichloro-2-propanol. They found that both methods successfully enriched microorganisms able to degrade the contaminant but that the constituting strains obtained in both methods were different and the continuous method seemed to favor microbial interactions.

1.3.3.2. Longevity

There are several factors that affect the lifetime of an SR-PRZ such as the amount and characteristics of the substrate, the reactions that occur in the barrier and their rates, and reduction of the surface area caused by preferential flow paths and clogging, among others. The rates of the reactions change over time (usually decline), which complicates the estimation of the lifetime. Reisman (Reisman et al. 2003) warns that the evaluation of longevity based on fixed amounts of organic carbon and limestone and the consumption rates observed is useless due to the high variability in kinetics of sulfate reduction during the treatment. In addition, not all the substrate is going to be used in reactions involved in remediation. Another problem is that the differences in design, type of substrate and inoculum, AMD chemistry, and environmental conditions make it hard to extrapolate results to other systems.

Benner and others (1997) estimated the longevity of the Nickel Rim SR-PRZ by assuming that 10% of the carbon in the barrier was available for degradation, calculating

how much iron could be precipitated as sulfide with that carbon, and comparing that quantity to the annual load of iron to the SR-PRZ. The calculation estimated a lifetime of 15 years. However, it did not take into account factors that might affect performance *in situ* such as preferential flow paths and inhibition of microbial activity.

In some cases, longevity estimates come from previous experiences with similar systems. For example, Cohen (Cohen 2006) estimated that the lifetime of 100-gallon upflow reactors filled with composted livestock manure would be approximately 4 to 6 years for a single load of substrate.

Excess biomass and heavy metal precipitates can potentially reduce the lifetime of an SR-PRZ by causing clogging of the pore space in the reactor. Jong and Parry (2003) proposed that this can be avoided by intermittently flushing the system by increasing the influent velocity. Although this might be possible in laboratory systems, it might not be an option in field SR-PRZs. In general, upflow systems are better at retaining hydraulic conductivity and ensuring contact with the substrate (Cohen 2006).

Tsukamoto and others (2004) proposed that once the organic substrate is depleted, the lifetime of the reactor can be extended by adding simple organic compounds. These compounds do not serve to stimulate the microbial community to better degrade the organic carbon already present in the SR-PRZ but act as direct carbon and energy sources for the SRB in the microbial community. Although this alternative might be successful, it requires energy input to deliver the organic compounds and might not be possible in remote, inaccessible sites.

1.3.3.3. Performance in Cold Weather

Performance in cold weather is an important aspect of SR-PRZ performance because many of these systems operate most of the year under freezing or slightly above-zero conditions. Usually in below-ground systems freezing of the AMD is not a problem but the low temperatures could slow down or stop microbial activity.

Sagemann and others (1998) investigated the effect of temperature on the sulfate reduction rates in cold anoxic sediments and reported that the rates of sulfate reduction increased 4 to 10-fold from -1.7/2.6 °C to 25/30 °C. Heal and Salt (1999) observed a decrease in metal removal and pH neutralization in a constructed wetland during winter. On the other hand, other studies have not found a significant effect of temperature. For example, the SRB in a wetland in Canada were very active during winter (Fortin et al. 2000). Tsukamoto and others (2004) studied performance of manure-based columns supplemented with ethanol or methanol in low temperature and found no effect. Passive on-site bioreactors operated successfully for 32 months at temperatures between 2 and 16 °C (Zaluski et al. 2003) and over 2 years at 1-8°C (Kuyucak et al. 2006; Reisinger et al. 2000).

1.3.3.4. Failures

A variety of factors can lead to the failure of an SR-PRZ, for example: inadequate selection of the substrate or the inoculum, short residence times that do not allow enough contact of AMD with microorganisms, and poor flexibility of the systems to handle overloads. However, every failure represents an opportunity to learn from the mistakes and improve the design. For example, a constructed wetland that received the water from

the underground mines in the Jones Branch watershed, Kentucky, failed after six months of operation (Barton and Karathanasis 1999). The wetland consisted of two ponds that contained crushed limestone and spent mushroom compost. The reasons of the failure were attributed to insufficient utilization of the treatment area, inadequate alkalinity production, and metal overloading. The design was improved by the addition of two anoxic limestone drains before a successive alkalinity producing system of limestone beds overlain by compost. The idea of the new design was to provide sufficient alkalinity in the drains and anaerobic zones to promote metal precipitation and compensate for the acidity generated in the aerobic zones. After the renovation, the performance of the system improved and a survey conducted 19 months after the renovation indicated that performance was stable.

1.4. Future Research

Although there has been substantial improvement in our knowledge of the principles and operation of SR-PRZs over the past years, several knowledge gaps remain.

Because of the critical role that microorganisms play in SR-PRZ performance, research efforts should continue to improve the understanding of the microbial community of AMD bioremediation. Biomolecular research has provided valuable insight into the microbial composition of SR-PRZs. The extraordinary phylogenetic diversity of cellulose degraders, fermenters, SRB, and methanogens, however, poses a challenge for 16S rRNA gene-based methods. In particular, information on the relative proportion of the microbial groups, which could be very useful in the selection of inocula, would require the use of hundreds of 16S rRNA gene probes. In light of the characteristics of the SR-PRZ microbial community, a more fruitful approach would

likely be to target functional genes. In the field of AMD bioremediation, functional genes (*dsrA* and *apsA*) have been used to study SRB. This approach could be expanded to include cellulose degraders, fermenters, and methanogens. In addition, the role of acetogens should be investigated as they might play a significant role in the community dynamics and, thus, in SR-PRZ performance. These are also phylogenetically diverse microorganisms but biomolecular methods targeting functional genes of acetogens have been developed.

Genetic engineering of inocula might also be worth exploring, particularly to enhance cellulose degradation which might be impaired by the low pH of some AMD. Flint (1997) suggested the introduction of cellulolytic capacity in low-pH-tolerant *Prevotella* spp. by genetic manipulation. However, given the constraints posed by the cell wall structure of the plant and the highly adapted nature of cellulose degraders, transfer of cellulolytic capabilities to non-cellulolytic species is challenging (Weimer 1996).

The SR-PRZ technology will also benefit from research on the performance after environmental stresses. Field systems are subject to metal and sulfate overloads, changes in influent pH, aeration during seasons of low flow, and low temperatures during winter. Understanding how these stresses affect the microbial community may help improve SR-PRZ design and reliability.

More research is needed to determine whether the presence of multiple taxa/species with overlapping functional abilities actually results in functional stability. Several studies have cited the importance of diversity in community stability. For example, von Canstein and others (2002), reported that increased microbial diversity improved the efficiency of mercury-reducing biofilms under changing environmental

conditions by providing a reservoir of strains with complementary ecological niches. However, other studies suggest that functional redundancy plays a more important role than microbial diversity (Franklin and Mills 2006).

A final note that should be considered for future studies has to do with the experimental setups employed to study the effect of different factors on performance. Batch setups are suitable for preliminary feasibility studies but they do not reflect the *in situ* conditions (Geets et al. 2005). A comparison of DNA sequences retrieved from laboratory (batch and column) and field SR-PRZ systems revealed that the microbial communities originating from laboratory and field systems were distinct. This only serves to demonstrate that the field conditions are extremely difficult to simulate in the laboratory environment and, although laboratory tests are useful to understand fundamental principles, they might need to be accompanied by field experimentation to ensure successful practical application.

1.5. References

- Augustin G, Wallace RJ, Flint HJ. 1997. Phenotypic diversity among ruminal isolates of *Prevotella ruminicola*: Proposal of *Prevotella brevis* sp nov, *Prevotella bryantii* sp nov, and *Prevotella albensis* sp nov and redefinition of *Prevotella ruminicola*. Int. J. Syst. Bacteriol. 47(2):284-288.
- Babel S, Kurniawan TA. 2003. Low-cost adsorbents for heavy metals uptake from contaminated water: a review. J. Hazard. Mater. 97(1-3):219-243.
- Baker BJ, Banfield JF. 2003. Microbial communities in acid mine drainage. FEMS Microbiol. Ecol. 44(2):139-152.

- Banfalvi G. 2006. Removal of insoluble heavy metal sulfides from water. *Chemosphere* 63(7):1231-1234.
- Banks D, Younger PL, Arnesen RT, Iversen ER, Banks SB. 1997. Mine-water chemistry: the good, the bad and the ugly. *Environ. Geol.* 32(3):157-174.
- Barton CD, Karathanasis AD. 1999. Renovation of a failed constructed wetland treating acid mine drainage. *Environ. Geol.* 39(1):39-50.
- Bastos F, Bessa JE, Pacheco CC, De Marco P, Castro PML, Silva M, Jorge RF. 2002. Enrichment of microbial cultures able to degrade 1,3-dichloro-2-propanol: A comparison between batch and continuous methods. *Biodegradation* 13(3):211-220.
- Baumgartner LK, Reid RP, Dupraz C, Decho AW, Buckley DH, Spear JR, Przekop KM, Visscher PT. 2006. Sulfate reducing bacteria in microbial mats: Changing paradigms, new discoveries. *Sediment. Geol.* 185(3-4):131-145.
- Bayer EA, Belaich JP, Shoham Y, Lamed R. 2004. The cellulosomes: Multienzyme machines for degradation of plant cell wall polysaccharides. *Annu. Rev. Microbiol.* 58:521-554.
- Bayer EA, Shimon LJW, Shoham Y, Lamed R. 1998. Cellulosomes - Structure and ultrastructure. *J. Struct. Biol.* 124(2-3):221-234.
- Bayer EA, Shoham Y, Lamed R. 2000. Cellulose-decomposing prokaryotes and their enzyme systems. In: Dworkin M, Falkow S, Rosenberg E, Schleifer K-H, Stackebrandt E, editors. *The Prokaryotes: An Evolving Electronic Resource for the Microbiological Community*, 3rd edition (latest update release 3.7, September 2001): Springer-Verlag, New York.

- Bechard G, Yamazaki H, Gould WD, Bedard P. 1994. Use Of Cellulosic Substrates For The Microbial Treatment Of Acid-Mine Drainage. *J. Environ. Qual.* 23(1):111-116.
- Beguin P, Aubert JP. 1994. The Biological Degradation Of Cellulose. *Fems Microbiol. Rev.* 13(1):25-58.
- Benner SG, Blowes DW, Ptacek CJ. 1997. A full-scale porous reactive wall for prevention of acid mine drainage. *Ground Water Monit. Rem.* 17(4):99-107.
- Benner SG, Gould WD, Blowes DW. 2000. Microbial populations associated with the generation and treatment of acid mine drainage. *Chem. Geol.* 169(3-4):435-448.
- Blowes DW, Ptacek CJ, Benner SG, McRae CWT, Bennett TA, Puls RW. 2000. Treatment of inorganic contaminants using permeable reactive barriers. *J. Contam. Hydrol.* 45(1-2):123-137.
- Boga HI, Brune A. 2003. Hydrogen-dependent oxygen reduction by homoacetogenic bacteria isolated from termite guts. *Appl. Environ. Microbiol.* 69(2):779-786.
- Brauman A, Kane MD, Labat M, Breznak JA. 1992. Genesis Of Acetate And Methane By Gut Bacteria Of Nutritionally Diverse Termites. *Science* 257(5075):1384-1387.
- Carrillo-Chavez A, Morton-Bermea O, Gonzalez-Partida E, Rivas-Solorzano H, Oesler G, Garcia-Meza V, Hernandez E, Morales P, Cienfuegos E. 2003. Environmental geochemistry of the Guanajuato Mining District, Mexico. *Ore Geol. Rev.* 23(3-4):277-297.
- Castro HF, Williams NH, Ogram A. 2000. Phylogeny of sulfate-reducing bacteria. *FEMS Microbiol. Ecol.* 31(1):1-9.

- Chang JJ, Chen WE, Shih SY, Yu SJ, Lay JJ, Wen FS, Huang CC. 2006. Molecular detection of the clostridia in an anaerobic biohydrogen fermentation system by hydrogenase mRNA-targeted reverse transcription-PCR. *Appl. Microbiol. Biotechnol.* 70(5):598-604.
- Chassard C, Bernalier-Donadille A. 2006. H₂ and acetate transfers during xylan fermentation between a butyrate-producing xylanolytic species and hydrogenotrophic microorganisms from the human gut. *FEMS Microbiol. Lett.* 254(1):116-122.
- Cohen RRH. 2006. Use of microbes for cost reduction of metal removal from metals and mining industry waste streams. *J. Clean Prod.* 14(12-13):1146-1157.
- Conrad R, Babbel M. 1989. Effect Of Dilution On Methanogenesis, Hydrogen Turnover And Interspecies Hydrogen Transfer In Anoxic Paddy Soil. *FEMS Microbiol. Ecol.* 62(1):21-28.
- Cravotta CA. 2003. Size and performance of anoxic limestone drains to neutralize acidic mine drainage. *J. Environ. Qual.* 32(4):1277-1289.
- de Mello JWV, Dias LE, Daniel AM, Abrahao WAP, Deschamps E, Schaefer C. 2006. Preliminary evaluation of acid mine drainage in Minas Gerais State, Brazil. *Rev. Bras. Cienc. Solo* 30(2):365-375.
- Dehority BA. 1969. Pectin-Fermenting Bacteria Isolated From Bovine Rumen. *J. Bacteriol.* 99(1):189-&.
- Dehority BA. 1991. Effects Of Microbial Synergism On Fiber Digestion In The Rumen. *Proc. Nutr. Soc.* 50(2):149-159.

- Desbarats AJ, Dirom GC. 2007. Temporal variations in the chemistry of circum-neutral drainage from the 10-Level portal, Myra Mine, Vancouver Island, British Columbia. *Appl. Geochem.* 22(2):415-435.
- Drake HL. 1994. Acetogenesis. New York: Chapman & Hall.
- Drake HL, Daniel SL, Kusel K, Matthies C, Kuhner C, Braus-Stromeyer S. 1997. Acetogenic bacteria: what are the *in situ* consequences of their diverse metabolic versatilities? *Biofactors* 6(1):13-24.
- Drake HL, Kusel K, Matthies C. 2002. Ecological consequences of the phylogenetic and physiological diversities of acetogens. *Antonie Van Leeuwenhoek* 81(1-4):203-213.
- Druschel GK, Baker BJ, Gehrke TM, Banfield JF. 2004. Acid mine drainage biogeochemistry at Iron Mountain, California. *Geochem. Trans.* 5(2):13-32.
- Dvorak DH, Hedin RS, Edenborn HM, McIntire PE. 1992. Treatment Of Metal-Contaminated Water Using Bacterial Sulfate Reduction - Results From Pilot-Scale Reactors. *Biotechnol. Bioeng.* 40(5):609-616.
- Elliott P, Ragusa S, Catcheside D. 1998. Growth of sulfate-reducing bacteria under acidic conditions in an upflow anaerobic bioreactor as a treatment system for acid mine drainage. *Water Res.* 32(12):3724-3730.
- Environmental Protection Agency. 1992. Managing Nonpoint Source Pollution. Final Report to Congress on Section 319 of the Clean Water Act. EPA.
- Espana JS, Pamo EL, Santofimia E, Aduvire O, Reyes J, Barettino D. 2005. Acid mine drainage in the Iberian Pyrite Belt (Odiel river watershed, Huelva, SW Spain):

- Geochemistry, mineralogy and environmental implications. *Appl. Geochem.* 20(7):1320-1356.
- Flint HJ. 1997. The rumen microbial ecosystem - some recent developments. *Trends Microbiol.* 5(12):483-488.
- Ford KL. 2003. Passive Treatment Systems for Acid Mine Drainage. Bureau of Land Management, National Science and Technology Center. Report nr Technical Note 409.
- Fortin D, Roy M, Rioux JP, Thibault PJ. 2000. Occurrence of sulfate-reducing bacteria under a wide range of physico-chemical conditions in Au and Cu-Zn mine tailings. *FEMS Microbiol. Ecol.* 33(3):197-208.
- Franklin RB, Mills AL. 2006. Structural and functional responses of a sewage microbial community to dilution-induced reductions in diversity. *Microb. Ecol.* 52(2):280-288.
- Garcia JL, Patel BKC, Ollivier B. 2000. Taxonomic phylogenetic and ecological diversity of methanogenic *Archaea*. *Anaerobe*. 6(4):205-226.
- Geets J, Borremans B, Vangronsveld J, Diels L, van der Lelie D. 2005. Molecular monitoring of SRB community structure and dynamics in batch experiments to examine the applicability of in situ precipitation of heavy metals for groundwater remediation. *J. Soils Sediments* 5(3):149-163.
- Gibert O, De Pablo J, Cortina JL, Ayora C. 2002. Treatment of acid mine drainage by sulphate-reducing bacteria using permeable reactive barriers: A review from laboratory to full-scale experiments. *Rev. Environ. Sci. Biotechnol.* 1:327-333.

- Gibert O, de Pablo J, Cortina JL, Ayora C. 2004. Chemical characterisation of natural organic substrates for biological mitigation of acid mine drainage. *Water Res.* 38(19):4186-4196.
- Gibert O, de Pablo J, Cortina JL, Ayora C. 2005. Municipal compost-based mixture for acid mine drainage bioremediation: Metal retention mechanisms. *Appl. Geochem.* 20(9):1648-1657.
- Gyure RA, Konopka A, Brooks A, Doemel W. 1990. Microbial Sulfate Reduction In Acidic (Ph-3) Strip-Mine Lakes. *FEMS Microbiol. Ecol.* 73(3):193-201.
- Hallberg KB, Rolfe S, Johnson DB. The microbiology of passive remediation technologies for mine drainage treatment. In: P. JA, Dudgeon BA, Younger PL, editors; 2004 19-23 September; Newcastle upon Tyne, U.K. University of Newcastle upon Tyne. p 227-233.
- Hammack RW, Edenborn HM, Dvorak DH. 1994. Treatment Of Water From An Open-Pit Copper Mine Using Biogenic Sulfide And Limestone - A Feasibility Study. *Water Res.* 28(11):2321-2329.
- Heal KV, Salt CA. 1999. Treatment of acidic metal-rich drainage from reclaimed ironstone mine spoil. *Water Sci. Technol.* 39(12):141-148.
- Henrissat B. 1991. A Classification Of Glycosyl Hydrolases Based On Amino-Acid-Sequence Similarities. *Biochem. J.* 280:309-316.
- Henrissat B, Bairoch A. 1993. New Families In The Classification Of Glycosyl Hydrolases Based On Amino-Acid-Sequence Similarities. *Biochem. J.* 293:781-788.

- Henrissat B, Davies G. 1997. Structural and sequence-based classification of glycoside hydrolases. *Curr. Opin. Struct. Biol.* 7(5):637-644.
- Herlihy AT, Mills AL. 1985. Sulfate Reduction In Fresh-Water Sediments Receiving Acid-Mine Drainage. *Appl. Environ. Microbiol.* 49(1):179-186.
- Hespell RB, Whitehead TR. 1990. Physiology And Genetics Of Xylan Degradation By Gastrointestinal-Tract Bacteria. *J. Dairy Sci.* 73(10):3013-3022.
- Hiibel SR, Pereyra LP, Inman LY, Tischer A, Reisman DJ, Reardon KF, Pruden A. 2008. Microbial community analysis of two field-scale sulfate-reducing bioreactors treating mine drainage. *Environ. Microbiol.* 10(8):2087-2097.
- Hu ZH, Yu HQ, Yue ZB, Harada H, Li YY. 2007. Kinetic analysis of anaerobic digestion of cattail by rumen microbes in a modified UASB reactor. *Biochem. Eng. J.* 37(2):219-225.
- Hudson-Edwards KA, Schell C, Macklin MG. 1999. Mineralogy and geochemistry of alluvium contaminated by metal mining in the Rio Tinto area, southwest Spain. *Appl. Geochem.* 14(8):1015-1030.
- Isa Z, Grusenmeyer S, Verstraete W. 1986. Sulfate Reduction Relative To Methane Production In High-Rate Anaerobic-Digestion - Microbiological Aspects. *Appl. Environ. Microbiol.* 51(3):580-587.
- Johnson DB, Hallberg KB. 2002. Pitfalls of passive mine water treatment. *Rev. Environ. Sci. Biotechnol.* 1(4):335-343.
- Johnson DB, Hallberg KB. 2003. The microbiology of acidic mine waters. *Res. Microbiol.* 154(7):466-473.

- Johnson DB, Hallberg KB. 2005. Acid mine drainage remediation options: a review. *Sci. Total Environ.* 338(1-2):3-14.
- Johnson DB, Hallberg KB. 2005. Biogeochemistry of the compost bioreactor components of a composite acid mine drainage passive remediation system. *Sci. Total Environ.* 338(1-2):81-93.
- Johnson RH. 1993. The physical and chemical hydrogeology of the Nickel Rim mine tailings, Sudbury, Ontario. [M.Sc.]. Waterloo, Ontario: University of Waterloo.
- Jong T, Parry DL. 2003. Removal of sulfate and heavy metals by sulfate reducing bacteria in short-term bench scale upflow anaerobic packed bed reactor runs. *Water Res.* 37(14):3379-3389.
- Jong T, Parry DL. 2004. Adsorption of Pb(II), Cu(II), Cd(II), Zn(II), Ni(II), Fe(II), and As(V) on bacterially produced metal sulfides. *J. Colloid Interface Sci.* 275(1):61-71.
- Kalin M, Cairns J, McCready R. 1991. Ecological engineering methods for acid-mine drainage treatment of coal wastes. *Resour. Conserv. Recycl.* 5:265-275.
- Kalin M, Fyson A, Wheeler WN. 2006. The chemistry of conventional and alternative treatment systems for the neutralization of acid mine drainage. *Sci. Total Environ.* 366(2-3):395-408.
- Kotrba P, Ruml T. 2000. Bioremediation of heavy metal pollution exploiting constituents, metabolites and metabolic pathways of living. A review. *65(8):1205-1247.*
- Krekeler D, Teske A, Cypionka H. 1998. Strategies of sulfate-reducing bacteria to escape oxygen stress in a cyanobacterial mat. *FEMS Microbiol. Ecol.* 25(2):89-96.

Kudo H, Cheng KJ, Costerton JW. 1987. Interactions Between Treponema-Bryantii And Cellulolytic Bacteria In The Invitro Degradation Of Straw Cellulose. *Can. J. Microbiol.* 33(3):244-248.

Kuyucak N. 1998. Mining, the environment and the treatment of mine effluents. *Int. J. Environ. Pollut.* 10(2):315-325.

Kuyucak N, Chabot F, Martschuk J. Successful implementation and operation of a passive treatment system in an extremely cold climate, northern Quebec, Canada.; 2006 March 26-30; St. Louis, MO. American Society of Mining and Reclamation. p 3131-3138.

Kuyucak N, St-Germain P. Possible options for in situ treatment of acid mine seepages; 1994. U.S. Bureau of Mines Special Publication. p 311-318.

Labrenz M, Banfield JF. 2004. Sulfate-reducing bacteria-dominated biofilms that precipitate ZnS in a subsurface circumneutral-pH mine drainage system. *Microb. Ecol.* 47(3):205-217.

Lagowski JM, Sell HM, Huffman CF, Duncan CW. 1958. The Carbohydrates In Alfalfa Medicago-Sativa.1. General Composition, Identification Of A Nonreducing Sugar And Investigation Of The Pectic Substances. *Arch. Biochem. Biophys.* 76(2):306-316.

Laube VM, Martin SM. 1981. Conversion Of Cellulose To Methane And Carbon-Dioxide By Triculture Of Acetivibrio-Cellulolyticus, Desulfovibrio Sp, And Methanosarcina-Barkeri. *Appl. Environ. Microbiol.* 42(3):413-420.

Leschine SB. 1995. Cellulose degradation in anaerobic environments. *Annu. Rev. Microbiol.* 49:399-426.

- Logan MV, Reardon KF, Figueroa LA, McLain JET, Ahmann DM. 2005. Microbial community activities during establishment, performance, and decline of bench-scale passive treatment systems for mine drainage. *Water Res.* 39(18):4537-4551.
- Lovell CR, Leaphart AB. 2005. Community-level analysis: Key genes of CO₂-reductive acetogenesis. *Environmental Microbiology*. San Diego: Elsevier Academic Press Inc. p 454-469.
- Lovley DR. 1993. Dissimilatory Metal Reduction. *Annu. Rev. Microbiol.* 47:263-290.
- Lovley DR, Coates JD. 2000. Novel forms of anaerobic respiration of environmental relevance. *Curr. Opin. Microbiol.* 3(3):252-256.
- Lovley DR, Phillips EJP. 1987. Competitive Mechanisms For Inhibition Of Sulfate Reduction And Methane Production In The Zone Of Ferric Iron Reduction In Sediments. *Appl. Environ. Microbiol.* 53(11):2636-2641.
- Lyew D, Sheppard JD. 1997. Effects of physical parameters of a gravel bed on the activity of sulphate-reducing bacteria in the presence of acid mine drainage. *J. Chem. Technol. Biotechnol.* 70(3):223-230.
- Lynd LR, Weimer PJ, van Zyl WH, Pretorius IS. 2002. Microbial cellulose utilization: Fundamentals and biotechnology (vol 66, pg 506, 2002). *Microbiol. Mol. Biol. Rev.* 66(4):739-739.
- Macy JM, Probst I. 1979. Biology Of Gastro-Intestinal Bacteroides. *Annu. Rev. Microbiol.* 33:561-594.
- Matlock MM, Howerton BS, Atwood DA. 2002. Chemical precipitation of heavy metals from acid mine drainage. *Water Res.* 36(19):4757-4764.

- McInerney MJ, Bryant MP. 1981. Anaerobic Degradation Of Lactate By Syntrophic Associations Of Methanosarcina-Barkeri And Desulfovibrio Species And Effect Of H₂ On Acetate Degradation. *Appl. Environ. Microbiol.* 41(2):346-354.
- Mohan D, Chander S. 2006. Removal and recovery of metal ions from acid mine drainage using lignite - A low cost sorbent. *J. Hazard. Mater.* 137(3):1545-1553.
- Morales TA, Dopson M, Athar R, Herbert RB. 2005. Analysis of bacterial diversity in acidic pond water and compost after treatment of artificial acid mine drainage for metal removal. *Biotechnol. Bioeng.* 90(5):543-551.
- Morvan B, RieuLesme F, Fonty G, Gouet P. 1996. In vitro interactions between rumen H₂-producing cellulolytic microorganisms and H₂-utilizing acetogenic and sulfate-reducing bacteria. *Anaerobe* 2(3):175-180.
- Neculita CM, Zagury GJ, Bussiere B. 2007. Passive treatment of acid mine drainage in bioreactors using sulfate-reducing bacteria: Critical review and research needs. *J. Environ. Qual.* 36(1):1-16.
- Nordstrom DK, Alpers CN. 1999. Negative pH, efflorescent mineralogy, and consequences for environmental restoration at the Iron Mountain Superfund site, California. *Proc. Natl. Acad. Sci.* 96:3455-3462.
- Office of Inspector General. 1991. Noncoal Reclamation. Abandoned Mine Land reclamation Program, Office of Surface Mining Reclamation and Enforcement. U.S. Department of the Interior. Report No.91-I-1248 p.
- Pereyra LP, Hiibel SR, Pruden A, Reardon KF. 2008. Comparison of microbial community composition and activity in sulfate-reducing batch systems remediating mine drainage. *Biotechnol. Bioeng.* 101(4):702-713.

- Pohlschroeder M, Leschine SB, Canaleparola E. 1994. Spirochaeta Caldaria Sp-Nov, A Thermophilic Bacterium That Enhances Cellulose Degradation By Clostridium- Thermocellum. *Arch. Microbiol.* 161(1):17-24.
- Pruden A, Messner N, Pereyra L, Hanson RE, Hiibel SR, Reardon KF. 2007. The effect of inoculum on the performance of sulfate-reducing columns treating heavy metal contaminated water. *Water Res.* 41(4):904- 914.
- Rabinovich ML, Melnik MS, Boloboba AV. 2002. Microbial cellulases (Review). *Appl. Biochem. Microbiol.* 38(4):305-321.
- Rabus R, Hansen T, Widdel F. 2000. Dissimilatory sulfate- and sulfur-reducing prokaryotes. In: Dworkin M, Falkow S, Rosenberg E, Schleifer KH, Stackebrandt E, editors. *The Prokaryotes: An Evolving Electronic Resource for the Microbiological Community* (3rd ed.). New York.
- Rainey FA, Stackebrandt E. 1993. 16s Rdna Analysis Reveals Phylogenetic Diversity Among The Polysaccharolytic Clostridia. *FEMS Microbiol. Lett.* 113(2):125-128.
- Reisinger RW, Gusek JJ, Richmond TC. Pilot-scale passive treatment test of contaminated waters at the historic Ferris-Haggarty Mine, Wyoming.; 2000 21-24 May; Denver, CO. p 1071-1077.
- Reisman DJ, Gusek JJ, Bishop M. A pre-treatability study to provide data for construction of a demonstration bioreactor.; 2003 October 12-15; Vail, CO. p 305-315.
- Sagemann J, Jorgensen BB, Greeff O. 1998. Temperature dependence and rates of sulfate reduction in cold sediments of Svalbard, Arctic Ocean. *Geomicrobiol. J.* 15(2):85-100.

- Schauder R, Widdel F, Fuchs G. 1987. Carbon Assimilation Pathways In Sulfate-Reducing Bacteria.2. Enzymes Of A Reductive Citric-Acid Cycle In The Autotrophic Desulfobacter-Hydrogenophilus. *Arch. Microbiol.* 148(3):218-225.
- Schink B. 1994. Diversity, Ecology, and Isolation of Acetogenic Bacteria. In: Drake HL, editor. *Acetogenesis*. New York: Chapman & Hall. p 197-227.
- Schink B. 1997. Energetics of syntrophic cooperation in methanogenic degradation. *Microbiol. Mol. Biol. Rev.* 61(2):262-&.
- Seal RR, Hammarstrom JM, Johnson AN, Piatak NM, Wandless GA. 2008. Environmental geochemistry of a Kuroko-type massive sulfide deposit at the abandoned Valzinco mine, Virginia, USA. *Appl. Geochem.* 23(2):320-342.
- Sigalevich P, Meshorer E, Helman Y, Cohen Y. 2000. Transition from anaerobic to aerobic growth conditions for the sulfate-reducing bacterium *Desulfovibrio oxyclinae* results in flocculation. *Appl. Environ. Microbiol.* 66(11):5005-+.
- Singer PC, Stumm W. 1970. Acidic Mine Drainage. Rate-Determining Step. *Science* 167(3921):1121-&.
- Skinner SJW, Schutte CF. 2006. The feasibility of a permeable reactive barrier to treat acidic sulphate- and nitrate-contaminated groundwater. *Water SA* 32(2):129-135.
- Song H, Clarke WP, Blackall LL. 2005. Concurrent microscopic observations and activity measurements of cellulose hydrolyzing and methanogenic populations during the batch anaerobic digestion of crystalline cellulose. *Biotechnol. Bioeng.* 91(3):369-378.

- Spain JC, Pritchard PH, Bourquin AW. 1980. Effects Of Adaptation On Biodegradation Rates In Sediment-Water Cores From Estuarine And Fresh-Water Environments. *Appl. Environ. Microbiol.* 40(4):726-734.
- Stams AJM, Plugge CM, de Bok FAM, van Houten B, Lens P, Dijkman H, Weijma J. 2005. Metabolic interactions in methanogenic and sulfate-reducing bioreactors. *Water Sci. Technol.* 52(1-2):13-20.
- Sylvia DM, Fuhrmann JJ, Hartel PG, Zuberer DA. 2005. Principles and Applications of Soil Microbiology, 2nd Edition. Upper Saddle River, New Jersey: Pearson Prentice Hall.
- Tsukamoto TK, Killion HA, Miller GC. 2004. Column experiments for microbiological treatment of acid mine drainage: low-temperature, low-pH and matrix investigations. *Water Res.* 38(6):1405-1418.
- Turner D, McCoy D. Anoxic alkanine drain treatment system, a low cost acid mine drainage treatment alternative. In: Graves DH, editor; 1990; Lexington, KY. University of Kentucky. p 73-75.
- Tyrrell WR, Mulligan DR, Sly LI, Bell LC. 1997. Trialing wetlands to treat coal mining wastewaters in a low rainfall, high evaporation environment. *Water Sci. Technol.* 35(5):293-299.
- Utgikar VP, Tabak HH, Haines JR, Govind R. 2003. Quantification of toxic and inhibitory impact of copper and zinc on mixed cultures of sulfate-reducing bacteria. *Biotechnol. Bioeng.* 82(3):306-312.

- vandenEnde FP, Meier J, vanGemerden H. 1997. Syntrophic growth of sulfate-reducing bacteria and colorless sulfur bacteria during oxygen limitation. *FEMS Microbiol. Ecol.* 23(1):65-80.
- Vaughan DJ, Jambor JL. 2006. Mineralogy and geochemistry of acid mine drainage and metalliferous minewastes. *Appl. Geochem.* 21(8):1249-1250.
- von Canstein H, Kelly S, Li Y, Wagner-Dobler I. 2002. Species diversity improves the efficiency of mercury-reducing biofilms under changing environmental conditions. *Appl. Environ. Microbiol.* 68(6):2829-2837.
- Voordouw G. 1995. The Genus *Desulfovibrio* - The Centennial. *Appl. Environ. Microbiol.* 61(8):2813-2819.
- Waite R, Gorrod ARN. 1959. The comprehensive analysis of grasses. *J. Sci. Food Agr.* 10:317.
- Waybrant KR, Blowes DW, Ptacek CJ. 1998. Selection of Reactive Mixtures for Use in Permeable Reactive Walls for Treatment of Mine Drainage. *Environ. Sci. Technol.* 32:1972-1979.
- Waybrant KR, Ptacek CJ, Blowes DW. 2002. Treatment of mine drainage using permeable reactive barriers: Column experiments. *Environ. Sci. Technol.* 36(6):1349-1356.
- Weimer PJ. 1992. Cellulose degradation by ruminal microorganisms. *Crit. Rev. Biotechnol.* 12(3):189-223.
- Weimer PJ. 1996. Why don't ruminal bacteria digest cellulose faster? *J. Dairy Sci.* 79(8):1496-1502.

Whitehead PG, Prior H. 2005. Bioremediation of acid mine drainage: an introduction to the Wheal Jane wetlands project. *Sci. Total Environ.* 338(1-2):15-21.

Wilkin RT, McNeil MS. 2003. Laboratory evaluation of zero-valent iron to treat water impacted by acid mine drainage. *Chemosphere* 53(7):715-725.

Wood HG, Ljungdahl LG. 1991. Autotrophic Character of the acetogenic bacteria. In: Shively JM, Barton LL, editors. *Variations in Autotrophic Life*. New York: Academic Press.

Xing DF, Ren NQ, Rittmann BE. 2008. Genetic diversity of hydrogen-producing bacteria in an acidophilic ethanol-H₂-coproducing system, analyzed using the [Fe]-hydrogenase gene. *Appl. Environ. Microbiol.* 74(4):1232-1239.

Younger PL, Jayaweera A, Elliot A, Wood R, Amos P, Daugherty AJ, Martin A, Bowden L, Aplin AC, Johnson DB. 2003. Passive treatment of acidic mine waters in subsurface-flow systems: exploring RAPS and permeable reactive barriers. *Land Contam. Reclam.* 9:127-135.

Zagury GJ, Kulnieks VI, Neculita CM. 2006. Characterization and reactivity assessment of organic substrates for sulphate-reducing bacteria in acid mine drainage treatment. *Chemosphere* 64(6):944-954.

Zaluski MH, Trudnowski JM, Harrington-Baker MA, Bless DR. Post-mortem findings on the performance of engineered SRB field-bioreactors for acid mine drainage control.; 2003 12-18 July; Cairns, QLD. p 845-853.

Chapter 2 Research Approach and Dissertation Overview

2.1. Research Approach

This dissertation integrates several studies that were aimed at understanding various aspects of the microbiology of mine drainage (MD) remediation starting from two basic questions: do microorganisms play a role in the remediation performance of sulfate-reducing permeable reactive zones (SR-PRZs)? If they do, how do different microbial communities perform? Other important questions that were explored are:

- What are the differences in the microbial communities of good- and poor-performing SR-PRZs? Are there specific microbial groups that are key for successful remediation?
- How does the organic substrate shape the microbial community? Are there differences in the microbial community composition of lignocellulose-based and ethanol-fed SR-PRZs?
- Does a functional gene-based approach provide a more robust characterization of the SR-PRZ microbial community compared to a 16S rRNA gene-based approach?
- What are differences from a functional perspective in the microbial communities of SR-PRZs with different inocula or carbon sources? Do they correlate with performance?

The approach used to explore these questions involved a combination of different biomolecular methods. These methods interrogate the genetic information of the microorganisms and, thus, bypass the bias of culture-dependent methods which can only detect approximately 1% of the microorganisms in a community. The methods applied in this research include quantitative polymerase chain reaction (Q-PCR) for the determination of the abundance of total bacteria and microbial groups, denaturing gradient gel electrophoresis (DGGE) to obtain a fingerprint of the microbial community and monitor its changes over time, and cloning for the identification of microorganisms through DNA sequencing.

The results from biomolecular analyses were combined with data relating to MD remediation performance to identify characteristics of the microbial community that are associated with good and poor performance.

2.2. Research Objectives

The main objective of this research is to understand how different characteristics of the microbial community such as diversity, functional redundancy, size, composition, and relative abundance of microorganisms relate to MD remediation performance and use this information to improve SR-PRZ design. This general objective was broken down into the following specific objectives:

- Determine if the type of microbial inoculum has an impact on the bioremediation of MD in continuous-flow and batch systems and identify differences in microbial composition and relative abundance of microorganisms in good- and poor-performing inocula

- Characterize the microbial communities that originated from a lignocellulose-based and an ethanol-fed pilot-scale SR-PRZ using quantitative and qualitative biomolecular techniques.
- Design and/or optimize probes targeting functional genes for cellulose degradation, fermentation, sulfate reduction, and methanogenesis.
- Apply a functional gene-based approach to study the microbial community in columns simulating SR-PRZs implementing different bioaugmentation or biostimulation strategies.

2.3. Dissertation Overview

This research started by tackling the question of whether the type of inoculum played a role in performance in continuous-flow and batch setups (Chapters 3 & 4). Systems that received different inocula performed differently and 16S rRNA gene-based analysis of the microbial communities also indicated differences in community structure and relative abundance of specific groups of sulfate-reducing bacteria (SRB) in the different systems.

These studies revealed that cellulose-degrading bacteria, fermenters, and SRB were present in the communities of the systems with good performance and that SRB were a small fraction of the microbial community. In addition, these studies brought to light the great phylogenetic diversity of the SR-PRZ microbial community.

The influence of a complex (lignocellulose) versus a simple (ethanol) organic substrate on the microbial community was investigated in pilot-scale SR-PRZs (Chapter 5). Biomolecular analysis targeting the 16S rRNA gene indicated important differences in terms of community composition and size. The ethanol-fed bioreactors contained less bacteria and were highly dominated by SRB. On the other hand, the lignocellulose-based

reactors contained a larger and more diverse community. This study also implemented methods targeting the adenosine 5'-phosphosulfate reductase (*apsA*) gene, a functional gene of microorganisms involved in the sulfur cycle. This gene provided better resolution of the sulfate-reducing microorganisms.

The initial suite of studies provided basic insight into the microbial community of SR-PRZs and their role in performance. The high microbial diversity in these systems might be a positive attribute for good performance but poses a challenge for the 16S rRNA gene-based analyses. Cellulose degraders, fermenters, and SRB span broad phylogenetic groups, thus a 16S rRNA gene-based approach would require hundreds of probes to target all the microorganisms of interest. In addition, the low proportion of SRB in the microbial community makes their detection particularly challenging. Therefore, a functional gene-based approach appears to be superior for the study of the complex SR-PRZ community. It can also be used to examine other functions of interest such as methanogenesis. In Chapter 6, the selection of appropriate functional genes for cellulose degradation, fermentation, sulfate reduction, and methanogenesis is discussed and PCR primers targeting these genes are designed and applied to characterize the microbial community in two pilot-scale SR-PRZs.

Chapter 7 describes the application of the functional gene-based approach to characterize the microbial community of six different types of lignocellulose-based laboratory columns during startup and steady state. This approach proved to be a very useful way to ‘zoom in’ into the different microbial groups of interest and to monitor them during column operation.

Finally, general conclusions and opportunities for future research are presented in Chapter 8.

Chapter 3 The Effect of Inoculum on the Performance of Sulfate-Reducing Columns Treating Heavy Metal Contaminated Water

Pruden, A., Messner, N.L., Pereyra, L.P., Hiibel, S.R., Hanson, R.E., and K.F. Reardon. (2007). *Water Research*. 41 (4): 904-914

Approximate contributions of each author are as follows:

N.L. Messner performed 70% of the data collection and 20% of the manuscript preparation.

L.P. Pereyra performed 20% of the data collection, 30% of the statistical analysis, and 40% of the manuscript preparation.

S.R. Hiibel performed 70% of the statistical analysis and 40% of the manuscript preparation.

R.E. Hanson performed 10% of the data collection.

A. Pruden and K.F. Reardon assisted with experimental design and manuscript preparation.

3.1. Abstract

Sulfate-reducing permeable reactive zones (SR-PRZs) are a passive means of immobilizing metals and neutralizing the pH of mine drainage through microbially mediated reactions. In this bench-scale study, the influence of inoculum on the performance of columns simulating SR-PRZs was investigated using chemical and biomolecular analyses. Columns inoculated from two sources (bovine dairy manure (DM) and a previous sulfate-reducing column (SRC)) and uninoculated columns (U) were fed a simulated mine drainage and compared on the basis of pH neutralization and removal of cadmium, zinc, iron, and sulfate. Cadmium, zinc, and sulfate removal was significantly higher in SRC columns than in the DM and U columns, while there was no significant difference between the DM and U columns. Denaturing gradient gel electrophoresis (DGGE) analysis revealed differences in the microbial community

composition among columns with different inocula, and indicated that the microbial community in the SRC columns was the first to reach a pseudo-steady state. In the SRC columns, a higher proportion of the DGGE band DNA sequences were related to microorganisms that carry out cellulose degradation, the rate limiting step in SR-PRZ energy flow, than was the case in the other columns. The proportion of sulfate-reducing bacteria of the genus *Desulfobacterium* was monitored using real-time quantitative PCR and was observed to be consistently higher in the SRC columns. The results of this study suggest that the inoculum plays an important role in SR-PRZ performance. This is the first report providing a detailed analysis of the effect of different microbial inocula on the remediation of acid mine drainage.

3.2. Introduction

The waters emanating from mine sites are typically characterized by low pH, high sulfate concentrations, and the presence of toxic heavy metals. Although some mine drainage issues are associated with large urban areas, many sites are located in remote areas and are subject to extreme weather conditions, which makes remediation challenging. This is particularly true in the case of abandoned mine land (AML) sites and affected streams. Researchers have estimated that there are over 200,000 AML sites and 5000 to 10,000 miles of impacted streams scattered throughout the US (EPA, 1997).

There are two general approaches for remediating mining influenced waters: active or passive. Active treatments (chemical treatment) require continuous inputs of resources to sustain the process, whereas passive treatments (biological treatment or anoxic limestone drains) require minimal inputs of resources once in operation (Johnson and Hallberg, 2005). Passive methods are preferred due to their low cost, low required

maintenance, and because they produce minimal hazardous waste requiring disposal. In particular, sulfate-reducing permeable reactive zones (SR-PRZs), such as wetlands and subsurface reactive zones, are an attractive passive means of treating mine drainage. SR-PRZs contain solid organic substrates that support the growth of anaerobic microbial communities, including sulfate-reducing bacteria (SRB), which reduce sulfate in the mine drainage to sulfide. The sulfide in turn reacts with the heavy metals and immobilizes them within the zone as solid precipitates. SR-PRZs are typically inoculated with microbial communities from animal manure.

While there are many desirable aspects of SR-PRZs, there is little guidance available regarding their design. For this reason, it is not known why some have been observed to be subject to short lifetimes, low performance, and/or long startup times while others function well for several years (Benner et al., 1999, 2002; Blowes et al., 2000; Waybrant et al., 2002). Previous studies have attempted to address the issue of poor performance by focusing on the organic substrates used, and have evaluated straw (Bechard et al., 1994), sawdust (Wakao et al., 1979), peat (Eger and Lapakko, 1988), spent mushroom compost (Dvorak et al., 1992), whey (Christensen et al., 1996), and oak chips (Chang et al., 2000). However, no clear solution has been provided.

Although SR-PRZs are biologically catalyzed treatment systems, their microbial communities have not been well characterized. A few recent studies have investigated the kinds of microorganisms present in these systems using a combination of culture-based and molecular biological techniques (Benner et al., 2000; Hallberg and Johnson, 2005a; Johnson and Hallberg, 2003; Pereyra et al., 2005; Pruden et al., 2006). The results of these studies correlate well with the results of parallel research focusing on the carbon

flow dynamics in these systems (Logan et al., 2005), and generally emphasize the complexity of the microbial communities responsible for remediation. Although SRB catalyze the final reaction of the SR-PRZ, they rely on the activity of anaerobic cellulolytic bacteria and fermentative bacteria to break down complex organic materials, such as cellulose from wood chips, to provide them with carbon and energy sources. Therefore, efforts to improve microbiological design criteria for SR-PRZs must consider the entire microbial community and not merely SRB.

The purpose of this study was to investigate the effect of inoculum on the performance of sulfate-reducing columns (SRC) simulating SR-PRZs. To gain a deeper understanding, denaturing gradient gel electrophoresis (DGGE) and real-time quantitative polymerase chain reaction (Q-PCR) were used to investigate the microbial community dynamics of the columns during startup and pseudo-steady-state operation. The results of this research provide insights for inoculum selection and may help improve the reliability of SR-PRZ performance in the field.

3.3. Materials and Methods

3.3.1. Column Specifications and Packing

Six acrylic columns, 5 cm ID_15cm height, with six 34-in vertical sampling ports, were supported vertically with upward flow at an average rate of 40 mL/d. Each column was packed under a nitrogen atmosphere with 100 g dry weight of a homogenized mixture consisting of 22% beech wood chips, 2% crushed alfalfa, 11% pine shavings, 45% silica sand, 5% limestone, and 15% inoculum by weight. This mixture is typical of SR-PRZs and includes slow-release carbon and nitrogen sources (woody material and alfalfa), a

source of alkalinity (limestone), and an inert material for porosity enhancement (sand) (Waybrant et al., 1998, 2002). The bottom layer (1.9 cm) of all columns was packed with a 90/10wt% mixture of silica sand/crushed pyrite to scavenge oxygen, as described by Waybrant et al. (2002). The top layer (0.6 cm) of all columns was packed with silica sand, separated from the organic layer by a stainless steel mesh to prevent organic material loss. All columns were covered in aluminum foil to inhibit photolithotrophic bacterial growth (Waybrant et al., 2002).

3.3.2. Inocula

Two inocula were compared in this study: (1) fresh bovine dairy manure (DM) collected from a dairy near Fort Collins, CO, and (2) contents from a previous column containing a sulfate-reducing community (SRC) (Logan et al., 2005). Two columns of each type (DM1, DM2, SRC1, SRC2) were prepared and compared to two uninoculated columns (U1, U2).

3.3.3. Influent Composition

Columns were fed simulated mine drainage water from a common feed bottle. Due to problems with precipitation of iron in the influent bottle, the composition of the influent was variable during the initial 10 d of startup. During this time, the influent pH was adjusted from 6.0 to 5.6 and the influent Fe(II)SO₄ concentration was lowered from 0.49 to 0.034 g/L to reduce the extent of iron precipitation. The final influent composition was 1.32 g/L Na₂SO₄, 0.03 g/L NH₄Cl, 0.05 g/L ZnSO₄, 0.03 g/L Fe(II)SO₄, and 0.01 g/L CdCl₂ at a target pH of 5.6 (adjusted with HCl and NaOH as needed). Before adding the metals, the deionized water for the influent was bubbled with nitrogen for 2 d to remove

dissolved oxygen. The final influent solution was continuously bubbled with a slow stream of nitrogen (10 mL/min) to replace the headspace as the influent was pumped to the six columns. No precipitate was noted in the influent bottle for the remainder of the experiment.

3.3.4. Column and Effluent Sampling

Effluent was collected from the top of each column in 250-mL flasks initially containing 25mL of deionized water in which the column effluent tube was submerged to prevent entry of oxygen into the column. This initial volume was considered in the calculation of sulfate and metal concentrations. Column material (approx. 0.5 g) was removed weekly from the middle sampling port of the DM and SRC columns for the first 6 weeks to monitor microbial community development. The uninoculated columns were sampled only at Week 6. Columns were disconnected from the flow system and manipulated under a nitrogen atmosphere during sampling.

3.3.5. Analytical Methods

Sulfate was quantified using the turbidimetric SulfaVers 4 method (Hach Co., Loveland, CO) with an Odyssey DR/2500 spectrophotometer (Hach Co.). After collection, aqueous samples were immediately filtered through 0.2-mm syringe tip filters and diluted with deionized water to achieve a concentration within the detection range of 2–70 mg/L. In order to verify that characteristics of the samples did not interfere with the turbidimetric method, samples were spiked with standard sulfate solutions. Based on these tests, no matrix effects were found.

Metals were analyzed by inductively coupled plasma absorbance emission spectroscopy (ICP-AES) (Thermo Jarrell Ash IRIS Advantage). Aqueous samples were filtered through 0.2-mm syringe-tip filters, diluted with deionized water, and acidified with trace metals-grade nitric acid (Mallinckrodt, Hazelwood, MO). The acidified solution was then boiled down to one-tenth of the initial volume and diluted to 50mL with deionized water for direct analysis by ICP-AES. Detection limits were 0.01 mg/L for iron and zinc, and 0.005 mg/L for cadmium. In every independent set of measurements, a deionized water blank was also measured. The calibration of the ICP-AES instrument was checked every 10 runs.

To determine the distribution of metals in the solid substrate of the columns at the end of operation, the column contents were divided approximately in thirds by volume into top, middle, and bottom sections. The material of these sections was well mixed and subsequently digested in a CEM microwave digester (MS-2000, Mathews, NC) per EPA Method SW-3015. The digested material was analyzed by ICP-AES as described above.

3.3.6. DNA Extraction

DNA extractions were carried out using the FastDNAs Spin Kit for Soil (Q-BIOGene, Irvine, CA) according to the manufacturer's protocol using approximately 0.5 g of homogenized column material (the exact amount was recorded for quantification). Concentrations of DNA were determined spectrophotometrically (Hewlett Packard 8452A diode array spectrophotometer, Houston, TX) by measuring the absorbance at 260 nm. All DNA extracts were diluted 1:3 with sterile deionized water in preparation for polymerase chain reaction (PCR).

3.3.7. PCR Amplification of 16S rDNA

A nested PCR approach was used to amplify the variable V3 region of the 16S rDNA molecule using primers 8F and 1492R (Weisburg et al., 1991) followed by I341F and I533R (Watanabe et al., 2001). The reaction (total volume 25 mL) included 12.9 mL purified water, 2.5 mL 10X Taq Reaction Buffer, 5.0 mL TaqMaster PCR Enhancer (Eppendorf, Hamburg, Germany), 5 pM of each dNTP, 0.25pM of each primer, 0.25 mL formamide, 1.75U Taq DNA polymerase (Eppendorf), and 1 mL DNA template. The temperature conditions for PCR were those described by Weisburg et al. (1991) for 8F and 1492R primers and by Watanabe et al. (2001) for I341F and I533R primers.

3.3.8. Denaturing Gradient Gel Electrophoresis (DGGE)

Gels (8% acrylamide/bisacrylamide 19:1, BioRad) were cast using a denaturing gradient of 20–55%, with 100% denaturant defined as 7M urea and 20% v/v formamide. A standard prepared with a mixture of DNA from pure cultures was loaded in all gels to verify the gradient. Gels were exposed to at 45V for 20h at 57.5 1C and stained with SybrGold nucleic acid stain (Molecular Probes, Inc., Eugene, OR). Gels were documented using a UVP BioChem gel documentation system and images were analyzed using Labworks software (UVP, Upland, CA). This software was used to identify the bands in the gels and to obtain the intensity profiles for each of the lanes. The intensity profiles were used to assess the degree of similarity between replicates at different times. The relative diversity was calculated using the Shannon diversity index (Equation 3.1)

$$H = -\sum \left[\frac{n_i}{N} \log \left(\frac{n_i}{N} \right) \right] \quad \text{Eq. 3.1}$$

where n_i is the intensity of the individual bands and N is the sum of the intensity of all the bands (Cox, 1972; Xia et al., 2005). Representative visible DGGE bands (33 total) were excised with sterile razor blades and stored in 2-mL tubes with 36 mL of sterile water.

3.3.9. DNA Sequence Analysis

DNA present in the DGGE bands was PCR amplified and purified for sequencing using the GeneClean Spin Kit (Q-BIOGene). Sequencing of the 200 bp product was performed by Davis Sequencing (Davis, CA). The closest matches to known microorganisms available in the National Center for Biotechnology Information database were determined using the BLAST alignment tool (<http://www.ncbi.nlm.nih.gov/BLAST/>). A literature survey was conducted to characterize the properties of the closest matches with respect to substrate utilization and sulfate reduction.

3.9.10. Cloning

Eighteen of the 33 cut DGGE bands resulted in mixed sequences. To separate these, the excised bands were PCR amplified using primers I341F and I533R as described above, purified using the GeneClean Spin Kit (Q-BIOGene), and cloned into Escherichia coli using the TOPO TA Cloning Kit for Sequencing (Invitrogen, Carlsbad, CA) according to the manufacturers' protocols. Inserts were PCR amplified directly from colonies using M13F and M13R primers. At least three clones per band were analyzed. PCR products were purified using the GeneClean Spin Kit (Q-BIOGene) and sequenced by Davis Sequencing (Davis, CA).

3.9.11. Real Time Q-PCR

Q-PCR targeting the 16S rDNA of total bacteria and the SRB genus *Desulfobacterium* (DSB), which has commonly been identified in mine drainage systems (Hallberg and Johnson, 2005b; Morales et al., 2005), was performed using a Cepheid SmartCycler (Sunnyvale, CA). Primers were designed for the DSB subgroup in the δ -proteobacteria subdivision using FastPCR software (Kalendar, 2005). The sequences of the DSB primers were 5'-AGT ARA GTG GCG YAC GGG TGA G for the forward primer (HDBM52f) and 5'-WTC AYY CAC GCG GCG TYG CTG C for the reverse primer (HDBM372r), yielding a product of approximately 320 bp. The specificity of the primers was verified both by a BLAST search and by shotgun cloning and sequencing of amplified products. Qiagen SybrGreen MasterMix (Valencia, CA) was used to adapt the primers to Q-PCR. The template used for calibration was purified 16S rDNA PCR product obtained from *Desulfobacterium autotrophicum* ATCC43914D (American Type Culture Collection, Rockville, MD). Calibration curves were constructed using six points with four replicates for each point. In every Q-PCR run, three standards were included. The Ct values of these standards were compared to the corresponding values in the calibration curve, and if the difference was more than 75%, the data from that run were discarded. The limit of quantification of the DSB assay was 917 copies per reaction. For total bacteria, the conditions described by Suzuki et al. (2000) were used, including universal 16S rDNA primers and probe. A six-point calibration curve was generated using amplified 16S rDNA from a sample collected from a sulfate-reducing bioreactor as the template, with four replicates in two independent runs for each point. For both assays,

a dilution series was performed on all samples and analyzed by Q-PCR to identify the linear range unaffected by inhibitors. A dilution of 1:20 was sufficient for most samples.

3.9.12. Statistical and Mathematical Analyses

Mixed linear regressions were fit to all data sets using the PROC MIXED function of SAS 9.1 (SAS Institute Inc., Cary, NC). Log transformation of all data sets was required to achieve homoscedasticity, and all comparisons were made in log scale. Degrees-of-freedom calculations were performed using the Kenward–Roger method with repeated time measurements. Significance was defined by a Type III p-value p0.05. Dixon's Extreme Value test was used to test for statistical outliers.

Column pore volume was estimated using the ratio of pore volume to empty column volume based on Logan et al. (2005) as similar column materials and packing techniques were utilized in the present study. The pore volume was found to be 166cm³ with a residence time of 4 d at an average flow rate of 40 mL/d.

For cumulative sulfate and metal removal analyses, cubic splines were fit to the effluent concentrations and flow rate data and then interpolated for direct comparison with the discrete influent data. Splines and interpolation were performed with the 'cspline' and 'interp' functions of MathCAD 12 (Mathsoft Engineering & Education, Inc., Cambridge, MA).

3.4. Results

3.4.1. Qualitative Observations

Between the first and seventh weeks of operation, the color of the column material changed only slightly (from dark to light green) in the columns inoculated with DM (DM1, DM2), and there was some darkening (from light brown to gray) in the uninoculated columns (U1, U2). By contrast, the columns inoculated with preacclimated column substrate (SRC1, SRC2) changed markedly from light brown to black. Hydrogen sulfide odor was also detectable in the effluents of the SRC columns after 2 wk, whereas this odor was not apparent in the effluents of the other two sets of columns.

3.4.2. Cumulative Sulfate Removal

Cumulative sulfate removal (**Error! Reference source not found.**) was negligible in the DM and U columns until Day 30, while sulfate was removed at low rates in the SRC columns during this period. After this time, an increase in the rate of removal was observed in all columns, with the highest sustained rates occurring in the SRC columns. The DM and U columns maintained the higher removal rate for approximately 60 d, while the SRC columns maintained the rate for an additional 30 d (through Day 120). Significantly greater cumulative sulfate removal was observed in the SRC columns than in the DM ($p = 0.004$) and U columns ($p < 0.001$), and no statistical difference was determined between the DM and U columns ($p = 0.2731$).

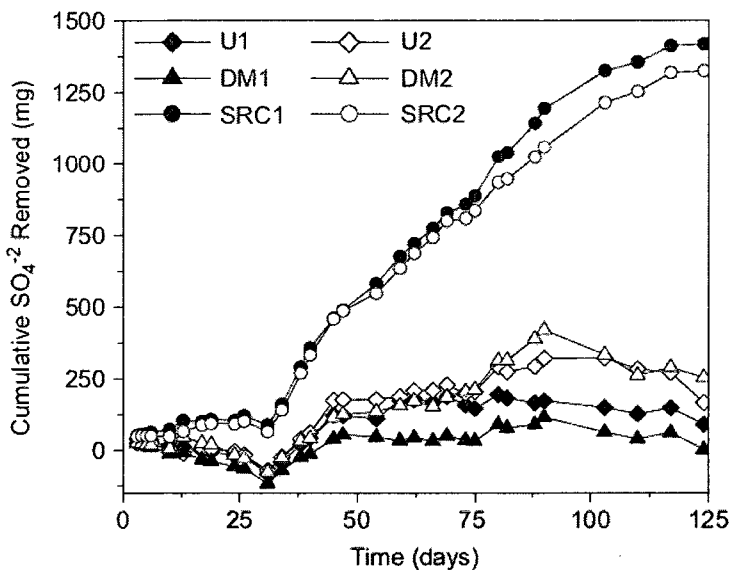


Figure 3. 1: Cumulative sulfate removal in duplicate SR-PRZ columns that were uninoculated (U) or inoculated with an acclimated culture (SRC) or with bovine dairy manure (DM). Cubic splines were fit to the effluent sulfate concentrations and flow rate data and then interpolated for direct comparison with the discrete influent data using a residence time of 4d. The negative cumulative removal values for the DM and U columns during the first 30d can be attributed to variable influent concentrations at the beginning of the experiment and to the propagation of error associated with the mathematical treatment of the minimal sulfate removal during this time.

3.4.3. pH

The effluent pH varied significantly with startup, followed by a gradual increase in all columns throughout the experiment. Between 40 and 125 d of operation, the pH of the SRC column effluent was consistently higher than that of the DM or U columns and fluctuated near pH 8 after Day 60. However, due to the fluctuation of the influent pH, no statistically valid distinction could be made among the columns. Because the influent was not buffered, a consistent pH in the influent was not attained (pH range 4–8, with an average and standard deviation of 5.61 ± 1.06). However, the buffering capacity was increased by the column contents, yielding a relatively stable effluent pH.

3.4.4. Cumulative Metal Removal

Calculated cumulative mass removals (**Error! Reference source not found.**) revealed that the total mass of cadmium and zinc removed by the SRC columns was greater than that removed by the DM ($p < 0.001$ for both metals) and U columns ($p < 0.0001$ for both metals). No statistical difference in cumulative cadmium removal was observed between the U and DM columns ($p = 0.552$), and cumulative zinc removal in the DM columns was statistically greater than the removal in the U columns ($p = 0.002$). For the duration of the experiment, the rate of removal for both cadmium and zinc was greater in the SRC columns than in the DM and U columns. In the case of iron (data not shown), cumulative removal in the SRC and U columns was significantly higher than in the DM columns ($p < 0.001$ for both column sets) but no significant differences in removal were observed between SRC and U columns ($p = 0.972$).

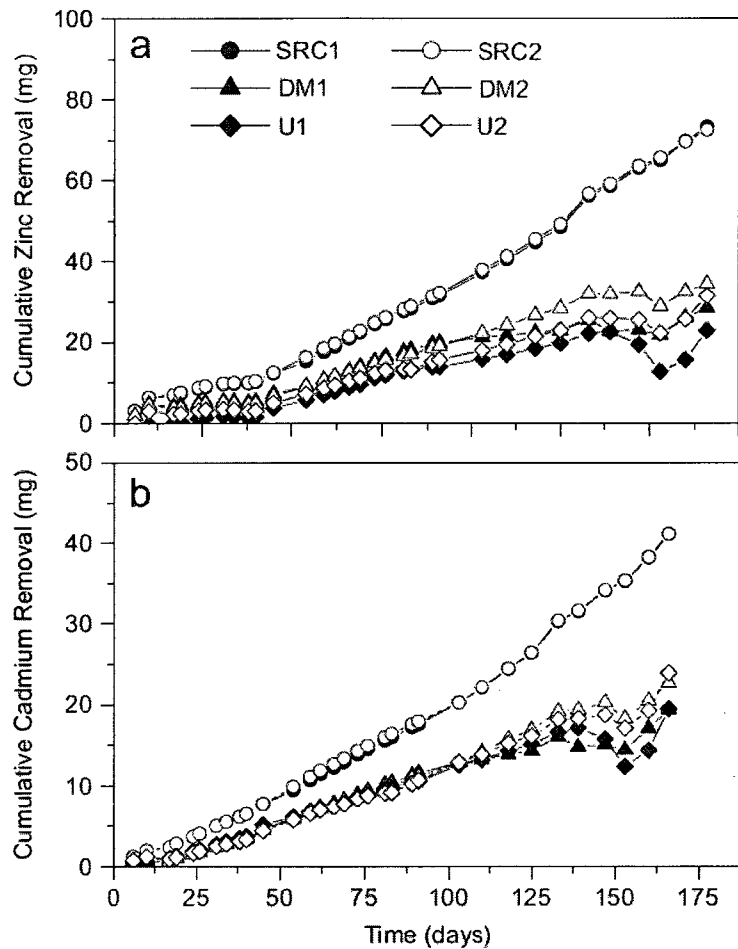


Figure 3.2: Cumulative zinc (a) and cadmium (b) removal in the uninoculated columns (U) and columns inoculated with an acclimated inoculum (SRC) or with bovine dairy manure. Cubic splines were fit to effluent metal concentrations and flow rate data and then interpolated for direct comparison with the discrete influent data using a residence time of 4d.

3.4.5. Distribution of Metals within the Columns

In the solids of the DM1 and U2 columns, the cadmium and zinc concentrations did not differ between the top, middle, and bottom ($p > 0.1$) (Error! Reference source not found.).

In the DM2 columns, the concentrations of these metals were slightly lower in the bottom (inlet) portion. In the SRC columns, concentrations of cadmium and zinc were lower in the upper section than in the middle and bottom. However, in the SRC1 column, most of

the cadmium and zinc was near the inlet, whereas these metals were equally concentrated in the bottom and middle of the SRC2 column.

Iron concentrations were highest in the inlet section of the DM and U columns (data not shown). In the SRC columns, however, the iron concentrations were more equally distributed among the three portions of the columns, with the highest concentration in the middle (SRC2) or in the bottom (SRC1).

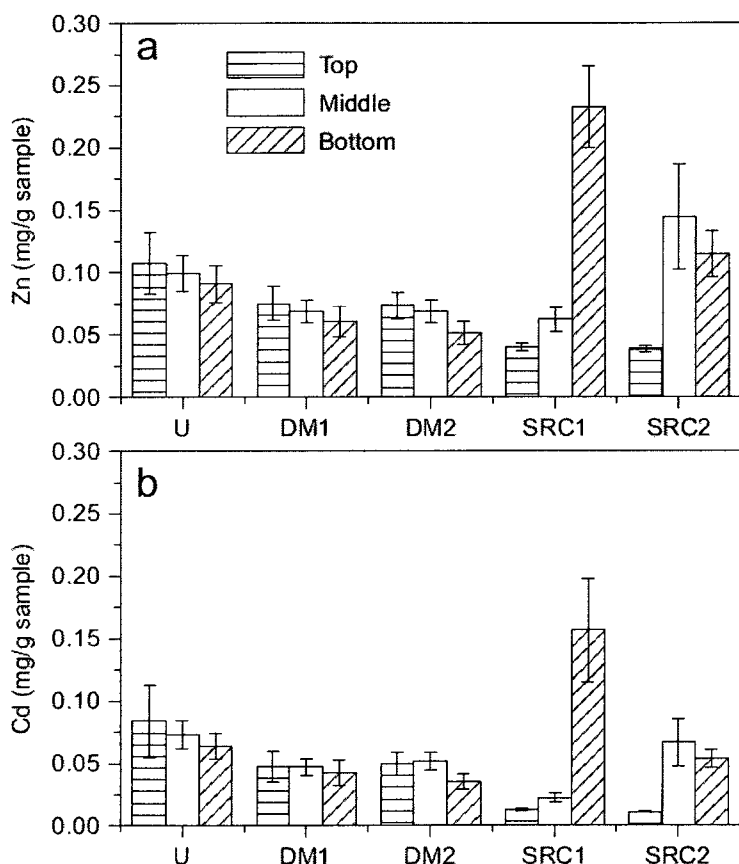


Figure 3. 3: Distribution of (a) cadmium and (b) zinc in the columns determined by ICP-AES analysis of digested column material collected from the top, middle, and bottom sections of each column after 170d of operation. The influent entered the columns from the bottom. Results for only one uninoculated column are shown because the second was used for tracer test. Error bars represent standard deviation of the means of five replicates.

3.4.6. DGGE of Columns Microbial Communities

Using the criterion that a microbial community reached a pseudo-steady state when no new DGGE bands were detected and no existing bands disappeared, the microorganisms in the SRC columns formed a stable community (after Week 2) before the other columns (**Error! Reference source not found.a**). By contrast, the DM columns still had new detectable bands at Week 4, while three bands faded gradually after this time in the DM1 column (**Error! Reference source not found.b**). More bands were observed in the DGGE gels for SRC columns than in the gels for DM or U columns. However, the Shannon diversity indices for the SRC and DM columns were not significantly different ($p = 0.136$). Diversity indices for the two SRC columns were highly similar and ranged from a value of $H = 1$ at the beginning of the experiment to $H = 1.37$ at Week 6. Diversity indices for column DM2 were consistently lower than those for column DM1 until Week 6, at which time the index values for both columns converged. Diversity index for column DM2 increased from an initial value of $H = 0.5$ to a value of $H = 1.12$ at Week 6. The initial average diversity index in column DM1 was $H = 1.26$. This index decreased to an average value of $H = 1.08$ by Week 1 and remained constant at all other sampling points. **Error! Reference source not found.** summarizes the results obtained by sequencing DGGE bands. Of the 30 unique bands of the SRC columns, 15 were sequenced, while eight of 27 unique bands were sequenced from the DM columns. Several cellulose-degrading bacteria belonging to the *Eubacterium*, *Clostridium*, and *Bacteroides* genera were found in the SRC columns. Fermentative bacteria in SRC columns were related to the classes Enterobacteria, Clostridia, and Bacteroidetes. In DM columns, the majority of the fermenters and the one cellulose degrader identified were

related to members of the genus *Clostridium*. An SRB was identified in the SRC columns, and an SRB was also detected in one of the U columns (data not shown). No SRB were detected in the eight sequenced DGGE bands from the DM columns.

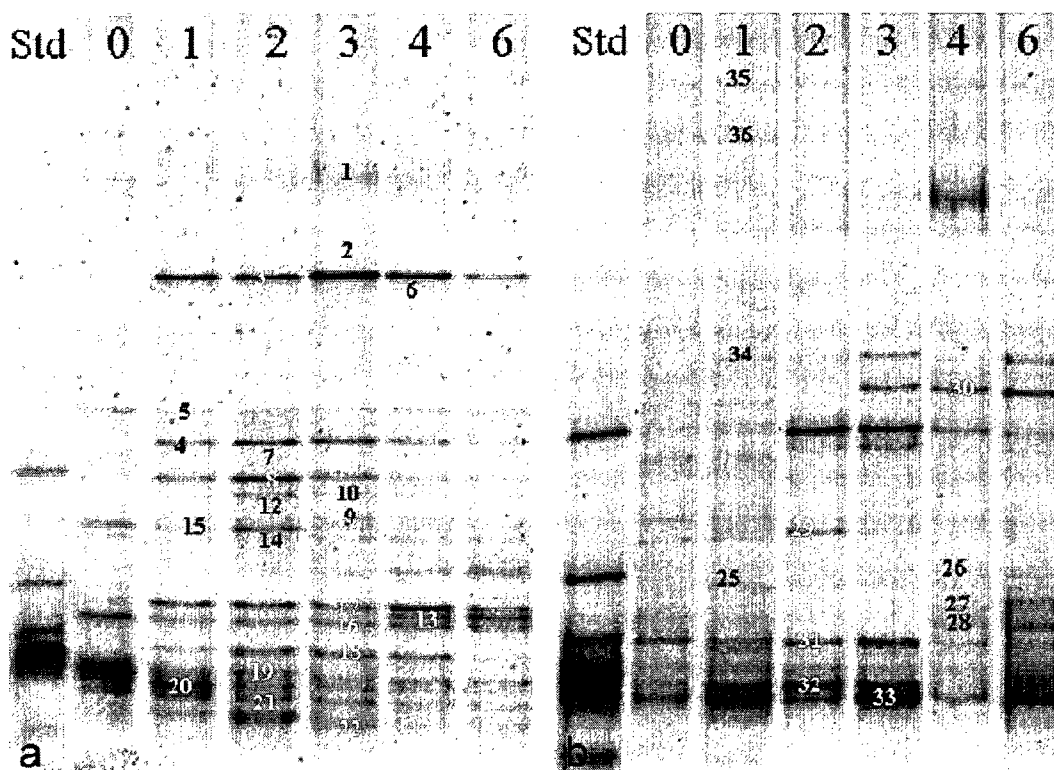


Figure 3.4: DGGE gel image of nested I341F and I533R PCR products of DNA extracted from (a) column SRC1 and (b) columns DM1 during the first 6 wk. Lane numbers correspond to the sampling week. 'std' is the positive control. Twenty-three of the labeled bands were sequenced and their identities are indicated in Table 3.1.

Table 3. 1: Characterization of microorganisms represented by DGGE bands. Band numbers correspond to numbering on Figure 3.4. A: cellulose degradation; B: fermentation of polysaccharides; C: fermentation of monosaccharides (and/or disaccharides); D: sulfate reduction. Where more than one sequence had the same similarity with the DGGE sequence, all the results corresponding to the highest match are presented. When the DGGE band sequence corresponded to an uncultured bacterium the function of the microorganisms was assigned based on the functions of the closest known relative.

Band ⁺	Highest Match (GenBank accession number)	% Match	A*	B*	C*	D*	Ref.
SRC							
1	<i>Clostridium indolis</i> strain DSM 755 (Y18184) <i>Clostridium celerecrescens</i> strain EIB 5 (AY458859)	99% 99%	- +	+- -	+- +	- -	(Dworkin, 2000; Holt, 1984; Leschine, 1995; Palop et al., 1989)
2	Uncultured bacterium BTCE-T2 IF 16S ribosomal RNA gene (AY217446)	96%					
3	<i>Clostridium fmetarum</i> (AF126687)	99%	-	-	+	-	(Kotsyurbenko et al., 1995)
4	<i>Eubacterium cellulodosolvens</i> strain Ce2 (AY178842)	100%	+	+	+	-	(Bryant et al., 1958)
6	<i>Bacteroides</i> sp. 253c (AY082449)	94%	+	+	+	-	(Dworkin, 2000)
7	<i>Desulfovibrio vulgaris</i> strain 15 (AY362360)	96%	-	-	-	+	
8	<i>Clostridium longisporum</i> strain DSM 8431	98%	+	+	+	-	(Varel, 1989)
10	Uncultured bacterium clone BCf5-21 (AB062828) that was 92% similar to an uncultured <i>Clostridiaceae</i> bacterium (AB089033)	91%					
12	<i>Klebsiella pneumoniae</i> (AY369139)	92%	-	-	+	-	(Dworkin, 2000)
13	Uncultured isopod gut bacterium clone RKP8AM (AF395327) that was 93.6% similar to an unidentified <i>Bacteroides</i> spp. (AF150715)	88%	+	+	+	-	
14	Uncultured <i>Clostridiaceae</i> bacterium clone: RS-Q69 (AB089029)	96%			+		(Dworkin, 2000)
16	<i>Clostridium longisporum</i> strain DSM 8431 (X76164)	99%	+	+	+	-	(Varel, 1989)
20	<i>Escherichia vulneris</i> (AF530476)	87%	-	-	+	-	(Brenner et al., 1982)
21	<i>Clostridium longisporum</i> strain DSM 8431 (X76164)	99%	+	+	+	-	(Varel, 1989)
22	<i>Escherichia senegalensis</i> (AY217654)	93%	-	-	+	-	(Dworkin, 2000)
DM							
25	Uncultured bacterium RSa32 (AJ289204). Related to <i>Clostridium polysaccharolyticum</i> (X77839)	99%	+	+	+	-	(Holt, 1984; Vangylswyk, 1980)
26	Uncultured bacterium clone HuCB56 (AJ409006) that was 94% similar to <i>Eubacterium xylanophilum</i> (L34628).	99%	-	+	+	-	(Vangylswyk and Vandertoorn, 1985)
27	<i>Clostridiaceae</i> bacterium 80Kb (AB084627) that was 91.5% Similar to <i>Clostridium leptum</i> (AF262239)	95%	-	-	+	-	(Holt, 1984; Moore et al., 1976)
28	<i>Sporomusa malonica</i> strain DSM 5090 (AJ279799)	81%	-	-	+	-	(Dehning et al., 1989)
29	<i>Clostridium indolis</i> strain DSM 755 (Y18184)	95%	-	+	+	-	(Dworkin, 2000; Holt, 1984)
32	Uncultured bacterium clone Thompsons76 (AY854354)	88%					
34	<i>Clostridium butyricum</i> strain EIB 3-4 (AY458857)	94%	-	+	+	-	(Dworkin, 2000; Holt, 1984)
35	<i>Clostridium lituseburense</i> strain EIB 6 (AY458860)	82%	-	-	+	-	(Holt, 1984)

3.4.7. Q-PCR

Although the total bacterial population in the DM columns was initially larger than that in the SRC columns, it rapidly decreased during the first 3 wk and was similar to the SRC columns for the remainder of the experiment (data not shown). At Week 6, the final sampling point, the bacterial populations of DM and SRC columns were not significantly different in size from those of the U columns.

Overall, the DSB populations in the SRC columns were significantly larger than in the DM columns ($p = 0.027$) (**Error! Reference source not found.a**). The number of DSB 16S rRNA gene copies increased in the SRC columns at Week 2 while it decreased in the DM columns. At Week 6, the DSB populations in the U columns were significantly smaller than those in the SRC ($p = 0.021$) and the DM ($p = 0.010$) columns.

The DSB population also constituted a much larger fraction of the bacterial community in the SRC columns than in the DM and U columns (**Error! Reference source not found.b**). At the beginning of the experiment, the ratio of DSB to total bacteria was smaller in the DM columns ($p = 0.022$). By Week 2, this ratio had increased in the SRC columns while it did not change in the DM columns. The ratios of DSB to bacteria in the SRC and DM columns were significantly different ($p < 0.001$). The higher ratios for the SRC columns are in agreement with the superior metal and sulfate removal observed for these columns.

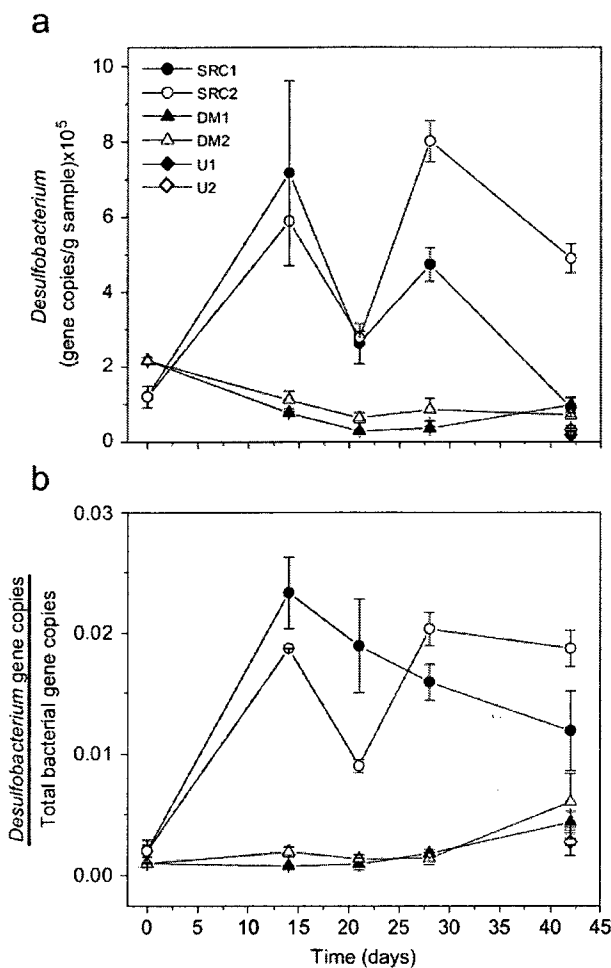


Figure 3.5: Quantification of *Desulfobacterium* with time by Q-PCR for SRC, DM, and U columns (a) normalized to mass of sample used for DNA extraction and (b) normalized to total bacteria. Error bars represent standard deviation of the means of two to six replicates.

3.5. Discussion

3.5.1. Effect of Inoculum on Column Performance

Metal removal, pH neutralization, and sulfate removal can be used as indicators of column performance. This work indicates that the microbial inoculum significantly affects the performance of columns remediating acid mine drainage (AMD). The rates of removal of sulfate and metals in the SRC columns were superior to those in the DM and U columns (except in the case of iron, which was removed by both the SRC and U

columns better than by the DM columns). Interestingly, the columns inoculated with DM, a common source of inoculum (Castro et al., 1999; Christensen et al., 1996), did not perform better than the uninoculated columns. This suggests that the ‘wrong’ inoculum may not provide an advantage over no inoculum at all.

In addition to remediation performance, the startup time and duration of active remediation (pseudo-steady state) are important parameters in determining the overall column performance. For comparison, startup time was taken as the point when sulfate or metal removal was observed, independent of removal rate, and pseudo-steady state was considered as the time during which the rate of removal was constant. Cadmium and zinc removal was observed in all columns from the start of the study, indicating an immediate startup to a pseudo-steady state. The pseudo-steady state was maintained throughout the experiment in the SRC columns, while the DM and U columns displayed a decline in removal rate after Days 125 and 133 for zinc and cadmium, respectively, indicating the end of the pseudo-steady state period. The startup was also immediate in terms of sulfate removal in the SRC columns, but required more than 4wk for the DM and U columns. Pseudo-steady state did not begin until Day 30 for all columns. The active remediation lasted for 90 d (through Day 120) in the SRC columns at a significantly higher removal rate than the DM and U columns, which remained in pseudo-steady state for only 60 d (through Day 90). These results suggest that the type of inoculum does not affect the startup time for metal removal (which may have been achieved partly by sorption in the first several days); however, inoculation with a preacclimated culture resulted in a shorter startup time for sulfate removal and maintenance of remediation capabilities for a longer period than the use of DM or no inoculum. A longer experiment would be required to

fully simulate operation times in the field, which vary from 2 to 20 years (Benner et al., 1999, 2002; Blowes et al., 2000; Waybrant et al., 2002).

These findings agree with results of other studies that show an effect of microbial inoculum on system performance. Moreno et al. (2005a) found that inoculating a submerged filter for biological denitrification with a pure culture of denitrifying bacteria increased system stability and performance indicators compared to inoculation with a mixed culture from a wastewater treatment plant's activated sludge. In the same system, Moreno et al. (2005b) also showed that the choice of microbial inoculum can also influence startup time. Pereira et al. (2001) verified that the degradation of oleic acid in anaerobic filters was improved by inoculating the system with acclimated biomass compared to nonacclimated biomass.

3.5.2. Spatial Distribution of Metal Removal

Analysis of cadmium, zinc, and iron in the column material revealed spatial heterogeneity in the SRC columns (Figure 3.3). In particular, zinc and cadmium concentrations in the bottom and middle portions of the SRC columns may have been higher because the higher levels of sulfate reduction in the SRC columns precipitated the metals more efficiently near the inlet, preventing them from reaching the upper layers at high concentration.

3.5.3. Microbial Community Composition and Dynamics

Microbial community profiling by DGGE provided data to determine the time required to reach a pseudo-stable microbial community, to identify microorganisms, and to compare the relative diversity. Based on DGGE, the microbial communities in the SRC columns

achieved a stable composition sooner than the populations in the DM and U columns. This correlates well with the performance data, and is a promising suggestion that the composition of the microbial inoculum can influence the startup time of a SR-PRZ, an issue that is significant for field operation. In a bench-scale study of AMD treatment using microbial-driven sulfate reduction, Christensen et al. (1996) demonstrated that inoculating the system with SRB shortened the initial lag phase.

The majority of the bands sequenced from the SRC columns corresponded to microorganisms that degrade cellulose and other polysaccharides, such as pectin and starch, and ferment the products of the hydrolysis (e.g., *Clostridium longisporum* and *Eubacterium cellulosolvens*). Sequences related to *Bacteroides* spp. were found only in SRC columns. *Bacteroides* spp. are saccharolytic microorganisms and, as a group, are able to utilize a wide variety of compounds as carbon and energy sources, including cellulose, hemicellulose, starch, and pectin (Dworkin, 2000). The mechanisms of polysaccharide digestion in *Bacteroides* spp. are highly effective (Dworkin, 2000). By contrast, only one of the sequences from the DM columns (DGGE Band 25) was confirmed to be related to a cellulose degrader. In the DM columns, 88% of the sequenced bands corresponded to microorganisms that ferment di- and/or monosaccharides and 57% of these microorganisms were also able to degrade polysaccharides such as starch and pectin. Since the degradation of cellulose has been shown to be the rate-limiting step in the carbon flow dynamics in SR-PRZs of the type tested here (Logan et al., 2005), the presence of *Bacteroides* spp. together with a diverse population of additional polysaccharide fermenters in the SRC columns might have constituted an advantage of these columns over the DM columns.

Although sulfate was removed by the DM columns, no SRB were found in the sequenced DGGE bands. In the SRC columns, the sequence from Band 7 showed 96% similarity to the sulfate reducer *Desulfovibrio vulgaris* strain I5. This band was detected by DGGE in Week 2. Both *Desulfovibrio* spp. and DSB spp., which were quantified by Q-PCR, have been identified as major SRB in AMD treatment systems (Hallberg and Johnson, 2005a; Labrenz and Banfield, 2004). SRB have been observed to represent a relatively low proportion of the microbial community in other sulfate-reducing mine drainage treatment systems (Hallberg and Johnson, 2005b; Johnson and Hallberg, 2003; Morales et al., 2005). This may explain why more SRB were not detected by DGGE and is corroborated by the low proportion of DSB (0.1–2%) detected by Q-PCR in all of the columns. This also supports the hypothesis of the importance of the upstream microorganisms that provide SRB with carbon substrates for growth (cellulose degraders and fermenters). A higher proportion of SRB in the SRC columns together with a variety of microorganisms capable of degrading complex organic materials might have caused the increased metal removal and pH neutralization observed in these columns compared to the DM columns.

Q-PCR analysis also revealed that the DM columns initially contained more total bacteria than the SRC columns. The decrease in total bacteria in DM columns in the following weeks could be an indication that the conditions were not favorable for a large portion of the original microbial community. This is not surprising considering the stark contrast in environmental conditions between the columns and the thermophilic lower intestinal tract of a dairy cow. It is also possible that the nutrient availability at the beginning of the experiment (especially the presence of readily available soluble

organics) caused competition of different microbial groups that ultimately lead to the survival of only those that were better at procuring these nutrients, but not necessarily better at the activities that lead to heavy metal precipitation.

3.6. Conclusions

The results of this study demonstrate that the nature of the inoculum influences the performance of sulfate-reducing systems treating heavy metal contaminated water. An inoculum previously acclimated to sulfate-reducing conditions and complex organic substrates outperformed DM, a typical SR-PRZ inoculum. The application of biomolecular tools provided deeper insights into the composition and overall dynamics of the microbial communities in the columns. The results of this study provide justification and basic information needed to support future efforts in the development of SR-PRZ inocula for improving reliability and performance in the field.

3.7. Acknowledgements

The authors thank EPA STAR Grant number R8395101-0 for funding this project and the Hazardous Substance Research Center at Colorado State University. Financial assistance was also provided by the National Science Foundation Research Experience for Undergraduates program in Water Research at Colorado State University. The authors would like to thank Ruoting Pei, HyunSuk Hong, Carmen Sans, and Santiago Esplugas for their help in performing effluent tests and substrate extractions, and Tom Sale and Dave Gilbert for providing assistance in column design and laboratory space for experiments.

3.8. References

- Bechard, G., Yamazaki, H., Gould, W.D., Bedard, P., 1994. Use of cellulosic substrates for the microbial treatment of acid-mine drainage. *J. Environ. Qual.* 23 (1), 111–116.
- Benner, S.G., Blowes, D.W., Gould, W.D., Herbert, R.B.J., Ptacek, C.J., 1999. Geochemistry of a permeable reactive barrier for metals and acid mine drainage. *Environ. Sci. Technol.* 33, 2793–2799.
- Benner, S.G., Gould, W.D., Blowes, D.W., 2000. Microbial populations associated with the generation and treatment of acid mine drainage. *Chem. Geol.* 169 (3–4), 435–448.
- Benner, S.G., Blowes, D.W., Ptacek, C.J., Mayer, K.U., 2002. Rates of sulfate reduction and metal sulfide precipitation in a permeable reactive barrier. *Appl. Geochem.* 17 (3), 301–320.
- Blowes, D.W., Ptacek, C.J., Benner, S.G., McRae, C.W.T., Bennett, T.A., Puls, R.W., 2000. Treatment of inorganic contaminants using permeable reactive barriers. *J. Contam. Hydrol.* 45 (1–2), 123–137.
- Brenner, D.J., McWhorter, A.C., Knutson, J.K.L., Steigerwalt, A.G., 1982. *Escherichia vulneris* - a new species of *Enterobacteriaceae* associated with human wounds. *J. Clin. Microbiol.* 15 (6), 1133–1140.
- Bryant, M.P., Small, N., Bouma, C., Robinson, I.M., 1958. Characteristics of ruminal anaerobic cellulolytic cocci and *Cillobacterium cellulosolvens* n. sp. *J. Bacteriol.* 76 (5), 529–537.

- Castro, J.M., Wielinga, B.W., Gannon, J.E., Moore, J.N., 1999. Stimulation of sulfate-reducing bacteria in lake water from a former open-pit mine through addition of organic wastes. *Water Environ. Res.* 71 (2), 218–223.
- Chang, S., Shin, P.K., Kim, B.H., 2000. Biological treatment of acid mine drainage under sulphate-reducing conditions with solid waste materials as substrates. *Water Res.* 34 (4), 1269–1277.
- Christensen, B., Laake, M., Lien, T., 1996. Treatment of acid mine water by sulfate-reducing bacteria: results from bench scale experiments. *Water Res.* 30 (7), 1617–1624.
- Cox, G.W., 1972. *Laboratory Manual of General Ecology*. W.C. Brown, Dubuque, IA, pp. 120–124.
- Dehning, I., Stieb, M., Schink, B., 1989. *Sporomusa malonica* sp. nov., a homoacetogenic bacterium growing by decarboxylation of malonate or succinate. *Arch. Microbiol.* 151 (5), 421–426.
- Dvorak, D.H., Hedin, R.S., Edenborn, H.M., McIntire, P.E., 1992. Treatment of metal-contaminated water using bacterial sulfate reduction: results from pilot-scale reactors. *Biotechnol. Bioeng.* 40, 609–616.
- Dworkin, M. (Ed.), 2000. *The Prokaryotes: An Evolving Electronic Resource for the Microbiological Community*. Springer, New York.
<<http://141.150.157.117:8080/prokPUB/index.htm>>.

Eger, P., Lapakko, K., 1988. Nickel and copper removal from mine drainage by a natural wetland. Bureau of Mines, US Department of Interior.

Hallberg, K.B., Johnson, D.B., 2005a. Microbial populations of compost wetlands constructed to remediate acidic coal spoil drainage. In: Harrison, S.T.L., Rawlings, D.E., Peteren, J. (Eds.), The 16th International Biohydrometallurgy Symposium (IBS), Cape Town, South Africa, pp. 713–722.

Hallberg, K.B., Johnson, D.B., 2005b. Microbiology of a wetland ecosystem constructed to remediate mine drainage from a heavy-metal mine. *Sci. Total Environ.* 338, 53–66.

Holt, J.H. (Ed.), 1984. Bergey's Manual of Systematic Bacteriology, vol. 2. Williams & Wilkins, Baltimore.

Johnson, D.B., Hallberg, K.B., 2003. The microbiology of acidic mine waters. *Res. Microbiol.* 154 (7), 466–473.

Johnson, D.B., Hallberg, K.B., 2005. Acid mine drainage remediation options: a review. *Sci. Total Environ.* 338 (1–2), 3–14.

Kalendar, R., 2005. FastPCR: PCR primer design, DNA and protein tools, repeats and own database searches program.

<<http://www.biocenter.helsinki.fi/bi/programs/fastpcr.htm>>.

Kotsyurbenko, O.R., Nozhevnikova, A.N., Osipov, G.A., Kostrikina, N.A., Lysenko, A.M., 1995. A new psychoactive bacterium *Clostridium fimetarium*, isolated from cattle manure digested at low temperature. *Microbiology* 64 (6), 681–686.

Labrenz, M., Banfield, J.F., 2004. Sulfate-reducing bacteria-dominated biofilms that precipitate ZnS in a subsurface circumneutral-pH Mine drainage system. *Microb. Ecol.* 47, 205–217.

Leschine, S.B., 1995. Cellulose degradation in anaerobic environments. *Ann. Rev. Microbiol.* 49, 399–426.

Logan, M.V., Reardon, K.F., Figueroa, L., McLain, J.E.T., Ahmann, D., 2005. Microbial community activities during establishment, performance, and decline of bench-scale passive treatment systems for mine drainage. *Water Res.* 39, 4537–4551.

Moore, W.E.C., Johnson, J.L., Holdeman, L.V., 1976. Emendation of *Bacteroidaceae* and *Butyrivibrio* and descriptions of *Desulfomonas* gen. nov. and 10 new species in genera *Desulfomonas*, *Butyrivibrio*, *Eubacterium*, *Clostridium*, and *Ruminococcus*. *Int. J. Syst. Bacteriol.* 26 (2), 238–252.

Morales, T.A., Dopson, M., Athar, R., Herbert Jr., R.B., 2005. Analysis of bacterial diversity in acidic pond water and compost after treatment of artificial acid mine drainage for metal removal. *Biotechnol. Bioeng.* 90 (5), 543–551.

Moreno, B., Gómez, M.A., González-López, J., Hontoria, E., 2005a. Inoculation of a submerged filter for biological denitrification of nitrate polluted groundwater: a comparative study. *J. Hazardous Mater.* 117 (2–3), 141–147.

Moreno, B., Gomez, M.A., Ramos, A., Gonzalez-Lopez, J., Hontoria, E., 2005b. Influence of inocula over start up of a denitrifying submerged filter applied to nitrate contaminated groundwater treatment. *J. Hazardous Mater.* 127 (1–3), 180–186.

Palop, M.L., Valles, S., Pinaga, F., Flors, A., 1989. Isolation and characterization of an anaerobic, cellulolytic bacterium, *Clostridium celerecrescens* sp. nov. Int. J. Syst. Bacteriol. 39 (1), 68–71.

Pereira, A., Mota, M., Alves, M., 2001. Degradation of oleic acid in anaerobic filters: the effect of inoculum acclimatization and biomass recirculation. Water Environ. Res. 73 (5), 612–621.

Pereyra, L.P., Hanson, R.E., Hiibel, S.R., Pruden, A., Reardon, K.F., 2005. Comparison of Inocula Applied in the Remediation of Acid Mine Drainage by Sulfate Reduction. American Society for Mining and Reclamation (ASMR), Breckenridge CO.

Pruden, A., Pereyra, L.P., Hiibel, S.R., Reardon, K.F., 2006. Microbiology of sulfate-reducing passive treatment systems. In: Seventh International Conference on Acid Rock Drainage (ICARD), St. Louis, MO.

Suzuki, M.T., Taylor, L.T., DeLong, E.F., 2000. Quantitative analysis of small-subunit rRNA genes in mixed microbial populations via 50-nuclease assays. Appl. Environ. Microbiol. 66 (11), 4605–4614.

US EPA, 1997. EPA's national hardrock mining framework. United States Environmental Protection Agency Office of Water.

Vangylswyk, N.O., 1980. A *Fusobacterium polysaccharolyticum* sp. nov., gram-negative rod from the rumen that produces butyrate and ferments cellulose and starch. J. Gen. Microbiol. 116, 157–163.

- Vangylswyk, N.O., Vandertoorn, J.J.T.K., 1985. *Eubacterium uniforme* sp. nov. and *Eubacterium xylanophilum* sp. nov., fiber-digesting bacteria from the rumina of sheep fed corn stover. *Int. J. Syst. Bacteriol.* 35 (3), 323–326.
- Varel, V.H., 1989. Reisolation and characterization of *Clostridium longisporum*, a ruminal sporeforming cellulolytic anaerobe. *Arch. Microbiol.* 152 (3), 209–214.
- Wakao, N., Takahashi, T., Sakurai, Y., Shiota, H., 1979. A treatment of acid mine water using sulfate-reducing bacteria. *J. Ferment. Technol.* 57 (5), 445–452.
- Watanabe, K., Kodama, Y., Harayama, S., 2001. Design and evaluation of PCR primers to amplify bacterial 16S ribosomal DNA fragments used for community fingerprinting. *J. Microbiol. Methods* 44 (3), 253–262.
- Waybrant, K.R., Blowes, D.W., Ptacek, C.J., 1998. Selection of reactive mixtures for use in permeable reactive walls for treatment of mine drainage. *Environ. Sci. Technol.* 32 (13), 1972–1979.
- Waybrant, K.R., Ptacek, C.J., Blowes, D.W., 2002. Treatment of mine drainage using permeable reactive barriers: column experiments. *Environ. Sci. Technol.* 36, 1349–1356.
- Weisburg, W.G., Barns, S.M., Pelletier, D.A., Lane, D.J., 1991. 16S ribosomal DNA amplification for phylogenetic study. *J. Bacteriol.* 173 (2), 697–703.

Xia, S.Q., Shi, Y., Fu, Y.G., Ma, X.M., 2005. DGGE analysis of 16S rDNA of ammonia-oxidizing bacteria in chemical-biological flocculation and chemical coagulation systems. *Appl. Microbiol. Biotechnol.* 69 (1), 99–105.

Chapter 4 Comparison of Microbial Community Composition and Activity in Sulfate-Reducing Batch Systems Remediating Mine Drainage

Pereyra, L.P., Hiibel, S.R., Pruden, A., and K.F. Reardon. (2008). Comparison of. *Biotechnology and Bioengineering*. (In Press, DOI: 10.1002/bit.21930)

Approximate contributions of each author are as follows:

LP Pereyra performed 60% of experimental setup, 50% of the analytical measurements, 50% of the DNA extractions, 60% of the PCR amplification, 60% of the DGGE, 40% of the DNA sequence analysis, 100% of the Q-PCR, 40% of the statistical analyses, and 60% of the manuscript preparation.

SR Hiibel performed 40% of experimental setup, 50% of the analytical measurements, 50% of the DNA extractions, 40% of the PCR amplification, 40% of the DGGE, 60% of the DNA sequence analysis, 100% of the Q-PCR, 60% of the statistical analyses, and 40% of the manuscript preparation.

A Pruden and KF Reardon assisted with experimental design and manuscript preparation.

4.1. Abstract

Five microbial inocula were evaluated for the ability to remediate for mine drainage in batch tests. Twice-acclimated inoculum (ACC), dairy manure (DM), anaerobic digester sludge (ADS) and substrate from the Luttrell (LUTR) and Peerless Jenny King (PJK) sulfate-reducing permeable reactive zones (SR-PRZs) were compared in terms of sulfate and metal removal and pH neutralization. The microbial communities were characterized over 14 weeks using denaturing gradient gel electrophoresis (DGGE) and quantitative polymerase chain reaction (Q-PCR) analysis targeting sulfate-reducing bacteria (SRB) of the genus *Desulfovibrio*. The cultures inoculated with the LUTR, PJK, and DM materials demonstrated significantly higher rates of sulfate and metal removal, and contained all the microorganisms necessary for the desired functioning of SR-PRZs (i.e.,

polysaccharide degraders, fermenters, and sulfate reducers) as well as a relatively high proportion of *Desulfovibrio* spp. These results demonstrate that inoculum influences performance and also provide insights into key aspects of inoculum composition that impact performance. This is the first systematic examination of the relationship between microbial community composition and mine drainage remediation capabilities.

4.2. Introduction

Mine drainage (MD) is a critical environmental problem, with treatment costs estimated in the tens of billions of dollars (Benner *et al.*, 1997). It is formed by the chemical and biological oxidation of sulfide minerals, which results in highly acidic to mildly alkaline waters enriched in sulfate and heavy metals (Benner *et al.*, 1997; Johnson & Hallberg, 2002).

Passive treatment options for MD based on biogeochemical processes are gaining ground over traditional (active) techniques such as limestone addition, which are expensive and require extensive operation and maintenance to function properly (Johnson & Hallberg, 2002). Passive alternatives such as sulfate-reducing permeable reactive zones (SR-PRZs) are minimal-maintenance, low-cost, *in situ* technologies that produce minimal hazardous waste (Johnson & Hallberg, 2002). SR-PRZs are installed in the flow path of the contaminated groundwater and contain a mixture of relatively biodegradable and recalcitrant materials that supply electron donors to a consortium of anaerobic microorganisms responsible for the remediation of the MD (Blowes *et al.*, 2000). The principle mode of function of SR-PRZs is metal sulfide precipitation due to bacterial dissimilatory sulfate reduction. Sulfate-reducing bacteria (SRB) use sulfate as an electron acceptor and reduce it to hydrogen sulfide, which reacts with divalent dissolved metals to

form insoluble metal sulfides that precipitate in the barrier. Thus, the activity of the SRB results in decreased sulfate and metal concentrations and an increase in alkalinity and pH due to the production of bicarbonate (Johnson & Hallberg, 2005). Despite the advantages, passive MD treatment systems have been implemented in the field and at laboratory scale with mixed success. Many perform as designed (Benner *et al.*, 1997) while others fail to remove contaminants to the required levels (Barton & Karathanasis, 1999; Johnson & Hallberg, 2002).

Cellulosic materials such as straw, mushroom compost and sawdust are used to provide a long-term source of carbon and energy for the SR-PRZ microorganisms (Johnson & Hallberg, 2002). These complex polymeric compounds cannot be directly degraded by SRB, which only utilize simple organic acids or molecular hydrogen as electron donors. As a consequence, a complex microbial community is responsible for MD remediation in SR-PRZs (Logan *et al.*, 2005). This microbial community includes cellulose-degrading and fermenting bacteria that hydrolyze cellulose and other polymeric compounds and transform the degradation products into simpler organic compounds that can be utilized by the SRB (Logan *et al.*, 2005).

The controlling influence of microbial inoculum on the treatment of MD (Chang *et al.*, 2000; Jong & Parry, 2003; Pruden *et al.*, 2007) as well as on the bioremediation of other contaminants such as nitrate (Moreno *et al.*, 2005), hydrocarbons (Juteau *et al.*, 2003), chlorinated aliphatics (Hourbron *et al.*, 2000) and polychlorinated biphenyls (Fava & Bertin, 1999) has been demonstrated. However, no studies have systematically examined the relationship between the microbial composition of several types of inocula and their ability to remediate MD. Thus, the main objective of the study was to identify

key characteristics of microbial inocula for optimizing SR-PRZ performance and reliability using a combination of biomolecular tools and multivariate statistics. The composition and activities of five inocula were compared in batch tests with respect to sulfate and metal removal and pH neutralization. Batch tests are simple to perform in large numbers and, while not exact analogs of the continuous-flow SR-PRZs, they serve as a valuable tool to evaluate and compare several conditions in parallel. The composition of the microbial community over time was monitored with denaturing gradient gel electrophoresis (DGGE) and quantitative polymerase chain reaction (Q-PCR) targeting all bacteria and *Desulfovibrio* spp.. The UniFrac algorithm (Lozupone *et al.*, 2006) was used to compare the microbial communities and identify microorganisms that contributed to major differences among the cultures.

4.3. Materials and Methods

4.3.1. Inocula

Five inocula were investigated: twice-acclimated inoculum (ACC), dairy manure (DM), anaerobic digester sludge (ADS), and substrate collected from two SR-PRZs operating at field sites (Luttrell (LUTR) and Peerless Jenny King (PJK), near Helena, MT). The ACC material was collected from a column simulating a SR-PRZ (Pruden *et al.*, 2007) that had been inoculated with contents from a column containing a sulfate-reducing community (Logan *et al.*, 2005). The dairy manure was obtained from a dairy in Wellington, CO and was included in this study for comparison purposes as it is an inoculum type commonly used in field SR-PRZs (Johnson & Hallberg, 2005). The ADS material was provided by the Drake Water Reclamation Facility of the City of Fort Collins, CO.

4.3.2. Batch Tests Setup

Inoculum, simulated mine water, solid organic substrate, and limestone were added to serum bottles (125 mL) in an anaerobic hood under a nitrogen atmosphere. To avoid inoculation with material that could have been exposed to oxygen, each inoculum was sampled from the core of its storage container. The organic substrate added to each bottle consisted of 7.27 g of beech wood chips (particle size 2.00 mm – 13.33 mm), 0.66 g of pulverized alfalfa (particle size < 0.85 mm), and 3.64 g of pine shavings (particle size 2.00 mm – 9.42 mm). Limestone (1.65 g per bottle, particle size 0.29 mm – 0.85 mm) was added as a source of alkalinity. The simulated mine water was a solution with pH between 5.5 and 6.0 containing: 1.32 g/L MgSO₄; 0.03 g/L NH₄Cl; 0.09 g/L ZnSO₄·7H₂O; 0.06 g/L FeSO₄·7H₂O, and 0.01 g/L CdCl₂ in deionized water purged with nitrogen. Ammonium was included to ensure that microbial growth was not nitrogen limited. Ninety milliliters of simulated acidic MD were added to each bottle. The amount of inoculum added to each bottle was such that all the bottles would initially have the same number of viable bacterial cells (2×10^{10} cells per bottle), as determined by total phospholipid quantification (Findlay *et al.*, 1989). ACC bottles received 80% fewer cells than the other bottles due to limited availability of this inoculum. Uninoculated bottles (“Control”) were also tested. Silica sand (particle size 0.42 mm – 0.85 mm) was used to reach the target weight of 33 g per bottle. The bottles were capped with ¼-inch butyl rubber septa (Bellco Glass Inc., Vineland, NJ), sealed with aluminum crimp seals, and maintained upside down in the dark.

Thirteen bottles were prepared for each type of inoculum and two bottles of each type were sacrificed after 0, 2, 4, 9, and 14 weeks. The liquid from the sacrificed bottles

was collected in 60-mL Nalgene® bottles and stored at 4 °C. The solid material was stored in 50-mL sterile centrifuge tubes at -80 °C.

4.3.3. Analytical Methods

Sulfate was measured using the SulfaVer® 4 method (Hach Company, Loveland, CO) and a DR/3000 spectrometer (Hach Company). Aqueous samples were filtered through 0.45- μm filters and diluted with deionized water to achieve a concentration within the detection range of 2-70 mg/L. To verify that the characteristics of the samples did not interfere with the method, samples were spiked with standard sulfate solutions. No matrix effects were found.

To determine the metal concentrations, 10 mL of the filtered liquid phase were digested in a CEM microwave digester model MS-2000 (Matthews, NC) using EPA Method SW-3015 and analyzed by inductively coupled plasma atomic emission spectroscopy (ICP-AES) with a Thermo Jarrell Ash IRIS Advantage ICP (Thermo Electron Corp., Milford, MA). Detection limits were 0.01 mg/L for zinc, 0.005 mg/L for cadmium, and 0.01 mg/L for magnesium.

The pH in the liquid phase was measured with an Accumet® AB15 Basic pH meter (Fisher Scientific, Pittsburgh, PA).

4.3.4. DNA Extraction

DNA extractions were carried out on the substrate of the sacrificed bottles using the Ultraclean™ Soil DNA kit (MO BIO, Carlsbad, CA) according to the manufacturer's protocol. Approximately 0.5 g of material was used per extraction and the extracted DNA

was PCR amplified and then analyzed by DGGE. For Q-PCR analysis, eight independent DNA extractions were performed and the extracts were pooled together.

4.3.5. PCR Amplification

The variable V3 region of the 16S rDNA was amplified using primers I341F (with a GC clamp) and I533R (Watanabe *et al.*, 2001). The master mix composition and temperature conditions for PCR were described by Pruden et al.(2007) and Watanabe et al. (2001), respectively. The PCR products were quantified using Low DNA MassTM Ladder (Invitrogen, Carlsbad, CA) in a 1.2% agarose gel.

4.3.6. Denaturing Gradient Gel Electrophoresis (DGGE)

Gels (8% acrylamide/bisacrylamide 19:1, BioRad) were cast using a denaturing gradient of 20 to 55% (PJK, LUTR, and DM samples) or 30 to 50% (ADS and ACC samples), with 100% denaturant defined as 7 M urea and 20% v/v formamide. Electrophoresis was performed at 45 V for 20 hours at 57.5 °C and gels were stained with SybrGold nucleic acid stain (Molecular Probes, Inc., Eugene, OR). For each inoculum, the PCR products corresponding to the different time points sampled were loaded in the same DGGE gel. In each gel, equal masses of the PCR products were loaded in each lane to allow for a semi-quantitative comparison among lanes. The PCR product from one of the LUTR samples was also loaded in the DGGE gels with the ACC and ADS samples to characterize gel-to-gel variations. Gel images were captured using a UVP BioChemi Gel Documentation System (UVP, Upland, CA) and analyzed using Labworks software (UVP). Representative visible DGGE bands were excised with sterile razor blades and stored in

0.5-mL tubes with 36 µL of sterile water. A total of 9, 10, 12, 7, and 13 DGGE bands from the PJK, LUTR, DM, ADS, and ACC gels were sequenced, respectively.

Labworks software was used to identify the bands in the gels and to quantify their relative proportion in each lane. The relative diversity of the microbial community in each sample was calculated using the Shannon Diversity Index (Equation 4.1) (Cox, 1972; Xia *et al.*, 2005):

$$H = -\sum \left[\frac{n_i}{N} \log \left(\frac{n_i}{N} \right) \right] \quad \text{Eq. 4.1}$$

where n_i is the intensity of the individual bands and N is the sum of the intensity of all the bands in the lane.

4.3.7. DNA Sequence Analysis

DNA present in the DGGE bands was re-amplified with primers I341F and I533R as described above and the ~200 bp PCR product was sequenced by SeqWright DNA Technology Services (Houston, TX). The closest matches to known microorganisms available in the National Center for Biotechnology Information database were determined using the BLAST alignment tool (<http://www.ncbi.nlm.nih.gov/BLAST/>). A literature survey was conducted to characterize the properties of the closest matches with respect to substrate utilization and sulfate reduction.

A phylogenetic tree was constructed with the DGGE sequences and 39 reference bacterial sequences belonging to *Prevotella*, *Bacteroides*, *Lactobacillus*, *Anoxibacillus*, *Sulfurospirillum*, *Acetobacterium*, *Flavobacterium*, *Acinetobacter*, *Spirochaetaceae*, *Enterobacteriaceae* and Clostridia. The sequences were aligned with ClustalX (Thompson *et al.*, 1997). The phylogenetic tree was estimated by the neighbor-joining

method using PAUP* 4.0 Beta Trial Version (Swofford, 2002) and was analyzed with the UniFrac application (Lozupone *et al.*, 2006). UniFrac was used to compare the different cultures as well as the microbial community in each culture over time to determine if there were significant differences (UniFrac significance test), to identify the microorganisms that led to major differences (lineage-specific analysis), and to find patterns of similarity (principal coordinate analysis (PCoA)). The comparisons made by these three tests were based on the phylogenetic distances among the samples.

4.3.8. Quantitative PCR (Q-PCR)

Q-PCR targeting the 16S rDNA of total bacteria (B) and the SRB genus *Desulfovibrio* (DSV) was performed using a 7300 Real-Time PCR System (Applied Biosystems, Foster City, CA). The primers used to quantify DSV were described by Daly *et al.* (2000). For the DSV primers, Q-PCR amplification was performed in a 25 µL reaction mixture using 1X *Power SYBR®* Green PCR Master Mix (Applied Biosystems), 0.30 µM of each primer, 0.2 mM Mg(OAc)₂, and 1µL of template with a temperature program of 10 min at 95 °C followed by 60 cycles of 15 s at 95 °C, 37 s at 64 °C, and 60 s at 72 °C. TaqMan® Universal PCR Master Mix (Applied Biosystems) was used to quantify total bacterial 16S rDNA using the conditions, universal 16S rDNA primers and probe described by Suzuki *et al.* (2000). For each sample and set of primers, a suppression factor that takes into account the impact of PCR inhibitors in the DNA extract was determined as described in Pei *et al.* (2006).

4.3.9. Statistical Analyses

Mixed linear regressions were fit to the data sets using the PROC MIXED function of SAS 9.1 (SAS Institute Inc., Cary NC). Log transformation of all data sets was required to achieve homoscedasticity, and thus all comparisons were made in log scale. Degrees-of-freedom calculations were performed using the Kenward-Roger method. Significance was defined by a pair-wise comparison p-value ≤ 0.05 .

4.4. Results

4.4.1. Effect of Inoculum on Performance

4.4.1.1. Sulfate Removal

Liquid-phase sulfate concentrations decreased 46-66% in the LUTR, DM, and PJK bottles. No significant removal was observed in the ADS, ACC, or Control bottles, which were not statistically different from each other (**Error! Reference source not found.**). The highest extent of sulfate removal occurred in the LUTR bottles, in which nearly 70% of the sulfate had been removed by Week 9.

The sulfate concentrations in the liquid phase of the bottles sacrificed at Weeks 2 and 9 were also measured two weeks before the sacrifice in order to calculate the average rates of sulfate removal in these two periods (Figure 4.2). At Week 2, the removal rates in the LUTR and DM bottles were significantly higher than those in the other bottles. At Week 9, the rates in the LUTR and DM bottles had decreased and there were no significant differences among the different bottles.

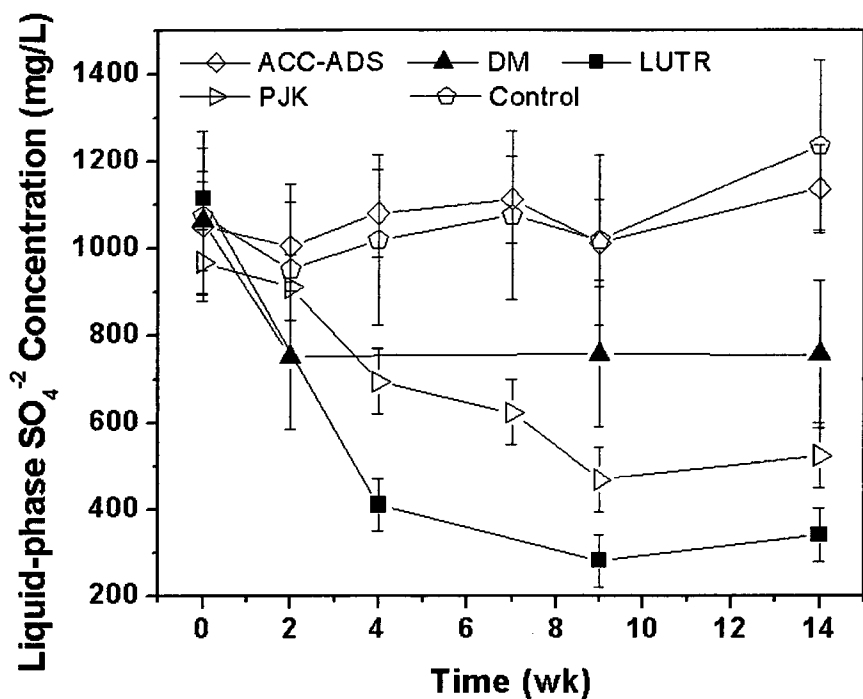


Figure 4. 1: Sulfate concentration in the liquid phase of the bottles. Data points represent the average of technical triplicates and biological duplicates, and error bars correspond to the pooled standard error. Since ACC and ADS bottles were not significantly different, one curve is shown to represent the trend observed in both types of inocula.

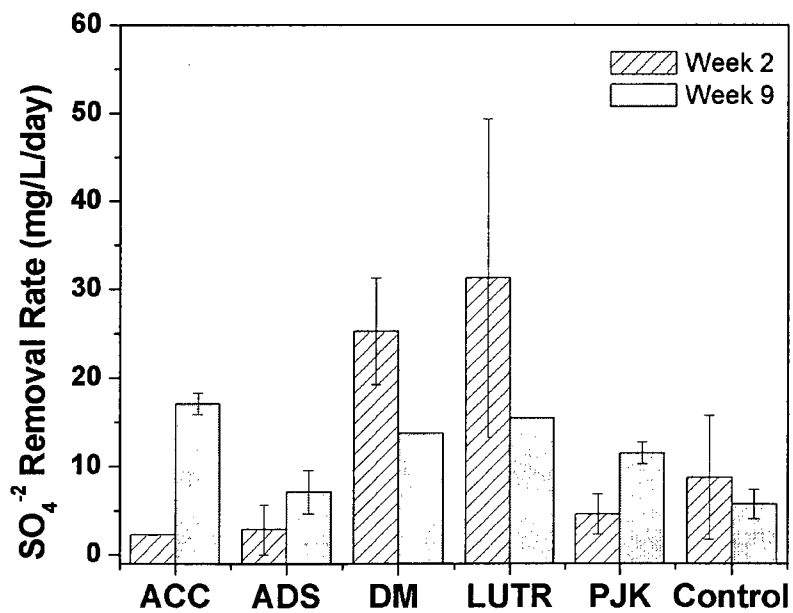


Figure 4. 2: Sulfate removal observed at Weeks 2 and 9 of the experiment. Column heights are the average of biological duplicates, and the error bars are the corresponding pooled standard error.

4.4.1.2. Metal Removal

With respect to the extent of zinc removal, two significantly different groups were observed: zinc removal was high (80-100%) in LUTR- and DM-inoculated bottles, and low (20-40%) in the others (Figure 4.3). A similar trend was observed in cadmium removal (data not shown). Within each group there were no significant differences among bottles ($p>0.05$). In all bottles, the highest rates of removal occurred in the first two weeks. Due to difficulties during the acid digestion of the substrate, no zinc data were obtained for the PJK bottles. Magnesium removal was minimal in all bottles (data not shown).

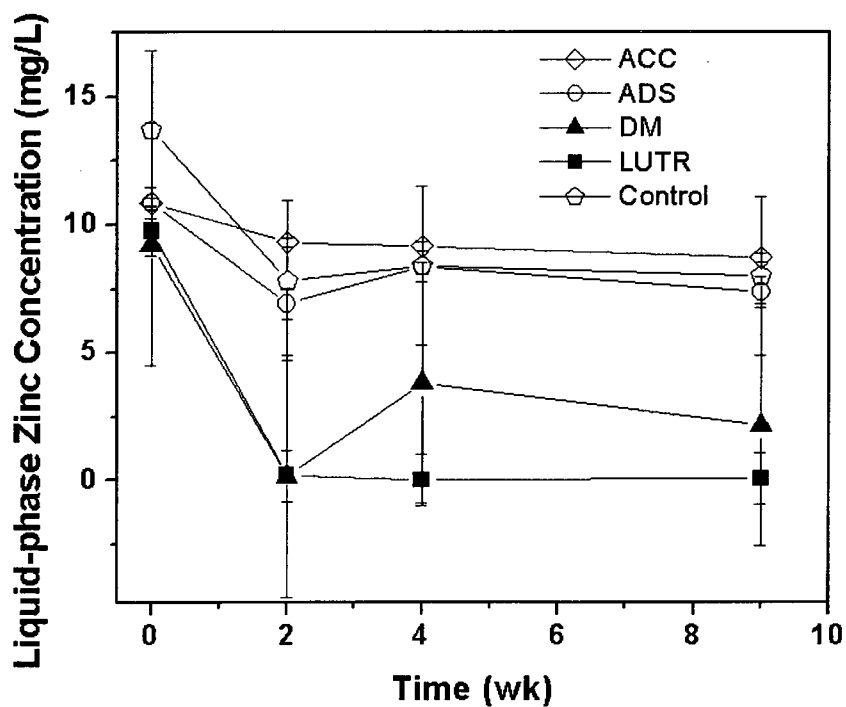


Figure 4. 3: Concentration of soluble zinc in the bottles determined by ICP-AES analysis of digested liquid-phase material. Data points represent the average of technical triplicates and biological duplicates, and error bars correspond to the pooled standard error. PJK data could not be obtained due to technical difficulties with the acid digestion.

4.4.1.3. pH

The initial pH in the bottles was 5.25-5.75 (Figure 4.4). Over the course of the experiment, the pH in the LUTR and PJK bottles was significantly higher than the pH in the other bottles, and no significant differences were found among the others. The pH increased until Week 9 in all bottles except those inoculated with the ADS material, in which the pH decreased during the first four weeks.

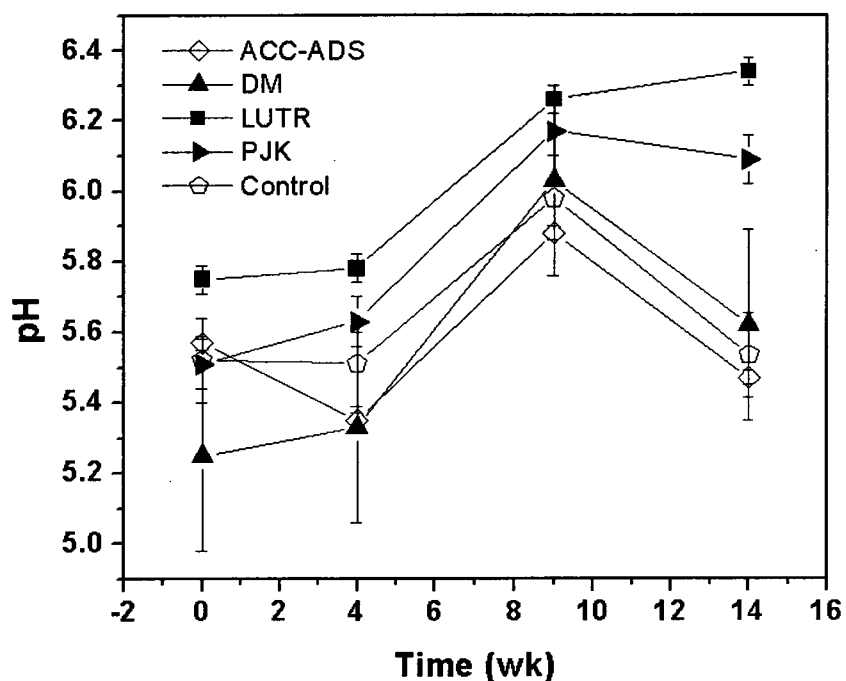


Figure 4. 4: pH in the liquid phase of the bottles. Data points represent the means of biological duplicates, and error bars correspond to the pooled standard error. Since ACC and ADS bottles were not significantly different one curve is shown to represent the trend observed in both types of inocula.

4.4.2. Microbial Community Composition

4.4.2.1. Microbial Diversity

In the ADS, ACC, and PJK cultures, the DGGE banding patterns changed with time with more bands being detected by the end of the experiment. In the LUTR cultures, the

DGGE banding pattern between Weeks 2 and 14 also changed with time but approximately the same number of bands was detected at each time point. In the DM cultures, there was a high similarity in the DGGE banding patterns between Weeks 2 and 14. Values of the Shannon Diversity Index in DM and LUTR cultures remained constant throughout the experiment ($H = 0.82 \pm 0.05$ for DM cultures and 0.86 ± 0.05 for LUTR cultures). In the ADS and ACC cultures, diversity increased between Weeks 0 and 2 and then remained constant at H values of 1.07 ± 0.10 and 1.10 ± 0.19 , respectively. The Shannon Diversity Index of the PJK culture increased until Week 4 and then remained constant at 1.12 ± 0.05 . A comparison of Shannon Diversity Index values among different cultures was not carried out because of apparent gel-to-gel variations. However, cloning of 16S rDNA (data not shown) indicated that the initial microbial diversity was higher in the LUTR, DM, and PJK cultures than in the ADS culture.

4.4.2.2. Microbial Composition of the Cultures

Sequencing of DGGE bands revealed the identity of some of the members of the microbial communities and gave insight into their function (Table 4.1). The majority of the DNA sequences were related to *Bacteroides*, *Prevotella*, Spirochaetes and *Clostridium*. In the DM cultures, an uncultured microorganism whose closest cultured phylogenetic relative is the SRB *Desulfosalina propionicus* was detected during Weeks 0, 2, and 14. A microorganism that produces H₂S (*Sulfurospirillum*) from sulfur or thiosulfate (MacRae *et al.*, 2007) was detected in the LUTR culture during Weeks 4, 9, and 14.

Table 4. 1: Characterization of major constituents of the microbial communities in the cultures represented by DGGE bands.

	Highest Match (GenBank accession number) /number of matching DGGE bands/	Closest Cultured Relative (GenBank accession number) % Match			C*	P*	F*
		WK*	% Match				
PJK	Uncultured bacterium clone anNSG06 (EF034865) /1/ Uncultured bacterium clone ASG2 (AJ514430) /3/	0,2,4,9,14 0,2,4,9,14	95 90-99	<i>Bacteroides ovatus</i> (X83952) 93% <i>Prevotella albensis</i> (AJ011683) 90%	-	+	+
	Uncultured <i>Bacteroidaceae</i> bacterium clone dgD-135 (AB264075) /2/ Uncultured bacterium clone up.21 (AY212542) /2/ Uncultured bacterium clone CFT214H12 (DQ456399) /1/	2,4,9,14 0,2,4,9,14 2,4,9	86-99 97-98 83	<i>Bacteroides vulgatus</i> (M58762) 99% <i>Prevotella bryantii</i> (AJ006457) 87% <i>Bacteroides vulgatus</i> (CP000139) 97%	-	+	+
	Uncultured bacterium clone ASG2 (AJ514430) /3/ Uncultured <i>Sulfurospirillum</i> sp. clone KB-1 16S ribosomal RNA (AY780560) /1/ <i>Clostridium fmetarium</i> (AF126687)/1/	2,4,9,14 4,9,14 0,2,4,9	97-100 92 86	<i>Prevotella albensis</i> (AJ011683) 90% <i>Sulfurospirillum multivorans</i> (X82931) 98%	-	-	-
	Uncultured bacterium clone CFT214H12 (DQ456399) /1/ Uncultured Bacteroidetes bacterium clone edNE10 (DQ886174) /2/ <i>Acetobacterium</i> sp. LS2 (DQ767880)/1/ <i>Flavobacterium xanthum</i> strain R-9010 (AJ601392) /1/	2,4,9,14 2,4,9,14 0,2,4,14 0,4,9,14	97 98-99 98 96	<i>Bacteroides vulgatus</i> (CP000139) 97% <i>Bacteroides eggerthii</i> (AB050107) 92%	±	±	±
LUTR	Uncultured bacterium clone ASG2 (AJ514430) /2/ <i>Bacteroides pectinophilus</i> (DQ497993)/3/	0,2,4,9,14 0,2,4,9,14	92-97 90-98	<i>Prevotella albensis</i> (AJ011683) 90%	-	+	+
	Uncultured bacterium clone: 1-H07 (AB107581) /2/ Uncultured <i>Treponema</i> sp. clone L0008 (AY739142) /1/ Uncultured <i>Treponema</i> sp. clone MgMJD-083 (AB234369) /1/ Uncultured delta proteobacterium clone ESB8 (EF061191)/1/ <i>Clostridium botulinum</i> strain F550 (EF030541) /1/ <i>Clostridium fmetarium</i> (AF126687)/1/	0,2,4,9,14 0,2,4,9,14 0,2,4,9,14 0,2,14 0,2,4,9,14 0,2,9,14	96-99 98 98 94 84 88	<i>Clostridium ramosum</i> (M23731) 89% <i>Treponema primitia</i> (AF093252) 88& <i>Treponema primitia</i> (AF093251) 88% <i>Desulfosalina propionicus</i> (DQ067422) 81% <i>Roseiflexus castenholzii</i> (CP000804) 78%	-	-	+
ADS	Uncultured bacterium clone H2-2D.74 (DQ423665) /1/ <i>Lactobacillus curvatus</i> subsp. <i>curvatus</i> (AY204894) /1/ <i>Lactobacillus bifementans</i> (LBARR16SH) /1/	0,4,9,14 0,2,9 0,2,4,9,14	83 94 97	<i>Prevotella albensis</i> (AJ011683) 90%	-	-	-
	Uncultured bacterium clone ASG2 (AJ514430) /4/ Uncultured Bacteroidetes bacterium clone edNE14a (EF152337) /1/	0,2,4,9,14 0,2,4,9,14	88-98 97	<i>Bacteroides intestinalis</i> (AB214329) 91%	-	+	+
	Uncultured bacterium clone ASG2 (AJ514430) /3/ <i>Lachnospira pectinoschiza</i> isolate M56 (AY699283) /1/	0,2,4,9,14 0,2,4	85-98 94	<i>Prevotella albensis</i> (AJ011683) 90%	±	±	±
	<i>Brevundimonas</i> sp. 28/28 (DQ310472) /1/ <i>Bacteroides helcogenes</i> strain: JCM 6927 (AB200227) /1/	0,14 0,2,4,9,14	97 97	<i>Prevotella bryantii</i> (AF396925) 92%	-	-	-
	Uncultured bacterium G1Clone107 (EF149120) /4/ Uncultured bacterium clone: 1-H07 (AB107581) /1/ Uncultured Bacteroidetes bacterium clone edNE65a (EF152339) /2/	0,2,4,9,14 0,2,4,9,14 0,2,4,9,14	86-97 96 89-99	<i>Clostridium ramosum</i> (M23731) 89% <i>Prevotella ouabra</i> (L16472) 92%	-	-	+

A WK, weeks of the experiment in which the band was detected on the DGGE gel, putative functions-C, cellulose degradation; P, degradation of polysaccharides other than cellulose (e.g., pectin, starch, and xylan); F, fermentation of monosaccharides (and/or disaccharides); +, function is present; -, function is absent, ±, function might be present. Where more than one sequence had the same similarity with the DGGE sequence, all the results corresponding to the highest matches are presented. When the DGGE band sequence corresponded to an uncultured bacterium, the function of the microorganism was assigned based on the functions of the closest known relative.

4.4.2.3. Analysis of Microbial Community Differences and Temporal Changes

An overall comparison of the cultures using the UniFrac Significance test revealed that the microbial communities were significantly different ($p=0.00$). According to the UniFrac lineage-specific analysis, the main differences among cultures were due to the presence of *Treponema* spp. and *Bacteroides pectinophilus* in the DM culture, *Lactobacillus* spp. and an uncultured bacterium (NCBI Accession Number DQ423665) in the ADS cultures, and *Lachnospira pectinophila* in the ACC culture. PCoA did not identify any clear clustering of the communities (Figure 4.5.a). The changes in the clustering at the beginning and end of the experiment were also examined with PCoA and no significant differences were found (Figure 4.5.b).

The UniFrac lineage-specific analysis and PCoA were also used to study the changes in the microbial community in the same culture over time (Figure 4.5). In the LUTR cultures, Bacteroidetes, Clostridia, *Acetobacterium*, *Sulfurospirillum*, and *Flavobacterium* spp. were abundant at Week 9, and differences in the culture at this point vs. all other times was captured by the first principal coordinate, which explained 61.3% of the variability observed in the data. In the DM cultures, PCoA revealed that there was a high similarity among the microbial communities at Weeks 2, 4, and 9 with *Bacteroides pectinophilus* as the dominant microorganism. In the PJK cultures, the PCoA clustering suggested that the microbial communities in Weeks 4, 9, and 14 were more similar to each other than they were to the communities present at Weeks 0 and 2. An uncultured bacterium (NCBI Accession number AY212542) that is related to *Prevotella bryantii* was dominant during Weeks 9 and 14 and an uncultured bacterium related to *Bacteroides vulgatus* was dominant at Week 4. In the ACC cultures, the initial microbial community

was different from the community at all other times and *Bacteroides* spp. were dominant in Weeks 2, 4, and 9 but not initially. In the ADS bottles, the microbial communities at Weeks 0 and 2 were different from each other and from the communities at Weeks 4, 9, and 14. *Lactobacillus* spp. were dominant during Weeks 2 and 9 and an uncultured bacterium (NCBI Accession number DQ423665) was dominant at the beginning of the experiment.

4.4.2.4. Quantification of Total Bacteria and SRB

Throughout the experiment, the lowest numbers of bacterial 16S rDNA gene were observed in the LUTR and Control cultures and the highest numbers in the DM and PJK cultures (Figure 4.6.a). In the LUTR culture, the concentration of bacterial 16S rDNA copies did not change significantly for the duration of the experiment.

Desulfovibrio spp. were detected by Q-PCR in all the cultures at the five time points analyzed. Among the ACC, ADS, and Control cultures, there were no significant differences in the ratio of *Desulfovibrio* to total bacteria, which ranged from 1×10^{-6} to 0.002 (**Error! Reference source not found.b**). In the PJK and LUTR cultures, this ratio was higher, ranging from 0.025 to 0.3. Only in the LUTR culture was a continuous increase in the proportion of *Desulfovibrio* observed (6.5-fold increase by Week 14). In the DM culture, the ratio of *Desulfovibrio* to total bacteria at Weeks 0, 4, and 9 was comparable to that of the ACC, ADS, and Control cultures while at Weeks 2 and 14 the ratio was higher and comparable to that of the PJK and LUTR cultures.

The average sulfate removal rates observed at Weeks 2 and 9 were compared to the corresponding values of *Desulfovibrio* normalized to total bacteria. A direct relationship was found only in the ACC and PJK bottles.

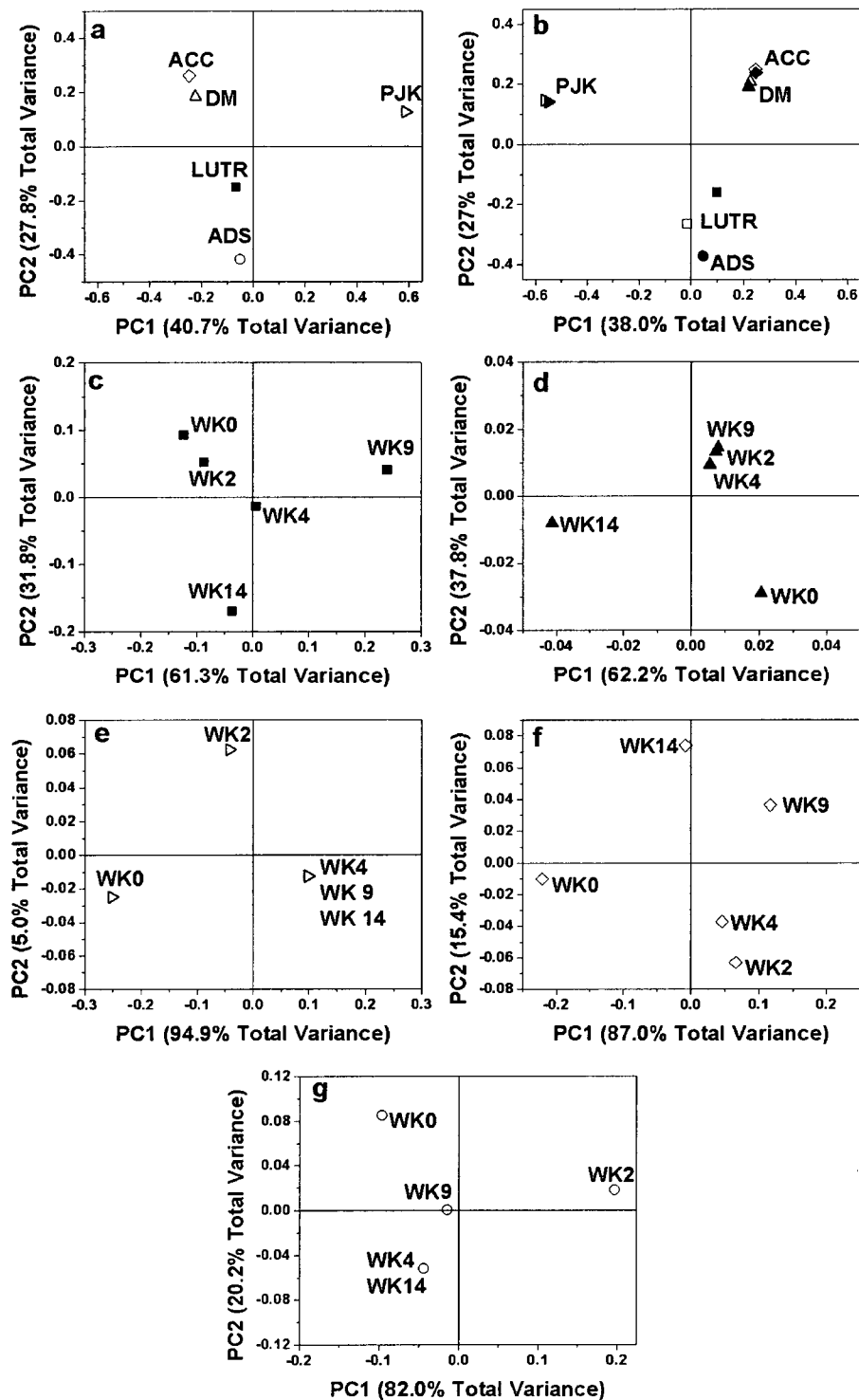


Figure 4. 5: Principal coordinates analysis of the microbial communities in the bottles. Bottles inoculated with different materials, overall comparison (a), and at Weeks 0 (solid symbols) and 14 (open symbols) (b), and LUTR (c), DM (d), PJK (e), ACC (f), and ADS (g) bottles over time.

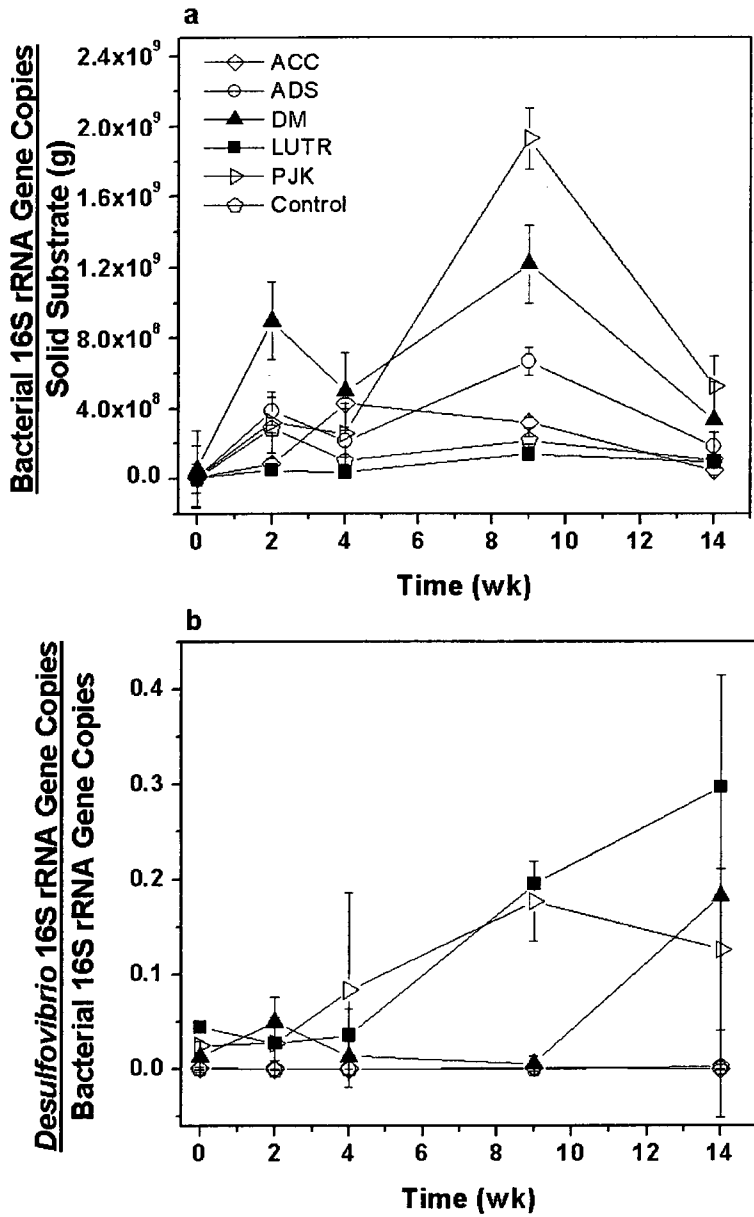


Figure 4.6: Quantification of total bacteria, and the SRB of the genus *Desulfovibrio* with time by Q-PCR. Total bacterial 16S rRNA gene copies normalized to mass of substrate (a), and total *Desulfovibrio* 16S rRNA gene copies normalized to total bacteria (b). Data points are the average of technical triplicates and biological duplicates. Error bars represent pooled standard error.

4.5. Discussion

4.5.1. Effect of Inoculum on Performance

The results of this study demonstrate that inoculum affected performance based on sulfate removal, zinc removal, and pH neutralization. The best performance was observed in the bottles inoculated with the LUTR, DM, and PJK materials. Performance in the ADS and ACC bottles was poor and was comparable to that of the uninoculated Control bottles.

The major differences in sulfate and zinc removal rates occurred in the first two weeks of the experiment, when these chemical species were removed at higher rates in the DM and LUTR bottles. This suggests that the type of inoculum influences the startup time and is consistent with results from a previous study in columns simulating SR-PRZs (Pruden *et al.*, 2007). The minimal removal of Mg in all the bottles is presumably due to the high solubility product of MgS and is consistent with results obtained by Jong and Parry (2003).

In LUTR and PJK bottles, pH neutralization was higher than in the other bottles. Since all of the bottles received an equivalent dose of limestone, the differences in pH response among them can be attributed to the buffering effect of the bicarbonate generated due to microbial activity. Reduction of the acidity of the water helps improve its quality and also favors microbial activity. For example, cellulose hydrolysis is particularly sensitive to acidic conditions (Weimer, 1992). Thus, low pH in the liquid phase of the cultures might slow cellulose degrading organisms and affect downstream microbial processes, resulting in a deleterious effect on the ability to remediate MD.

4.5.2. Microbial Community Composition and Performance

SRB typically represent a small fraction of the microbial community in the systems treating MD (Hong *et al.*, 2007; Morales *et al.*, 2005; Pruden *et al.*, 2007) and, as a consequence, they are likely to be difficult to detect with DGGE (Muyzer *et al.*, 1993a). For these reasons, DGGE was used here to study only the major constituents of the microbial communities while the SRB were studied with Q-PCR.

Bacteroides, *Prevotella*, *Treponema*, and *Clostridium* were the major constituents of the microbial community in the different cultures. This is consistent with the findings of other studies (Labrenz & Banfield, 2004; Pruden *et al.*, 2007). In the PJK and DM cultures, comparison of the PCoA plots and performance data revealed that in each culture the microbial communities were highly similar during the periods of greatest sulfate removal. However, this relationship between PCoA clustering and sulfate removal was not evident in the LUTR culture, in which sulfate removal was also significant. Interestingly, the points in the PCoA plots for the ACC and ADS cultures were spread across the x- and y-axes, and no clear clustering of the communities in relation to the performance was observed. This suggests that the microbial communities in these cultures changed with time without being able to adapt to the environmental conditions.

The microbial communities in the cultures at the beginning and end of the experiment were compared to determine whether the cultures became more similar over time. The convergence of communities to the same composition from different starting conditions has been observed in fixed-film reactors treating aromatic hydrocarbons (MassolDeya *et al.*, 1997) and in soil contaminated with aromatic hydrocarbons (Greene *et al.*, 2000). In this study, however, the microbial communities did not seem to become

more similar, suggesting that a variety of communities with different compositions can be active in the remediation of MD and that the inoculum composition plays a significant role in driving this.

4.5.3. Potential Indicators of Inoculum Suitability for MD Remediation

Demonstration of the impact of the inoculum source on performance leads to the question of precisely which inoculum characteristics predict performance. This knowledge may help guide enrichment of inocula known to have the desired microorganisms.

4.5.3.1. Inoculum Source

In this study, it appears that pre-acclimated material from a SR-PRZ (e.g., LUTR or PJK) is ideal while ADS is not recommended. Our previous column study also indicated that acclimated material is associated with superior performance (Pruden *et al.*, 2007). However, because of variability, caution is necessary in this approach. For example, the performance of systems inoculated with dairy manure was poor in a previous study (Pruden *et al.*, 2007) but good in the present study. Although dairy manure is a common source of inoculum for SR-PRZs, its microbial activity and composition are variable and depend on many factors such as animal species, feed composition, manure pH, and manure handling (Leggett *et al.*, 1998). Since a different source of manure was used in both studies, it is likely that the manure microbial composition had an effect. Therefore, while general inoculum sources might provide some guide, more specific information about the inoculum composition is needed.

Handling and storage of the inoculum are also important aspects that must be taken into account. For example, the poor performance of the ACC bottles was

unexpected because the ACC inoculum came from a column that was actively removing sulfate and metals from MD (Pruden *et al.*, 2007). Despite the fact that 80% fewer cells were inoculated to the ACC bottles, it was expected that the “MD-adapted” microorganisms in this inoculum would quickly increase in number and remove sulfate at high rates. The poor performance of this culture might be due to extensive manipulation prior to use in this study, including exposure to air.

4.5.3.2. Overall Biomass and Diversity

While higher total biomass concentrations should relate to higher microbial activity, no such trend was apparent. This emphasizes the need for a suitable microbial community composition rather than overall number of bacteria.

Diversity has also been considered to potentially correlate with performance. Von Canstein *et al.* (2002) reported that species diversity correlated with the efficiency of a mercury-reducing biofilm, and Kaksonen *et al.* (2004) suggested that diversity and flexibility of the microbial community may enhance the robustness of sulfate-reducing reactors. The microbial communities in LUTR and DM bottles, which performed well, were the most functionally and phylogenetically diverse on the basis of the DGGE analysis. In these cultures, diversity did not change throughout the experiment, whereas the initial diversity of the poorly performing cultures was low and increased later in the experiment.

4.5.3.3. Presence of Key Functional Groups

Cellulose degraders, polysaccharide degraders, fermenters, and sulfate reducers play key roles in SR-PRZ function (Logan *et al.*, 2005) and therefore are of particular interest. In

this study, the best performing cultures had in common the presence of microorganisms from all levels of the carbon flow. For example, the LUTR bottles had reached their maximum sulfate removal at Week 9 and the corresponding microbial community contained a variety of microorganisms, including cellulose degraders and fermenters (*Bacteroides* spp. and Clostridia) and H₂S producers (*Sulfurospirillum* and *Desulfovibrio* spp.).

4.5.3.3.1. Cellulose and other Polysaccharide Degraders

Members of *Clostridium*, a genus known to include highly efficient cellulose-degrading bacteria, were found only in LUTR and DM cultures. Since cellulose was the major constituent of the carbon substrate in the bottles, and its degradation has been reported to be the rate-limiting step in SR-PRZs (Logan *et al.*, 2005), the presence of *Clostridium* may be a desirable characteristic of the inocula (Labrenz & Banfield, 2004). Clostridia were also found in high-performing sulfate-reducing columns in a previous study (Hong *et al.*, 2007). *Bacteroides* spp., which were detected in all the cultures, are extremely versatile in terms of their growth substrate and they can ferment several poly-, oligo-, and monosaccharides (Holt, 1984a). Some *Bacteroides* spp. are able to ferment cellulose.

Microorganisms that hydrolyze polysaccharides other than cellulose were detected in some cultures. Examples of these microorganisms are *Bacteroides pectinophilus* and spirochetes of the genus *Treponema* found in the DM culture, *Prevotella bryantii* detected in the PJK culture and an uncultured bacterium (NCBI Accession Number AJ514430) related to *Prevotella albensis* that was detected in all the cultures. Some *Treponema* spp. can degrade hemicellulosic material such as xylan, the main component of hemicellulose (Leschine, 1995). *B. pectinophilus* uses pectin, a

polysaccharide of high molecular weight, as the only fermentable substrate for growth (Jensen & Canaleparola, 1986). *Prevotella* spp. can utilize plant polysaccharides such as starch, pectins and xylan (Avgustin *et al.*, 1997). The activity of these polysaccharide degraders may benefit cellulose-degrading bacteria by rendering cellulose more accessible (Weimer, 1992) and/or by keeping a low concentration of the products of cellulose hydrolysis (Leschine, 1995).

In general, the best performing cultures contained a variety of polysaccharide-degrading microorganisms that do not degrade cellulose, but that form close associations with cellulose degraders. These microorganisms may be used as indicators of the suitability of the inoculum for MD remediation.

4.5.3.3.2. Fermenters

While all of the cellulose and polysaccharide degraders described above are also capable of fermentation, microorganisms with metabolism restricted to fermentation of simpler molecules were also found in all cultures (Table 4.1). Although the presence of fermentative bacteria is crucial to supply electron donors to the SRB, not all fermenters might be beneficial to the SRB. For example, *Lactobacillus curvatus* and *L. bif fermentans* were present throughout the experiment in the poorly performing ADS culture. Lactic acid, the main product of the fermentative metabolism of Lactobacilli (Holt, 1984b), has been reported to inhibit cellulolytic activity in the rumen (Weimer, 1992). Thus, it is possible that *Lactobacillus* spp. have an inhibitory effect on the desired functioning of the microbial food chain, reducing the supply of simple organic compounds to SRB and resulting in a reduction of the sulfate and metal removal rates of these cultures.

4.5.3.3.3. Sulfate Reducers

Desulfovibrio spp. have been identified as major SRB in MD treatment systems (Labrenz & Banfield, 2004) suggesting that they play a role in remediation. In this study, Q-PCR data indicated that the cultures with better performance generally had a higher fraction of *Desulfovibrio* spp. over time.

The ACC and PJK cultures reduced sulfate at rates proportional to the fraction of *Desulfovibrio* in the microbial community, which suggests that, for these cultures, the SRB population limited the rate of sulfate reduction. For the other cultures, different factors (e.g., slow cellulose hydrolysis) may have influenced the rate of sulfate reduction. This observation, along with the fact that the SRB are generally a small fraction of the total bacterial community, emphasizes the need to also consider other members of the microbial community.

4.6. Conclusions

This study demonstrates the influence of microbial inoculum on the remediation of MD and supports our previous findings from column experiments (Pruden *et al.*, 2007) by examining a wider range of inocula and combining biomolecular analyses with multivariate statistical analyses to identify key characteristics. Batch cultivation proved to be a viable experimental format that enabled higher throughput testing than column experiments. The best overall performance with respect to sulfate and zinc removal and pH neutralization was observed in systems inoculated with LUTR, PJK, and DM materials, which contained fermentative and sulfate-reducing bacteria and a variety of polysaccharide degraders. The results of this study suggest that enrichment of inocula

known to have the desired microorganisms is a promising low cost means of improving the performance of SR-PRZs.

4.7. Acknowledgements

We are grateful for funding through EPA STAR Grant R 8395101-0, which supported the Rocky Mountain Regional Hazardous Substance Research Center and this project. Additional funding was provided by the National Science Foundation Award CBET-0651947. We also thank Rachel Hanson, Nella Kashani, and April Tischer for laboratory assistance.

4.8. References

- Avgustin G, Wallace RJ, Flint HJ. 1997. Phenotypic diversity among ruminal isolates of *Prevotella ruminicola*: Proposal of *Prevotella brevis* sp nov, *Prevotella bryantii* sp nov, and *Prevotella albensis* sp nov and redefinition of *Prevotella ruminicola*. Int. J. Syst. Bacteriol. 47(2):284-288.
- Barton CD, Karathanasis AD. 1999. Renovation of a failed constructed wetland treating acid mine drainage. Environ. Geol. 39(1):39-50.
- Benner SG, Blowes DW, Ptacek CJ. 1997. A full-scale porous reactive wall for prevention of acid mine drainage. Ground Water Monit. Rem. 17(4):99-107.
- Blowes DW, Ptacek CJ, Benner SG, McRae CWT, Bennett TA, Puls RW. 2000. Treatment of inorganic contaminants using permeable reactive barriers. J. Contam. Hydrol. 45(1-2):123-137.

Chang IS, Shin PK, Kim BH. 2000. Biological treatment of acid mine drainage under sulphate-reducing conditions with solid waste materials as substrate. *Water Res.* 34(4):1269-1277.

Cox GW. 1972. *Laboratory Manual of General Ecology*. Brown WC, editor. Dubuque, IA. 120-124 p.

Daly K, Sharp RJ, McCarthy AJ. 2000. Development of oligonucleotide probes and PCR primers for detecting phylogenetic subgroups of sulfate-reducing bacteria. *Microbiology-(UK)* 146:1693-1705.

Dworkin M, editor. 2000. *The Prokaryotes: An Evolving Electronic Resource for the Microbiological Community*. New York: Springer.

Fava F, Bertin L. 1999. Use of exogenous specialized bacteria in the biological detoxification of a dump site-polychlorobiphenyl-contaminated soil in slurry phase conditions. *Biotechnol. Bioeng.* 64(2):240-249.

Fields MW, Russell JB, Wilson DB. 1998. The role of ruminal carboxymethylcellulases in the degradation of beta-glucans from cereal grain. *FEMS Microbiol. Ecol.* 27(3):261-268.

Findlay RH, King GM, Watling L. 1989. Efficacy of phospholipid analysis in determining microbial biomass in sediments. *Appl. Environ. Microbiol.* 55(11):2888-2893.

Foti M, Sorokin DY, Lomans B, Mussman M, Zacharova EE, Pimenov NV, Kuenen JG, Muyzer G. 2007. Diversity, activity, and abundance of sulfate-reducing bacteria in saline and hypersaline soda lakes. 73(7):2093-2100.

Greene EA, Kay JG, Jaber K, Stehmeier LG, Voordouw G. 2000. Composition of soil microbial communities enriched on a mixture of aromatic hydrocarbons. Appl. Environ. Microbiol. 66(12):5282-5289.

Hanada S, Takaichi S, Matsuura K, Nakamura K. 2002. *Roseiflexus castenholzii* gen. nov., sp nov., a thermophilic, filamentous, photosynthetic bacterium that lacks chlorosomes. 52:187-193.

Holt JG, editor. 1984a. Bergey's Manual of Systematic Bacteriology. Baltimore, MD: Williams & Wilkins.

Holt JG, editor. 1984b. Bergey's Manual of Systematic Bacteriology. Baltimore, MD: Williams & Wilkins.

Hong H, Pruden A, Reardon KF. 2007. Comparison of CE-SSCP and DGGE for monitoring a complex microbial community remediating mine drainage. J. Microbiol. Methods 69:52-64.

Hourbron E, Escoffier S, Capdeville B. 2000. Trichloroethylene elimination assay by natural consortia of heterotrophic and methanotrophic bacteria. Water Sci. Technol. 42(5-6):395-402.

Jensen NS, Canaleparola E. 1986. *Bacteroides pectinophilus* sp. nov. and *Bacteroides galacturonicus* sp. nov. 2 pectinolytic bacteria from the human intestinal tract. *Appl. Environ. Microbiol.* 52(4):880-887.

Johnson DB, Hallberg KB. 2005. Acid mine drainage remediation options: a review. *Sci. Total Environ.* 338(1-2):3-14.

Johnson DJ, Hallberg KB. 2002. Pitfalls of passive mine water treatment. *Rev. Environ. Sci. Biotechnol.* 1(4):335-343.

Jong T, Parry DL. 2003. Removal of sulfate and heavy metals by sulfate reducing bacteria in short-term bench scale upflow anaerobic packed bed reactor runs. *Water Res.* 37(14):3379-3389.

Juteau P, Bisaillon JG, Lepine F, Ratheau V, Beaudet R, Villemur R. 2003. Improving the biotreatment of hydrocarbons-contaminated soils by addition of activated sludge taken from the wastewater treatment facilities of an oil refinery. *Biodegradation* 14(1):31-40.

Kaksonen AH, Plumb JJ, Franzmann PD, Puhakka JA. 2004. Simple organic electron donors support diverse sulfate-reducing communities in fluidized-bed reactors treating acidic metal- and sulfate-containing wastewater. *FEMS Microbiol. Ecol.* 47(3):279-289.

Kotsyurbenko OR, Nozhevnikova AN, Osipov GA, Kostrikina NA, Lysenko AM. 1995. A new psychoactive bacterium *Clostridium fimetarium*, isolated from cattle manure digested at low temperature. *Microbiology* 64(6):681-686.

Labrenz M, Banfield JF. 2004. Sulfate-reducing bacteria-dominated biofilms that precipitate ZnS in a subsurface circumneutral-pH mine drainage system. *Microb. Ecol.* 47(3):205-217.

Leggett JA, Lanyon LE, Graves RE. 1998. Biological manipulation of manure: Getting what you want from animal manure. University Park, PA.: The Pennsylvania State University. Department of Agricultural and Biological Engineering. PSU/96.

Leschine SB. 1995. Cellulose degradation in anaerobic environments. *Annu. Rev. Microbiol.* 49:399-426.

Logan MV, Reardon KF, Figueroa LA, McLain JET, Ahmann DM. 2005. Microbial community activities during establishment, performance, and decline of bench-scale passive treatment systems for mine drainage. *Water Res.* 39(18):4537-4551.

Lozupone C, Hamady M, Knight R. 2006. UniFrac - An online tool for comparing microbial community diversity in a phylogenetic context. *BMC Bioinformatics* 7.

MacRae JD, Lavine IN, McCaffery KA, Ricupero K. 2007. Isolation and characterization of NP4, arsenate-reducing *Sulfurospirillum*, from Maine groundwater. *J. Environ. Eng.-ASCE* 133(1):81-88.

MassolDeya A, Weller R, RiosHernandez L, Zhou JZ, Hickey RF, Tiedje JM. 1997. Succession and convergence of biofilm communities in fixed-film reactors treating aromatic hydrocarbons in groundwater. *Appl. Environ. Microbiol.* 63(1):270-276.

- Matsui H, Ogata K, Tajima K, Nakamura M, Nagamine T, Aminov RI, Benno Y. 2000. Phenotypic characterization of polysaccharidases produced by four *Prevotella* type strains. *Curr. Microbiol.* 41(1):45-49.
- Morales TA, Dopson M, Athar R, Herbert RB. 2005. Analysis of bacterial diversity in acidic pond water and compost after treatment of artificial acid mine drainage for metal removal. *Biotechnol. Bioeng.* 90(5):543-551.
- Moreno B, Gomez MA, Gonzalez-Lopez J, Hontoria E. 2005. Inoculation of a submerged filter for biological denitrification of nitrate polluted groundwater: a comparative study. *J. Hazard. Mater.* 117(2-3):141-147.
- Muyzer G, Dewaal EC, Uitterlinden AG. 1993. Profiling of complex microbial populations by denaturing gradient gel electrophoresis analysis of polymerase chain reaction-amplified genes coding for 16S rRNA. *Appl. Environ. Microbiol.* 59(3):695-700.
- Pei RT, Kim SC, Carlson KH, Pruden A. 2006. Effect of River Landscape on the sediment concentrations of antibiotics and corresponding antibiotic resistance genes (ARG). *Water Res.* 40(12):2427-2435.
- Pruden A, Messner N, Pereyra L, Hanson RE, Hiibel SR, Reardon KF. 2007. The effect of inoculum on the performance of sulfate-reducing columns treating heavy metal contaminated water. *Water Res.* 41(4):904- 914.
- Russell JB, Rychlik JL. 2001. Factors that alter rumen microbial ecology. *Science* 292(5519):1119-1122.

Suzuki MT, Taylor LT, DeLong EF. 2000. Quantitative analysis of small-subunit rRNA genes in mixed microbial populations via 5'-nuclease assays. *Appl. Environ. Microbiol.* 66(11):4605-4614.

Swofford DL. 2002. PAUP*: Phylogenetic Analysis Using Parsimony (and Other Methods) 4.0 Beta, 4.0b10. Sinauer Associates I, editor. Sinauer Associates, Inc.

Thompson JD, Gibson TJ, Plewniak F, Jeanmougin F, Higgins DG. 1997. The CLUSTAL_X windows interface: flexible strategies for multiple sequence alignment aided by quality analysis tools. *Nucleic Acids Res.* 25(24):4876-4882.

von Canstein H, Kelly S, Li Y, Wagner-Dobler I. 2002. Species diversity improves the efficiency of mercury-reducing biofilms under changing environmental conditions. *Appl. Environ. Microbiol.* 68(6):2829-2837.

Watanabe K, Kodama Y, Harayama S. 2001. Design and evaluation of PCR primers to amplify bacterial 16S ribosomal DNA fragments used for community fingerprinting. *J. Microbiol. Methods* 44(3):253-262.

Weimer PJ. 1992. Cellulose degradation by ruminal microorganisms. *Crit. Rev. Biotechnol.* 12(3):189-223.

Xia SQ, Shi Y, Fu YG, Ma XM. 2005. DGGE analysis of 16S rDNA of ammonia-oxidizing bacteria in chemical-biological flocculation and chemical coagulation systems. *Appl. Microbiol. Biotechnol.* 69(1):99-105.

Chapter 5 Effect of Organic Substrate on the Microbial Community Structure of Pilot-Scale Sulfate-Reducing Permeable Reactive Zones Treating Mine Drainage

Pereyra, L.P., Hiibel, S.R., Prieto, M.V., Figueroa, L.A., Reisman, D.J., Reardon, K.F., and A. Pruden

(*in preparation for submission to Applied and Environmental Microbiology*)

Approximate contributions of each author are as follows:

L.P. Pereyra performed 50% of the sample collection, 100% of the Q-PCR, 75% of the Q-PCR data analysis, 20% of the sequence BLAST analysis, 75% of the PCoA, and 40% of the manuscript preparation.

S.R. Hiibel performed 50% of the sample collection, 25% of the Q-PCR data analysis, 20% of the 16S cloning, 100% of the *apsA* cloning, 50% of the sequence BLAST analysis, 25% of the PCoA, and 40% of the manuscript preparation.

M.V. Prieto performed 100% of the DNA extractions, 80% of the 16S cloning, 30% of the sequence BLAST analysis, and 20% of the manuscript preparation.

L.A. Figueroa assisted with experimental design.

D.J. Reisman assisted with experimental design and manuscript preparation.

K.F. Reardon and A. Pruden assisted with manuscript preparation.

5.1. Abstract

Passive biological systems such as sulfate-reducing permeable reactive zones (SR-PRZs) have shown promise for the treatment of mine drainage (MD) because of their low cost and minimal maintenance. However, few criteria exist for their design and operation and, in particular, the impact of the choice of carbon substrate is poorly understood. The purpose of this study was to explore the effect of the type of organic substrate on microbial communities present in pilot-scale SR-PRZs treating MD in order to understand how substrate-microbe interactions drive performance. Three organic substrates were evaluated: ethanol (ETOH); and two lignocellulose-based mixtures: hay and wood chips (HYWD), and corn stover and wood chips (CSWD). The microbial

community compositions were characterized by cloning and sequencing of 16S rRNA and *apsA* genes. Quantitative polymerase chain reaction was applied to quantify *Desulfovibrio-Desulfomicrobium* spp. and methanogens. Results revealed differences in microbial compositions and relative quantities of total and sulfate-reducing bacteria (SRB) among the SR-PRZs. In particular, the greatest proportion of SRB was observed in the ETOH SR-PRZs. In these reactors, the copies of the bacterial 16S rRNA gene were significantly lower than in the lignocellulose-based SR-PRZs. The HYWD and CSWD SR-PRZs contained highly similar bacterial communities, which were highly complex in composition relative to the ETOH SR-PRZs. Methanogens were found to be present in all SR-PRZs at low levels and were the highest in the lignocellulose-based reactors. This study demonstrates that substrate influences microbial community composition and diversity, which, in turn, may have an effect in SR-PRZ performance.

5.2. Introduction

Mine drainage (MD) is acidic to near-neutral; metal-rich water formed when sulfide minerals from abandoned or active mines are exposed to and react with oxygen and water. MD represents a worldwide concern due to its potential to cause contamination of drinking water systems, disruption of growth and reproduction of aquatic life, and other problems related to its toxicity (Banks et al. 1997). Because most remediation sites are remote or associated with abandoned mines, treatment systems that are efficient, cost-effective, and require minimal maintenance are highly desirable.

A variety of abiotic and biological remediation systems have been developed and used for the treatment of MD. Abiotic methods usually involve the addition of neutralizing agents or other chemicals and, although they might be effective, they can

require impractically high levels of operation and maintenance (Cohen 2006; Johnson and Hallberg 2005). Alternatively, bioremediation technologies have shown promise because of the low operational costs and minimal external energy requirements. In particular, sulfate-reducing permeable reactive zones (SR-PRZs) have been applied with success, for example, at the Wheal Jane (Whitehead and Prior 2005) and Nickel Rim (Benner et al. 1997) mines. However, reports from the field are variable in terms of the overall performance and reliability of these systems (Barton and Karathanasis 1999; Benner et al. 1997; Johnson and Hallberg 2002). The basic principle of SR-PRZs is the cultivation of sulfate-reducing bacteria (SRB) that reduce the sulfate in the mine drainage to sulfide, which, in turns, reacts with heavy metals and precipitates them as metal sulfides. Metal sulfides are immobilized within the SR-PRZ and thus removed from the water (Johnson and Hallberg 2005). Significant levels of alkalinity are also produced, which help neutralize the acidity.

A significant aspect of SR-PRZ design is the choice of organic substrate (Waybrant et al. 1998). Relatively simple substrates, such as organic acids or alcohols, have the advantage of providing a carbon and energy source that SRB can directly utilize for growth. The disadvantage, however, is that these compounds are used quickly and need to be continuously fed into the system, which increases the cost and maintenance (Cohen 2006). Alternatively, complex lignocellulose-based organic materials (e.g., wood chips) are biodegraded slowly providing a long-term source of carbon and energy compounds. In this case, SRB rely on the activities of anaerobic cellulose degraders and fermenters to break down the complex material into simpler molecules that support their growth (Logan et al. 2005).

Recent studies that used molecular biological tools have revealed the complexity of microbial communities in lignocellulose-based SR-PRZs (Hiibel et al. 2008; Johnson and Hallberg 2005; Pruden et al. 2007). In addition, the effect of the type of organic substrate on MD remediation has been extensively studied (Bechard et al. 1994; Figueroa et al. 2004; Waybrant et al. 1998) and recently reviewed by Neculita (2007). However, direct comparison of the microbial communities resulting from complex versus simple carbon substrates has not been determined previously. Differences in the recalcitrance of the substrate in SR-PRZs are likely to drive the development of distinct microbial communities in terms of types of microorganisms present, their relative abundance, and overall diversity. This, in turn, can have an impact on performance given that microbes are the primary catalysts of SR-PRZ function and that the composition of the microbial community impacts SR-PRZ performance (Pereyra et al. 2008; Pruden et al. 2007).

The purpose of this study is to explore the effect of the type of organic substrate on the resulting microbial communities in parallel pilot-scale SR-PRZs treating MD. Six pilot-scale SR-PRZs were operated in Black Hawk, Colorado, and were fed with discharge from the National Tunnel, which is a major contributor of contaminants to this area (Buccambuso et al. 2007). Three types of organic substrate were compared in duplicate: ethanol (ETOH 1,2), hay and wood chips (HYWD 3,4), and corn stover and wood chips (CSWD 5,6). Biomolecular characterization of the microbial populations included cloning of 16S rRNA gene and the adenosine-5'-phosphosulfate reductase (*apsA*) gene, and quantitative polymerase chain reaction (Q-PCR) targeting total bacteria, the *Desulfovibrio*-*Desulfomicrobium* genera of SRB, and methanogens. This is the first biomolecular comparison of the microbial communities involved in the remediation of

MD that originate from different organic substrates. A better understanding of substrate-microbe interactions can improve our understanding of the fundamentals of SR-PRZs function and therefore help develop better criteria for their design, operation, and overall performance.

5.3. Materials and methods

5.3.1. Sample Site and Collection

Six pilot-scale SR-PRZs were installed under the Mill Street Bridge in Black Hawk, Colorado on June 28-29, 2006 (Buccambuso et al. 2007) and fed with a water discharge from the National Tunnel. The discharge contains elevated levels of sulfate and heavy metals (zinc, copper, manganese, cadmium, lead, and arsenic) resulting from historic gold mining. The SR-PRZs consisted of 55-gallon drums that were filled or fed with one of three different organic substrates: ethanol, hay, or corn stover. The ethanol-fed SR-PRZs (ETOH 1,2) were packed with limestone and a zero valence iron slag layer on the top and inoculated with approximately 5 lb of horse manure layered on top of the limestone. Ethanol was added to the top of the reactors periodically. The lignocellulose-based SR-PRZs (HYWD 3,4 and CSWD 5,6) contained a mixture of wood chips, limestone, horse manure, and hay or corn stover in the proportions presented in Table 5.1.

During the SR-PRZs setup, five removable mesh bags were filled with the respective substrate and stacked in the center of each reactor within a vertical perforated PVC pipe to facilitate sampling. For sample collection, one mesh bag from each reactor (second from the topmost) was removed and placed on ice for immediate transport to the

laboratory where they were stored at -80 °C for biomolecular analyses. Sampling was performed on May 2007.

Table 5. 1: Proportion of solid substrate components in the HYWD and CSWD SR-PRZs

SR-PRZ		
	HYWD	CSWD
Component	Percentage (%)	
Wood Chips	50	35
Limestone	30	20
Horse Manure	10	15
Hay	10	0
Corn Stover	0	30

5.3.2. DNA Extraction

DNA was extracted from approximately 5 g of each of the collected samples using the PowerMax Soil DNA Isolation Kit (MO BIO, Carlsbad, CA) according to the manufacturer's protocol, and stored at -80 °C. The exact mass of material used in each extraction was determined and recorded for downstream quantification purposes.

5.3.3. 16S rDNA and *apsA* PCR Amplification and Cloning

To characterize the overall composition of the bacterial community and to identify dominant bacteria, cloning of 16S rRNA gene was performed. To specifically target SRB, *apsA* gene cloning was also performed. The 16S rRNA gene and *apsA* gene (Friedrich 2002) were amplified using primer sets 341F and 1492R (primer 1 of (Muyzer et al. 1993; Weisburg et al. 1991) and 7F and 8R (Friedrich 2002), respectively. PCR

products were cloned with the TOPO TA Cloning Kit (Invitrogen, Carlsbad, CA) according to the manufacturer's protocol. Inserts were amplified using the vector-specific primers T7 and T3. Amplified rDNA restriction analysis (ARDRA) was performed visually from PCR-amplified inserts digested with the *MspI* restriction enzyme (Promega, Madison, WI). Shannon Diversity Indices (H) were calculated as (Cox 1972):

$$H = - \sum_{i=1}^S p_i \ln(p_i)$$

where S is the size of the clone library and p_i is the relative abundance of each restriction pattern

The 16S rRNA gene clones with ARDRA patterns appearing two or more times and all *apsA* gene clones with unique enzymatic restriction patterns were sequenced. Because of the labor and cost associated with cloning of the 16S rRNA genes, cloning of these genes was performed on only one of each of the duplicate SR-PRZs.

5.3.4. Sequence Analyses

The DNA sequences obtained from cloning were aligned to the sequences of the most similar microorganisms identified by the Basic Local Alignment Search Tool (BLAST) (<http://www.ncbi.nlm.nih.gov/BLAST/>) and the Ribosomal Database Project II (RDP) (<http://rdp.cme.msu.edu/>). A literature review was performed to assign a putative function to the identified microorganisms. A phylogenetic tree was constructed using the 16S rRNA gene sequences of each of the unique clones identified, and 16S rRNA gene sequences of related microorganisms obtained from the National Center for Biotechnology Information Database.

5.3.5. Q-PCR

Total bacteria and the SRB genera *Desulfovibrio*-*Desulfomicrobium* were quantified by targeting the 16S rRNA gene. To quantify methanogens, primers targeting the gene that encodes the alpha subunit of the methyl coenzyme-M reductase (*mcrA*) were used.

All reactions were performed in a 7300 Real Time PCR cycler (Applied Biosystems, Foster City, CA). Reactions were set up in triplicate using 12.5 µL 1X Power SYBR Green PCR Master Mix (Applied Biosystems, Foster City, CA), 0.3 µM of primers DSV230f/DSV838r (Daly et al. 2000), and 0.25 mM of Mg(OAc)₂ for the *Desulfovibrio*-*Desulfomicrobium* Q-PCR, or 0.2 µM of *mcrA*-targeted primers designed by Luton and coworkers (2002) and 1mM of Mg(OAc)₂ for the methanogens Q-PCR. In addition, 1 µL of template DNA and deionized water to a final volume of 25 µL were added to the master mix. The temperature programs included 10 min at 95 °C followed by 60 cycles of 95 °C for 30 s, 64 °C for 37 s, and 72 °C for 60 s for the DSV primers or 50 cycles of 95 °C for 30 s, 56 °C for 40 s, and 72 °C for 40 s for the *mcrA* primers. Total bacterial 16S rRNA gene was quantified using the conditions, universal BACT1369F and PROK1492R primers, and the TM1389F probe described by Suzuki and coworkers (2000).

For the total bacteria and *Desulfovibrio*-*Desulfomicrobium* Q-PCRs, a five to six-point calibration curve was constructed using as standard purified PCR product amplified with primers 8F and 1492R (Eden et al. 1991; Weisburg et al. 1991) from a sample of the CSWD6 SR-PRZ and from a *Desulfovibrio salexigens* pure culture, respectively. Genomic DNA from *Methanococcus maripaludis* (ATCC 43000D) served as standard for the methanogens Q-PCR. Standards were analyzed in triplicate. The calibration curves

were used for absolute quantification of the target genes under the assumption that the amplification efficiency of standards and samples was the same. To ensure that only samples for which this assumption was valid were analyzed, the procedure proposed by Chervoneva and others (2006) was applied on the Q-PCR amplification efficiencies calculated with LinRegPCR (Ramakers et al. 2003).

5.3.6. Statistical Analyses

The phylogenetic trees of the 16S rRNA and *apsA* genes were analyzed directly using PCoA and the UniFrac significance tests of the UniFrac algorithm (Lozupone and Knight 2005). PCoA differs from principal component analysis in that the input data are the phylogenetic distances between each pair of sampling locations rather than the number of times each clone sequence was observed at each location. The UniFrac significance test was used to determine whether two microbial communities were significantly different (Lozupone and Knight 2005). For all analyses, non-normalized abundance data, based on the ARDRA screening, were incorporated in the UniFrac significance test. Reference strains used to construct the phylogenetic trees were not included in the analysis. A p-value ≤ 0.05 was considered to be statistically significant.

Q-PCR data was analyzed using the PROC GLM function of SAS 9.1 (SAS Institute Inc., Cary NC). Significance was defined by a pair-wise comparison p-value ≤ 0.05 .

5.4. Results

5.4.1. SR-PRZ Performance

Seasonal variations were observed in the rates of sulfate reduction in all the bioreactors. However, zinc removal was more than 95% in all the bioreactors and effluent zinc concentrations were below 0.1 mg/L (Buccambuso et al. 2007). Copper removal typically exceeded 95% (Venot et al. 2008). Before sampling for biomolecular analyses, operational problems resulted in the exposure to oxygen of the material in the EtOH1 and HYWD3.

5.4.2. Microbial Community Diversity and Composition

Rarefaction analysis of ARDRA patterns revealed that the overall bacterial diversity of the lignocellulose-based CSWD 5 SR-PRZ was significantly higher than that of the ethanol-fed ETOH 2 SR-PRZ (Figure 5.1). The overall diversity of the HYWD 3 reactor was similar to that of the ETOH 2 reactor.

Sequencing the 16S rRNA gene of the dominant clones also revealed differences between the SR-PRZs. Notably, the proportion of SRB in the ETOH 2 reactor was almost 70%, whereas SRB were only 2-5% in the HYWD 3 and CSWD 5 reactors (Figure 5.2). Other putative functional groups such as cellulose degraders were identified in the lignocellulose-based reactors and not in the ETOH reactor. Fermenters were estimated to be 25-30% of the lignocellulose-based communities and only 5% of the ETOH community.

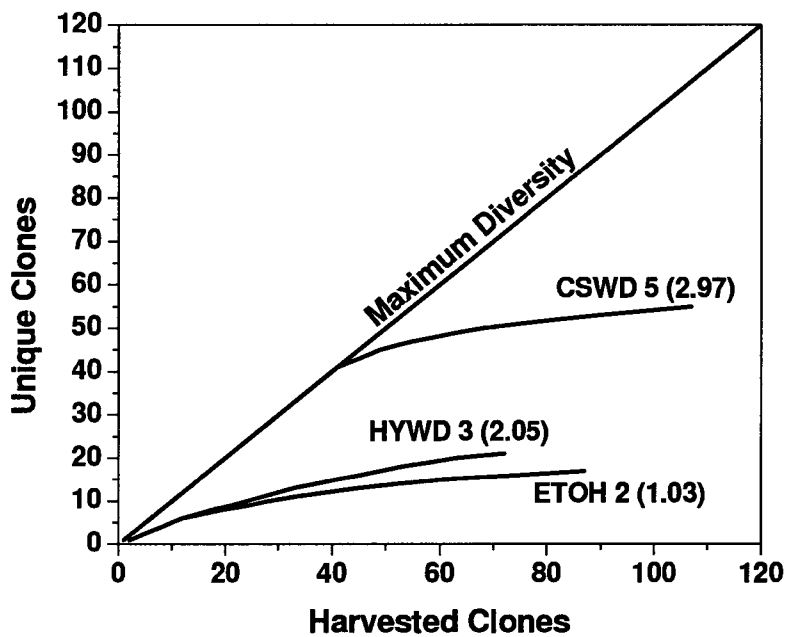


Figure 5.1: Relative diversity of the ETOH 2, HYWD 3, and CSWD 5 SR-PRZs determined by cloning of the 16S rRNA gene. Shannon diversity indices for each SR-PRZ are indicated in parenthesis and were calculated based on the frequency of each clone in the clone library.

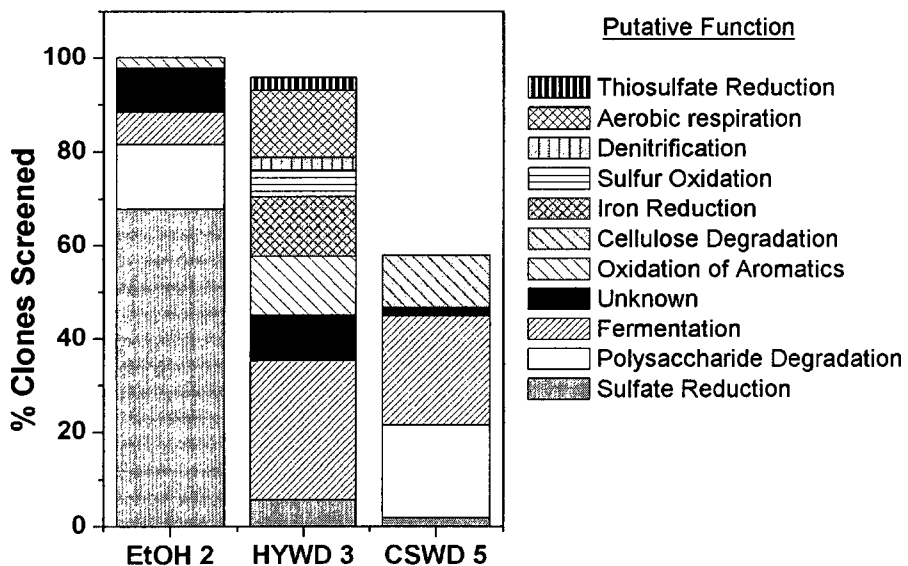


Figure 5.2: Distribution of microbial functions in each SR-PRZ based on the identity of the microorganisms identified through 16S rRNA gene cloning and DNA sequencing.

ApsA gene profiling revealed some overlaps and some differences between the lignocellulose and ETOH SR-PRZs (Figure 5.3). *Desulfovibrio aerotolerans* and an SRB most closely related to *Desulfovibrio* sp. JD160 were found in almost all of the SR-PRZs.

A *Desulfomicrobium baculum* relative was only found in two of the SR-PRZs, ETOH 1 and HYWD 3. In the lignocellulose SR-PRZs, some additional bacteria carrying the *apsA* gene were found: an uncultured bacterium that was present at about 10% in the HYWD 4, CSWD 5, and CSWD 6 SR-PRZs; *Thiobacillus* spp. (only in HYWD 3); and *D. desulfuricans* and *D. burkinensis*. *Thiobacillus* spp. have been recognized in the literature as aerobic and denitrifying organisms that reverse the process of sulfate reduction (Baker and Banfield 2003).

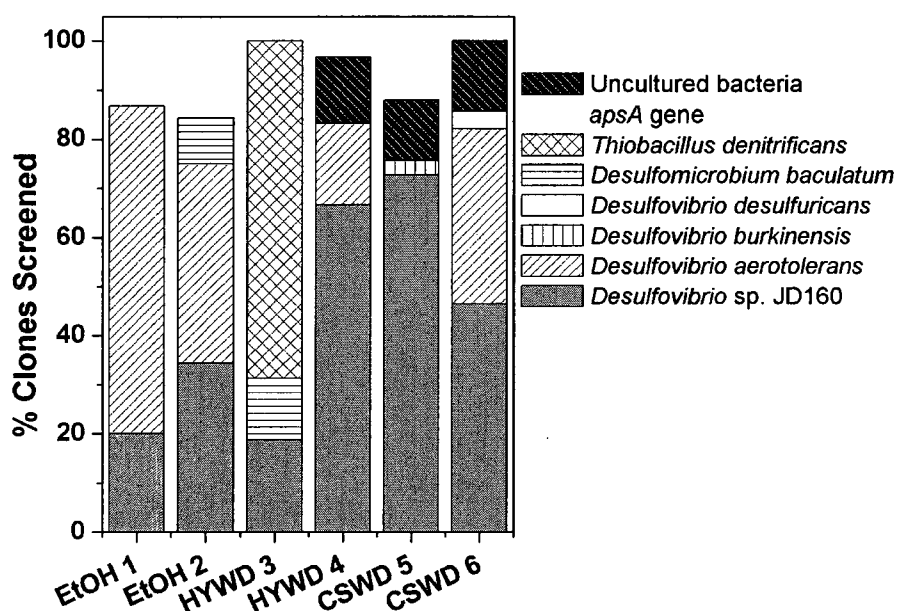


Figure 5. 3: Identity and percentages of *apsA*-containing microorganisms in ETOH, HYWD, and CSWD SR-PRZs.

PCoA provided a means to statistically compare the microbial communities (Figure 5. 4). PCoA analysis of 16S rDNA indicated that the ETOH 2, HYWD 3, and CSWD 6 communities were distinct across both coordinates. PCoA analysis of *apsA* genes, however, demonstrated that all of the SR-PRZs except HYWD 3 were relatively similar along the first coordinate, which explained 73% of the variability observed.

5.4.3. Quantification of Total Bacteria, SRB, and Methanogens

The results from the total bacteria, *Desulfovibrio-Desulfomicrobium*, and *mcrA* Q-PCRs were used to estimate the size of the bacterial community in each SR-PRZ (expressed as number of 16S rRNA gene copies per mass of substrate) and the relative proportion of the specific microbial groups (Figure 5.5). The ETOH 1 SR-PRZ contained a high percentage of SRB ($75\pm12\%$). However, the total number of bacteria was significantly lower in both ETOH SR-PRZs compared to the lignocellulose reactors. Methanogens were also significantly lower in the ETOH than in the lignocellulose reactors. In general, methanogens were present at a lower proportion than SRB. Overall, there were no significant differences in total bacteria or the two specific microbial groups among the lignocellulose-based SR-PRZs.

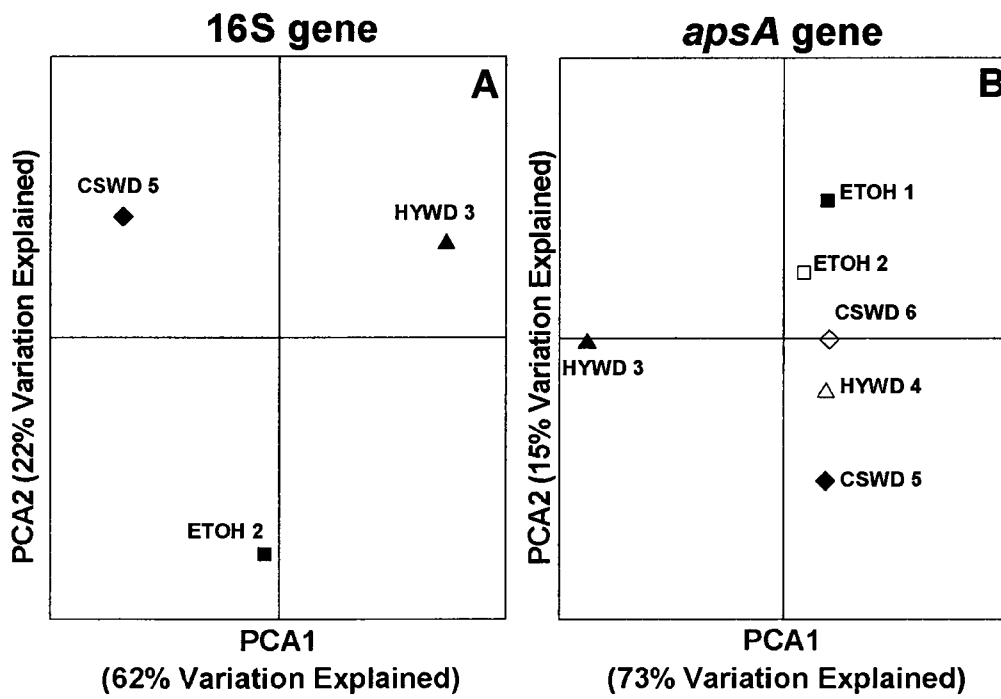


Figure 5.4: Principal coordinates analyses (PCoA) of the (A) total bacterial community based on 16S rRNA gene sequences and the (B) *apsA* gene-containing community based on *apsA* gene sequences.

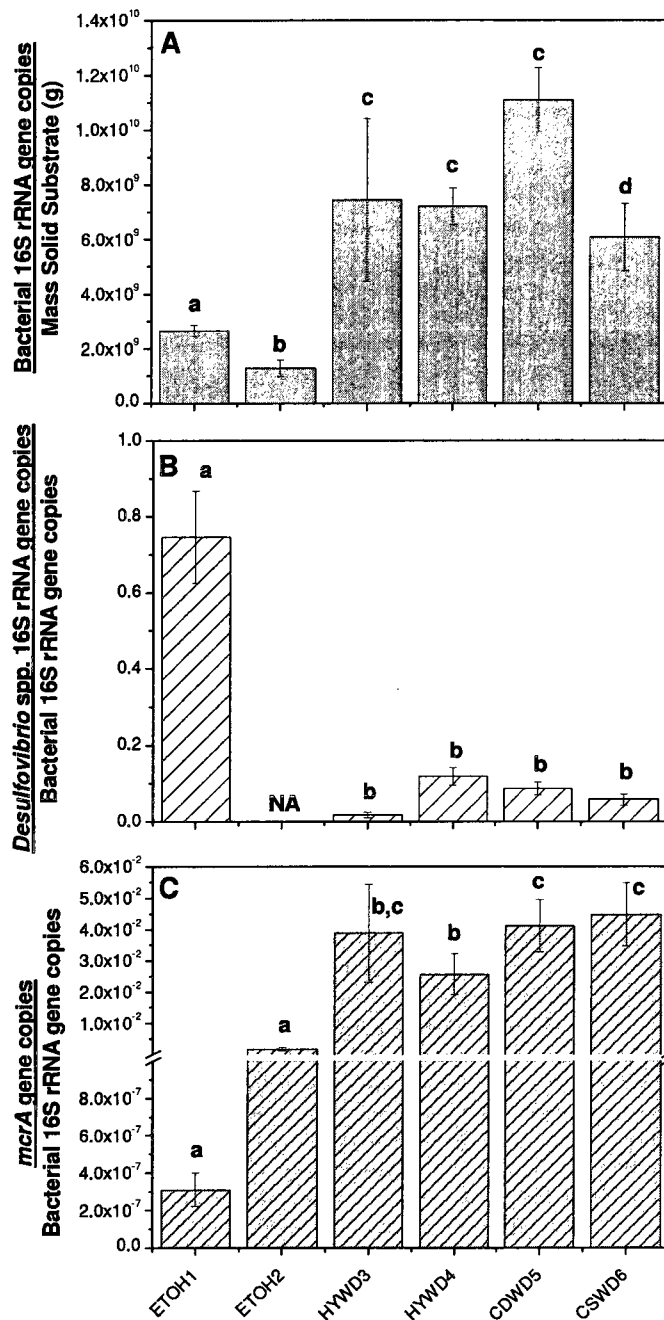


Figure 5. 5: Quantification of total bacteria, the SRB of the genus *Desulfovibrio*, and methanogenic microorganisms for the ETOH, HYWD, and CSWD SR-PRZs by Q-PCR. Total bacteria 16S rRNA gene copies normalized to mass of substrate (A), total *Desulfovibrio* spp. 16S rRNA gene copies normalized to total bacteria (B), and *mcrA* genes normalized to total bacteria (C). Bars with the same letter are not significantly different at the 0.05 level. NA – not analyzed.

5.5. Discussion

5.5.1. Effect of Type of Substrate on Community Composition

This study investigated the effect of different organic substrates on the microbial communities in pilot-scale SR-PRZs treating MD. As expected, different organic substrates yielded distinct communities. Key differences were observed between lignocellulose and ethanol-fed SR-PRZs in terms of total biomass, kinds of bacteria present, kinds of SRB present, and overall diversity.

Overall diversity of bacteria was found to be higher in the lignocellulose-based SR-PRZs. This was likely a result of the complexity of the substrate, which required a broader array of microbial functional groups for its breakdown compared to ethanol. In terms of the diversity of the SRB, there appeared to be a slight edge for the lignocellulose-based SR-PRZs. Between 3 and 4 different kinds of SRB were identified in the lignocellulose SR-PRZs compared to the ethanol-fed ones where only 2 to 3 different kinds were identified. Although all SRB carry out dissimilatory sulfate reduction, their substrate utilization capabilities, kinetics and other characteristics such as tolerance to oxygen exposure and other stresses may differ (Warren et al. 2005). This could have a significant impact on SR-PRZ performance. Though the proportion of SRB was higher in ETOH SR-PRZs, the total bacterial biomass was lower. This likely resulted from the reactor design in which the abiotic support material provided a small surface area to mass ratio as compared to the lignocellulosic material. A few other bacteria besides SRB were detected in the ETOH SR-PRZs, including putative fermenters and polysaccharide degraders. Their low-level presence is not necessarily surprising

considering that the horse manure used to inoculate the reactors would likely provide some residual substrate.

Both 16S rRNA gene cloning and Q-PCR indicated that the ethanol-fed SR-PRZs were dominated by SRB. Ethanol is a simple organic alcohol that can be directly utilized by most species of SRB (Rabus et al. 2000) and was the prevailing carbon source in the ETOH 1 and 2 SR-PRZs. This created a selective pressure that enriched the microbial community with microorganisms that could utilize this carbon source. Ethanol can also be consumed by some methanogens (Garcia et al. 2000). However, the proportion of these microorganisms in the ETOH SR-PRZs was lower than in the lignocelluloses based SR-PRZs, possibly because they could not outcompete the highly dominant SRB. Assuming that methanogens had an overall negative impact on SR-PRZ performance due to their competitive relationship with SRB, the low proportion of methanogens might be an advantage of ethanol-based SR-PRZs. However, methanogens may play a positive role as well. For example, some SRB have been inhibited in the presence of high concentrations of acetate, which can be easily removed by methanogens (Raskin et al. 1996).

The low levels of SRB in the lignocellulose-based SR-PRZs were typical of what has been observed by others (Hong et al. 2007; Morales et al. 2005; Pereyra et al. 2008; Pruden et al. 2007). In lignocellulose-based reactors, SRB depend on other microorganisms to obtain sources of energy. Cellulose degradation is a slow process and this limits the supply to microorganisms downstream of cellulose degradation such as SRB and methanogens (Logan et al. 2005). In addition, the greater microbial diversity

supported by the complex material could also lead to competitive interactions. These factors might explain the low numbers of SRB in the HYWD and CSWD SR-PRZs.

5.5.2. Microbial Composition and Operational Problems

During operation, the ETOH 1 and HYWD 3 SR-PRZs experienced problems that resulted in temporary exposure to the atmosphere. Interestingly, the microbial communities in these SR-PRZs presented some corresponding peculiarities. For example, methanogens were found to be lowest in the ETOH 1 SR-PRZ. Methanogens are strictly anaerobic microorganisms and the exposure to air might have had a detrimental effect on their survival in the SR-PRZ. In HYWD 3, *Thiobacillus* spp. were detected by *apsA* gene analysis. *Thiobacillus* spp. are aerobic or denitrifying organisms that convert sulfides to sulfates, thus reversing the process applied in remediation (Friedrich 1998). The presence of sulfur-oxidizing bacteria is consistent with a study of the field SR-PRZ Peerless Jenny King that is also periodically exposed to the atmosphere during seasonal low flow (Hiibel et al. 2008).

5.5.3. Implications for Response to an Environmental Stress

Interestingly, the performance of the six SR-PRZs was comparable (Venot et al. 2008), though the ETOH SR-PRZs offered some advantage in terms of overall sulfate and metals removal. The results of this study indicate that different microbial compositions and diversities can produce consistent sulfate and metal removal. This, however, raises the question of how these communities would perform in response to an environmental stress. In the field, SR-PRZs are exposed to below-freezing temperatures during winter, overloads of sulfate and metals, and exposure to air, among others. These factors are

likely to have an effect on the microorganisms and, thus, on the remediation performance. The higher microbial diversity of the lignocellulose-based SR-PRZs might represent an important advantage in terms of resilience to stress. Several studies have sited the importance of diversity in community stability. For example, von Canstein and others (2002), reported that increased microbial diversity improved the efficiency of mercury-reducing biofilms under changing environmental conditions by providing a reservoir of strains with complementary ecological niches. Given the regularity of changing environmental conditions in SR-PRZs and the potential effects that they can have on performance, the relationship between microbial community and stress in SR-PRZs should be further explored.

5.6. Conclusions

The results from this study suggest that ethanol-based bioreactors are effective for MD remediation and might be useful in locations that can be accessed year-round. Lignocellulose-based SR-PRZs still represent a less expensive and lower maintenance option since the organic substrate is made up of waste material that can indirectly support the SRB via a complex microbial community, without having to be constantly replenished. In addition, there may be advantages of lignocellulose-based SR-PRZs in terms of the overall diversity of the microbial community, which may aid in providing resilience to stress. Future research exploring this hypothesis, as well as the effects of other substrates, could be helpful in improving design and performance of SR-PRZs.

5.7. Acknowledgements

Financial assistance was provided by the EPA Office of Research and Development's Engineering Technical Support Center, under contract with Golder Associates, Inc., Contract # GS-10F00130N DO #1101 (David Reisman, Project Officer; reisman.david@epa.gov); and by the Water Research Experience for Undergraduates program at CSU sponsored by the National Science Foundation. Funding was also provided by the National Science Foundation Award CBET-0651947. This research has undergone EPA peer and policy review, and has been cleared for publication. Mention of commercial products does not constitute endorsement by the Agency.

5.8. References

- Baker BJ, Banfield JF. 2003. Microbial communities in acid mine drainage. FEMS Microbiol. Ecol. 44(2):139-152.
- Banks D, Younger PL, Arnesen RT, Iversen ER, Banks SB. 1997. Mine-water chemistry: the good, the bad and the ugly. Environ. Geol. 32(3):157-174.
- Barton CD, Karathanasis AD. 1999. Renovation of a failed constructed wetland treating acid mine drainage. Environ. Geol. 39(1):39-50.
- Bechard G, Yamazaki H, Gould WD, Bedard P. 1994. Use Of Cellulosic Substrates For The Microbial Treatment Of Acid-Mine Drainage. J. Environ. Qual. 23(1):111-116.
- Benner SG, Blowes DW, Ptacek CJ. 1997. A full-scale porous reactive wall for prevention of acid mine drainage. Ground Water Monit. Rem. 17(4):99-107.

Buccambuso E, Ruhs A, Figueroa L, Gusek J, Wildeman T, Holmes M, Reisman D.

Ethanol-fed or Solid-phase organic sulfate reducing bioreactors for the National Tunnel Drainage, Clear Creek/Central City Superfund Site?" 2007 June 2-7; Gillette, WY. p 95-105.

Chervoneva I, Hyslop T, Iglewicz B, Johns L, Wolfe HR, Schulz S, Leong E, Waldman S. 2006. Statistical algorithm for assuring similar efficiency in standards and samples for absolute quantification by real-time reverse transcription polymerase chain reaction. *Anal. Biochem.* 348(2):198-208.

Cohen RRH. 2006. Use of microbes for cost reduction of metal removal from metals and mining industry waste streams. *J. Clean Prod.* 14(12-13):1146-1157.

Cox GW. 1972. *Laboratory Manual of General Ecology*. Brown WC, editor. Dubuque, IA. 120-124 p.

Daly K, Sharp RJ, McCarthy AJ. 2000. Development of oligonucleotide probes and PCR primers for detecting phylogenetic subgroups of sulfate-reducing bacteria. *Microbiology-(UK)* 146:1693-1705.

Eden PA, Schmidt TM, Blakemore RP, Pace NR. 1991. Phylogenetic Analysis Of Aquaspirillum-Magnetotacticum Using Polymerase Chain Reaction-Amplified 16s Ribosomal-Rna-Specific Dna. *Int. J. Syst. Bacteriol.* 41(2):324-325.

Figueroa LA, Seyler J, Wildeman T. Characterization of organic substrates used for anaerobic bioremediation of mining impacted waters. In: Jarvis A, editor; 2004 International Mine Water Association Conference, September 20-25, 2004; Newcastle, England.

Friedrich CG. 1998. Physiology and genetics of sulfur-oxidizing bacteria. Advances In Microbial Physiology, Vol 39. London: Academic Press Ltd. p 235-289.

Friedrich MW. 2002. Phylogenetic analysis reveals multiple lateral transfers of adenosine-5'-phosphosulfate reductase genes among sulfate-reducing microorganisms. *J. Bacteriol.* 184(1):278-289.

Garcia JL, Patel BKC, Ollivier B. 2000. Taxonomic phylogenetic and ecological diversity of methanogenic Archaea. *Anaerobe* 6(4):205-226.

Hiibel SR, Pereyra LP, Inman LY, Tischer A, Reisman DJ, Reardon KF, Pruden A. 2008. Microbial community analysis of two field-scale sulfate-reducing bioreactors treating mine drainage. *Environ. Microbiol.* 10(8):2087-2097.

Hong H, Pruden A, Reardon KF. 2007. Comparison of CE-SSCP and DGGE for monitoring a complex microbial community remediating mine drainage. *J. Microbiol. Methods* 69(1):52-64.

Johnson DB, Hallberg KB. 2002. Pitfalls of passive mine water treatment. *Rev. Environ. Sci. Biotechnol.* 1(4):335-343.

Johnson DB, Hallberg KB. 2005. Acid mine drainage remediation options: a review. *Sci. Total Environ.* 338(1-2):3-14.

Johnson DB, Hallberg KB. 2005. Biogeochemistry of the compost bioreactor components of a composite acid mine drainage passive remediation system. *Sci. Total Environ.* 338(1-2):81-93.

Logan MV, Reardon KF, Figueroa LA, McLain JET, Ahmann DM. 2005. Microbial community activities during establishment, performance, and decline of bench-scale passive treatment systems for mine drainage. *Water Res.* 39(18):4537-4551.

- Lozupone C, Knight R. 2005. UniFrac: a new phylogenetic method for comparing microbial communities. *Appl. Environ. Microbiol.* 71(12):8228-8235.
- Luton PE, Wayne JM, Sharp RJ, Riley PW. 2002. The *mcrA* gene as an alternative to 16S rRNA in the phylogenetic analysis of methanogen populations in landfill. *Microbiology-(UK)* 148:3521-3530.
- Morales TA, Dopson M, Athar R, Herbert RB. 2005. Analysis of bacterial diversity in acidic pond water and compost after treatment of artificial acid mine drainage for metal removal. *Biotechnol. Bioeng.* 90(5):543-551.
- Muyzer G, Dewaal EC, Uitterlinden AG. 1993. Profiling of complex microbial populations by denaturing gradient gel electrophoresis analysis of polymerase chain reaction-amplified genes coding for 16S rRNA. *Appl. Environ. Microbiol.* 59(3):695-700.
- Neculita CM, Zagury GJ, Bussiere B. 2007. Passive treatment of acid mine drainage in bioreactors using sulfate-reducing bacteria: Critical review and research needs. *J. Environ. Qual.* 36(1):1-16.
- Pereyra LP, Hiibel SR, Pruden A, Reardon KF. 2008. Comparison of microbial community composition and activity in sulfate-reducing batch systems remediating mine drainage. *Biotechnology and bioengineering* 101(4):702-713.
- Pruden A, Messner N, Pereyra L, Hanson RE, Hiibel SR, Reardon KF. 2007. The effect of inoculum on the performance of sulfate-reducing columns treating heavy metal contaminated water. *Water Res.* 41(4):904- 914.
- Rabus R, Hansen T, Widdel F. 2000. Dissimilatory sulfate- and sulfur-reducing prokaryotes. In: Dworkin M, Falkow S, Rosenberg E, Schleifer KH, Stackebrandt

- E, editors. *The Prokaryotes: An Evolving Electronic Resource for the Microbiological Community* (3rd ed.). New York.
- Ramakers C, Ruijter JM, Deprez RHL, Moorman AFM. 2003. Assumption-free analysis of quantitative real-time polymerase chain reaction (PCR) data. *Neurosci. Lett.* 339(1):62-66.
- Raskin L, Rittmann BE, Stahl DA. 1996. Competition and coexistence of sulfate-reducing and methanogenic populations in anaerobic biofilms. *Appl. Environ. Microbiol.* 62(10):3847-3857.
- Suzuki MT, Taylor LT, DeLong EF. 2000. Quantitative analysis of small-subunit rRNA genes in mixed microbial populations via 5'-nuclease assays. *Appl. Environ. Microbiol.* 66(11):4605-4614.
- Venot C, Figueroa L, Brennan RA, Wildeman TR, Reisman D, Sieczkowski M. Comparing chitin and organic substrates on the National Tunnel waters in Blackhawk, Colorado, for manganese removal.; 2008 June 14 to 19; Richmond, VA.
- von Canstein H, Kelly S, Li Y, Wagner-Dobler I. 2002. Species diversity improves the efficiency of mercury-reducing biofilms under changing environmental conditions. *Appl. Environ. Microbiol.* 68(6):2829-2837.
- Warren YA, Citron DM, Merriam CV, Goldstein EJC. 2005. Biochemical differentiation and comparison of *Desulfovibrio* species and other phenotypically similar genera. *J. Clin. Microbiol.* 43(8):4041-4045.

Waybrant KR, Blowes DW, Ptacek CJ. 1998. Selection of Reactive Mixtures for Use in Permeable Reactive Walls for Treatment of Mine Drainage. Environ. Sci. Technol. 32:1972-1979.

Weisburg WG, Barns SM, Pelletier DA, Lane DJ. 1991. 16s Ribosomal Dna Amplification For Phylogenetic Study. J. Bacteriol. 173(2):697-703.

Whitehead PG, Prior H. 2005. Bioremediation of acid mine drainage: an introduction to the Wheal Jane wetlands project. Sci. Total Environ. 338(1-2):15-21.

**Chapter 6 Development of PCR Primers Targeting Functional Genes for the
Detection and Quantification of Cellulose-Degrading, Fermentative,
and Sulfate-Reducing Bacteria, and Methanogenic Archaea.**

Pereyra, L.P., Pruden, A., and Reardon, K.F.

(*In preparation for submission to Applied and Environmental Microbiology*)

6.1. Abstract

Cellulose degradation, fermentation, sulfate reduction, and methanogenesis are microbial processes that coexist in a variety of natural and engineered environments such as rumen, sediments, soil, wetlands and sulfate-reducing bioreactors. 16S rRNA genes are poor targets for study of these functional guilds due to their broad phylogenetic diversity. Targeting genes encoding the enzymes that catalyze these functions is advantageous because it provides direct functional information. However, methods are not available for their quantification in complex environments. In this study, consensus degenerate hybrid oligonucleotide primers were designed and validated to amplify both sequenced and unsequenced cellulase genes of anaerobic cellulose-degrading bacteria, *hydA* genes of fermentative bacteria, *dsrA* genes of sulfate-reducing bacteria, and *mcrA* genes of methanogenic archaea. Specificity was verified *in silico* and by cloning and sequencing of the polymerase chain reaction (PCR) products obtained from a complex sulfate-reducing environmental sample. The primer pairs were further adapted to

quantitative PCR (Q-PCR) and demonstrated on samples obtained from a lignocellulose-based and an ethanol-fed sulfate-reducing bioreactor. As expected, Q-PCR indicated that the lignocellulose-based bioreactor contained higher numbers of cellulose degraders, fermenters and methanogens, while the ethanol-fed bioreactor was enriched in sulfate reducers. The suite of tools developed in this study represent a significant advance in terms of their specificity to key functional guilds, their quantitative nature, and the access they provide to uncultured and unsequenced environmental targets. These attributes will be of particular value for characterizing microbial communities that drive important biogeochemical processes in the environment.

6.2. Introduction

The advent of biomolecular techniques has significantly improved our knowledge of the composition, diversity, and distribution of microbial populations (Amann and Ludwig 2000). In particular, they have allowed the identification of microorganisms (including as of yet not cultured bacteria) through their DNA sequence. This circumvents the need for cultivation and provides a more complete and unbiased description of microbial communities.

Traditionally, the gene that encodes the 16S small subunit of the ribosomes (16S rRNA gene) has served as a highly suitable target for studying bacterial species for several reasons: it is present in all microorganisms, its size provides enough genetic diversity, and it contains both conserved and variable regions (Amann and Ludwig 2000). Upon obtaining 16S rRNA gene sequence information, function may be inferred from an identical match to a well-characterized pure culture. More commonly, however, the similarity to pure cultures is low and/or the highest similarities correspond to 16S rRNA

gene sequences identified without isolation or phenotypic characterization of the microorganisms. Either situation, however, is prone to erroneous conclusions because several distinct phenotypes (e.g., strict anaerobic metabolism, dissimilatory Fe(III) reduction, and chlorate reduction) are found in microorganisms with highly similar (e.g. 99.5%) 16S rRNA gene sequences (Achenbach and Coates 2000). In addition, 16S rRNA gene surveys of broad phylogenetic groups can be time, labor, and cost intensive. For example, the 16S rRNA gene-based polymerase chain reaction (PCR) detection of all recognized lineages of sulfate-reducing bacteria (SRB) would require approximately one hundred and thirty two 16S rRNA gene-targeted primer sets (Loy et al. 2002). Handelsman (2004) estimated that approximately one million clones would have to be sequenced to cover the phylogenetic diversity of the more than 10,000 species in soil.

The 16S rRNA gene-based approach has been used to characterize the microbial communities of a variety of natural and engineered anaerobic environments such as rumen (Whitford et al. 1998), termites' gut (Warnecke et al. 2007), decomposing wood (Borsodi et al. 2005), sulfate-reducing and methanogenic sediments (Cardenas et al. 2008; Heijs et al. 2007), wetlands (Ibekwe et al. 2003), and sulfate-reducing bioreactors (Hiibel et al. 2008). In these environments, mineralization of complex organic matter occurs through the concerted action of a variety of microorganisms. Primary fermenters such as cellulose degraders break down the complex molecules and ferment the hydrolysis products. Secondary fermenters also ferment the hydrolysis products. In sulfate-rich environments, SRB utilize the fermentation products as carbon and energy sources. In addition, methanogens can also grow on some of the fermentation products. 16S rRNA gene sequences from these environments are affiliated to a variety of major

phyla such as *Cytophaga-Flexibacter-Bacteroides*, *Proteobacteria*, *Spirochetes*, *Firmicutes*, and *Fibrobacteres*. Studies based on the 16S rRNA gene revealed the complexity of these communities and their high level of phylogenetic and functional diversity. In some of these environments, important members of the microbial community such as SRB are a small fraction of the community (Morales et al. 2005; Pereyra et al. 2008) which makes difficult their detection with 16S rRNA gene-targeted fingerprinting methods such as denaturing gradient gel electrophoresis. Furthermore, the phylogenetic diversity of SRB, cellulose degraders and fermenters prevents their quantification using a small number of 16S rRNA gene-targeted probes.

For the study of microbial groups that span phylogenetic groups, a more fruitful approach is to target them as a physiological coherent guild by using specific genetic markers for the functions of interest (a.k.a. functional genes) instead of the 16S rRNA gene (Sun et al. 2004). Functional genes have been targeted in bioremediation studies to investigate microbial populations responsible for the degradation of contaminants. Some examples include the use of the large alpha subunit of benzylsuccinate synthase to monitor anaerobic hydrocarbon-degrading bacteria (Beller et al. 2002), the monitoring of *ars* genes for the identification and quantification of arsenic-metabolizing bacteria (Sun et al. 2004), and the detection of catechol 1,2-dioxygenase in aromatic-hydrocarbon-degrading *Rhodococcus* spp. (Tancsics et al. 2008). Analysis of functional genes has also been useful in the investigation of microorganisms involved in nutrient cycling such as the phylogenetically widespread denitrifying bacteria (Braker et al. 1998). In the field of mine drainage remediation, functional genes have been used to target SRB (Geets et al. 2006; Hiibel et al. 2008). However, a major limitation has been the relative lack of

characterization and available sequences of functional genes. As a consequence, the few methods that are available tend to be more relevant to pure cultures, rather than complex environmental samples.

In this study, we develop, validate, and demonstrate PCR primers for the amplification of previously sequenced and unsequenced genetic markers of anaerobic cellulose-degrading bacteria, fermentative bacteria, sulfate-reducing bacteria, and methanogenic archaea.. The specificity of the primers to key functional guilds, their adaptability to quantitative PCR (Q-PCR), and their suitability for complex environmental samples will be of significant value for characterizing the microbial role in important biogeochemical processes.

6.3. Materials and Methods

6.3.1. Primer Design

Although a functional gene-based approach has several advantages over the 16S rRNA gene-based approach, its success greatly depends on the proper selection of target functional genes. These genes not only have to be present in all the microorganisms that perform a function of interest but they also have to be exclusive to that function. In addition, there can be different degrees of sequence divergence which might require the design of more than one primer set to cover the gene diversity. The genes encoding for the glycoside hydrolases of the Families 5 and 48 (collectively designated in this study as *cel5* and *cel48* genes) were selected as functional markers for cellulose degradation. The genes encoding for the alpha subunits of iron hydrogenase (*hydA*), dissimilatory sulfite

reductase (*dsrA*), and methyl coenzyme M reductase (*mcrA*) were selected to target fermenters, SRB, and methanogens, respectively.

The COnsensus-DEgenerate Hybrid Oligonucleotide Primer (CODEHOP) strategy (Rose et al. 1998) was used to design all primer sets. CODEHOPs are hybrid primers that contain a relatively short 3' degenerate core and a 5' non-degenerate consensus clamp which stabilizes the hybridization of the 3' end (Rose et al. 1998). This design approach overcomes the problem of having weak or undetectable bands due to low concentration of any single primer in degenerate PCR and the lack of amplification of distantly related sequences due to primer-to-template mismatches observed when a consensus primer set is used. The CODEHOP strategy is based on reverse translation of multiply aligned sequences across the conserved regions of proteins (blocks). The protein sequences used to design primers were downloaded from the National Center Biotechnology Information (NCBI) database and a subset representative of the diversity within each functional group was selected (Table 6.1).

For each set of sequences, the Block Maker program (Henikoff et al. 1995) was used to create an alignment and identify conserved regions or 'blocks' using two different algorithms (MOTIF and Gibbs). Optimal blocks contain 3-4 highly conserved amino acids with restricted codon multiplicity and five or more conserved amino acids. The blocks found with the Gibbs algorithm were used as input for the CODEHOP program (<http://bioinformatics.weizmann.ac.il/blocks/codehop.html>). Primers were designed using all codon possibilities for 3' degenerate core and the most frequent nucleotide in each position for the 5' consensus clamp. The primers were arranged in pairs that would yield

an amplicon of suitable size for Q-PCR amplification (150 bp is considered ideal and 450 bp was selected as the maximum allowable size).

Table 6. 1: Sequences used for the design of the *cel5*, *cel48*, *hydA*, *dsrA*, and *mcrA* primer sets.

Primer Set	Target Gene	Microorganism	NCBI Accession #	
			Gene Bank	Gene Pept
<i>cel48</i>	<i>celS</i>	<i>Clostridium thermocellum</i>	L06942	AAA23226
	<i>celY</i>	<i>Clostridium thermocellum</i>	AJ863163	CAI06105
	<i>celA</i>	<i>Bacteroides cellulosolvens</i>	AY374129	AAR23324
	<i>celD</i>	<i>Clostridium josui</i>	AB004845	BAA32430
	<i>celF</i>	<i>Clostridium cellulolyticum</i>	U30321	AAB41452
	<i>celF</i>	<i>Clostridium acetobutylicum</i>	AE001437	AAK78887
	<i>celA</i>	<i>Ruminococcus albus</i>	AY422811	AAR01217
<i>cel5</i>	<i>celG</i>	<i>Fibrobacter succinogenes</i>	U33887	AAB38548
	<i>endA</i>	<i>Ruminococcus flavefaciens</i>	S55178	AAB19708
	<i>endI</i>	<i>Butyrivibrio fibrisolvens</i>	X17538	CAA35574
	<i>egl</i>	<i>Bacteroides ruminicola</i>	M38216	AAA22909
	<i>engE</i>	<i>Clostridium cellulovorans</i>	AF105331	AAD39739
	<i>celA</i>	<i>Clostridium longisporum</i>	L02868	AAC37035
<i>hydA</i>	<i>hydA</i>	<i>Clostridium acetobutylicum</i> ATCC 824	U15277	AAB03723
	<i>hydA</i>	<i>Clostridium pasteurianum</i> ATCC 6013	M81737	AAA23248
	<i>hydA</i>	<i>Clostridium perfringens</i> NCTC 8237	AB016775	BAA74726
	<i>hydA</i>	<i>Clostridium saccharobutylicum</i>	U09760	AAA85785
	<i>hydA</i>	<i>Clostridium difficile</i> strain 630	NC_009089	YP_001089927
	<i>hydA</i>	<i>Clostridium novyi</i> NT	NC_008593	YP_877778
	<i>hydA</i>	<i>Clostridium thermocellum</i> ATCC 27405	AF148212	AAD33071
<i>dsrA</i>	<i>dsrA</i>	<i>Desulfobacterium aniline</i>	AF482455	AAQ05939
	<i>dsrA</i>	<i>Desulfobacterium autotrophicum</i>	AF418182	AAL57437
	<i>dsrA</i>	<i>Desulfococcus multivorans</i>	U58126	AAC24101
	<i>dsrA</i>	<i>Desulfobacter curvatus</i>	AF418199	AAL57471
	<i>dsrA</i>	<i>Desulfobacter postgatei</i>	AF418198	AAL57469
	<i>dsrA</i>	<i>Desulfotomaculum ruminis</i>	U58118	AAC24103
	<i>dsrA</i>	<i>Desulfobulbus propionicus</i>	AF218452	AAG28585
	<i>dsrA</i>	<i>Desulfovibrio aerotolerans</i>	AY749039	AAU95684
	<i>dsrA</i>	<i>Desulfovibrio alkalitolerans</i>	AY864856	AAW83205
	<i>dsrA</i>	<i>Desulfovibrio burkenensis</i>	AF418186	AAL57445
	<i>dsrA</i>	<i>Desulfovibrio desulfuricans</i>	DQ092635	AAZ04355
<i>mcrA</i>	<i>dsrA</i>	<i>Desulfovibrio vulgaris</i>	U16723	AAA70107
	<i>mcrA</i>	<i>Methanococcus voltae</i>	X07793	CAA30633
	<i>mcrA</i>	<i>Methanococcus vannielii</i>	M16893	AAA72595
	<i>mcrA</i>	<i>Methanothermus fervidus</i>	J03375	AAA72197
	<i>mcrA</i>	<i>Methanosarcina barkeri</i>	Y00158	CAA68357
	<i>mcrA</i>	<i>Methanocaldococcus jannaschii</i>	L77117	AAB98851
	<i>mcrA</i>	<i>Methanothermobacter thermautotrophicus</i>	NC_000916	NP_276292
	<i>mcrA</i>	<i>Methanopyrus kandleri</i>	U57340	1E6VA

6.3.2. Primer Validation

6.3.2. Environmental Samples

Two environmental samples collected from pilot-scale sulfate-reducing biochemical reactors receiving acid mine drainage from the National Tunnel in Black Hawk, CO, were selected for primer validation. The sample sources were particularly suitable because they differ only in the type of carbon substrate applied to support the microbial community. The first sample contained a complex lignocellulose-based substrate [wood chips (35%), limestone (20%), and corn stover (30%)] and, therefore, was expected to maintain a complex community including cellulose degraders, fermenters, sulfate reducers and methanogens. The second received ethanol as its primary substrate. Since ethanol contains no cellulose and is a fermentation product, this community was expected to be dominated by sulfate reducers. In addition the ethanol bioreactor was packed with limestone and a zero valent iron (ZVI) slag layer on the top. Both bioreactors were inoculated with horse manure.

6.3.2.2. Genomic DNA from Pure Cultures

Genomic DNA from the following microorganisms was used as positive/negative control for PCR: *Clostridium thermocellum* (ATCC 27405D), *Methanococcus maripaludis* (ATCC 43000D), *Desulfobacterium autotrophicum* (ATCC 43914D).

Pure cultures of the following microorganisms were grown in the laboratory and their DNA was used as positive/negative control for PCR: *Escherichia coli*, *Clostridium cellulovorans* (ATCC 35296), *Ruminococcus flavefaciens* (ATCC 49949), and *Fibrobacter succinogenes* strain B1 (ATCC 51214).

6.3.3. DNA Extraction

DNA was extracted from approximately 5 g of each of the environmental samples using the PowerMax Soil DNA Isolation Kit (MO BIO, Carlsbad, CA) according to the manufacturer's protocol, and stored at -80 °C for subsequent studies.

For the pure cultures, DNA was extracted using the UltraClean™ Microbial DNA Isolation Kit (Mo BIO) according to the manufacturer's instructions and stored at -80 °C.

6.3.4. Optimization of PCR Conditions

An annealing temperature optimization was performed for all the primer sets. The following temperatures were tested: 52.9 °C, 54.3 °C, 55.8 °C, 59.2 °C, and 60.7 °C (*cel48*); 52 °C, 52.8 °C, 53.9 °C, 55.3 °C, 56.9 °C, 58.5 °C, 60.2 °C, 61.7 °C, 63 °C, and 64 °C (*cel5*); 56 °C, 58.8 °C, 62.8 °C, and 65.2 °C (*hydA*), 60.0 °C and 63 °C (*dsrA*), and 53.6 °C, 54.7 °C, 56.0 °C, 58.8 °C, and 60.1 °C (*mcrA*). The annealing temperature was chosen based on the presence of one band of PCR product of the expected size in a 1.2% agarose gel for the positive controls and the absence of PCR product in the negative controls. In addition, a magnesium optimization at the chosen annealing temperature was done for the environmental samples.

6.3.5. Cloning

PCR products from the lignocellulose-based substrate collected from the National Tunnel site were cloned with the TOPO TA Cloning Kit (Invitrogen, Carlsbad, CA) according to the manufacturer's protocol. Inserts were PCR amplified directly from colonies using M13F and M13R primers for further analysis.

6.3.6. Selection of Restriction Enzymes

The Restriction Enzyme Database (REBASE) (Roberts et al. 2007) was used to select restriction endonucleases to digest the PCR products from the following primer sets: *cel5_392F/754R*, *cel48_490F/920R*, *hydA_1290F/1538R*, *dsrA_290F/660R*, and *mcrA_1035F/1530R*. The priming site of each primer was identified by aligning the primer sequence to a DNA alignment of the reference sequences used in their design. The DNA sequence comprised between the priming sites was submitted to the NEBcutter V2.0 tool of REBASE which provided a list of the restriction enzymes that could cut the DNA sequence and the cleavage sites along the sequence. Only restriction enzymes that could cut all the sequences used to design a given primer set were considered. From these enzymes, one was selected per primer set based on their ability to differentiate among different sequences and the feasibility of differentiating patterns in a 3% agarose gel (i.e., enzymes that cut the sequences into several fragments of less than 100 bp were not considered). The restriction enzymes Hpy188III, MboI, MnII, NlaIII, and MboII (New England Biolabs, Ipswich, MA) were chosen to digest the PCR products from the primer sets *cel5*, *cel48*, *hydA*, *dsrA*, and *mcrA*, respectively.

6.3.7. Restriction Enzyme Digestion and DNA Sequencing

Enzymatic digestion conditions were optimized to minimize the time and amount of reagents required to completely digest the DNA. The template for all reactions was the insert recovered from the clones through PCR with M13 primers. For all the enzymes, the optimized master mix contained 1X of the corresponding buffer (provided with the enzyme), 0.5 U (*hydA*), 1 U (*cel48*, *dsrA*, and *mcrA*), or 2 U (*cel5*) of the corresponding

enzyme, 1 μ L (*hydA* and *dsrA*) or 2 μ L (*cel5*, *cel48*, *mcrA*) of the M13 PCR product, and sterilized deionized water to a final volume of 20 μ L. The master mix for the *cel5*, *hydA*, and *dsrA* PCR products also contained 100 μ g/mL of bovine serum albumin. The reactions were incubated at 37 °C for 1 h (*mcrA*), 1.5 h (*cel5* and *hydA*), or 3 h (*cel48* and *dsrA*) followed by an inactivation step of 20 minutes at 65 °C. The digestion products were run in a 3% agarose gel and restriction patterns were visually inspected. For each unique restriction pattern, at least one clone was sequenced. Sequencing was performed by the Proteomics and Metabolomics Facility (Colorado State University, Fort Collins, CO). The closest matches to microorganisms available in the NCBI database were determined using the Basic Local Alignment Search Tool X (BLASTX) (<http://blast.ncbi.nlm.nih.gov/Blast.cgi>) which searches the protein database using a translated nucleotide query.

6.2.8. Q-PCR

The *cel5*, *cel48*, *hyd*, *dsrA*, and *mcrA* primer sets were adapted to Q-PCR and further validated by quantifying the functional genes in samples collected from the lignocellulose- and ethanol-based sulfate-reducing bioreactors. In addition, total bacterial 16S rRNA gene was quantified using the conditions, universal BACT1369F and PROK1492R primers and the TM1389F probe described by Suzuki et al. (2000). For the functional gene primers, Q-PCR amplification was performed on a 7300 Real-Time PCR System (Applied Biosystems, Foster City, CA) using a 12.5- μ L reaction mixture of 1X *Power SYBR® Green PCR Master Mix* (Applied Biosystems); 0.15 μ M (*cel48*, *hydA*, and *dsrA*), 0.2 μ M (*mcrA*), or 0.25 μ M (*cel5*) of each primer; 1 mM (*mcrA* and *hydA*), 1.5

mM (*dsrA*) or 2.5 mM (*cel5*) Mg(OAc)₂ 25 mM; additional 0.25 U (*dsrA*) or 0.375 U (*cel5*) of iTaq DNA polymerase (Bio-Rad); and 1 µL of template with a temperature program of 10 min at 95 °C followed by 40 (*cel48* and *mcrA*), 45 (*hydA* and *cel5*) or 50 (*dsrA*) cycles of 40 s at 95 °C, 30 s at the corresponding annealing temperature (Table 6.2), and 30 s at 72 °C. Samples were diluted 1:10 and analyzed in five replicates.

Table 6. 2: Temperature programs used for PCR amplification of *cel5*, *cel48*, *hydA*, *dsrA*, and *mcrA* genes using the primer sets selected after specificity validation.

Primer Set	Initial Denaturation	Denaturation	Annealing	Extension	Final Extension
<i>cel48_490F/ cel48_920R</i>	95 °C, 3 min	95 °C, 40 s	56 °C, 30 s	72 °C, 30 s	72 °C, 7 min
			40 cycles		
<i>cel5_392F/ cel5_754R</i>		95 °C, 40 s	52 °C, 30 s	72 °C, 30 s	
			45 cycles		
<i>hydA_1290F/ hydA_1538R</i>		95 °C, 40 s	59 °C, 30 s	72 °C, 30 s	
			35 cycles		
<i>dsrA_290F/ dsrA_660R</i>		95 °C, 40 s	60 °C, 30 s	72 °C, 30 s	
			50 cycles		
<i>mcrA_1035F/ mcrA_1530R</i>		95 °C, 40 s	56 °C, 30 s	72 °C, 30 s	
			35 cycles		

For each functional gene primer set, a 4 to 6-point calibration curve was constructed using a mixture of purified PCR products obtained with the plasmid-specific primers T3-T7 from sequenced clones as standard. For the 16S rRNA gene primer set, purified PCR product amplified from an environmental sample with primers 8F and 1492R (Eden et al. 1991; Weisburg et al. 1991) was used as standard. Standards were analyzed in triplicate. The calibration curves were used for absolute quantification of the target genes under the assumption that the amplification efficiency of standards and samples was the same. To ensure that only samples for which this assumption was valid were analyzed, the procedure proposed by Chervoneva et al (Chervoneva et al. 2006) was applied. Briefly, LinRegPCR (Ramakers et al. 2003) was used to calculate the

amplification efficiency from the amplification curve of each replicate sample and standard. A box plot outlier detection rule was applied to the amplification efficiency of the standards to identify calibration standards that amplified with dissimilar efficiencies. These standards were not used in the data analysis. The Kinetic Outlier Detection (KOD) method (Bar et al. 2003) was used to compare the average efficiency of the remaining standards and the efficiency of each replicate to detect samples with dissimilar efficiencies from the standards. A more detailed explanation of the role of PCR efficiency in Q-PCR and the different methods to calculate it is presented in Appendix A.

6.4. Results

6.4.1. Primers Design

Using the Gibbs algorithm of the Block Maker program, a total of 12, 5, 7, 5, and 8 blocks of conserved amino acids were found in the multiple alignments of the *cel5*, *cel48*, *hydA*, *dsrA*, and *mcrA* protein sequences presented in Table 6.1, respectively (additional details available in Appendix B). These blocks were used as input to the CODEHOP program to design primers specific to each of the target genes. The output of the CODEHOP program consists of a series of forward and reverse primers for each block with their corresponding degeneracies of the '3' core and annealing temperature. The CODEHOP default parameters were used for the design of all primer sets. For each block, the primer with the lowest degeneracy was selected and its sequence was compared *in silico* against the NCBI nucleotide database to confirm target specificity. Primer sequences that did not match the desired target were discarded and the primer with the next lowest degeneracy was compared to the sequences in the NCBI database.

The primers that were identified as specific were aligned with the DNA sequences of the proteins used for the design and manually modified by increasing the degeneracy to improve the match of the primer with the reference sequences or by decreasing it where the degeneracy in the primer was higher than that observed in the alignment of reference sequences. This process is illustrated in Figure 6.1 for the design of one of the *cel48* primers. Based on this process, a total of three primer sets for the *mcrA*, two for the *cel5*, *cel48*, and *dsrA*, and one for the *hydA* sequences were selected for optimization and validation by PCR (Table 6.3). One of the *dsrA* primer sets contains a modified version of the reverse primer RH3-dsr-R designed by Ben-Dov (Ben-Dov et al. 2007) and an in-house-designed forward primer. One of the *mcrA* primer sets (*mcrA_1035F/1530R*) was designed by Luton et. al. (2002). The other two *mcrA* primer pairs combine one of the Luton primers with one in-house-designed primer.

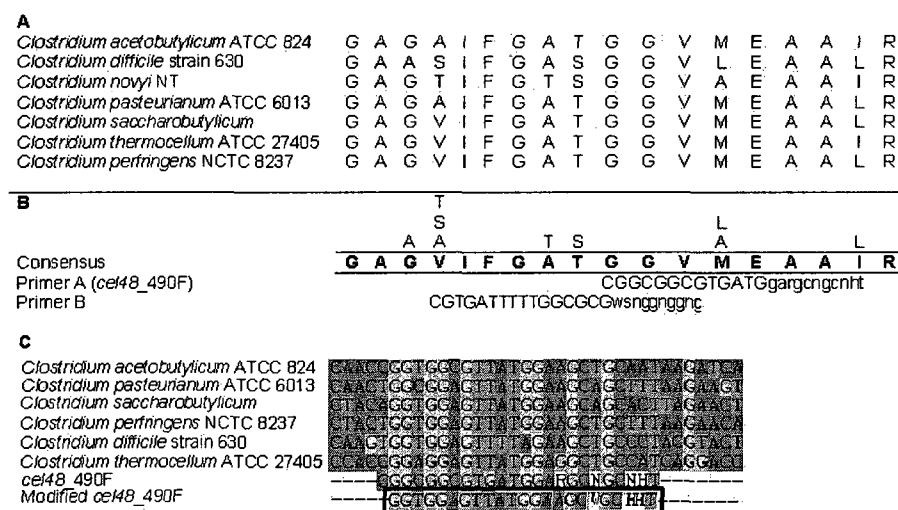


Figure 6.1: CODEHOP primer design strategy (A) Block of conserved sequence in a multiple protein sequence alignment of seven glycoside hydrolases of the Family 48 identified with the Blockmaker program (B) Consensus amino acid sequence as determined by the CODEHOP algorithm (in bold and boxed). The other amino acids found at each position are aligned vertically above the consensus amino acid. Two primers (A and B) are indicated with the 5'consensus clamp in upper case and the 3'degenerate region in lower case (C) DNA alignment of the *cel48_490F* primer with reference sequences used for its design. The primer sequence was modified (boxed sequence) to adjust for differences in the degeneracy of the primer and the different nucleotides present in the DNA alignment of the reference sequences at a particular position.

Table 6. 3: Primer combinations designed by the CODEHOP strategy and selected for further validation PCR. The primers *mcrA_1035F/1530R* were designed by Luton and others (2002) and the primer RH3-dsr_R' is a modified version of the primer RH3-dsr-R designed by Ben-Dov and others (2007). Primer sets that were selected after specificity validation are indicated in bold.

Target	Primer	'5-3' sequence	Primer Combinations	Approximate Amplicon Size (bp)
Family 48 glycoside hydrolases	<i>cel48_490F</i>	TNATGGTTGAAGCTCCDGAYTAYGG		
	<i>cel48_880F</i>	CAYTGG HTNNTG GAYGTTGAY AACTGGTA	<i>cel48_490F/cel48_920R</i>	430
	<i>cel48_920R</i>	CCAAANCRTACCACTTCAACRTC	<i>cel48_880F/cel48_980R</i>	100
	<i>cel48_980R</i>	CCTGTTCACCTCTYTGRWARGTRTT		
Family 5 glycoside hydrolases	<i>cel5_392F</i>	GAGCATGGGCTGGAAYHTNGGNAA		
	<i>cel5_525R</i>	GAAAGGAATAACGGACGGYNNTRAAHCC	<i>cel5_392F/cel5_525R</i>	133
	<i>cel5_754R</i>	CATCATAATCTTGAAAGTGGTTGCAATYTGDKTCCA	<i>cel5_392F/cel5_754R</i>	362
Alpha subunit iron hydrogenases	<i>hydA_1290F</i>	GGTGGAGTTATGGAAGCWGCHHT		
	<i>hydA_1538R</i>	CATCCACCWGGRCAHGCCAT	<i>hydA_1290F/hydA_1538R</i>	248
Alpha subunit dissimilatory sulfite reductase	<i>dsrA_290F</i>	CGGC GTTGC GCATTTYCAYACVVT		
	RH3-dsr-R'	GTGGM GCCGTGCATGTT	<i>dsrA_290F/RH3-dsr-R'</i>	140
	<i>dsrA_660R</i>	GCCGGACGATGCAGHTCRTCCTGRWA	<i>dsrA_290F/dsrA_660R</i>	370
Alpha subunit of methyl coenzyme M reductase	<i>mcrA_1035f</i>	GGTGGTGTMGGATTCACACARTAYGCWACAGC		
	<i>mcrA_1530r</i>	TTCATTGCRTAGTTWGGRTAGTT	<i>mcrA_1035f/mcrA_1530r</i>	495
	<i>mcrA_1450r</i>	TTTGAAGCWCCRCAYTGGTCYT	<i>mcrA_1035f/mcrA_1450r</i>	415
	<i>mcrA_1430f</i>	TTCTATGGTTACGACTVCAGGACCARTGYGG	<i>mcrA_1430f/mcrA_1530r</i>	100

6.4.2. PCR Optimization

Annealing temperature and magnesium concentration were optimized for the selected *cel48*, *cel5*, *hydA*, *dsrA*, and *mcrA* primer sets. The primer combination *cel48_490F/920R* amplified targets from the environmental samples and positive control (*C. thermocellum*). The combination *cel48_880F/980R* amplified the positive control only.

No amplification of environmental samples or positive controls (*R. flavefaciens*, *F. succinogenes*, *C. cellulovorans*, and *C. thermocellum*) was achieved with the *cel5_392F/525R* primer pair. The primer set *cel5_382F/754R* yielded PCR product in the environmental samples and positive controls.

Amplification of some negative controls (*M. maripaludis*, *C. thermocellum*) was observed with the *dsrA_290F/RH3-dsr-R'* set but not with the *dsrA_290F/660R* combination. Both combinations amplified the positive control (*D. autotrophicum*) and the environmental samples.

PCR product was obtained with the *hydA* primer set but the positive control (*C. thermocellum*) amplified poorly.

The three *mcrA* primer combinations yielded products of the expected size from the environmental samples and positive control (*M. maripaludis*) but the pair *mcrA_1430F/1530R* also amplified one of the negative controls (*E. coli*). According to DNA sequencing of clones of PCR product from the *mcrA_1035F/1530R* and *mcrA_1035F/1450R*, the *mcrA_1035F/1530R* combination captures more *mcrA* gene diversity than the *mcrA_1035F/1450R* one (data not shown). Based on the amplification of environmental samples and positive and negative controls the following primer sets

were selected to amplify the desired functional markers: *cel48_490F/cel48_920R*, *cel5_392F/cel5_754R*, *hydA_1290F/hydA_1538R*, *dsrA_290F/dsrA_660R*, and *mcrA_1035F/mcrA_1530R*. The optimized PCR mixture and temperature program for each primer set is presented in Tables 6.4 and 6.2, respectively.

Table 6. 4: Optimized PCR master mix for *cel5*, *cel48*, *hydA*, *dsrA*, and *mcrA* primer sets selected after specificity validation.

Reagent	Primer Set				
	<i>cel5_392F/754R</i>	<i>cel48_490F/920R</i>	<i>hydA_1290F/1538R</i>	<i>dsrA_290F/660R</i>	<i>mcrA_1035F/1530R</i>
Deionized autoclaved water	to 11.5 µL	to 11.5 µL	to 12 µL	to 11.5 µL	to 11.5 µL
10X reaction buffer ¹			1X		
5X PCR enhancer ¹			1X		
Deoxynucleoside triphosphates			0.05 mM each		
Mg(OAc) ₂ 25 mM ¹	2.5 mM	--	--	1.5 mM	1 mM
Primers	0.25 µM	0.15 µM	0.15 µM	0.15 µM	0.2 µM
Formamide			0.125 µL		
Taq DNA polymerase ¹			0.875 U		
iTaq DNA polymerase ²	0.25 U	--	--	0.375 U	--
DNA template	1 µL	1 µL	0.5 µL	1 µL	1 µL

¹ 5 Prime Gaithersburg, MD

² Biorad, Hercules, CA

6.4.3. Validation of Specificity

PCR products obtained from the lignocellulose-based bioreactor sample were cloned and DNA sequences were obtained from 10, 30, 29, 30, and 25 unique clones resulting from the *cel48*, *cel5*, *hyd*, *dsrA*, and *mcrA* primer sets, respectively. The sequencing results confirmed that the primer sets amplified the desired targets (Table 6.5). All the *cel48* and *cel5* clones matched with exo- or endoglucanases belonging to the Families 48 and 5 of

glycoside hydrolases, respectively. The sequences obtained with the *hydA* primers matched the C-terminal domain in the large subunit of iron-hydrogenases, which contains the H-cluster used to design the primers. All the sequences obtained with the *dsrA* primers matched the alpha subunit of the dissimilatory sulfite reductase of uncultured sulfate-reducing bacteria. The entirety of the *mcrA* sequences matched the alpha subunit of the methyl coenzyme M reductase and the majority of the sequences matched an uncultured *Methanosaecinaeae* archaeon. Good's coverage (Good 1953), calculated from the results from the restriction digest analysis, were 96.6%, 90%, 84.6%, 93.3%, and 82.1% for the *cel5*, *cel48*, *hydA*, *dsrA*, and *mcrA* clones, respectively. This suggested that the number of clones screened was representative of the genetic diversity captured by each primer set.

6.4.4. Adaptation and Validation of Q-PCR

The selected primer sets were adapted to Q-PCR and applied in the quantification of the functional genes in the lignocellulose-based and the ethanol-fed bioreactors. All functional genes were successfully quantified in both samples (Figure 6.2). In the lignocellulose-based bioreactor, the number of *cel48*, *cel5*, and *mcrA* genes was approximately 2.5 orders of magnitude higher than in the ethanol-fed bioreactor. The number of *hydA* genes in the lignocellulose-based bioreactor was also higher (approximately 1.5 orders of magnitude) than in the ethanol-fed reactor. On the other hand, the ethanol-fed reactor contained approximately 30 times more *dsrA* genes than the lignocellulose-based reactor. Based on the quantification of the 16S rRNA gene, the lignocellulose-based bioreactor contained a larger bacterial biomass than the ethanol bioreactor.

Table 6. 5: DNA sequencing results of clones of PCR product obtained with the *cel5*, *cel48*, *hydA*, *dsrA*, and *mcrA* primer sets on a sample from a lignocellulose-based sulfate-reducing bioreactor. Clone sequences were compared to those in the NCBI database using the BLASTX tool that searches the protein database using a translated nucleotide query

	Microorganism	BLASTX Identity (% match)*	% screened clones	GenPept Accession #
<i>cel48</i>	<i>Clostridium josui</i>	exoglucanase S, glycosyl hydrolase Family 48 (75%)	14.3	AAC38571
	<i>Clostridium acetobutylicum</i> ATCC 824	processive endoglucanase, glycosyl hydrolase Family 48 (56%)	14.3	NP_347547
	<i>Clostridium cellulolyticum</i> H10	glycoside hydrolase, Family 48 (69%)	28.6	ZP_01575465
	<i>Clostridium cellulovorans</i>	exoglucanase S, glycosyl hydrolase Family 48 (53-61%)	42.9	AAC38571
<i>cel5</i>	<i>Saccharophagus degradans</i> 2-40	endoglucanase-like protein, glycoside hydrolase Family 5 (45-59%)	46.7	ABD81896
	<i>Clostridium cellulovorans</i>	endoglucanase engB, Glycoside hydrolase Family 5 (43%)	3.3	AAA23231
	<i>Flavobacterium johnsoniae</i> UW101	hypothetical protein EUBSIR_0099, glycoside hydrolase Family 5 (44%)	6.7	ABQ03808
	<i>Eubacterium siraeum</i> DSM 15702	hypothetical protein EUBSIR_00991, Glycoside hydrolase Family 5 (52-53%)	43.3	EDS01174
<i>hydA</i>	<i>Clostridium botulinum</i> B1 str. Okra	[Fe] hydrogenase (72%)	3.7	YP_001781395
	<i>Clostridium cellulolyticum</i> H10	hydrogenases, Fe-only (75-82%)	7.4	ZP_01573883
	<i>Bacteroides capillosus</i> ATCC 29799	hypothetical protein BACCAP 02746, iron hydrogenase large subunit C-terminal domain (73%)	7.4	ZP_02037133
	<i>Thermosinus carboxydovorans</i> Nor1	hydrogenases, Fe-only (74%)	11.1	EAX48145
	<i>Pelotomaculum thermopropionicum</i> SI	hydrogenase subunit (63%)	11.1	YP_001212560
	<i>Clostridium bolteae</i> ATCC BAA-613	hypothetical protein CLOBOL 01023, iron hydrogenase large subunit, C-terminal domain (60-74%)	22.2	ZP_02083500
	<i>Clostridium thermocellum</i>	hydrogenase-1(67-69%)	37.0	AAD33071
<i>dsrA</i>	uncultured sulfate-reducing bacterium AAQ7928	dissimilatory sulfite reductase alpha subunit (96%)	3.3	AAQ7928
	uncultured sulfate-reducing bacterium ACD37519	dissimilatory sulfite reductase alpha subunit (90-91%)	63.3	ACD37519

Table 6.5 continued

	Microorganism	BLASTX Identity (% match)*	% screened clones	GenPept Accession #
<i>dsrA</i>	uncultured sulfate-reducing bacterium ABR45803	dissimilatory sulfite reductase subunit A (82-88%)	13.3	ABR45803
	uncultured sulfate-reducing bacterium ABR09856	dissimilatory sulfite reductase alpha subunit (89-92%)	3.3	ABR09856
	uncultured sulfate-reducing bacterium ABW69247	dissimilatory sulfite reductase alpha subunit (96%)	16.7	ABW69247
<i>mcrA</i>	uncultured <i>Methanosarcinaceae</i> archaeon	methyl Coenzyme M reductase alpha subunit (96%)	3.6	AAN02199
	uncultured euryarchaeote	methyl Coenzyme M reductase alpha subunit (90-91%)	3.6	AAR22542
	uncultured methanogenic archaeon	methyl Coenzyme M reductase alpha subunit (96%)	7.1	CAN99766
	uncultured archaeon	methyl Coenzyme M reductase alpha subunit (97-98%)	21.4	ABX75060
	uncultured euryarchaeote	methyl Coenzyme M reductase alpha subunit (96%)	25.0	AAR24558
	<i>Methanobacterium ivanovii</i>	methyl Coenzyme M reductase alpha subunit (99%)	39.3	ABO93183

* when several clones matched the same protein, the range of % match is given

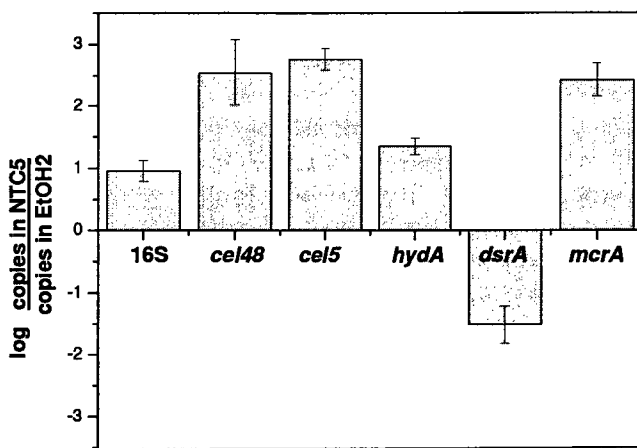


Figure 6. 2: Number of *cel5*, *cel48*, *hydA*, *dsrA*, and *mcrA* copies in the lignocellulose-based bioreactor with respect to the ethanol-fed bioreactor as determined by Q-PCR.

6.5. Discussion

6.5.1. Advantages of the Functional Gene –Based Approach

Traditionally, the 16S rRNA gene has been used for the biomolecular characterization of microbial communities. This approach is highly effective for studying microorganisms that form a tight phylogenetic cluster, such as ammonia-oxidizing bacteria, but becomes impractical when used to capture the diversity of microorganisms that span phylogenetic groups, such as denitrifying bacteria. In the case of natural environments undergoing sulfate reduction, microorganisms with a variety of phylogenetic affiliations are key. In this study, primer sets targeting genetic functional markers of cellulose degradation, fermentation, sulfate reduction, and methanogenesis were designed, validated and demonstrated on samples from two sulfate-reducing bioreactors.

The designed primer sets were demonstrated for the quantification of different target genes in a lignocellulose-based and an ethanol-fed sulfate-reducing bioreactor. The presence of a simple carbon source such as ethanol, a fermentation product, as the only

energy source was expected to directly stimulate SRB and produce a microbial community enriched in SRB. On the other hand, the complex lignocellulosic carbon source was expected to produce a more functionally diverse microbial community. Q-PCR results supported these assumptions and were in general agreement with a prior 16S rRNA gene-based study (Chapter 5). Compared to the ethanol-fed bioreactor, the lignocelluloses-based bioreactor contained higher numbers of *cel5*, *cel48*, *hydA*, and *mcrA* genes. In contrast, the ethanol-fed bioreactor contained approximately 1.5 orders of magnitude more *dsrA* genes. While genetic markers for cellulose degradation and fermentation were detected in the ethanol-fed bioreactor, these were likely a result of the residual horse manure used to inoculate the bioreactor.

The CODEHOP strategy proved to be effective for primer design particularly for the *cel5*, *cel48*, and *hydA* sequences which were more challenging because of their lower degree of conservation compared to the *mcrA* and *dsrA* sequences. Although it was possible to identify blocks of conserved protein sequences and design primers from them for all the target genes, the divergence of the *cel5*, *cel48*, and *hydA* sequences limited the number of primer combinations that could be designed for these genes and, in general, increased the degeneracy of their 3' degenerate core.

Interestingly, the similarity of the sequences from the lignocellulose-based bioreactor to the sequences in the NCBI database was lower than what is typically observed for 16S rRNA gene sequences (>90%), particularly for the *cel5*, *cel48*, and *hydA* sequences. Other studies that investigated functional genes in mixed microbial communities also reported low percent similarity of their sequences with the ones in the NCBI database (Healy et al. 1995; Henry et al. 2004). The degree of genetic diversity is

higher in *cel48*, *cel5*, and *hydA* genes than in *dsrA* and *mcrA* genes. In addition, from a search done on November 4th, 2008 on the NCBI database using the keywords ‘glycoside hydrolase Family 48, glycoside hydrolase Family 5, iron hydrogenase large subunit, *dsrA* and dissimilatory sulfite reductase, and methyl coenzyme M reductase’, it is apparent that the database contains a higher number of *dsrA* and *mcrA* sequences than it does *cel5*, *cel48*, and *hydA* sequences. The search reported a total of 2,798, 108, 1,495, 3,497, and 4,548 sequences corresponding to the *cel48*, *cel5*, *hyd*, *dsrA*, and *mcrA* genes, respectively. Thus, the low percent of similarity observed can result from a combination of limited sequence information in the database and the high degree of genetic diversity of the target genes.

6.5.2. Quantification of Genetic Markers for Cellulose Degradation

The majority of the anaerobic cellulose degraders have a very efficient cellulose-degrading multicomponent extracellular enzymatic complex known as the cellulosome (Figure 6.3) (Bayer et al. 1998). The genes encoding for the different components of the cellulosome (e.i., cohesin-containing scaffolding subunit, the dockerin-containing cellulases, and the carbohydrate-binding domain) are potential targets for cellulose degradation. Although the participation of all of these components is necessary for cellulose hydrolysis, the cellulases are the actual catalysts of this reaction and, thus, the genes encoding for these enzymes make an ideal target for cellulose degradation. Of the more than seventy glycoside hydrolase families defined based on amino acid sequence identity in their catalytic domains (Gilkes et al. 1991), cellulases are found in fifteen families (5, 6, 7, 8, 9, 10, 11, 12, 26, 44, 45, 48, 51, 60, and 61) (Henrissat 1991; Rabinovich et al. 2002) and most of the cellulases of anaerobic cellulose degraders

belong to just three families: 5, 9, 48 (Figure 6.4). All cellulolytic microorganisms produce cellulases that belong to different families and, on the other hand, cellulases of the same family occur in widely different microorganisms (Beguin 1990). For example, both Family 5 and 9 cellulases are found in phylogenetically distant microorganisms (Figure 6.4). For this reason, it was not considered necessary to design primers for the three protein families. Instead, the genes encoding for the cellulases of the Families 5 (*cel5*) and 48 (*cel48*) were selected as functional markers for cellulose degradation.

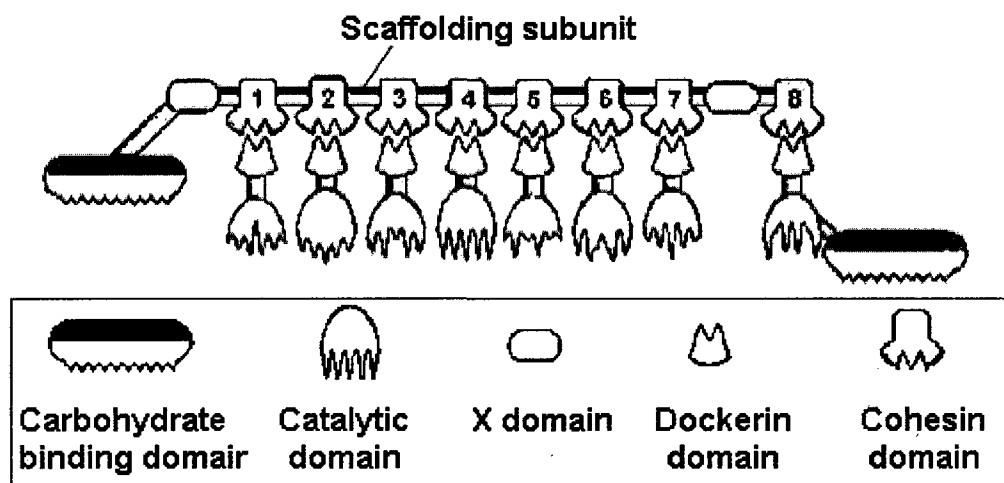


Figure 6.3: Schematic of the cellulosome of anaerobic bacteria.

Of the known glycoside hydrolases of the Family 48, the majority are found in *Clostridium* spp. (Figure 6.4) although *Bacteroides cellulosolvens* and *Ruminococcus albus* are also known to have at least one *cel48* gene. Glycoside hydrolases of the Family 5 are found in a wider range of phylogenetic groups. The *cel5* primer set is supposed to provide a wider coverage of anaerobic cellulose degraders. *In silico* analysis of this primer set (Appendix B) indicates that it amplifies *cel5* genes of several *Clostridium*, *Fibrobacter*, *Ruminococcus*, *Butyrivibrio*, and *Bacteroides* spp. DNA sequencing results

suggest that this primer pair also amplifies *cel5* genes of some *Eubacterium* spp. and *Saccharophagus* spp.

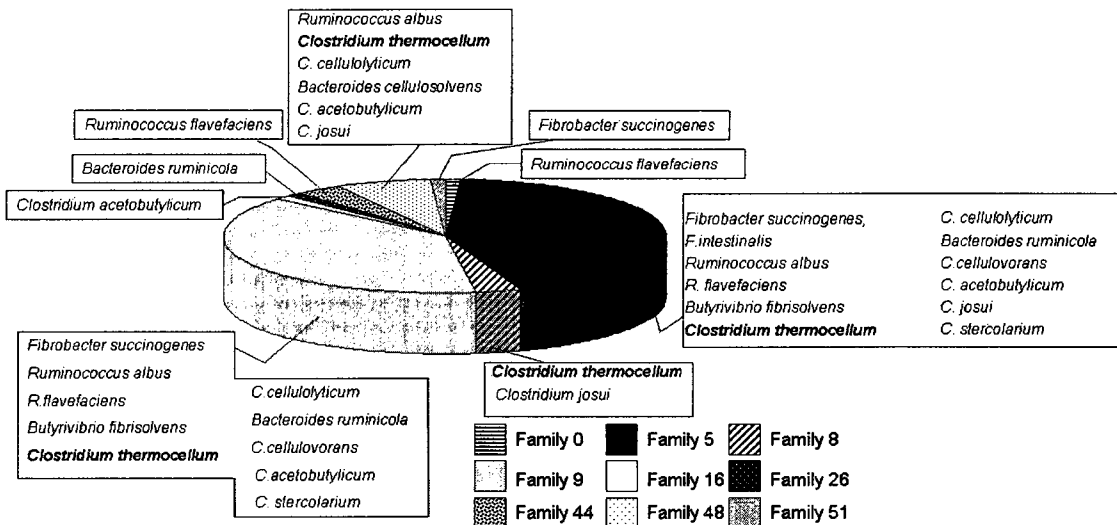


Figure 6.4: Distribution of cellulases of anaerobic bacteria into glycoside hydrolases families. Thermophilic microorganisms are indicated in bold. The chart was constructed using information from the Carbohydrate Active enzymes database (CAZy, <http://www.cazy.org/index.html>).

6.5.3. Quantification of Genetic Markers for Fermentation

Fermentation is supported by a variety of microorganisms. The end products of this process depend on the microbial species and the environmental conditions. As a consequence, there is a variety of enzymes involved in this pathway, many of which are not exclusive to fermentation. Fermentation is mostly associated with hydrogen evolution (Das et al. 2006). In a vast number of fermentative bacteria, the electrons from the reduced electron carriers are channeled to H₂ via iron hydrogenases (Adams et al. 1980). All iron hydrogenases contain a highly conserved region of 350 amino acids known as the H-cluster domain in their alpha subunit (Meyer 2007; Vignais et al. 2001) which is ideal for primer design.

The *hydA* primers were designed from the two conserved protein regions GAGVIFGA and MACPGGCING. The second region is one of the characteristic sequence signatures of the H-cluster domain of iron hydrogenases (Vignais et al. 2001) and was also used by Xing et al. (2008) to design a reverse primer to amplify the *hydA* gene of H₂-producing bacteria in acidophilic communities. Xing and others designed the forward primer from the ADLTIMEE signature sequence of the H-cluster domain to produce a PCR product of 500 to 600 bp. In our study, the forward primer was designed from a conserved region closer to the MACPGGCING region so that the primers would produce a smaller product (~248 bp) which is preferable for Q-PCR applications (Mohammadi and Day 2004). Although the *hydA* primers were designed using sequences of *hydA* from *Clostridium* species only, the DNA sequencing results suggest that a broader range of *hydA* sequences is amplified by the primer set.

6.5.4. Quantification of Genetic Markers for Sulfate Reduction

The dissimilatory reduction of sulfate to hydrogen sulfide in SRB is performed in three steps (Wagner et al. 2005):



where APSR and DSR are adenosine 5'-phosphosulfate and dissimilatory sulfite reductase, respectively. The APSR and DSR genes are evolutionary conserved among SRB (Hipp et al. 1997; Wagner et al. 1998). ATP sulfurylase, APSR and DSR appear to be involved in both the oxidative and the reductive mode of the dissimilatory sulfur metabolism (Hipp et al. 1997). APSR has been found in several species of the sulfur-oxidizing photolithotrophic bacteria *Chromatiaceae* and *Chlorobiaceae* and in the sulfur-

oxidizing chemolithotrophic *Thiobacillus* spp. (Schwenn and Biere 1979). This represents a limitation to study SRB in systems where both sulfur-oxidizing bacteria (SOB) and SRB might coexist such as field sulfate-reducing bioreactors that treat mine drainage. In fact, cloning of APS7-F/APS8-R (Friedrich 2002) PCR products from samples of the Luttrell and Peerless Jenny King sulfate-reducing bioreactors confirmed that SRB as well as SOB of the genus *Thiobacillus* were being amplified by this set of primers (Hiibel et al. 2007). Since the *dsr* genes of SRB and SOB are more distantly related than the corresponding *aps* genes (Hipp et al. 1997), the *dsr* gene is a more adequate marker for SRB.

In silico analysis of the *dsrA* primer set indicated that there were several mismatches between known *dsrA* genes of *Thiobacillus* spp. and the primers (particularly at the '3 end of the reverse primer) to prevent amplification of these sequences. In addition, DNA sequencing of clones of PCR product obtained with the *dsrA* primer set from a sample of the Peerless Jenny King bioreactor, which was known to contain *Thiobacillus* spp. DNA (Hiibel et al. 2008), revealed that no *Thiobacillus* spp. *dsrA* sequences were amplified (data not shown).

6.5.5. Quantification of Genetic Markers for Methanogenesis

Methanogens are a metabolically diverse group of microorganisms. They can form methane from acetate, CO₂, H₂, and C₁ compounds (Garcia et al. 2000). A variety of enzymes involved in the methanogenic pathway and many are not exclusive to methanogenesis. For example, methylene tetrahydromethanopterin dehydrogenase and methenyl tetrahydromethanopterin cyclohydrolase are also found in methanotrophic microorganisms (Chistoserdova et al. 1998). With the exception of coenzyme M,

methyl-coenzyme M and methyl-coenzyme M reductase, all the other enzymes and coenzymes involved in methanogenesis are also present in sulfate-reducing Achaea (Thauer 1998). The fact that the genes encoding this enzyme appear to be unique to methanogens and are evolutionarily conserved (Friedrich 2005) make the *mcr* genes the ideal genetic markers for methanogens.

Two primers targeting the *mcrA* gene were designed with the CODEHOP strategy and combined with primers designed by Luton and others (2004) into two primer sets. In addition, the primer set from the Luton study was also tested. This primer set and one of the in-house combinations were specific to *mcrA* genes, as determined by sequencing of *mcrA* clones. However, the Luton combination seemed to provide better sequence diversity coverage and was selected to quantify methanogens in the environmental samples.

6.6. Conclusions

This study provides a useful new suite of tools for quantitative studies of anaerobic sulfate-reducing and methanogenic communities. The approach represents a significant advance over 16S rRNA gene approaches and prior functional gene methods developed primarily for pure cultures. The ability to detect functional genes corresponding to both cultured and uncultured organisms in complex environments is of particular value. With this approach, ubiquitous microbial functions such as cellulose degradation, fermentation, sulfate reduction, and methanogenesis can be studied with a small number of primer sets targeted at functional genes compared to the 16S rRNA gene-based approach.

6.7. References

- Achenbach LA, Coates JD. 2000. Disparity between Bacterial Phylogeny and Physiology
- Comparing 16S rRNA sequences to assess relationships can be a powerful tool,
but its limitations need to be considered. ASM News 66(12):714-715.
- Adams MWW, Mortenson LE, Chen JS. 1980. Hydrogenase. BIOCHIMICA ET
BIOPHYSICA ACTA 594(2-3):105-176.
- Amann R, Ludwig W. 2000. Ribosomal RNA-targeted nucleic acid probes for studies in
microbial ecology. Fems Microbiol. Rev. 24(5):555-565.
- Bar T, Stahlberg A, Muszta A, Kubista M. 2003. Kinetic Outlier Detection (KOD) in
real-time PCR. Nucleic Acids Res. 31(17).
- Bayer EA, Shimon LJW, Shoham Y, Lamed R. 1998. Cellulosomes - Structure and
ultrastructure. J. Struct. Biol. 124(2-3):221-234.
- Beguin P. 1990. Molecular-Biology Of Cellulose Degradation. Annu. Rev. Microbiol.
44:219-248.
- Beller HR, Kane SR, Legler TC, Alvarez PJJ. 2002. A real-time polymerase chain
reaction method for monitoring anaerobic, hydrocarbon-degrading bacteria based
on a catabolic gene. Environ. Sci. Technol. 36:3977-3984.
- Ben-Dov E, Brenner A, Kushmaro A. 2007. Quantification of Sulfate-reducing Bacteria
in Industrial Wastewater by Real-time Polymerase Chain Reaction (PCR) Using
dsrA and apsA Genes. Microbial Ecology 54(3):439-451.
- Borsodi AK, Micsinai A, Rusznyak A, Vladar P, Kovacs G, Toth EM, Marialigeti K.
2005. Diversity of alkaliphilic and alkalitolerant bacteria cultivated from
decomposing reed rhizomes in a Hungarian soda lake. Microb. Ecol. 50(1):9-18.

- Braker G, Fesefeldt A, Witzel KP. 1998. Development of PCR primer systems for amplification of nitrite reductase genes (*nirK* and *nirS*) to detect denitrifying bacteria in environmental samples. *Appl. Environ. Microbiol.* 64(10):3769-3775.
- Cardenas E, Wu WM, Leigh MB, Carley J, Carroll S, Gentry T, Luo J, Watson D, Gu B, Ginder-Vogel M and others. 2008. Microbial communities in contaminated sediments, associated with bioremediation of uranium to submicromolar levels. *Appl. Environ. Microbiol.* 74(12):3718-3729.
- Chervoneva I, Hyslop T, Iglewicz B, Johns L, Wolfe HR, Schulz S, Leong E, Waldman S. 2006. Statistical algorithm for assuring similar efficiency in standards and samples for absolute quantification by real-time reverse transcription polymerase chain reaction. *Anal. Biochem.* 348(2):198-208.
- Chistoserdova L, Vorholt JA, Thauer RK, Lidstrom ME. 1998. C-1 transfer enzymes and coenzymes linking methylotrophic bacteria and methanogenic Archaea. *Science* 281(5373):99-102.
- Das D, Dutta T, Nath K, Kotay SM, Das AK, Veziroglu TN. 2006. Role of Fe-hydrogenase in biological hydrogen production. *Curr. Sci.* 90(12):1627-1637.
- Eden PA, Schmidt TM, Blakemore RP, Pace NR. 1991. Phylogenetic Analysis Of Aquaspirillum-Magnetotacticum Using Polymerase Chain Reaction-Amplified 16s Ribosomal-Rna-Specific Dna. *Int. J. Syst. Bacteriol.* 41(2):324-325.
- Friedrich MW. 2002. Phylogenetic analysis reveals multiple lateral transfers of adenosine-5'-phosphosulfate reductase genes among sulfate-reducing microorganisms. *J. Bacteriol.* 184(1):278-289.

- Friedrich MW. 2005. Methyl-coenzyme M reductase genes: Unique functional markers for methanogenic and anaerobic methane-oxidizing Archaea. *Environmental Microbiology*. San Diego: Elsevier Academic Press Inc. p 428-442.
- Garcia JL, Patel BKC, Ollivier B. 2000. Taxonomic phylogenetic and ecological diversity of methanogenic Archaea. *Anaerobe* 6(4):205-226.
- Geets J, Vanbroekhoven K, Borremans B, Vangronsveld J, Diels L, Van der Lelie D. 2006. Column experiments to assess the effects of electron donors on the efficiency of *in situ* precipitation of Zn, Cd, Co and Ni in contaminated groundwater applying the biological sulfate removal technology. *Environ. Sci. Pollut. Res* 13(6):362-378.
- Gilkes NR, Henrissat B, Kilburn DG, Miller RC, Warren RAJ. 1991. Domains In Microbial Beta-1,4-Glycanases - Sequence Conservation, Function, And Enzyme Families. *Microbiol. Rev.* 55(2):303-315.
- Good IJ. 1953. The Population Frequencies Of Species And The Estimation Of Population Parameters. *Biometrika* 40(3-4):237-264.
- Handelsman J. 2004. Soils-The Metagenomics Approach. In: Bull AT, editor. *Microbial Diversity and Bioprospecting*. Washington DC.: ASM Press. p 109-119.
- Healy FG, Ray RM, Aldrich HC, Wilkie AC, Ingram LO, Shanmugam KT. 1995. Direct Isolation Of Functional Genes Encoding Cellulases From The Microbial Consortia In A Thermophilic, Anaerobic Digester Maintained On Lignocellulose. *Appl. Microbiol. Biotechnol.* 43(4):667-674.
- Heijs SK, Haese RR, van der Wielen P, Forney LJ, van Elsas JD. 2007. Use of 16S rRNA gene based clone libraries to assess microbial communities potentially involved in

- anaerobic methane oxidation in a Mediterranean cold seep. *Microb. Ecol.* 53(3):384-398.
- Henikoff S, Henikoff JG, Alford WJ, Pietrovski S. 1995. Automated Construction And Graphical Presentation Of Protein Blocks From Unaligned Sequences (Reprinted From Gene-Combis Vol 163, Pg Gc17-Gc26, 1995). *Gene* 163(2):GC17-GC26.
- Henrissat B. 1991. A Classification Of Glycosyl Hydrolases Based On Amino-Acid-Sequence Similarities. *Biochem. J.* 280:309-316.
- Henry S, Baudoin E, Lopez-Gutierrez JC, Martin-Laurent F, Baumann A, Philippot L. 2004. Quantification of denitrifying bacteria in soils by *nirK* gene targeted real-time PCR. *59(3):327-335.*
- Hiibel SR, Pereyra LP, Inman LY, Tischer A, Reisman DJ, Reardon KF, Pruden A. 2008. Microbial community analysis of two field-scale sulfate-reducing bioreactors treating mine drainage. *Environ. Microbiol.* 10(8):2087-2097.
- Hiibel SR, Pereyra LP, Inman LY, Tisher A, Reisman DJ, Reardon KF, Pruden A. 2007. Microbial Community Analysis of Two Field-Scale Sulfate-Reducing Bioreactors Treating Mine Drainage. In preparation for submission to Environmental Microbiology.
- Hipp WM, Pott AS, ThumSchmitz N, Faath I, Dahl C, Truper HG. 1997. Towards the phylogeny of APS reductases and sirohaem sulfite reductases in sulfate-reducing and sulfur-oxidizing prokaryotes. *Microbiology-(UK)* 143:2891-2902.
- Ibekwe AM, Grieve CM, Lyon SR. 2003. Characterization of microbial communities and composition in constructed dairy wetland wastewater effluent. *Appl. Environ. Microbiol.* 69(9):5060-5069.

- Loy A, Lehner A, Lee N, Adamczyk J, Meier H, Ernst J, Schleifer KH, Wagner M. 2002. Oligonucleotide microarray for 16S rRNA gene-based detection of all recognized lineages of sulfate-reducing prokaryotes in the environment. *Appl. Environ. Microbiol.* 68(10):5064-5081.
- Luton PE, Wayne JM, Sharp RJ, Riley PW. 2002. The *mcrA* gene as an alternative to 16S rRNA in the phylogenetic analysis of methanogen populations in landfill. *Microbiology-(UK)* 148:3521-3530.
- Meyer J. 2007. [FeFe] hydrogenases and their evolution: a genomic perspective. *Cell. Mol. Life Sci.* 64(9):1063-1084.
- Mohammadi M, Day PJR. 2004. Oligonucleotides used as template calibrators for general application in quantitative polymerase chain reaction. *Anal. Biochem.* 335(2):299-304.
- Morales TA, Dopson M, Athar R, Herbert RB. 2005. Analysis of bacterial diversity in acidic pond water and compost after treatment of artificial acid mine drainage for metal removal. *Biotechnol. Bioeng.* 90(5):543-551.
- Pereyra LP, Hiibel SR, Pruden A, Reardon KF. 2008. Comparison of microbial community composition and activity in sulfate-reducing batch systems remediating mine drainage. *Biotechnology and bioengineering* 101(4):702-713.
- Rabinovich ML, Melnik MS, Boloboba AV. 2002. Microbial cellulases (Review). *Appl. Biochem. Microbiol.* 38(4):305-321.
- Ramakers C, Ruijter JM, Deprez RHL, Moorman AFM. 2003. Assumption-free analysis of quantitative real-time polymerase chain reaction (PCR) data. *Neurosci. Lett.* 339(1):62-66.

- Roberts RJ, Vincze T, Posfai J, Macelis D. 2007. REBASE - enzymes and genes for DNA restriction and modification. Nucleic Acids Res. 35:D269-D270.
- Rose TM, Schultz ER, Henikoff JG, Pietrokovski S, McCallum CM, Henikoff S. 1998. Consensus-degenerate hybrid oligonucleotide primers for amplification of distantly related sequences. Nucleic Acids Res. 26(7):1628-1635.
- Schwenn JD, Biere M. 1979. Aps-Reductase Activity In The Chromatophores Of *Chromatium vinosum* strain D. FEMS Microbiol. Lett. 6(1):19-22.
- Sun YM, Polishchuk EA, Radoja U, Cullen WR. 2004. Identification and quantification of arsC genes in environmental samples by using real-time PCR. 58(3):335-349.
- Suzuki MT, Taylor LT, DeLong EF. 2000. Quantitative analysis of small-subunit rRNA genes in mixed microbial populations via 5'-nuclease assays. Appl. Environ. Microbiol. 66(11):4605-4614.
- Tancsics A, Szoboszlay S, Kriszt B, Kukolya J, Baka E, Marialigeti K, Revesz S. 2008. Applicability of the functional gene catechol 1,2-dioxygenase as a biomarker in the detection of BTEX-degrading Rhodococcus species. J. Appl. Microbiol. 105(4):1026-1033.
- Thauer RK. 1998. Biochemistry of methanogenesis: a tribute to Marjory Stephenson. Microbiology-(UK) 144:2377-2406.
- Vignais PM, Billoud B, Meyer J. 2001. Classification and phylogeny of hydrogenases. Fems Microbiol. Rev. 25(4):455-501.
- Wagner M, Loy A, Klein M, Lee N, Ramsing NB, Stahl DA, Friedrich MW. 2005. Functional marker genes for identification of sulfate-reducing prokaryotes.

Environmental Microbiology. San Diego: Elsevier Academic Press Inc. p 469-489.

Wagner M, Roger AJ, Flax JL, Brusseau GA, Stahl DA. 1998. Phylogeny of dissimilatory sulfite reductases supports an early origin of sulfate respiration. *J. Bacteriol.* 180(11):2975-2982.

Warnecke F, Luginbuhl P, Ivanova N, Ghassemian M, Richardson TH, Stege JT, Cayouette M, McHardy AC, Djordjevic G, Aboushadi N and others. 2007. Metagenomic and functional analysis of hindgut microbiota of a wood-feeding higher termite. *Nature* 450(7169):560-U17.

Weisburg WG, Barns SM, Pelletier DA, Lane DJ. 1991. 16s Ribosomal Dna Amplification For Phylogenetic Study. *J. Bacteriol.* 173(2):697-703.

Whitford MF, Forster RJ, Beard CE, Gong JH, Teather RM. 1998. Phylogenetic analysis of rumen bacteria by comparative sequence analysis of cloned 16S rRNA genes. *Anaerobe* 4(3):153-163.

Xing DF, Ren NQ, Rittmann BE. 2008. Genetic diversity of hydrogen-producing bacteria in an acidophilic ethanol-H₂-coproducing system, analyzed using the [Fe]-hydrogenase gene. *Appl. Environ. Microbiol.* 74(4):1232-1239.

Chapter 7 Application of Functional-Gene Profiling and Quantification for the Characterization of the Initial and Pseudo-Steady State Operation of Sulfate-Reducing Columns Treating Mine Drainage.

Pereyra, L.P., Hiibel, S.R., Perrault, E.M., Pruden, A., and Reardon, K.F.
(in preparation for submission to Applied and Environmental Microbiology)

Approximate contributions of each author are as follows:

LP Pereyra performed 45% of experimental setup, 40% of sample collection, 50% of metals and pH analysis, and 50% of DNA extraction, 100% of DGGE analysis, 100% of Q-PCR analysis, and 100% of manuscript preparation
SR Hiibel performed 45% of experimental setup, 40% of sample collection, 100% of sulfate analysis, 5% of the metals and pH analysis,
EM Perrault performed 10% of the experimental setup, 20% of sample collection, and 45% of the metals and pH analysis.
A Pruden and KF Reardon assisted with experimental design and manuscript preparation.

7.1. Abstract

The startup period of complex microbial systems represents a critical yet poorly understood aspect of engineering design and performance. In this study, a recently described approach for quantifying the functional genes of cellulose-degrading, fermenting, and sulfate-reducing bacteria as well as methanogens is applied in characterizing the initial and pseudo-steady-state microbial communities of sulfate-reducing columns remediating mine drainage (MD). A new method for characterizing the diversity of these functional genes by denaturing gradient gel electrophoresis (DGGE) is also developed. The columns were fed simulated MD containing sulfate, iron, zinc, and cadmium and were packed with a complex lignocellulose mixture to provide a slow-release carbon source. Six column conditions were studied in duplicate to compare the

effect of inoculum (dairy manure (DM), DM + sulfate-reducing enrichment (SRB), DM + cellulose-degrading enrichment (CD), and no inoculum (CR)) and supplemental carbon sources (soluble carboxymethyl cellulose (CMC) and ethanol (EtOH)). This model system was particularly suitable because it relies on a complex community of the target functional groups to anaerobically degrade the lignocellulose, producing substrates for fermenters, sulfate reducers (desired), and methanogens (undesired). Sulfate removal startup was approximately 15 days for all the columns. Sulfate removal achieved a pseudo-steady state by Day 30 (defined as $\pm 10\%$ effluent sulfate concentration for three hydraulic residence times (~12 days)). There was no significant difference among the columns in terms of sulfate removal or pH neutralization at pseudo-steady state, though CR columns performed marginally worse than DM and CMC columns. Near 99% removal of metals was achieved in all except the CMC columns. DGGE of the 16S rRNA and functional genes confirmed that the initial microbial community composition was distinct among the different kinds of inocula. Column communities generally experienced a shift from the initial to pseudo-steady-state time point, at which greater differences were observed among different column conditions than between replicates. Quantitative polymerase chain reaction demonstrated that there was a marked increase in the abundance of 16S rRNA and functional genes in all columns between the initial and the steady-state time point, except for the 16S genes in the CR columns. This study demonstrates the applicability of qualitative and quantitative functional gene analysis to the study of shifts in multiple functional guilds in a complex microbial system.

7.2. Introduction

Startup is a critical, yet poorly understood aspect of design and performance of engineered systems. The startup time is usually defined as the period until measurable removal or formation of a compound of interest is observed. Biological systems operate on the basis of reactions catalyzed by microorganisms. During startup, the microorganisms adapt to new conditions using a variety of mechanisms such as selective enrichment, enzyme regulation, exchange of genetic information, and alteration of their environment (Rittmann and McCarty 2001). Startup times vary from system to system. In aerobic communities they range from hours to days whereas in anaerobic communities they may be anywhere from weeks to months (Dabert et al. 2005; Linkfield et al. 1989). In biological systems, factors that have an impact on the microbial community may also affect the startup time. For example, in the degradation of methyl parathion and *p*-nitrophenol, startup time was influenced by the pre-exposure of the microorganisms to the contaminants (Spain et al. 1980). Sahinkaya and Dilek (2005) also observed that acclimation of activated sludge inoculum reduced the lag time in the biodegradation of 4-chlorophenol. In denitrifying submerged filters, startup was longer at low temperatures (De la Rua et al. 2008). Some studies have applied molecular techniques such as quantitative membrane hybridization and polymerase chain reaction (PCR)-single strand conformation polymorphism to monitor the microbiology of different systems during startup (Angenent et al. 2002; Dabert et al. 2005). However, there is still not a clear understanding of the influence of the microbial ecology of a system on startup and long-term performance, particularly for complex microbial communities.

Sulfate-reducing permeable reactive zones (SR-PRZs) treating mine drainage (MD) provide an important example of a remediation system relying on complex microbial communities for which the startup period is poorly understood. SR-PRZs are anaerobic systems that treat MD by precipitating the metals as metal sulfides with biogenically produced sulfide. The two main components of an SR-PRZ are the substrate and the microbial community. The substrate provides hydraulic conductivity and physical support and energy sources for the microbial community. Typically, the substrate is a lignocellulose-based inexpensive material such as wood chips or compost (Johnson and Hallberg 2005). The substrate is a slow-release, long-term source of carbon, the composition of which shapes the microbial community through selective enrichment. Sulfate-reducing bacteria (SRB) are of key importance for MD remediation because they produce sulfide, which ultimately binds heavy metals. However, SRB cannot utilize the lignocellulosic material present in SR-PRZs directly. Cellulose-degrading and fermentative bacteria are thus also critical members of the SR-PRZ microbial community as they transform the lignocellulosic material into carbon and energy sources for the SRB through hydrolytic and fermentative reactions, respectively. Methanogenic archaea are also of interest because they can compete with SRB for carbon and energy sources.

Several recent studies have examined the microbial communities in lab-scale (Geets et al. 2005; Hong et al. 2007; Pereyra et al. 2008; Pruden et al. 2007) and pilot-scale (Hiibel et al. 2008; Johnson and Hallberg 2005; Nicomrat et al. 2006) SR-PRZs targeting 16S rRNA genes. *Clostridium* spp., *Bacteroides* spp., *Treponema* spp., *Prevotella* spp., *Desulfovibrio* spp., *Acetobacterium* spp., and *Flavobacterium* spp. are a few of the species that were found in these studies. Interestingly, SRB are typically a

small fraction of these communities, which makes their detection difficult based on 16S rRNA gene-targeted fingerprinting methods (Hong et al., 2007). Because of the complexity of these systems and the dominance of uncultured microbes, information about the functional properties of the members of the microbial community is particularly desirable. Unfortunately, the phylogenetic diversity of SRB, anaerobic cellulose degraders and fermenters greatly hinders their quantification using a small number of 16S rRNA gene-targeted primers or probes. However, this limitation may be overcome by targeting functional genes that serve as genetic markers of the functions of interest. Functional genes have been used to study several processes of technological or environmental relevance such as biohydrogen production (Xing et al. 2008), remediation of xenobiotics (Beller et al. 2002), and nitrogen cycling. For example, genes encoding nitrate (*narG*, *napA*) and nitrite (*nirS*, *nrfA*) reductase were used to investigate dissimilatory nitrate reduction in estuarine sediments (Smith et al. 2007), and the genes encoding nitrogenase reductase (*nifH*) (Wakelin et al. 2007), nitric oxide reductase (*cnorB*) (Dandie et al. 2007), and ammonia monooxygenase (*amoA*) (Leininger et al. 2006) were used in agricultural soils as functional markers for nitrogen-fixation, denitrification and nitrification, respectively. With respect to SR-PRZs, functional genes have recently been applied to study SRB (Geets et al. 2006; Hallberg et al. 2004; Hiibel et al. 2008). However, a functional gene-based approach has never been applied to profile and quantify other equally important functional microbial groups, such as cellulose degraders, fermenters, and methanogens.

In this study, a new technique for denaturing gradient gel electrophoresis (DGGE) profiling of five different functional genes (*cel5*, *cel48*, *hydA*, *dsrA*, and *mcrA*) is

developed and combined with quantitative PCR (Q-PCR) targeting the same genes to characterize the microbial community before and after startup of columns simulating SR-PRZs. Six conditions were studied in duplicate to compare the effect of inoculum (dairy manure (DM), DM + sulfate-reducing enrichment (SRB), DM + cellulose-degrading enrichment (CD), and no inoculum (CR)) and supplemental carbon sources (soluble carboxymethyl cellulose (CMC) and ethanol (EtOH)). This study applies advanced qualitative and quantitative functional gene tools to provide key insight into the role of the initial inoculum and its stimulation with alternative carbon substrates on the microbial community of complex systems during startup and steady state.

7.3. Materials and Methods

7.3.1. Column Specifications

Twelve PVC columns (10.2 cm ID) with seven $\frac{1}{4}$ "sampling distributed alongside the 40.5 cm of operating height were operated vertically at an average upward flow of 250 mL/d to simulate field conditions. The influent port was located 10 cm from the bottom of the columns and the influent port, 2 cm from the top. The remaining five sampling ports (spaced 5-cm apart) were used for collection of substrate samples during column operation. The bottom (12 cm) and top (4 cm) layers of the columns were packed with gravel (particle size 0.131"-0.187") to ensure homogeneous flow distribution and were separated from the substrate by a Nylon mesh to prevent loss of substrate. Once filled, the columns were sealed with a monitoring well plug. The hydraulic residence time (HRT), determined by a tracer test with 10 g/L NaBr in a test column, was 6.4 days (Appendix C).

Each column received 866 g (dry wt) of substrate which consisted of 232 g beechwood (3.33 – 4.75 mm), 112 g pine shavings (3.33 – 4.75 mm), 17 g ground alfalfa, 51 g of limestone sand, and 454 g of playground sand. For each column, the dry materials were mixed in a ZipLoc® bag and stored opened in an anaerobic chamber under a 3% H₂/97% N₂ atmosphere. After 24 h, 743 mL of the corresponding inocula were added to each bag and mixed with the dry materials until the mixture appeared homogeneous. The bags were sealed and incubated overnight in the 3% H₂/97% N₂ atmosphere to facilitate attachment of the microorganisms to the substrate surface. The columns were filled with the inoculated substrate under a nitrogen atmosphere. Prior to column packing, the inoculated substrate material for each column was sampled and stored in 50-mL conical tubes at -80 °C for biomolecular analyses of the initial time point. When the columns were halfway filled, gentle pressure was applied on the top to help pack the substrate. Then, the remaining substrate was added and pressed again. After the columns were sealed, they were filled with simulated MD and allowed to incubate overnight. The next day, continuous flow was applied to all columns. This was considered Day 1 of operation.

7.3.2. Influent Composition

Columns were fed simulated MD consisting of 1,320 mg/L Na₂SO₄, 30 mg/L NH₄Cl, 90 mg/L ZnSO₄·7H₂O, 10 mg/L CdCl₂, and 0.92 mg/L FeSO₄·7H₂O in deionized water. The feed for the CMC columns also contained 500 mg/L of CMC. Feed solutions were adjusted to pH 5.5 and delivered to the columns via peristaltic pumps (Isamatec, Glattbrugg, Switzerland). The feed solutions were continuously bubbled with nitrogen in the feed tank. In addition to the simulated MD, the EtOH columns were fed 200 proof

ethanol at 2.8 μ L/h using a syringe pump (kd Scientific, Holliston, MA) connected into the feed line between the peristaltic pump and the columns. Because CMC is a solid substance, it could not be injected into the feed line. Therefore, while the other columns received feed from the same bottle, the CMC feed was prepared in the same manner, but in a separate feed bottle containing 0.507 g/L of CMC. The amount of CMC and ethanol in the feed corresponded to the equivalents required to reduce 50% of the sulfate based on the stoichiometry of the reactions and the yields described by Badger (2002).

7.3.3. Inocula

Fresh manure collected from a dairy in Wellington, CO and stored at 4 °C was used as inoculum. The manure was slurried by mixing 2032.5 g with 1098 mL of sterile deionized water and used to inoculate all but the CR columns.

The same mass of DM slurry was added to each column, with a target biomass concentration of 10^9 cells/g substrate (dry weight) as determined by 16S rRNA gene Q-PCR. The CD and SRB columns received an additional 10^9 cells/g substrate of a cellulose-degrading enrichment and a sulfate-reducing enrichment, respectively.

The cellulose-degrading bacteria inoculum was a mixture of three pure cultures of cellulose-degrading microorganisms (*Clostridium cellulovorans* ATCC 35296, *Fibrobacter succinogenes* ATCC 51214, and *Ruminococcus flavefaciens* ATCC 4994) and a mixed culture enriched for cellulose degraders. The pure cultures were grown anaerobically at 37 °C using the medium suggested by ATCC. Two different carbon sources (glucose and cellobiose) were used for the *C. cellulovorans* and *F. succinogenes* cultures. The growth medium for *R. flavefaciens* contained several carbon sources. Gas production was measured as an indicator of microbial activity and the cultures were

transferred to fresh medium every one or two days. Freezer stocks (in 70% glycerol) were prepared for each transfer and stored at -80 °C. The cultures used for the inoculation of the CD columns were cultivated anaerobically overnight from freezer stocks with cellobiose (*F. succinogenes* and *C. cellulovorans*) or glucose, cellobiose, maltose, and starch (*R. flavefaciens*) as the carbon source prior to inoculating the columns.

The initial inoculum for the enrichment culture of cellulose degraders consisted of ~50 g fresh sheep manure and ~70 g of sediment collected from the Cache la Poudre River in Fort Collins, CO, and slurried with 500 mL of sterile DI water. The enrichment culture was prepared and grown anaerobically in 60-mL serum bottles that contained 5 g/L crystalline cellulose, 2.5 g/L 2-bromoethane sulfonic acid (BESA) to inhibit methanogenic activity (Sparling and Daniels 1987), and 1.4 g/L sodium molybdate to inhibit SRB activity (Newport and Nedwell 1988) in M9 minimal salts medium (Fisher Scientific). The enrichments were maintained at 37 °C at 100 RPM for a minimum of eight days before being transferred to fresh medium. After two transfers, solid cellulosic material in the form of 12 g/L of beechwood (<0.841 mm) and 5 g/L of pine shavings (0.074 – 2.362 mm) was also added to the medium to encourage adaptation to more complex lignocellulose-based carbon sources. In the fourth transfer, M9 minimal salts medium was substituted for anaerobic cellulolytic medium (Atlas 1997) to ensure that adequate growth factors were present for the cellulose degraders. The enrichment culture obtained after the seventh transfer was used to inoculate the CD columns. Although no gas production was observed during the enrichment, visual inspection of the beechwood material suggested that cellulose degradation was occurring.

The SRB inoculum was an enrichment culture of a substrate sample collected from an ethanol-fed SR-PRZ treating MD at the National Tunnel site in Black Hawk, CO. The enrichment culture was grown in 60-mL serum bottles with 25-mL of ATCC Medium 1249 Modified Baar's medium and 1.2 mL of the SR-PRZ sample and maintained for 24 h at 20 °C and 100 RPM. Cultures were anaerobically transferred daily to 25 mL of medium for 48 days. The cultures from the last transfer were used as inoculum for the SRB columns.

7.3.4. Effluent Sampling

Effluent was collected from the top of each column in Nalgene bottles initially containing deionized water in which the column effluent tube was submerged to prevent entry of oxygen into the column. Liquid samples were collected in acid-washed, anaerobically sealed serum bottles and stored at 4 °C prior to chemical analysis to prevent oxidation of sulfides.

7.3.5. Column Substrate Sampling

When the effluent sulfate concentration in all the columns reached a pseudo-steady state (defined as changes in sulfate concentration of 10% or less for three HRTs) by Day 43 of operation, the substrate of the columns was sampled for biomolecular analyses. Approximately 3 g of packing material from the top, middle, and bottom sampling ports of each column were collected and mixed into 50-mL conical tubes using sterile tweezers and immediately snap frozen in liquid nitrogen. Samples were stored at -80 °C.

7.3.6. Analytical Methods

Sulfate was quantified by ion chromatography using a Metrohm 861 Advanced Compact IC with MSM and CO₂ Suppressor and a 250 mm Metrospec A Supp 5 High Resolution Anion Column (Houston, TX). The IC NET Chromatography Control and Data Acquisition System was used to calibrate the instrument and to collect and analyze chromatograms. Effluent samples were diluted 1:10 with deionized water to achieve a concentration within the detection range of 1-100 mg/L. Diluted samples were filtered via an inline filter. A four-point calibration curve (5, 10, 50, and 100 mg/L) was prepared in house via dilution from a 1000 g/L stock solution. Quality control measures included the preparation of fresh standards, analysis of at least one standard in triplicate, and repeat injection of every 20th sample of each analysis set.

Metals were analyzed using inductively coupled plasma absorbance emission spectroscopy (ICP-AES) (Thermo Jarrell Ash IRIS Advantage) following U.S. EPA Method 3015 (1994). Samples were filtered through 0.45-μm filters and 10 mL were digested according to EPA Method 3015 (1994) prior to analysis. Detection limits were 0.01 mg/L for zinc, and 0.005 mg/L for cadmium.

The pH was measured with an Accumet® AB15 Basic pH meter (Fisher Scientific, Pittsburgh, PA) immediately upon opening the anaerobically stored samples.

7.3.7. Biomolecular Analyses

7.3.7.1. DNA Extraction and Purification

Total genomic DNA was extracted from the column substrate sampled at the beginning of the experiment and at pseudo-steady state using the PowerMax™ Soil DNA Isolation Kit (MoBIO, Carlsbad, CA) according to the manufacturer's recommended protocol. DNA extracts were checked in a 1.2% agarose gel to verify the extraction and check the quality of the DNA.

The Geneclean® Spin Kit was used to purify 300 µL of the DNA extract following the manufacture's instructions. In the last step, 150 µL of sterile 10 mM tris buffer pH 8 were used instead of sterile deionized water to elute the DNA. The purified DNA extracts were verified on a 1.2% agarose gel. Aliquots of 50 µL of the purified DNA extract were stored at -80 °C and were used for downstream biomolecular analyses.

7.3.7.2. DGGE PCR

The *cel5*, *cel48*, *hydA*, *dsrA*, and *mcrA* primer sets (Chapter 6) were adapted for DGGE by the addition of a GC clamp in the 5'end of the forward primer. PCR conditions (magnesium and primer concentration) were optimized for the primer sets and used to amplify the purified DNA from the substrate samples collected at the beginning of the experiment, and at pseudo-steady state. The optimized PCR mixture contained 1X reaction buffer with 2 mM magnesium (5 Prime, Gaithersburg, MD); 1X PCR enhancer (5 Prime); 0.05 mM of each deoxynucleoside triphosphate; magnesium solution (5 Prime) at 1.0 mM (*hydA* and *mcrA*), 1.5 mM (*cel48* and *dsrA*), or 2 mM (*cel5*); 0.15µM

(for *cel48*, *hydA*, and *dsrA*) or 0.20 μ M (*cel5* and *mcrA*) of each primer; 0.25 μ L formamide; 1.75 U Taq DNA polymerase (5 Prime); 2 μ L DNA template; and water to a final volume of 25 μ L. To the *cel5* and *dsrA* master mixes, 0.75 units of iTaq DNA polymerase (Bio-Rad, Hercules, CA) were added. The temperature programs for each primer set are summarized in Table 7.1.

The 16S rRNA gene primer set I341F/I533R was used to amplify the variable V3 region of this gene (Watanabe et al. 2001). The master mix composition and temperature conditions for PCR were described by Pruden et al.(2007) and Watanabe et al. (2001), respectively. PCR products were verified on 1.2% agarose gels

Table 7. 1: PCR temperature conditions for the primer sets targeting at functional genes used in denaturing gradient gel electrophoresis.

Primer Set	Initial Denaturation	Denaturation	Annealing	Extension	Final Extension
GC <i>cel48</i> _490F/ <i>cel48</i> _920R	95 °C, 3 min	95 °C, 40 s	56 °C, 30 s	72 °C, 30 s	72 °C, 7 min
GC <i>cel5</i> _392F/ <i>cel5</i> _754R		40 cycles			
GC <i>hydA</i> _1290F/ <i>hydA</i> _1538R		95 °C, 40 s	52 °C, 30 s	72 °C, 30 s	
GC <i>dsrA</i> _290F/ <i>dsrA</i> _660R		45 cycles			
GC <i>mcrA</i> _1035F/ <i>mcrA</i> _1530R		95 °C, 40 s	59 °C, 30 s	72 °C, 30 s	
		45 cycles			
		95 °C, 40 s	60 °C, 30 s	72 °C, 30 s	
		50 cycles			
		95 °C, 40 s	56 °C, 30 s	72 °C, 30 s	
		40 cycles			

7.3.7.3. DGGE

Gels (8% acrylamide/bisacrylamide 19:1, BioRad) were cast using a denaturing gradient of 30 to 50% (PCR product from the *cel5*, *hydA*, and *mcrA* primer sets) or 30 to 60% (PCR product from the *cel48*, and 16S rRNA gene primer sets), with 100% denaturant defined as 7 M urea and 20% v/v formamide. Electrophoresis was performed at 57.5 °C at 130 V for 7 hours or 75 V for 14 hours. Gels were stained with SybrGold nucleic acid

stain (Molecular Probes, Inc., Eugene, OR). Gel images were captured using a UVP BioChemi Gel Documentation System (UVP, Upland, CA) and analyzed using Labworks software (UVP).

Labworks was used to identify the bands in the gels and to quantify their relative intensity in each lane. The relative diversity of the microbial community in each sample was calculated using the Shannon diversity index (Cox 1972; Xia et al. 2005):

$$H = -\sum \left[\frac{n_i}{N} \log \left(\frac{n_i}{N} \right) \right],$$

where n_i is the intensity of the individual bands and N is the sum of the intensity of all the bands in the lane.

The number of bands in each DGGE pattern was used as an indicator of species richness (S) and the evenness (E_H) was calculated as:

$$E_H = \frac{H}{\ln(S)}$$

7.3.7.4. Analysis of DGGE gels

DGGE fingerprints were analyzed with the Gelcompare II software version 5.10 (Applied Maths, Austin, TX). Since more than one DGGE gel was required per primer set, samples that were loaded in all of the DGGE gels were used as reference for gel-to-gel comparisons. The Dice coefficient was used to calculate pairwise similarity values between profiles and construct a similarity matrix. This matrix was converted to a dendrogram using the unweighted pair groups using mathematical averages clustering method. Dendograms and similarity matrices are presented in Appendix C.

7.3.7.5. Quantitative PCR.

The *cel5* and *cel48*, *hydA*, *dsrA*, and *mcrA* primer sets (Chapter 6) were used in Q-PCR to quantify cellulose-degrading bacteria, fermenters, SRB, and methanogens in the purified DNA extract from the samples collected at the beginning of the experiment and during the pseudo-steady state. In addition, total bacterial 16S rRNA genes were quantified using the conditions, universal BACT1369F and PROK1492R primers, and the TM1389F probe described by Suzuki et al. (2000). Q-PCR was performed in a 7300 Real-Time PCR System (Applied Biosystems, Foster City, CA). All samples were analyzed in triplicate. The master mix composition and temperature programs for all the primer sets were described in Chapter 6.

For each of the primer sets targeting functional genes, a four to six-point calibration curve was constructed using as standard a mixture of purified PCR products obtained with the plasmid-specific primers T3-T7 from sequenced clones. For the 16S rRNA gene primer set, purified PCR product amplified from an environmental sample with primers 8F and 1492R (Eden et al. 1991; Weisburg et al. 1991) was used as standard. Standards were analyzed in triplicate. The calibration curves were used for absolute quantification of the target genes under the assumption that the amplification efficiency of standards and samples was the same. To ensure that only samples for which this assumption was valid were analyzed, the procedure proposed by Chervoneva et al (Chervoneva et al. 2006) was applied. Briefly, LinRegPCR (Ramakers et al. 2003) was used to calculate the amplification efficiency from the amplification curve of each replicate sample and standard. A box plot outlier detection rule was applied to the amplification efficiencies of the standards to identify calibration standards that amplified

with dissimilar efficiencies. These standards were not used in the data analysis. The Kinetic Outlier Detection method (Bar et al. 2003) was used to compare the average efficiency of the remaining standards and the efficiency of each replicate to detect samples with dissimilar efficiencies from the standards. A more detailed explanation of the role of PCR efficiency in Q-PCR and the different methods to calculate it is presented in Appendix A.

7.3.8. Statistical Analyses

Mixed linear regressions were fit to the data sets using the PROC MIXED function of SAS 9.1 (SAS Institute Inc., Cary NC). Log transformation of all data sets was required to achieve homoscedasticity, and thus all comparisons were made in log scale. Degrees-of-freedom calculations were performed using the Kenward-Roger method. Significance was defined by a pair-wise comparison p-value ≤ 0.05 .

7.4. Results

7.4.1. Column Performance

7.4.1.1. Sulfate Removal and Column Startup

During the first 15 days (approximately 3.4 HRTs) of operation, the sulfate concentration in the effluent of all columns fluctuated around the influent values (Figure 7.1). After this startup time, the concentrations decreased sharply in all columns until about Day 20 when effluent concentrations began to level off to values between 304 and 505 mg/L. According to the criterion of changes of $\pm 10\%$ or less in sulfate concentration for 3 HRTs, pseudo-steady state was achieved between Days 30 and 42. During this time, the

sulfate concentration in the effluent of all columns was significantly lower than that in the feeds (p -value < 0.0001 for all columns) and there were no significant differences among the CD, CMC, DM, EtOH, and SRB columns. Sulfate removal in the CR columns, however, was lower than in the DM and CMC columns (p -value=0.05 for both comparisons).

7.4.1.2. Metal Removal

For the first 15 days of operation, the effluent concentration of cadmium and zinc in all the columns was significantly lower than the feed concentration (Figure 7.2). After this time, the concentration of both metals in the effluent of the CMC columns increased while it remained below 1 mg/L for cadmium and 5 mg/L for zinc in all the other columns.

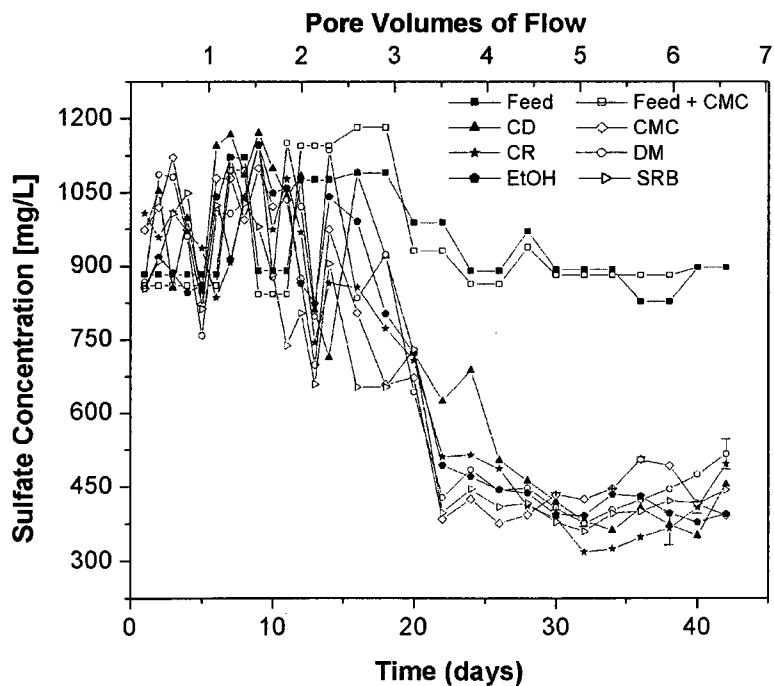


Figure 7. 1: Column feed and effluent sulfate concentrations determined by ion chromatography. Feed data were adjusted by 4 days to adjust for the hydraulic residence time. Data points represent the average of two biological replicates. Error bars represent the standard deviation of independently prepared technical replicates.

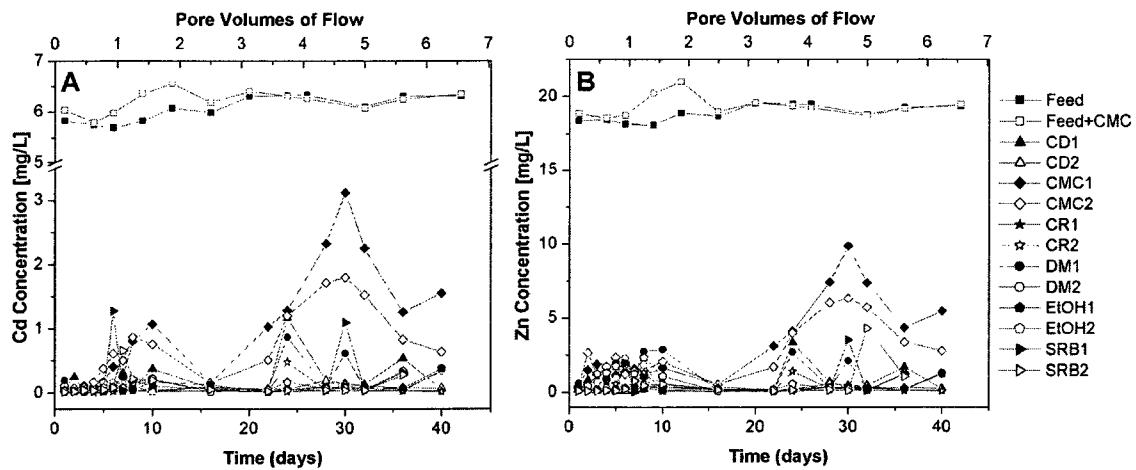


Figure 7. 2: Feed and effluent concentrations of (A) cadmium and (B) zinc as determined by ICP-AES. The error bars represent the standard deviation of independently prepared technical replicates

7.4.1.3. pH

For the first ten days of operation, pH values in the effluent of the columns were between 5.5 and 6.0 (Figure 7.3). After this time, pH increased in all columns to values between 6.5 and 7.5 which were significantly higher than the pH in the feed. There were no significant differences among the columns.

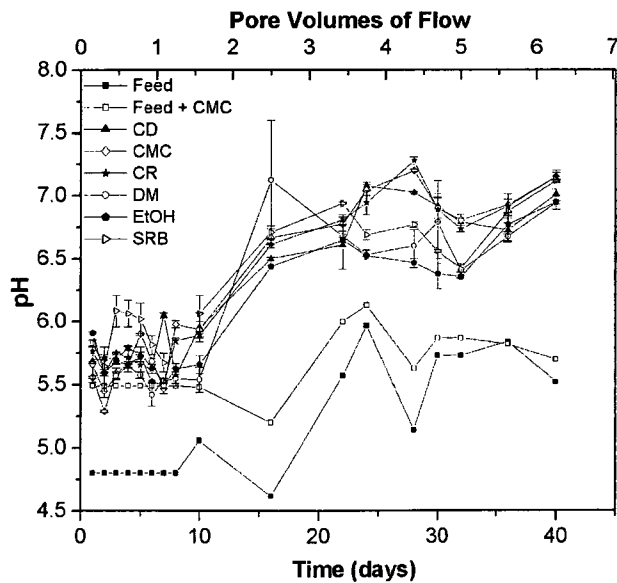


Figure 7. 3: Column feed and effluent pH. Data points represent the average of biological replicates and the error bars represent the average deviation of the biological replicates.

7.4.2. Functional Gene Characterization

7.4.2.1. DGGE Profiling of Functional and 16S rRNA genes

A representative cluster analysis is presented in Fig. 7.4 for reference. Cluster analysis of the 16S rRNA gene DGGE gels indicated a high degree of reproducibility in the initial DGGE patterns of the duplicate CD, CR, DM, and ETOH columns (similarity > 90%) (Appendix C). For the CMC and SRB columns, the similarity between duplicate columns was 71% and 61%, respectively. At the functional gene level, the level of reproducibility between biological duplicates at the beginning of the experiment depended on the functional gene analyzed. In the case of the *mcrA* patterns, the duplicate inoculated columns were highly reproducible whereas the CR columns were only 31% similar. For the *hydA* and *dsrA* fingerprints, the similarity between duplicates was between 66% and 75%. For the *cel5* DGGE, duplicate columns were from 34% to 52% similar and for the *cel48* DGGE, the similarity between duplicates ranged from 33% to 100%. In general, at pseudo-steady state, the similarity between duplicates decreased for the 16S rRNA, *cel5*, *hydA*, *dsrA*, and *mcrA* genes and increased for the *cel48* genes.

According to cluster analysis, the 16S rRNA gene DGGE banding patterns of the initial material in the DM, CMC, and EtOH columns, which all received the same inoculum, were highly similar (Appendix C). The majority of the bands detected in these columns were also found in the CD initial material. The banding patterns of the initial CR and SRB column material were distinct from each other and from all the other columns, as expected. At pseudo-steady state, no trends were evident from the cluster analysis. From visual inspection, the initial microbial communities were different from those at pseudo-steady state. In general, the diversity and richness decreased in the

columns after the startup except for the SRB #1 column where they remained the same. The evenness did not change from the startup to the steady state.

Presumably because of low relative abundance, *cel48* gene PCR products and DGGE profiles could only be obtained from the initial substrate of the CMC, DM, and EtOH columns. *Cel48* genes were successfully amplified from all pseudo-steady-state samples, suggesting that abundance of cellulose degraders increased during startup. The fingerprints from the available initial material and the steady state clustered separately. At pseudo-steady state, some bands were detected in all columns, but the overall patterns were distinct among different columns (similarity < 60%).

The initial and pseudo-steady state *cel5* DGGE patterns formed two separate clusters (Appendix C). During pseudo-steady state, the patterns in the DM columns were different from all the other columns. The EtOH and SRB columns and the CD, CMC, and CR columns formed two different clusters. In all columns, diversity and richness of *cel5* genes was higher at pseudo-steady state than in the initial inoculated substrate ($H = 1.02 \pm 0.66$ and 1.95 ± 0.23 , and $S = 4 \pm 2$ and 9 ± 3 bands for the initial material and the pseudo-steady state, respectively).

In the case of fermentative bacteria, the fingerprints from the initial material formed a unique cluster and the pseudo-steady state patterns separated into two groups, one with the DM and biostimulated columns (CMC and EtOH) and the other with the bioaugmented columns (SRB and CD). The diversity of *hydA* genes decreased from the initial material ($H=2.57 \pm 0.23$) to the pseudo-steady state ($H = 2.22 \pm 0.28$) in the DM, CMC, and EtOH columns. The banding patterns of the initial material from these columns were highly similar, comprised of three dominant bands. No PCR product could

be obtained from the initial substrate of the other columns. Based on the data from the initial time points available and from steady state for all columns, the richness of fermentative bacteria was higher than that of cellulose-degrading bacteria.

The *dsrA* DGGE patterns from the initial material in the CR columns were distinct from those in all the other columns (Appendix C). The banding patterns of the initial material from the DM, CMC, and EtOH columns were similar and distinct from the SRB and CR columns, further supporting the consistency in the initial material among these three column conditions. In the CD columns, the initial banding patterns were faint but they appeared to share bands with the DM, CMC, and EtOH columns. At pseudo-steady state, it was observed that the majority of the columns formed one cluster. In some cases, there was low similarity between samples that were loaded into different gels indicating some effect of gel-to-gel variation in the clustering. In the DM, CMC, and EtOH columns, the diversity of *dsrA* genes was higher in the initial material than at the pseudo-steady state. Diversity of *dsrA* genes at pseudo-steady state increased in the CD columns and remained constant in the CR and SRB columns. The same trend was observed for richness. In all columns, evenness decreased from startup to the pseudo-steady state.

In general, the *mcrA* diversity indices were comparable among the columns and remained relatively constant between the two time points (Appendix C). The DGGE patterns formed three clusters each of them containing fingerprints from the initial material and pseudo-steady state. At steady state, there was a high degree of similarity among the SRB and EtOH columns.

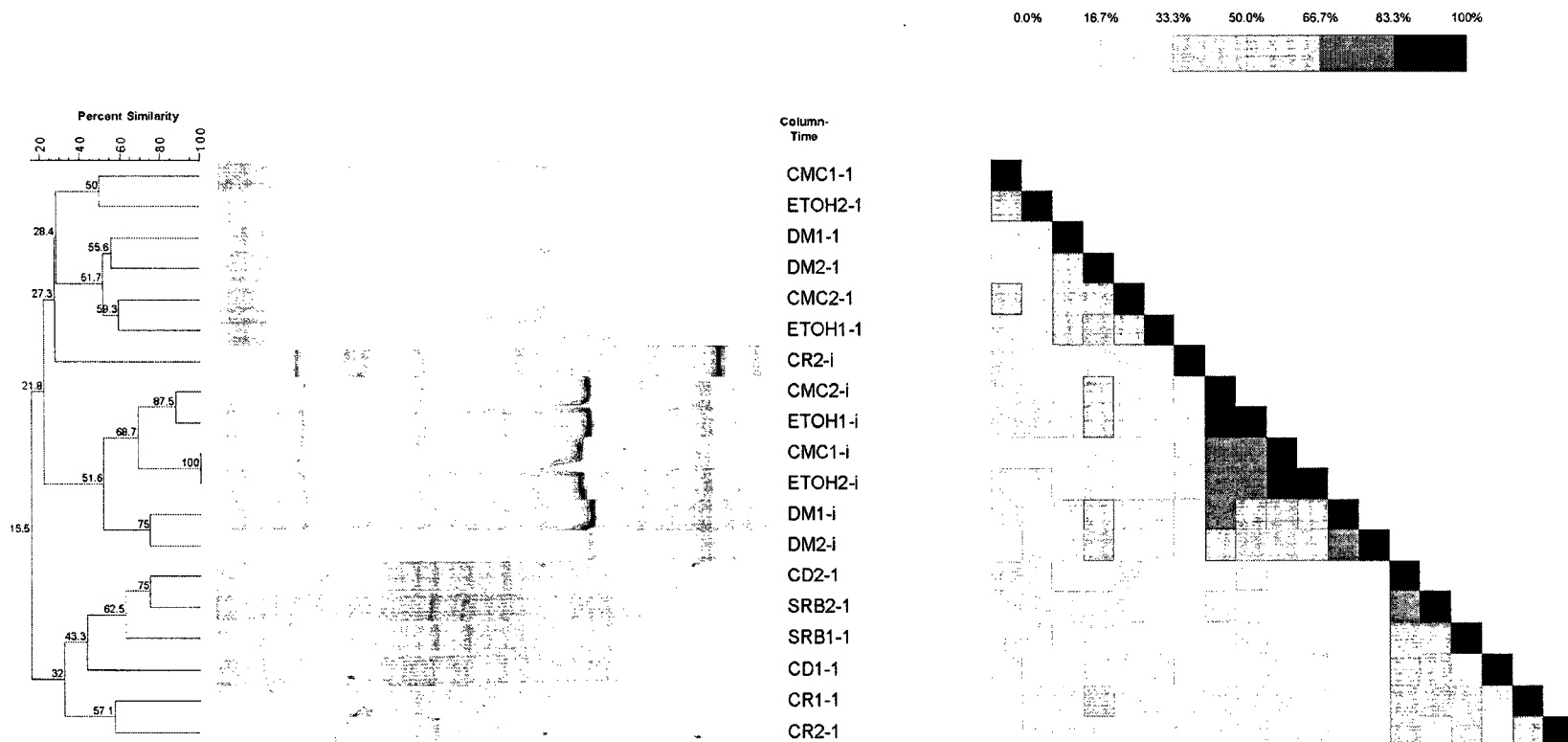


Figure 7.4: Cluster analysis of DGGE fingerprints of GChydA_1290F/hydA_1538R PCR products of DNA extracted from the columns at the beginning of the experiment (-i), and during the pseudo-steady state (-1) for the columns inoculated with dairy manure only (DM), dairy manure and an enrichment of SRB (SRB), dairy manure and an enrichment of cellulose degraders (CD), inoculated with dairy manure alone and supplemented with carboxymethyl cellulose (CMC) or ethanol (EtOH). 1 and 2 indicate the replicate number. Samples with a '#' in their label were used as reference to compare different gels.

7.4.2.2. Quantification of Microbial Functional Groups

The 16S rRNA gene was used as an indicator of the total bacterial density (Figure 7.5.A). In all except the CR columns, 16S rRNA genes significantly increased from the initial material to pseudo-steady state. The number of 16S rRNA genes at pseudo-steady state was not significantly different among the columns, except for the CR columns, which had significantly lower numbers. There was also not a significant difference among the columns in the initial material, except for the SRB and CD columns, which contained significantly fewer 16S genes initially.

The number of the genetic markers for cellulose-degrading bacteria (*cel5* and *cel48*) increased in all columns from the initial condition to pseudo-steady state (Figures 7.5.B &C). At pseudo-steady state, the SRB columns contained higher numbers of *cel5* and *cel48* genes than the other columns, except for EtOH #1 and DM #2 with respect to *cel5*.

In all the columns, the number of *hydA* genes increased from the initial to the pseudo-steady state condition (Figure 7.5.D). At pseudo-steady state, all the inoculated columns contained comparable numbers of *hydA* genes and significantly lower numbers were observed in the CR columns.

The number of *dsrA* genes increased in all columns from the initial to the pseudo-steady state condition (Figure 7.5.E). At pseudo steady state, the highest concentrations were observed in the SRB columns and in columns DM #2 and CMC #1.

In general, higher concentrations of *mcrA* genes were detected in the DM, CMC, and SRB columns than in the others (Figure 7.5.F). The lowest numbers of *mcrA* genes were found in the CR columns at both time points.

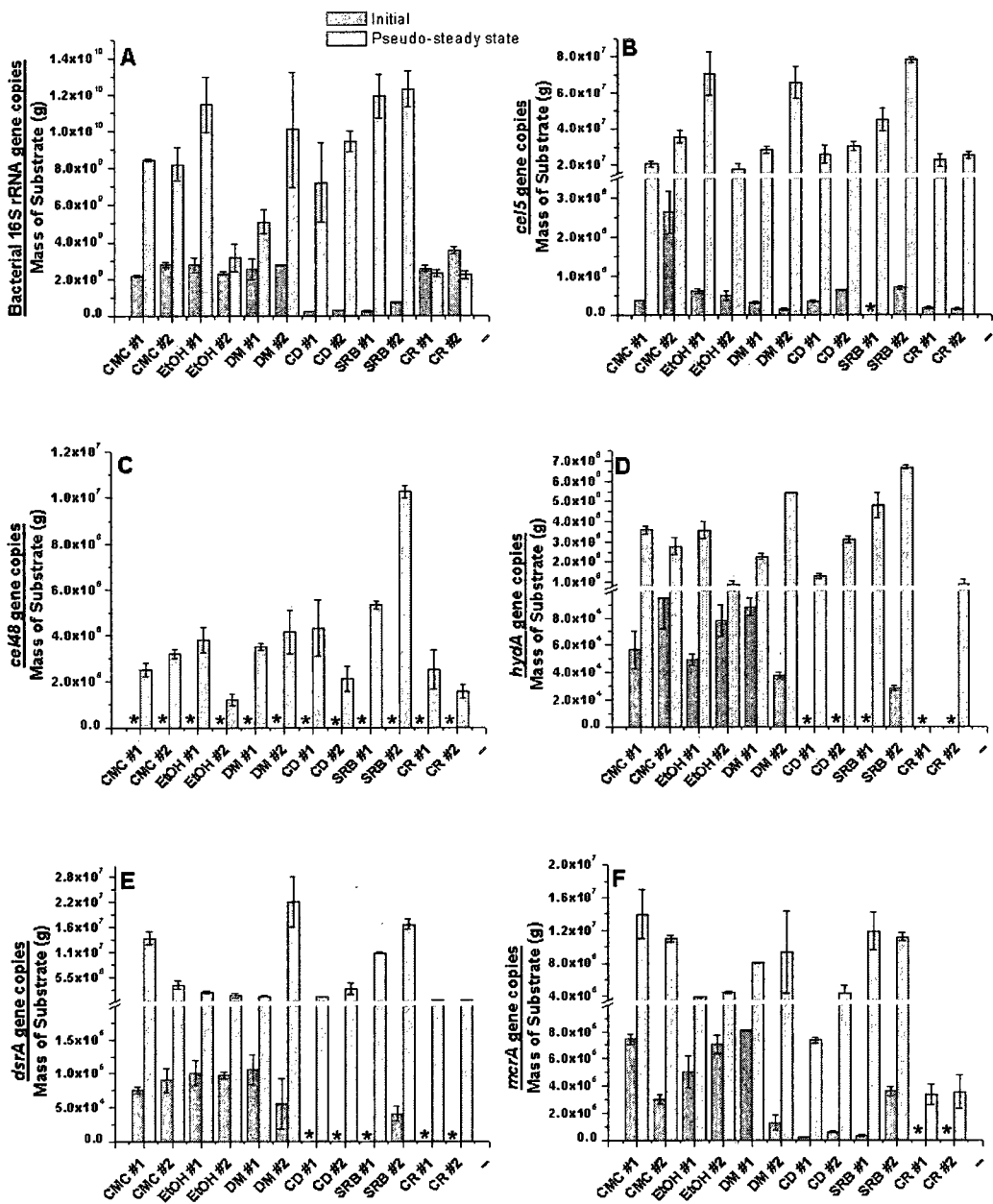


Figure 7. 5: Number of (A) 16S rRNA genes, (B) *cel5* genes, (C) *cel48* genes, (D) *hydA* genes, (E) *dsrA* genes, and (F) *mcrA* genes in the columns in the initial inoculated substrate and during the pseudo-steady state normalized to the mass of substrate as determined by Q-PCR. * indicates samples that were below the quantification limit.

7.5. Discussion

7.5.1. Effect of Inoculum on Pseudo-Steady-State Community

Of key interest in this study was the effect of the initial microbial composition on that of the steady-state community. Because all biotic and abiotic conditions were identical, it was expected that biological duplicates would develop identical pseudo-steady-state microbial communities. There was in fact a high level of similarity between biological replicates at pseudo-steady state based both on DGGE and Q-PCR analysis, but in general there was a slight reduction in similarity from what was observed for the initial condition. This suggests that the initial inoculum is a significant factor governing the composition of the steady-state community, but that there are random influences as well. Nonetheless, differences in the pseudo-steady-state communities among the column conditions investigated were more pronounced than those observed between replicates. Therefore, both biostimulation and bioaugmentation impacted the composition of the pseudo-steady-state community. It is also noteworthy that the methods applied in this study yielded a high level of repeatability for the analysis of the same material and also provided complementary information. For example, the same samples from the initial condition from which DGGE PCR products could not be obtained were confirmed to have low abundance of template by Q-PCR.

7.5.2. Effect of Inoculum on Performance

Sulfate removal started in all columns at about Day 15 and achieved pseudo-steady state by Day 28 which is comparable to other column studies (Logan et al. 2005; Pruden et al. 2007). Interestingly, the startup time and performance were similar among the columns,

including the CR columns, which performed marginally poorer than the DM and CMC columns. Although the CR columns were not directly inoculated, the substrate had not been sterilized and Q-PCR analysis of 16S rRNA genes demonstrated that the initial bacterial density after the overnight incubation prior to the beginning of column operation was not significantly different from the DM inoculated columns. Significant sulfate-reducing activity in uninoculated columns treating MD has been noted in other studies (Christensen et al. 1996; Pruden et al. 2007).

In terms of startup time, significant cadmium and zinc removal was observed before significant sulfate removal (approximately Days 1 and 20, respectively). The immediate startup for metal removal is not surprising and is likely associated with abiotic processes (Zagury et al. 2006) while the continuous removal can be attributed to precipitation as metal sulfides. Therefore, sulfate removal provides a better indicator of the startup time of biological activity than the metal removal.

Although sulfate reduction in the CMC columns was comparable to that of the other columns, the effluent concentrations of zinc and cadmium were significantly higher. The carboxymethyl and hydroxyl groups in CMC have chelating properties (Hosny et al. 1995) and might have formed complexes with the metals preventing their precipitation as metal sulfides.

7.5.3. Qualitative Changes in Microbial Community

Cluster analysis of DGGE banding patterns provided information about the similarities and differences in the microbial communities in the columns and the intensity and number of bands provided information on their diversity, richness, and evenness. Since the limit of detection of DGGE is approximately 1% (Muyzer et al. 1993), many

microorganisms that are a small fraction of the community (e.g., sulfate-reducing bacteria) are not typically detected by 16S rRNA-based DGGE. This limitation was eliminated by using DGGE primers specific to the microbial groups of interest: cellulose-degrading bacteria, fermenters, sulfate-reducing bacteria, and methanogens.

DGGE analyses of 5 different functional genes (*cel5*, *cel48*, *hydA*, *dsrA*, and *mcrA*) and the 16S rRNA gene confirmed that the initial microbial communities in the columns that were inoculated with dairy manure only (CMC, DM, and EtOH) were similar. The analyses also confirmed that the initial microbial community in the CR columns was distinct from the inoculated columns, as expected.

Although there were only marginal differences in performance among the columns during the pseudo-steady state, the microbial communities were different indicating that functional redundancy exists among microbes critical to MD remediation. Interestingly, the degree of similarity among columns depended on the gene analyzed. In general, a higher level of similarity was observed with the 16S rRNA gene than with the functional genes. Therefore, analysis of functional genes captured differences that 16S genes did not.

Cluster analysis of the *cel5*, *cel48*, *hydA*, and *dsrA* patterns indicated that the fingerprints of the initial material were different from the ones at pseudo-steady state. This suggests that these microbial groups underwent transformations to adapt to the conditions in the columns. In some cases, the net result was a loss in diversity, suggesting inability of the initial populations to adapt and/or enrichment of the most highly suited strains. This decrease in diversity was observed, for example, in the *dsrA* fingerprints of the CMC, DM, and EtOH columns. In other cases (e.g., the *hydA* and *dsrA* fingerprints of

the CD columns), diversity increased, which suggests enrichment of sub-dominant populations. Interestingly, SRB diversity remained constant in the SRB columns, suggesting that the bioaugmented SRB were well adapted to the column environment. Differences between initial and steady states were not apparent for *mcrA* patterns suggesting that methanogens were not particularly affected by the column environment.

DGGE analysis with functional-gene primers revealed some interesting aspects of the microbial communities in the columns. In general, the diversity of fermentative and sulfate-reducing bacteria was higher than that of cellulose degraders and methanogens. Of the four microbial functions targeted in this study, fermentation is probably the most widespread, and this was reflected in the DGGE banding patterns. The evenness of the different microbial groups was 0.8 or higher during column operation for the *cel5*, *cel48*, *hydA*, and *mcrA* genes and 0.6 or higher for the *dsrA* genes. Evenness is defined on a scale of 0 to 1, with 1 corresponding to equally distributed species. These results suggest that there were no dominant microorganisms within each functional group.

Since this is the first functional gene-based study of cellulose-degrading, fermentative, and sulfate-reducing bacteria, and methanogenic archaea of a lignocellulose-based environment, it is difficult to predict expected diversity. The primers targeting functional genes were designed to amplify the genes of both cultured and uncultured microorganisms and *in silico* analysis indicates that they are specific to phylogenetically diverse microorganisms (Chapter 6). However, given the significant sequence diversity in the target functional genes, particularly with respect to cellulose-degrading bacteria, it is possible that not all the target sequences were amplified by the primers. Thus the reported diversity indices may underestimate the actual diversity.

7.5.4. Quantitative Changes in Microbial Community

Q-PCR was used to monitor the total bacterial density (16S rRNA gene copies) and four functional groups in each column at the initial and pseudo-steady-state point. In all the columns, the numbers of *cel5*, *cel48*, *hydA*, *dsrA*, and *mcrA* genes were higher at pseudo-steady state than in the initial inoculated substrate, indicating that members of the microbial groups represented by these genes were able to survive and grow in the columns. Quantification of 16S rRNA genes also indicated an increase in the number of total bacteria in the inoculated columns. Although the uninoculated CR columns initially contained similar numbers of bacteria as the DM columns, the numbers remained constant (CR #1) or decreased (CR #2) at pseudo-steady state. Nevertheless, all of the other functional groups increased dramatically in the CR columns, especially cellulose degraders. This indicates that the proportional increase of these groups of interest was much greater in the CR than in the inoculated columns. Interestingly, *mcrA* genes representing methanogens were not detected in the CR column initial material and remained significantly lower than the other columns at steady-state. Since methanogens compete with SRB, this may have provided an additional unanticipated advantage to the CR columns.

Interestingly, bioaugmentation with cellulose-degrading bacteria and SRB did not lead to an obvious effect on sulfate removal. Unexpectedly, the initial number of 16S rRNA genes in the CD and SRB columns was lower than in the other columns. There was also no indication of higher numbers of cellulose degraders or sulfate reducers in their respective initial materials. Although additional cellulose-degrading and sulfate-reducing enrichments were added to the CD and SRB columns on top of the baseline level of dairy

manure present in all inoculated columns, these results suggest that the bioaugmentation attempt was confounded. Maintaining the enrichment cultures in a viable and active state via serial transfers was a significant challenge during column setup and it is possible that the populations had deteriorated by the time of the initial sampling point after the overnight incubation in the anaerobic chamber. Another possibility is that toxic by-products of the enrichment process were lethal to even the dairy manure bacteria during this incubation period. This would explain the overall lower initial bacterial density in these columns. Although the CD and SRB columns started with less bacterial mass, during column operation the 16S rRNA gene copies in these columns increased and were comparable to the other inoculated columns by pseudo-steady state. Also, *dsrA* genes were most abundant in the SRB columns at pseudo-steady state, suggesting that bioaugmentation did eventually have a net positive impact in these columns. However, neither *cel5* nor *cel48* was most abundant in the CD columns at pseudo-steady state.

Supplementation with carboxymethyl cellulose was expected to stimulate cellulose-degrading bacteria and increase their numbers. However, there did not seem to be an effect of CMC as the *cel5* and *cel48* gene numbers were comparable to those in the DM columns. The different types of cellulose (crystalline vs amorphous, soluble vs unsoluble) require the use of different enzymes for its hydrolysis and microorganisms differ in their affinities for the different types of cellulose. Therefore, CMC may have stimulated cellulose degraders not detectable by the *cel5* or *cel48* primer sets. The highest concentrations of these genes were actually in the SRB columns (along with *cel5* in one of the DM and one of the EtOH columns). This suggests that additional SRB may

have played an ecological role by removing toxic by-products that may have been inhibitory to anaerobic cellulose degraders.

Ethanol is a product of fermentation and can be directly utilized by sulfate reducers and similarly was expected to stimulate abundance of *dsrA* genes in the EtOH columns. However, the *dsrA* gene abundance at steady-state in these columns was still quite low, though comparable with all of the other columns. In fact, the EtOH columns in general were highly similar to the DM columns. This suggests that though EtOH is a substrate readily available to SRB and not to cellulose degraders or fermenters, it does not disrupt the lignocelluloses-degrading community. Therefore its temporary supplementation in the field should not have a negative impact on overall performance.

Although the similarity in performance among all the columns was unexpected, biomolecular analysis provided useful information to interpret the results and understand the underlying phenomena taking place. Biostimulation and bioaugmentation are remediation strategies that have worked successfully in SR-PRZs (Tsukamoto and Miller 1999) and other systems (Gentry et al. 2004; Mohan et al. 2007). However, there are also several cases where these strategies failed (Mohanty et al. 2008; Winchell and Novak 2008; Wright and Weaver 2004). In the case of bioaugmentation, growing specialized strains can be challenging particularly in the case of anaerobic and nutritionally fastidious microorganisms such as cellulose degraders. The biostimulation of microorganisms that grow on a variety of carbon sources (e.g., SRB) or that differ in their affinities for different forms of the same substrate (e.g., cellulose degraders) may also be less effective than biostimulation of more physiologically-constrained microorganisms. In addition, complex communities add an extra level of difficulty as the ecological interactions

among microbial groups and the effects of biostimulation and bioaugmentation on these interactions are difficult to predict.

7.6. Conclusions

This study provided a quantitative and qualitative characterization and comparison of genes corresponding to key functional groups of bacteria and methanogenic archaea at the beginning and pseudo-steady-state operation of lignocelluloses-based sulfate-reducing columns remediating mine drainage. Startup remains a dynamic and relatively unpredictable stage in operation of biological systems. The results indicate that while there is some effect of randomness on the ultimate composition, both biostimulation and bioaugmentation impact the composition achieved by the microbial community at steady-state operation.

7.8. Acknowledgements

Financial assistance was provided by the National Science Foundation Award CBET-0651947. Additional funding was provided by the EPA Office of Research and Development's Engineering Technical Support Center, under contract with Golder Associates, Inc., Contract # GS-10F00130N DO #1101 (David Reisman, Project Officer; reisman.david@epa.gov); and by the Water Research Experience for Undergraduates program at CSU sponsored by the National Science Foundation. The authors wish to thank Dr. Thomas Sale and Dr. Mitch Olson and the rest of the members of their contaminant hydrology lab for providing the columns and other equipment for the experimental setup and for their assistance in with the IC analysis. The authors also thank M.V. Prieto for her assistance in effluent sampling and biomolecular analyses.

7.8. References

- Angenent LT, Sung SW, Raskin L. 2002. Methanogenic population dynamics during startup of a full-scale anaerobic sequencing batch reactor treating swine waste. *Water Res.* 36(18):4648-4654.
- Atlas RM. 1997. *Handbook of Microbiological Media*. Boca Raton, FL.: CRC Press.
- Badger PC. 2002. Ethanol From Cellulose: A General Review. Janick J, Whipkey A, editors. Alexandria, VA: ASHS Press. 17-21 p.
- Bar T, Stahlberg A, Muszta A, Kubista M. 2003. Kinetic Outlier Detection (KOD) in real-time PCR. *Nucleic Acids Res.* 31(17).
- Beller HR, Kane SR, Legler TC, Alvarez PJ. 2002. A real-time polymerase chain reaction method for monitoring anaerobic, hydrocarbon-degrading bacteria based on a catabolic gene. *Environ. Sci. Technol.* 36:3977-3984.
- Chervoneva I, Hyslop T, Iglewicz B, Johns L, Wolfe HR, Schulz S, Leong E, Waldman S. 2006. Statistical algorithm for assuring similar efficiency in standards and samples for absolute quantification by real-time reverse transcription polymerase chain reaction. *Anal. Biochem.* 348(2):198-208.
- Christensen B, Laake M, Lien T. 1996. Treatment of acid mine water by sulfate-reducing bacteria; Results from a bench scale experiment. *Water Res.* 30(7):1617-1624.
- Cox GW. 1972. *Laboratory Manual of General Ecology*. Brown WC, editor. Dubuque, IA. 120-124 p.
- Dabert P, Delgenes JP, Godon JJ. 2005. Monitoring the impact of bioaugmentation on the start up of biological phosphorus removal in a laboratory scale activated sludge ecosystem. *Appl. Microbiol. Biotechnol.* 66(5):575-588.

- Dandie CE, Miller MN, Burton DL, ZebARTH BJ, Trevors JT, Goyer C. 2007. Nitric oxide reductase-targeted real-time PCR quantification of denitrifier populations in soil. *Appl. Environ. Microbiol.* 73(13):4250-4258.
- De la Rua A, Gonzalez-Lopez J, Nieto MAG. 2008. Influence of temperature on inoculation and startup of a groundwater-denitrifying submerged filter. *Environ. Eng. Sci.* 25(2):265-274.
- Eden PA, Schmidt TM, Blakemore RP, Pace NR. 1991. Phylogenetic Analysis Of Aquaspirillum-Magnetotacticum Using Polymerase Chain Reaction-Amplified 16s Ribosomal-Rna-Specific Dna. *Int. J. Syst. Bacteriol.* 41(2):324-325.
- Geets J, Borremans B, Vangronsveld J, Diels L, van der Lelie D. 2005. Molecular monitoring of SRB community structure and dynamics in batch experiments to examine the applicability of *in situ* precipitation of heavy metals for groundwater remediation. *J. Soils Sediments* 5(3):149-163.
- Geets J, Vanbroekhoven K, Borremans B, Vangronsveld J, Diels L, Van der Lelie D. 2006. Column experiments to assess the effects of electron donors on the efficiency of *in situ* precipitation of Zn, Cd, Co and Ni in contaminated groundwater applying the biological sulfate removal technology. *Environ. Sci. Pollut. Res* 13(6):362-378.
- Gentry TJ, Josephson KL, Pepper IL. 2004. Functional establishment of introduced chlorobenzoate degraders following bioaugmentation with newly activated soil - Enhanced contaminant remediation via activated soil bioaugmentation. *Biodegradation* 15(1):67-75.

- Hallberg KB, Rolfe S, Johnson DB. The microbiology of passive remediation technologies for mine drainage treatment. In: P. JA, Dudgeon BA, Younger PL, editors; 2004 19-23 September; Newcastle upon Tyne, U.K. University of Newcastle upon Tyne. p 227-233.
- Hiibel SR, Pereyra LP, Inman LY, Tischer A, Reisman DJ, Reardon KF, Pruden A. 2008. Microbial community analysis of two field-scale sulfate-reducing bioreactors treating mine drainage. *Environ. Microbiol.* 10(8):2087-2097.
- Hong H, Pruden A, Inman LY, Reardon KF. 2007. Comparison of microbial communities present in columns with varying sulfate-reducing activities remediating mine drainage. Submitted to *Water Research*.
- Hosny WM, Hadi AKA, Elsaied H, Basta AH. 1995. Metal-Chelates With Some Cellulose Derivatives.3. Synthesis And Structural Chemistry Of Nickel(Ii) And Copper(Ii) Complexes With Carboxymethyl Cellulose. *Polym. Int.* 37(2):93-96.
- Johnson DB, Hallberg KB. 2005. Acid mine drainage remediation options: a review. *Sci. Total Environ.* 338(1-2):3-14.
- Johnson DB, Hallberg KB. 2005. Biogeochemistry of the compost bioreactor components of a composite acid mine drainage passive remediation system. *Sci. Total Environ.* 338(1-2):81-93.
- Leininger S, Urich T, Schloter M, Schwark L, Qi J, Nicol GW, Prosser JI, Schuster SC, Schleper C. 2006. Archaea predominate among ammonia-oxidizing prokaryotes in soils. *Nature* 442(7104):806-809.

- Linkfield TG, Suflita JM, Tiedje JM. 1989. Characterization Of The Acclimation Period Before Anaerobic Dehalogenation Of Halobenzoates. *Appl. Environ. Microbiol.* 55(11):2773-2778.
- Logan MV, Reardon KF, Figueroa LA, McLain JET, Ahmann DM. 2005. Microbial community activities during establishment, performance, and decline of bench-scale passive treatment systems for mine drainage. *Water Res.* 39(18):4537-4551.
- Mohan SV, Mohanakrishna G, Raghavulu SV, Sarma PN. 2007. Enhancing biohydrogen production from chemical wastewater treatment in anaerobic sequencing batch biofilm reactor (AnSBBR) by bioaugmenting with selectively enriched kanamycin resistant anaerobic mixed consortia. *Int. J. Hydrol. Energy* 32(15):3284-3292.
- Mohanty SR, Kollah B, Hedrick DB, Peacock AD, Kukkadapu RK, Roden EE. 2008. Biogeochemical processes in ethanol stimulated uranium-contaminated suhsurface sediments. *Environ. Sci. Technol.* 42(12):4384-4390.
- Muyzer G, Dewaal EC, Uitterlinden AG. 1993. Profiling of complex microbial populations by denaturing gradient gel electrophoresis analysis of polymerase chain reaction-amplified genes coding for 16S rRNA. *Appl. Environ. Microbiol.* 59(3):695-700.
- Newport PJ, Nedwell DB. 1988. The Mechanisms Of Inhibition Of *Desulfovibrio* And *Desulfotomaculum* Species By Selenate And Molybdate. *J. Appl. Bacteriol.* 65(5):419-423.

- Nicomrat D, Dick WA, Tuovinen OH. 2006. Assessment of the microbial community in a constructed wetland that receives acid coal mine drainage. *Microb. Ecol.* 51(1):83-89.
- Pereyra LP, Hiibel SR, Pruden A, Reardon KF. 2008. Comparison of microbial community composition and activity in sulfate-reducing batch systems remediating mine drainage. *Biotechnology and bioengineering* 101(4):702-713.
- Pruden A, Messner N, Pereyra L, Hanson RE, Hiibel SR, Reardon KF. 2007. The effect of inoculum on the performance of sulfate-reducing columns treating heavy metal contaminated water. *Water Res.* 41(4):904- 914.
- Ramakers C, Ruijter JM, Deprez RHL, Moorman AFM. 2003. Assumption-free analysis of quantitative real-time polymerase chain reaction (PCR) data. *Neurosci. Lett.* 339(1):62-66.
- Rittmann BE, McCarty PL. 2001. *Environmental Biotechnology: Principles and Applications*. Boston: McGraw-Hill.
- Smith CJ, Nedwell DB, Dong LF, Osborn AM. 2007. Diversity and abundance of nitrate reductase genes (*narG* and *napA*), nitrite reductase genes (*nirS* and *nrfA*), and their transcripts in estuarine sediments. *Appl. Environ. Microbiol.* 73(11):3612-3622.
- Spain JC, Pritchard PH, Bourquin AW. 1980. Effects Of Adaptation On Biodegradation Rates In Sediment-Water Cores From Estuarine And Fresh-Water Environments. *Appl. Environ. Microbiol.* 40(4):726-734.
- Sparling R, Daniels L. 1987. The Specificity Of Growth-Inhibition Of Methanogenic Bacteria By Bromoethanesulfonate. *Can. J. Microbiol.* 33(12):1132-1136.

- Suzuki MT, Taylor LT, DeLong EF. 2000. Quantitative analysis of small-subunit rRNA genes in mixed microbial populations via 5'-nuclease assays. *Appl. Environ. Microbiol.* 66(11):4605-4614.
- Tsukamoto TK, Miller GC. 1999. Methanol as a carbon source for microbiological treatment of acid mine drainage. *Water Res.* 33(6):1365-1370.
- Wakelin SA, Colloff MJ, Harvey PR, Marschner P, Gregg AL, Rogers SL. 2007. The effects of stubble retention and nitrogen application on soil microbial community structure and functional gene abundance under irrigated maize. *FEMS Microbiol. Ecol.* 59(3):661-670.
- Watanabe K, Kodama Y, Harayama S. 2001. Design and evaluation of PCR primers to amplify bacterial 16S ribosomal DNA fragments used for community fingerprinting. *J. Microbiol. Methods* 44(3):253-262.
- Weisburg WG, Barns SM, Pelletier DA, Lane DJ. 1991. 16s Ribosomal Dna Amplification For Phylogenetic Study. *J. Bacteriol.* 173(2):697-703.
- Winchell LJ, Novak PJ. 2008. Enhancing polychlorinated biphenyl dechlorination in fresh water sediment with biostimulation and bioaugmentation. *Chemosphere* 71(1):176-182.
- Wright AL, Weaver RW. 2004. Fertilization and bioaugmentation for oil biodegradation in salt marsh mesocosms. *Water Air Soil Pollut.* 156(1-4):229-240.
- Xia SQ, Shi Y, Fu YG, Ma XM. 2005. DGGE analysis of 16S rDNA of ammonia-oxidizing bacteria in chemical-biological flocculation and chemical coagulation systems. *Appl. Microbiol. Biotechnol.* 69(1):99-105.

- Xing DF, Ren NQ, Rittmann BE. 2008. Genetic diversity of hydrogen-producing bacteria in an acidophilic ethanol-H₂-coproducing system, analyzed using the [Fe]-hydrogenase gene. *Appl. Environ. Microbiol.* 74(4):1232-1239.
- Zagury GJ, Kulnieks VI, Neculita CM. 2006. Characterization and reactivity assessment of organic substrates for sulphate-reducing bacteria in acid mine drainage treatment. *Chemosphere* 64(6):944-954.

Chapter 8 Conclusions and Future Work

8.1. Conclusions

The studies presented in this dissertation have demonstrated the importance of the microbial community in the bioremediation of mine drainage (MD) and promise to be useful in guiding the selection and enrichment of inocula for sulfate-reducing permeable reactive zones (SR-PRZs).

The initial batch and column studies to investigate the effect of the type of inoculum on performance revealed that three microbial groups are key for good performance: cellulose degraders, fermenters, and sulfate reducers. This finding also highlights the importance of studying all the members of the microbial community and not only the ones that are ultimately responsible for the removal of metals (i.e., sulfate-reducing bacteria (SRB)). In addition, these results suggested that selection of inocula is crucial for ensuring good performance. Opposite performance was observed in batch and continuous flow systems inoculated with dairy manure. This puts in evidence the importance of pre-screening the inocula before use for inoculation of large-scale systems. Although they are not continuous flow systems as the SR-PRZ, batch tests proved to be a useful tool for comparing a large number of inocula and could even be used to screen materials for inoculation of field SR-PRZs.

The influence of the complexity of the carbon substrate on the composition of the microbial community was also demonstrated. Not surprisingly, a complex carbon source

gave rise to a diverse microbial community whereas a simpler one favored the dominance of SRB in the community. Although there were no differences in performance, these results raise the question of how these different communities would perform after an environmental stress, which commonly occurs in field SR-PRZs.

Although the previous studies were important in helping understand the microbial ecology of SR-PRZs, they did not provide information on the composition of each on the key microbial groups and their abundance. The functional-gene based approach proved to be very useful in overcoming this limitation and it provided an efficient approach to obtain fingerprints and quantitative information of cellulose degraders, fermenters, sulfate reducers, and methanogens. In addition, its application in Q-PCR offers the possibility of high throughput, real-time monitoring of the microbial community. Although there was some degree of variability on the sequences of the functional genes, this diversity was captured with a smaller number of polymerase chain reaction (PCR) primers than what would be needed with a 16S rRNA gene-based approach. This research served as a proof of concept for the application of biomolecular tools targeted at functional genes in the study of complex anaerobic microbial communities. This approach is not limited to SR-PRZs as cellulose degraders, fermenters, SRB, and methanogens are found in a variety of environments and processes such as biohydrogen production, rumen, wastewater treatment, and anaerobic decomposition of litter.

The biomolecular characterization of the microbial communities in laboratory batch and continuous-flow systems and pilot-scale SR-PRZs revealed that functional diversity in these systems goes beyond cellulose degradation, fermentation, sulfate

reduction, and methanogenesis and reinforced the choice of a functional gene-based approach to the study the microbiology of SR-PRZs.

The studies presented in this dissertation have provided significant insight in the microbial communities involved in MD remediation at laboratory and pilot scale. They also presented a variety of biomolecular methods that can be used to explore different aspects of the microbial community such as diversity, structure, and relative abundance of specific microbial groups not only in SR-PRZs and but also in other systems with complex microbial communities. They demonstrated the great potential of biomolecular methods as monitoring tools for tracking the microbial community during MD remediation. Integration of biomolecular and performance data will provide a more complete understanding of SR-PRZ functioning that could be used to improve SR-PRZ performance and reliability.

8.2. Future Work

Because of the critical role that microorganisms play in SR-PRZ performance, research efforts should continue to improve the understanding of the microbial community of MD bioremediation.

Field SR-PRZs are subject to several environmental stresses such as metal and sulfate overloads, changes in influent pH, aeration during seasons of low flow, and low temperatures during winter. Unfortunately, there has not been much research on how these stresses affect the microbial community and, ultimately, SR-PRZ performance. Research in this area is critical to design SR-PRZs that operate well not only under normal conditions but also under sub-optimal conditions. In other systems, microbial functional redundancy appears to be related to the ability of a microbial community to

recover after a stress. If a microbial community includes different microorganisms that carry out the same biochemical functions but with different tolerance to stress, the community can still function or recover more rapidly after a stress even if some microorganisms do not survive. Biomolecular methods are an excellent tool to investigate the diversity and other characteristics of the microbial community in response to stress. In particular, a combination of a 16S rRNA gene-based approach and the functional gene-based approach presented in Chapters 6 and 7 would help address this question not only at the overall-community level but also at each of the functional levels. This would help identify vulnerabilities in the microbial community and guide remedial actions.

Although development of inocula by mixing pure cultures known to have the desired microbial functions is a possible alternative, the complexity of the natural microbial communities in SR-PRZs poses a significant challenge to this strategy. A more fruitful approach might be the enrichment of microorganisms desirable for MD remediation through directed enrichment from environmental samples. The biomolecular tools presented in this dissertation in combination with multivariate techniques for comparing microbial communities provide an efficient and complete way of monitoring the enrichment.

On the methodological side, future research should focus on expanding the functional gene-based approach to target additional microbial functions. Hydrogen metabolism plays a key role in the SR-PRZ microbial community and is central to many microbial interactions. Acetogens are key players in interspecies hydrogen transfer as they can compete with SRB and methanogens for this energy source. Competition between acetogens and SRB could be detrimental to sulfate removal and SR-PRZ

performance. However, the role of acetogens in SR-PRZs has not received much attention. These microorganisms could be easily detected with the functional gene-based approach by targeting the gene encoding for formyltetrahydrofolate synthetase. The functional gene approach could expand even further to target microorganisms responsible for MD generation such as sulfur and iron oxidizers. These microorganisms have been found in SR-PRZs and could counteract the remediation process.

Continuing with the improvement of the functional gene-based approach, the next logical step for this method would be its application on messenger RNA. This would allow the identification and quantification of the active members of each microbial group. The primers designed in this research can be converted to probes and applied in fluorescent *in situ* hybridization or implemented in reverse-transcription PCR and used in quantitative PCR, or fingerprinting methods such as denaturing gradient gel electrophoresis and capillary electrophoresis single-strand conformation polymorphism.

Appendix A PCR Efficiency

A.1. The Concept of PCR Efficiency

In polymerase chain reaction (PCR) DNA is exponentially amplified. For example, in a sample with one copy of the target double-stranded DNA, after the first cycle of PCR amplification there will be four copies, after the second cycle there will be eight copies and so forth. In mathematic terms, PCR can be described with the following formula:

$$\begin{aligned} \text{a. } N_n &= N_0 \cdot 2^n \\ \text{or} \quad &\qquad \text{Eq. A1} \\ \text{b. } R_n &= R_0 \cdot 2^n \end{aligned}$$

where N_n is the number of copies of target DNA at cycle n , N_0 is the initial amount of DNA copies, R_n is the amount of target DNA at cycle n in fluorescence units, R_0 is the initial amount of DNA expressed in fluorescence units, and n is the number of PCR cycles.

The reaction eventually reaches a plateau phase due to the consumption of reagents and molecular crowding produced by the accumulation of PCR products. Equation A1 only describes the exponential part of PCR and not the plateau phase.

In many cases, the amount of DNA after each PCR cycle does not double due to the presence of PCR inhibitors, poor quality of the DNA template, concentration of the DNA template, and unspecific annealing of the primers among other factors (Pfaffl 2004). Equation A1 can be written in a more general way to take this into account:

$$\begin{aligned} \text{a. } N_n &= N_0 \cdot E^n \\ \text{or} & \quad \quad \quad \text{Eq. A2} \\ \text{b. } R_n &= R_0 \cdot E^n \end{aligned}$$

where E is the PCR amplification efficiency and ranges from 1 (0% efficiency, no amplification) to 2 (100% efficiency, doubling of DNA after each cycle). The amplification efficiency of PCR is the relative increase in amplicon concentration per cycle (Nordgard et al. 2006) or, in other words, the rate of amplification of the amplicon.

A.2. Quantitative PCR (Q-PCR) and Absolute Quantification

In Q-PCR, the amplification of the target DNA is monitored in every cycle by measuring the fluorescence emitted by a reporter dye. The fluorescence is considered to be proportional to the amount of DNA in each cycle (Peirson et al. 2003).

At the beginning of the reaction, the fluorescence increases exponentially until it reaches a plateau (Figure A.1a). On a logarithmic scale (Figure A.1b), the small differences in the earlier cycles can be appreciated. The linear relationship between the increase in fluorescence and cycle number observed in a logarithmic scale indicates the region of exponential amplification. Note that in a regular scale, the region of exponential amplification (linear part of logarithmic plot) is the very early part of the curve (which is not the region that looks linear on the regular scale view).

Quantification of the initial amount of DNA in a sample must be done where the amplification is exponential, which is at the very beginning of the upturn of the curve. The cycle at which the fluorescence from a sample crosses a threshold value is known as C_t and is used for absolute quantification of target DNA. The value of C_t is inversely proportional to the initial amount of DNA in the sample. In general, for samples analyzed

under the same conditions (i.e., samples in the same run), the same threshold value is used. A calibration curve of Ct versus initial input amount of target DNA or copy number is constructed using serial dilutions of a standard of known concentration. The Ct values of the samples are converted into number of copies using this calibration curve. At the threshold value, Equation A2 can be written as:

a. $N_{Ct} = N_0 \cdot E^{Ct}$
or Eq. A3
b. $R_{Ct} = R_0 \cdot E^{Ct}$

where N_{Ct} and R_{Ct} are the threshold value expressed in number of DNA copies and the fluorescence units, respectively.

A mathematical formula for the calibration curve can be obtained by applying logarithm to both sides of Equation A3.a and rearranging the terms:

$$\log(N_{0, \text{std}}) = \log(N_{Ct}) - Ct \cdot \log(E_{\text{std}}) \quad \text{Eq.A4}$$

where the subscript std denotes the standard.

Thus, the y-intercept of the calibration curve is the logarithm of the threshold value used to determine the Ct and the slope is the negative logarithm of the average amplification efficiency of all the standards (E_{std}).

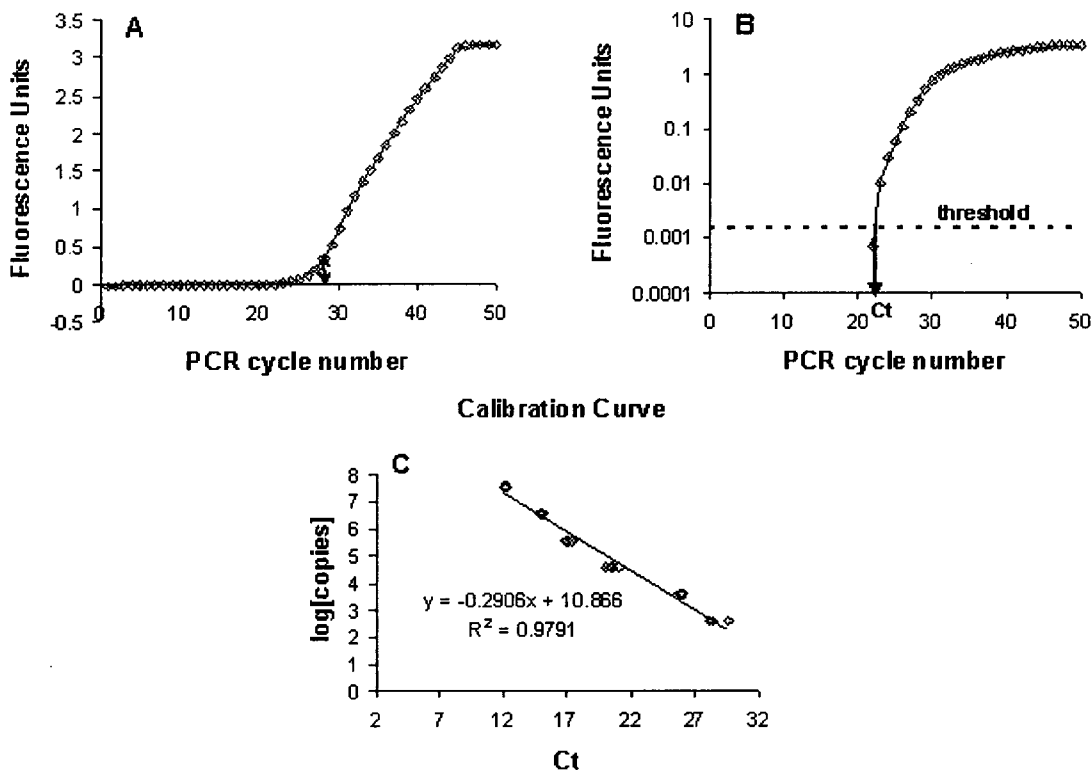


Figure A. 1: Absolute quantification using Q-PCR. (A) Amplification curve. The end of the exponential phase of amplification is indicated with a double arrow (B) Logarithmic plot of the amplification curve. The threshold value used to determine the Ct value is indicated with a dashed line (C) Calibration curve constructed using serial dilutions of a standard. The y-intercept is the logarithm of the threshold value and the slope is the negative logarithm of the average amplification efficiency of the standards.

A.3. PCR Efficiency and Q-PCR

Absolute quantification in Q-PCR is based on the assumption of similar amplification efficiencies between the calibration standards and the samples (Pfaffl 2001). However, in many cases, the efficiencies of samples and standards are different (Liu and Saint 2002; Ramakers et al. 2003).

The following is a theoretical example to demonstrate the importance of amplification efficiency in Q-PCR. Equation A4 was used to calculate a calibration curve

using a threshold value of 10^9 copies of target DNA for a calibration standard that amplifies with an efficiency of 95 % ($E=1.95$):

$$\log(\text{copies}) = 9 - 0.29 \cdot Ct \quad \text{Eq. A5}$$

The Ct values for six different samples that were amplified with 90% efficiency were calculated using Equation A3.a. The Ct values were converted into number of copies using Eq. A5. The number of copies in the samples estimated using the calibration curve were anywhere from 51% to 81% less than the actual number of copies in the sample (Table A1).

This example demonstrates how small differences in PCR amplification efficiency between samples and standards can translate into significant differences in the predicted number of copies in the samples. For this reason, it is important to estimate the amplification efficiency of samples and standards and check that they are not significantly different.

Table A 1: Example of how differences in amplification efficiency between samples and standards can impair absolute quantification in Q-PCR. In this example, the amplification efficiency is 95% for the standards and 90% for the samples and all Ct values are calculated at the same threshold value. The calibration curve (Eq. A5) was used to calculate the number of copies of target DNA in the sample (N_0 's) and compared to the actual number of copies in the sample ($N_{0,S}$)

Samples 90% efficiency ($E = 1.90$)			Conversion using calibration curve	
$N_{0,S}$ [copies target DNA]	Threshold value [copies target DNA]	Ct	N_0 's [copies target DNA]	% Fold difference (N_0 's/ $N_{0,S}$)100
5.E+06	1.E+09	8.25	4.04E+06	81
5.E+05	1.E+09	11.84	3.68E+05	74
5.E+04	1.E+09	15.43	3.35E+04	67
5.E+03	1.E+09	19.02	3.06E+03	61
5.E+02	1.E+09	22.60	2.78E+02	56
5.E+01	1.E+09	26.19	2.54E+01	51

A.4. Methods to Estimate Amplification Efficiency.

The methods to estimate amplification efficiency fall into two approaches (Karlen et al. 2007). A summary of these methods is provided in Table A2. In the first approach, the Ct values of serial dilutions of a sample are plotted against the logarithm of the dilution. A linear regression is performed and the amplification efficiency of the samples is obtained from the slope of the line. If there are PCR inhibitors in the sample, dilution of the sample will also dilute the inhibitors and therefore decrease their effect on PCR (Ramakers et al. 2003). As a result, the PCR amplification efficiency increases with each dilution step and the slope of the line represents the average efficiency. The serial dilutions approach is not feasible with samples with low copy numbers and is very laborious as several replicates of each dilution have to be analyzed (Bar et al. 2003). In the second approach, an efficiency value is calculated for each reaction by modeling either the exponential phase of PCR amplification or the entire amplification curve.

Table A 2: Methods used to calculate PCR amplification efficiency.

Method	Description	Reference
Serial dilution method	E is determined by performing a dilution series of a sample and is calculated from the slope of a plot of Ct versus log (dilution)	(Stahlberg et al. 2003)
LinRegPCR	Calculates the initial amount of target DNA (expressed in arbitrary fluorescent units) and E from linear regression analysis of log fluorescence data from the exponential phase of amplification.	(Ramakers et al. 2003)
DART-PCR	Uses linear regression of the log fluorescence data around the midpoint between the maximum fluorescence and background noise to calculate E and the initial amount of target DNA in fluorescence units.	(Peirson et al. 2003)
Exponential Model	Uses a sigmoidal model to fit the fluorescence data from the exponential phase of amplification. E is calculated from two arbitrary fluorescence thresholds.	(Liu and Saint 2002)
Sigmoid curve-fitting (SCF)	Uses a four-parameter sigmoid model to fit the full kinetics of the amplification (lag + exponential + plateau phases)	(Tichopad et al. 2002)
Exponential fitting	Fits amplification curve to exponential function:	(Karlen et al. 2007; Tichopad et al. 2003)

The LinRegPCR (Ramakers et al. 2003) and DART-PCR (Peirson et al. 2003) approaches use linear regression of the linear part of the log fluorescence plot (i.e., the exponential amplification phase) and estimate the amplification efficiency from the slope of the line. Both methods use a linearized form of Equation A2.b:

$$\log(R_n) = \log(R_0) + n \cdot \log(E) \quad \text{Eq.A6}$$

The methods only differ on the algorithm that is used to find the ‘window of linearity’ (i.e., the region of exponential amplification, which is the linear part of the log fluorescence plot). LinRegPCR uses an iterative algorithm formulated to search for lines consisting of at least four and no more than six data points with the highest R^2 value and a slope close to the maximum slope. The slope criterion is included in the algorithm to avoid fitting in the plateau phase.

The algorithm used by DART-PCR uses the fluorescence maximum (R_{\max}) and the background noise (R_{noise}) of each plot to determine a signal range in which the amplification rate can be accurately determined. The midpoint (M) of the log-transformed signal range is calculated as:

$$M = R_{\text{noise}} \cdot \sqrt{\frac{R_{\max}}{R_{\text{noise}}}} \quad \text{Eq.A7}$$

Linear regression is applied to calculate the slope of the log fluorescence around M and the amplification efficiency is calculated from the slope.

The exponential model method (Liu and Saint 2002) calculates the efficiency with the formula:

$$E = \left(\frac{R_{n,A}}{R_{n,B}} \right)^{\frac{1}{C_{t,A} - C_{t,B}}} - 1 \quad \text{Eq.A8}$$

where $R_{n,A}$ and $R_{n,B}$ are the fluorescence units at arbitrary thresholds A and B in an individual curve, and $C_{T,A}$ and $C_{T,B}$ are the threshold cycles at these arbitrary thresholds.

The Sigmoid curve-fitting (SCF) method (Tichopad et al. 2002) uses a four-parameter sigmoid model to fit the full kinetics of the amplification:

$$f = y_0 + \frac{a}{1 + e^{-\left(\frac{x-x_0}{b}\right)}} \quad \text{Eq.A9}$$

where f is the fluorescence at cycle x , y_0 is the ground fluorescence, a is the difference between maximal fluorescence in the run and ground fluorescence, x_0 is the inflection point of the curve and b is the slope. In this model, the smaller the value of b , the higher the amplification efficiency. A drawback of this method is that fluorescence data including at least the beginning of the plateau phase are needed. This can be a disadvantage when using small amounts of sample or quantifying genes with low copy numbers.

The exponential fitting method (Tichopad et al. 2003) fits the exponential part of the amplification curve to the following formula:

$$f = \gamma_0 + \alpha \cdot E^n \quad \text{Eq.A10}$$

where f is the fluorescence, γ_0 is the upward shift due to ground fluorescence, and α is the fluorescence due to nucleic acid input. Separate mathematical algorithms are applied to identify the PCR ground fluorescence phase and the non-exponential and plateau phases and exclude them from the calculation process.

The approaches presented above are only a small sample the methods that can be used to estimate the amplification efficiency. Although the methods in the second group differ in what type of curve is fitted to the data and the algorithms employed to select the

data points to be fitted, they are all based on the same concept which is the utilization of the amplification kinetics to estimate the rate at which the PCR product is amplified (i.e., the amplification efficiency).

If a correction is going to be applied to adjust for differences between the amplification efficiencies of standards and samples, special care has to be taken to ensure that an accurate estimate of the amplification efficiency is obtained. If not, errors in the estimation of the efficiency are going to be exponentially magnified and will have a considerable effect on the estimated number of copies (Peirson et al. 2003). Several studies have compared different methods to estimate the efficiency and explained their benefits and drawbacks (Cikos et al. 2007; Guescini et al. 2008; Karlen et al. 2007; Skern et al. 2005). Some studies have also proposed modifications to improve the prediction of the efficiency (Kontanis and Reed 2006).

Instead of correcting for different amplification efficiencies between samples and standards, a more conservative approach is to use the calibration curve to quantify the number of copies only in samples with efficiency not significantly different from that of the standards. In this case, even if the method used to calculate the efficiency does not produce accurate estimates, as long as the same method is used to calculate all the efficiencies, any significant difference between estimated efficiencies should reflect differences in true efficiencies (Bar et al. 2003). Bar (2003) proposed a kinetic outlier detection (KOD) method to identify samples that have efficiencies different from the standards. In this method, a sample is considered an outlier if:

$$P^* = 2 \cdot \left[1 - \Phi \left(\frac{|e_i - \mu_{\text{standards}}|}{\sigma} \right) \right] < 0.05 \quad \text{Eq. A11}$$

where Φ is the cumulative distribution function for the standard normal distribution, e_i is the observed efficiency of the sample, $\mu_{\text{standards}}$ is the mean efficiency of the calibration standards and σ is the standard deviation of the efficiency of the calibration standards.

Chervoneva (2006) proposed a modification of the KOD method to exclude calibration standards with outlying amplification efficiencies. The boxplot outlier detection rule is applied to the estimates of the amplification efficiency of the standards to eliminate inefficient reactions and ensure that only reactions with comparable efficiencies are included in the calibration curve. Observations that fall below the lower fence $LF = Q_1 - 1.5(Q_3 - Q_1)$ or above the upper fence $UF = Q_3 + 1.5(Q_3 - Q_1)$ are considered outliers. Q_1 and Q_3 are the first and third quartiles of the set of amplification efficiencies of the standards. Once the outlying standards are identified and discarded, the KOD method is applied to compare the amplification efficiencies of samples and standards.

A.5. Correction for Difference in Efficiency between Samples and Standards

For the calibration standards, the linearized form of Equation A3.a is:

$$\log(N_{ct}) = \log(N_{0,std}) + Ct \cdot \log(E_{std}) \quad \text{Eq.A12}$$

For the samples, Equation A3.a can be written as:

$$\log(N_{ct}) = \log(N_{0,s}) + Ct \cdot \log(E_s) \quad \text{Eq.A13}$$

where the subscripts std and s correspond to the calibration standards and samples, respectively.

For a given Ct value, when $E_s = E_{std}$, then $N_{0,std} = N_{0,s}$. This means that the calibration curve will accurately predict the number of copies of the target DNA in the samples. If $E_s > E_{std}$ or $E_s < E_{std}$, then the calibration curve will over estimate or under

estimate the number of copies in the sample, respectively. In this case, Equations A12 and A13 can be combined to produce a formula to calculate the number of copies of the target DNA in the sample as a function of the number of copies predicted by the calibration curve. Rearranging Equations A12 and A13:

$$C_t = \frac{[\log(N_{ct}) - \log(N_{0, \text{std}})]}{\log[E_{\text{std}}]} \quad \text{Eq. A14}$$

$$C_t = \frac{[\log(N_{ct}) - \log(N_{0,s})]}{\log[E_s]} \quad \text{Eq. A15}$$

Combining Equations A14 and A15 and rearranging the terms:

$$\log(N_{0,s}) = \log(N_{ct}) - [\log(N_{ct}) - \log(N_{0, \text{std}})] \cdot \frac{\log(E_s)}{\log(E_{\text{std}})} \quad \text{Eq. A16}$$

When the efficiencies of the standards and samples are different, Equation A16 can be used to correct for this difference. It should be noted, however, that application of corrections using individual E values may impair the quantification as it introduces systematic errors in the data analysis (Cikos et al. 2007; Karlen et al. 2007; Peirson et al. 2003). It is recommended that the mean efficiency be used because it provides a better representation of the amplification kinetics (Peirson et al. 2003). Applying a correction when samples do not exhibit comparable kinetics has the risk of exponentially magnifying errors in the estimation of the efficiency, which could render the estimated number of copies meaningless. For this reason, this type of correction should only be applied when there is sufficient statistical evidence to justify it.

To confirm that Equation A16 was correct, its formula was used to correct the number of copies of target DNA in the samples of the example in Table A1. The formula correctly predicted the number of copies in the samples (Table A3).

Table A 3: Number of copies (N_0 's,corr) in the samples of the example in Table A1 calculated using Equation A16 to correct for different amplification efficiencies between samples and standards.

Standards			
Average amplification efficiency = 95% Calibration curve: $\log(N_0) = 9 - 0.29 Ct$			
Samples			
Amplification efficiency 90%			
$N_{0,s}$ [copies target DNA]	Ct	N_0 's [copies target DNA]	N_0 's,corr [copies target DNA]
5.E+06	8.25	4.E+06	5.E+06
5.E+05	11.84	4.E+05	5.E+05
5.E+04	15.43	3.E+04	5.E+04
5.E+03	19.02	3.E+03	5.E+03
5.E+02	22.60	3.E+02	5.E+02
5.E+01	26.19	3.E+01	5.E+01

Jørgensen and Leser (2007) used Q-PCR to quantify *Bacillus licheniformis* CH200 and *Bacillus subtilis* CH201 spores in animal feed samples and applied the following formula to correct for different amplification efficiencies between samples and standards and obtain a corrected estimate of the spore content in the samples ($\log(Qty_{corr})$):

$$\log(Qty_{corr}) = 1 - (\log(E_{std,ave}) - \log(E_s)) \cdot \log(Qty) \quad Eq.A17$$

where $\log(Qty)$ is the log of colony forming units calculated from the calibration curve, $E_{std,ave}$ is the mean of the amplification efficiencies of the standards determined by LinRegPCR, and E_s is the amplification efficiency of the samples determined by LinRegPCR. The following table from their study summarizes their results:

Table A 4: Table 6 from Jørgensen and Leser (2007). The table summarizes the results of the quantification of *Bacillus licheniformis* CH200 and *Bacillus subtilis* CH201 spores in animal feed samples by multiplex Q-PCR.

Sample	Strain	Plate count (log CFU g ⁻¹)	<i>C_t</i>	Standard curve-1		Standard curve-2			
				Log Qty ^a	DIFF Log Qty (%)	Log Qty ^b	DIFF Log Qty (%)	Sample ^c Eff	Log Qty _{corr} ^d
1.1	CH200	6.13	26.33±0.22	6.69	9.04	7.06	15.07	1.73±0.10	6.66
	CH201	6.15	27.66±0.14	6.20	0.76	6.87	11.64	1.85±0.07	6.68
2.1	CH200	5.83	29.29±0.79	5.81	-0.26	6.25	7.31	1.56±0.07	5.62
	CH201	5.73	30.24±0.38	5.46	-4.75	6.16	7.48	1.93±0.07	6.10
5.2	CH200	5.83	30.00±0.23	5.60	-3.87	6.06	3.99	1.66±0.05	5.61
	CH201	5.73	29.83±0.40	5.57	-2.69	6.27	9.46	1.64±0.21	5.77
6.2	CH200	6.13	28.00±0.17	6.19	0.97	6.60	7.65	1.57±0.06	5.95
	CH201	6.15	28.95±0.12	5.83	-5.28	6.51	5.86	1.54±0.01	5.82
7.1	CH200	7.14	24.96±0.28	7.09	-0.60	7.43	4.12	1.84±0.04	7.21
	CH201	7.12	25.28±0.14	6.88	-3.31	7.52	5.67	1.83±0.04	7.28
8.2	CH200	7.23	25.04±0.09	7.07	-2.14	7.41	2.54	1.86±0.06	7.22
	CH201	7.14	25.92±0.10	6.70	-6.12	7.35	2.96	1.89±0.09	7.22
9.2	CH200	7.22	25.43±0.17	6.95	-3.71	7.30	1.11	1.92±0.05	7.22
	CH201	7.14	25.06±0.18	6.95	-2.65	7.59	6.28	1.99±0.04	7.61
10.2	CH200	8.20	23.83±0.53	7.43	-9.45	7.74	-5.68	1.68±0.09	7.21
	CH201	8.20	22.26±0.25	7.75	-5.48	8.36	1.86	1.89±0.03	8.20
Mean				-2.47		5.46			0.47

Spores were quantified using two different standard curves. Spore quantities (Log Qty) were estimated from the *C_t* values using the standard curves and compared to plate counts (log CFU).

Differences between Log Qty and plate counts (DIFF) were calculated as [(Log Qty - Log CFU)/Log CFU] × 100 (%).

^a Number of spores estimated from standard curve-1.

^b Number of spores estimated from standard curve-2.

^c Amplification efficiency calculated by LinRegPCR (Ramakers et al., 2003). Numbers are mean±S.D. of 3 replicate PCR.

^d Number of spores estimated from standard curve-2 and corrected for the difference in amplification efficiency between samples and the standards according to: Log Qty_{corr} = 1 - [Log(mean Eff_{standard}) - Log(Eff_{sample})] × Log Qty.

The log(Qty) values calculated with the standard curve-2 and the sample efficiencies from Table A4 were used in Equation A17 to calculate the corresponding log(Qty_{corr}) values. The average efficiency for the standards was 1.97. The log(Qty_{corr}) values obtained were different from the ones reported in Table A4. However, modifying the equation by rearranging the parenthesis (Eq.A18) yielded the values reported in the table.

$$\log(\text{Qty}_{\text{corr}}) = [1 - (\log(\text{E}_{\text{std,ave}}) - \log(\text{E}_{\text{sample}}))] \cdot \log(\text{Qty}) \quad \text{Eq.A18}$$

Equation A18 was used to correct the number of copies in the samples from the example in Table A1. The values predicted by this formula did not coincide with the expected ones (Table A5). In addition, the Equation A18 could not be derived using the mathematical model for PCR amplification used to derive Equation A16. No information is provided in Jorgensen and Leser (2007) regarding the derivation of this formula and the assumptions involved. For this reasons, the use of this formula is not advised.

Table A 5: Number of copies (N_0')_{S,Eq.A18} in the samples of the example in Table A1 calculated using Equation A18 to correct for different amplification efficiencies between samples and standards.

Standards			
Average amplification efficiency = 95% Calibration curve: $\log(N_0) = -0.2553Ct + 9$			
Samples			
Amplification efficiency 90%			
N_0 's [copies of target DNA]	Ct	N_0 's [copies of target DNA]	N_0' _{S,Eq.A18} [copies of target DNA]
5.E+06	8.E+00	4.E+06	3.E+06
5.E+05	1.E+01	4.E+05	3.E+05
5.E+04	2.E+01	3.E+04	3.E+04
5.E+03	2.E+01	3.E+03	3.E+03
5.E+02	2.E+01	3.E+02	3.E+02
5.E+01	3.E+01	3.E+01	2.E+01

A.6. References

- Bar T, Stahlberg A, Muszta A, Kubista M. 2003. Kinetic Outlier Detection (KOD) in real-time PCR. Nucleic Acids Res. 31(17).
- Chervoneva I, Hyslop T, Iglewicz B, Johns L, Wolfe HR, Schulz S, Leong E, Waldman S. 2006. Statistical algorithm for assuring similar efficiency in standards and samples for absolute quantification by real-time reverse transcription polymerase chain reaction. Anal. Biochem. 348(2):198-208.
- Cikos S, Bukovska A, Koppel J. 2007. Relative quantification of mRNA: comparison of methods currently used for real-time PCR data analysis. BMC Mol. Biol. 8.
- Guescini M, Sisti D, Rocchi MBL, Stocchi L, Stocchi V. 2008. A new real-time PCR method to overcome significant quantitative inaccuracy due to slight amplification inhibition. BMC Bioinformatics 9.

- Jorgensen C, Leser TD. 2007. Estimating amplification efficiency improves multiplex real-time PCR quantification of *Bacillus licheniformis* and *Bacillus subtilis* spores in animal feed. *J. Microbiol. Methods* 68(3):588-595.
- Karlen Y, McNair A, Persegues S, Mazza C, Mermod N. 2007. Statistical significance of quantitative PCR. *BMC Bioinformatics* 8.
- Kontanis EJ, Reed FA. 2006. Evaluation of real-time PCR amplification efficiencies to detect PCR inhibitors. *Anal. Biochem.* 351(4):795-804.
- Liu WH, Saint DA. 2002. A new quantitative method of real time reverse transcription polymerase chain reaction assay based on simulation of polymerase chain reaction kinetics. *Anal. Biochem.* 302(1):52-59.
- Nordgard O, Kvaloy JT, Farmen RK, Heikkila R. 2006. Error propagation in relative real-time reverse transcription polymerase chain reaction quantification models: The balance between accuracy and precision. *Anal. Biochem.* 356(2):182-193.
- Peirson SN, Butler JN, Foster RG. 2003. Experimental validation of novel and conventional approaches to quantitative real-time PCR data analysis. *Nucleic Acids Res.* 31(14).
- Pfaffl MW. 2001. A new mathematical model for relative quantification in real-time RT-PCR. *Nucleic Acids Res.* 29(9).
- Pfaffl MW. 2004. Determination of real-time PCR efficiency - an overview.
- Ramakers C, Ruijter JM, Deprez RHL, Moorman AFM. 2003. Assumption-free analysis of quantitative real-time polymerase chain reaction (PCR) data. *Neurosci. Lett.* 339(1):62-66.

- Skern R, Frost P, Nilsen F. 2005. Relative transcript quantification by Quantitative PCR: Roughly right or precisely wrong? *BMC Mol. Biol.* 6.
- Stahlberg A, Aman P, Ridell B, Mostad P, Kubista M. 2003. Quantitative real-time PCR method for detection of B-lymphocyte monoclonality by comparison of kappa and lambda immunoglobulin light chain expression. *Clin. Chem.* 49(1):51-59.
- Tichopad A, Dilger M, Schwarz G, Pfaffl MW. 2003. Standardized determination of real-time PCR efficiency from a single reaction set-up. *Nucleic Acids Res.* 31(20).
- Tichopad A, Dzidic A, Pfaffl MW. 2002. Improving quantitative real-time RT-PCR reproducibility by boosting primer-linked amplification efficiency. *Biotechnol. Lett.* 24(24):2053-2056.

Appendix B Primer Design

B.1. Design of *cel48* primers

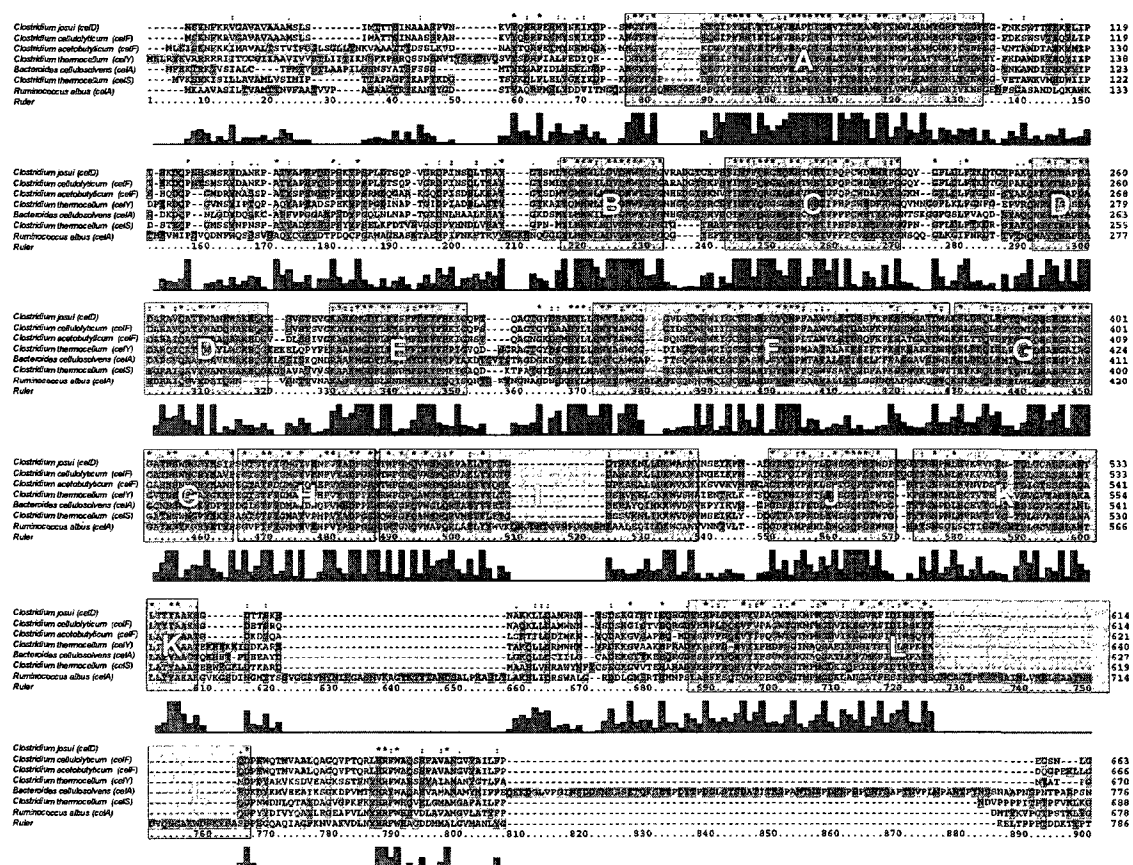


Figure B. 1: Multiple protein alignment of seven glycoside hydrolases of the family 48 and the blocks of conserved protein sequence (indicated with green boxes) identified by the Blocksmaker program. The alignment was constructed using ClustalX.

Primers found with the CODEHOP algorithm in each block of conserved protein sequence. The degeneracy (degen) of the 3' core and the melting temperature of the

primer (temp) are indicated. When the melting temperature is too low, the message 'Extend clamp' appears next to the primer:

Block unknown_A

```

N G Y F S E E G I P Y
oligo:5'-AATGGCTATTTAGCGAAGAAggnrtnccnta-3' degen=128 temp=60.1
G Y F S E E G I P Y H
oligo:5'-TGGCTATTTAGCGAAGAAAGGCrtncntayca-3' degen=64 temp=61.9
I E T M M V E A P D
oligo:5'-CATTGAAACCATGATGGTGGargcnccnga-3' degen=32 temp=61.6
E T M M V E A P D Y
oligo:5'-GAAACCATGATGGTGGAAgcncngayta-3' degen=32 temp=60.3
M V E A P D Y G
oligo:5'-TGATGGTGGAAAGCGccngaytaygg-3' degen=16 temp=60.3
V E A P D Y G H
oligo:5'-GGTGGAAAGCGCCGgaytaygnca-3' degen=16 temp=63.1

```

Complement of Block unknown_A

```

G I P Y H S I E T M M V
ccnyanggnatAGTATCGTAACCTTGGTACTACC oligo:5'-
CCATCATGGTTCAATGCTATGAtanggnayncc-3' degen=128 temp=62.0
P Y H S I E T M M V E
anggnatrgtrwCGTAACCTTGGTACTACCACC oligo:5'-
CCACCATCATGGTTCAATGCwrtgrtgtnangna-3' degen=128 temp=63.4
P Y H S I E T M M V E
ggnatrgtrwsGTAACTTGGTACTACCACCT oligo:5'-
TCCACCATCATGGTTCAATGSwrtgrtgtnangg-3' degen=64 temp=61.6
E A P D Y G H E T T
ctycngngnctaATACCGGTACTTGGTGG oligo:5'-GGTGGTTCATGCCATAAtcngngcytc-
3' degen=32 temp=61.3
A P D Y G H E T T S
cgnggnctratACCGGTACTTGGTGGT oligo:5'-TGGTGGTTCATGCCAtartcngngc-3'
degen=32 temp=60.7
P D Y G H E T T S
ggnctratrcGGTACTTGGTGGTCG oligo:5'-GCTGGTGGTTCATGGccrtartcngg-3'
degen=16 temp=62.5
D Y G H E T T S E A
ctratrcngtACTTGGTGGTCGCTTC oligo:5'-CTTCGCTGGTGGTTCAAtgnccrtartc-3'
degen=16 temp=60.2

```

Block unknown_B

```

Y G M H W
oligo:5'-TATbdnatgcaytg-3' degen=72 temp=-128.4 Extend clamp
Y G M H W
oligo:5'-TATbdnatgcaytgg-3' degen=72 temp=-128.4 Extend clamp
Y G M H W L
oligo:5'-TATGGCatgcaytgght-3' degen=6 temp=32.5 Extend clamp
M H W L M D V D N
oligo:5'-CATGCATTGGCTGATGGaygtngayaa-3' degen=16 temp=60.2
H W L M D V D N W
oligo:5'-TGCATTGGCTGATGGATgtngayaaytg-3' degen=16 temp=61.1
H W L M D V D N W
oligo:5'-TGCATTGGCTGATGGATgtngayaaytgg-3' degen=16 temp=61.1
H W L M D V D N W Y
oligo:5'-TGCATTGGCTGATGGATGTngayaaytgg-3' degen=16 temp=61.1

```

H W L M D V D N W Y
 oligo:5'-CATTGGCTGATGGATGTGgayaaytggta-3' degen=4 temp=62.9
Complement of Block unknown_B
 Y G M H W L M D V
 atrvhntacgtAACCGACTACCTAC oligo:5'-CATCCATCAGCCAAtgcatnhvrta-3'
 degen=72 temp=60.5
 M H W L M D V D N W Y G
 tacgtraccdaCTACCTACACCTATTAACCATAC oligo:5'-
 CATACCAATTATCCACATCCATCadccartgcat-3' degen=6 temp=60.7
 H W L M D V D N W Y G
 acgtraccdannACCTACACCTATTAACCATACCG oligo:5'-
 GCCATACCAATTATCCACATCCAnnadccartgca-3' degen=96 temp=62.8
 D V D N W Y G F G N
 ctrcanctrtaACCATAACGAAACCGTT oligo:5'-TTGCCAAAGCCATACCAAAttrtcnacrtc-3'
 degen=16 temp=60.3
 V D N W Y G F G N
 canctrtracCATACCGAAACCGTTA oligo:5'-ATTGCCAAAGCCATAccarttrtcnac-3'
 degen=16 temp=57.5 Extend clamp
 D N W Y G F G N
 anctrtraccaTACCGAAACCGTTA oligo:5'-ATTGCCAAAGCCATaccarttrtcna-3'
 degen=16 temp=57.5 Extend clamp
 D N W Y G F G N
 ctrtraccatACCGAAACCGTTA oligo:5'-ATTGCCAAAGCCAtaccarttrtc-3' degen=4
 temp=57.5 Extend clamp
 N W Y G F G N
 trttraccatryCGAAACCGTTA oligo:5'-ATTGCCAAAGCyrtaaccarttrt-3' degen=16
 temp=33.7 Extend clamp
 N W Y G F G N
 ttraccatryyGAAACCGTTA oligo:5'-ATTGCCAAAGyyrtaccartt-3' degen=16
 temp=24.1 Extend clamp
Block unknown_C
 Y I N T Y Q
 oligo:5'-TATATTaayacntwyca-3' degen=32 temp=-18.7 Extend clamp
 Y I N T Y Q R
 oligo:5'-TATATTAAATacntwycarmg-3' degen=64 temp=1.4 Extend clamp
 Y I N T Y Q R G
 oligo:5'-TATATTAAATACCTwycarmgnggg-3' degen=64 temp=17.3 Extend clamp
 G E Q E S C W E T I
 oligo:5'-GGCGAACAGGAAAGCTGCtkbgaracnrt-3' degen=96 temp=62.9
 Q E S C W E T I P
 oligo:5'-AACAGGAAAGCTGCTGGgaracnrtnc-3' degen=64 temp=60.9
Complement of Block unknown_C
 I N T Y Q R G E Q E
 tadtrtrgnawAGTCGCACCGCTTGTCC oligo:5'-CCTGTTGCCACGCTGAwangtrtdat-3'
 degen=48 temp=63.3
 N T Y Q R G E Q E
 ttrtgtnawrgtCGCACCGCTTGTCC oligo:5'-CCTGTTGCCACGCTgrwangtrtt-3'
 degen=32 temp=61.2
 T Y Q R G E Q E S C
 tgnawrgtykcACCGCTTGTCCCTTCGAC oligo:5'-CAGCTTCCTGTTGCCAckytgrwangt-3'
 degen=64 temp=61.9
 Y Q R G E Q E S C
 awrgtykcnccGCTTGTCCCTTCGACG oligo:5'-GCAGCTTCCTGTTGCCcnckytgrwa-3'
 degen=64 temp=62.1
 W E T I P H P C W

amvctytgnyaAGCGTAGGCACGAC oligo:5'-CAGCACGGATGCGGAayngtytcvma-3'
 degen=96 temp=61.6
 E T I P H P C W
 ctytgnyanggCGTAGGCACGACC oligo:5'-CCAGCACGGATGCggayngtytc-3' degen=64
 temp=62.2
Block unknown_D
 R Y T N A P D A D A
 oligo:5'-GCGTTATACCAATGCGCCNgaygcngang-3' degen=128 temp=60.1
Complement of Block unknown_D
 D A D A R A I Q A
 ctrcgncnccbCGCACGCTAAGTCCGC oligo:5'-CGCCTGAATCGCACGCbcntcngcrtc-3'
 degen=96 temp=63.9
Block unknown_E
 K A S K M G
 oligo:5'-AAAGCGdsnrararatggg-3' degen=96 temp=-6.9 Extend clamp
 K A S K M G D
 oligo:5'-AAAGCGAGNrararatgggng-3' degen=64 temp=10.3 Extend clamp
 K A S K M G D
 oligo:5'-AAAGCGAGCrararatgggnga-3' degen=16 temp=23.1 Extend clamp
 G D Y L R Y N M F D K
 oligo:5'-TGGGCGATTATCTGCCTTATAATwtbtwygayaa-3' degen=48 temp=61.8
 G D Y L R Y N M F D K Y
 oligo:5'-TGGGCGATTATCTGCCTTATAATATbtwygayaart-3' degen=48 temp=61.9
 G D Y L R Y N M F D K Y
 oligo:5'-GGGCGATTATCTGCCTTATAATATGtwygayaarta-3' degen=16 temp=62.4
Complement of Block unknown_E
 M G D Y L R Y N M F D K Y F R
 tytaccnctrmTAGACGCAATATTATACAAACTATTATAAAAAG oligo:5'-
 GAAAATATTATCAAACATATTATAACGCAGATmrtcncccatt-3' degen=32 temp=60.6
 M G D Y L R Y N M F D K Y F R
 tacccnctrmwAGACGCAATATTATACAAACTATTATAAAAAG oligo:5'-
 GAAAATATTATCAAACATATTATAACGCAGAwmrtcncccatt-3' degen=32 temp=60.4
 F D K Y F R K I G
 avawrctrtyaTAAAAGCATTAAACCG oligo:5'-GCCAATTTCAGAAAAtayttrtcrrwava-3'
 degen=48 temp=48.9 Extend clamp
 F D K Y F R K I G
 awrctrtyaTAAAAGCATTAAACCG oligo:5'-GCCAATTTCAGAAAAtayttrtcrrwa-3'
 degen=16 temp=48.9 Extend clamp
 D K Y F R K I G
 ctrttyatrwwAGCATTAAACCG oligo:5'-GCCAATTTCAGAwrrtayttrtc-3' degen=32
 temp=38.7 Extend clamp
Block unknown_F
 S H C H F G Y Q N P
 oligo:5'-CAGCCATTGCCATTGGntaycaraayc-3' degen=32 temp=61.0
 H C H F G Y Q N P
 oligo:5'-GCCATTGCCATTGGCtaycaraaycc-3' degen=8 temp=61.9
 H C H F G Y Q N P M
 oligo:5'-CCATTGCCATTGGCTATcaraayccnht-3' degen=48 temp=62.9
Complement of Block unknown_F
 Y Q N P M A A W
 atrgttytrggCTACCGCCGCAC oligo:5'-CACGCCGCATCggrttytgrta-3' degen=8
 temp=63.3
 Q N P M A A W V
 trgttytrggndACCGCCGCACCCA oligo:5'-ACCCACGCCGCCAdnggrttytgrt-3'
 degen=96 temp=60.3

Q N P M A A W V
 gtytrggndaCCGCCGCACCCA oligo:5'-ACCCACGCCGCAdnggrtttg-3' degen=48
 temp=60.3
Block unknown_G
 S E G A I A G G
 oligo:5'-CAGCGAAGGCGCGathgcnggngg-3' degen=48 temp=60.8
Complement of Block unknown_G
 I A G G C T N S W
 tadcgncncGACGTGGTTATCGACC oligo:5'-CCAGCTATTGGTGCAGCcncncdat-3'
 degen=48 temp=60.4
Block unknown_H
 S G T S T F Y G
 oligo:5'-AGCGGCACCAAGnacnttykayg-3' degen=128 temp=42.8 Extend clamp
 G T S T F Y G M
 oligo:5'-GCGGCACCAGCACCCttykaygrnat-3' degen=64 temp=62.1
 G T S T F Y G M
 oligo:5'-GCGGCACCAGCACCCttykaygrnatg-3' degen=64 temp=62.1
Complement of Block unknown_H
 T F Y G M M Y V W H P
 tgnarmtrcyGTACTACATACACACCGTAGGC oligo:5'-
 CGGATGCCACACATACATGycrtmraangt-3' degen=64 temp=64.4
 F Y G M M Y V W H P
 aarmtrcyntaCTACATACACACCGTAGGC oligo:5'-CGGATGCCACACATACATCatnycrtmraa-
 3' degen=64 temp=61.6
 Y G M M Y V W H P V
 armtrcyntacyACATACACACCGTAGGCCA oligo:5'-
 ACCGGATGCCACACATACAYcatnycrtmra-3' degen=128 temp=60.8
Block unknown_J
 S T L D W E G Q P D
 oligo:5'-GAGCACCCCTGGATTGGGAnggnarccng-3' degen=128 temp=62.1
 T L D W E G Q P D
 oligo:5'-CACCCCTGGATTGGGAAggnarccnga-3' degen=32 temp=61.3
Complement of Block unknown_J
 G Q P D T W T G
 ccngtyggncnctATGGACCTGGCCG oligo:5'-GCCGGTCCAGGTAtcnggytgncc-3' degen=32
 temp=52.4 Extend clamp
 Q P D T W T G
 gtyggncnctrdsGACCTGGCCG oligo:5'-GCCGGTCCAGsdrtnnggytg-3' degen=96
 temp=37.7 Extend clamp

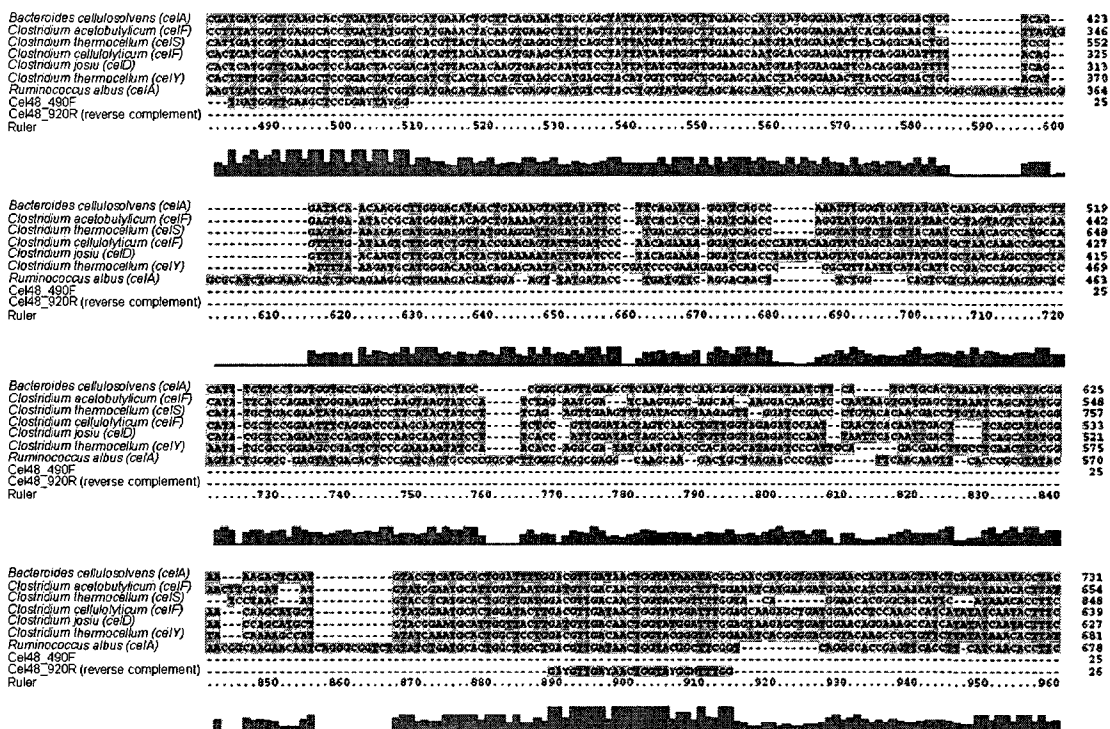


Figure B. 2: Multiple DNA alignment of the reference glycoside hydrolase genes of the family 48 and the primers selected for their amplification. The alignment was constructed with ClustalX.

B.2. Design of *cel5* primers

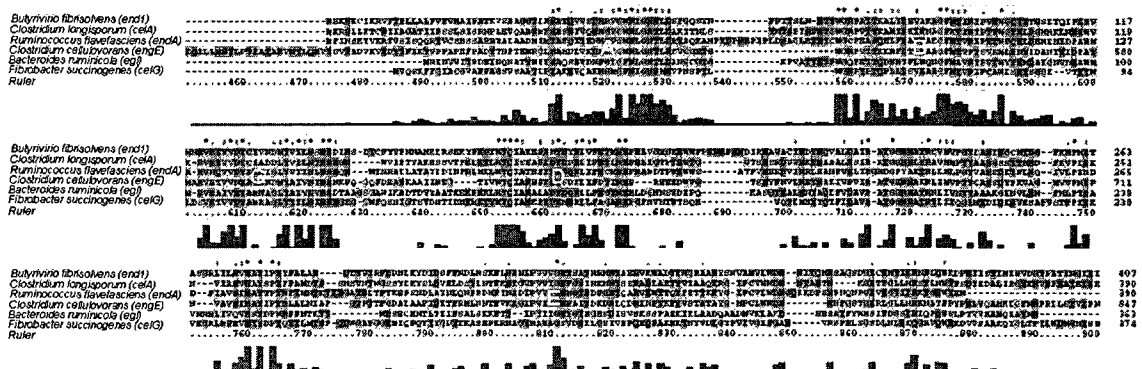


Figure B. 3: Multiple protein alignment of six glycoside hydrolases of the family 5 and the blocks of conserved protein sequence (indicated with green boxes) identified by the Blocksmaker program. The alignment was constructed using ClustalX.

Primers found with the CODEHOP algorithm in each block of conserved protein sequence. The degeneracy (degen) of the 3' core and the melting temperature of the primer (temp) are indicated. When the melting temperature is too low, the message 'Extend clamp' appears next to the primer:

Block unknown_A

Q N M G M G W N L
oligo:5'-TGCAGAATATGGGCATGggntkbaayht-3' degen=144 temp=62.8
Q N M G M G W N L G
oligo:5'-CAGAATATGGGCATGGGCTkbaayhtngg-3' degen=144 temp=60.8
G M G W N L G N
oligo:5'-GGGCATGGGCTGGGaayhtnggnaa-3' degen=96 temp=60.1

Complement of Block unknown_A

G W N L G N T M D
ccnamvttrdaCCCGTTATGGTACCTA oligo:5'-ATCCATGGTATTGCCAdrttvmancc-3'
degen=144 temp=55.3 Extend clamp
W N L G N T M D
amvtrdancCGTTATGGTACCTA oligo:5'-ATCCATGGTATTGccnadrttvma-3' degen=144
temp=46.5 Extend clamp
N L G N T M D
ttrdancnttATGGTACCTA oligo:5'-ATCCATGGTAttncnadrtt-3' degen=96
temp=26.8 Extend clamp

Block unknown_B

E T C W G
oligo:5'-GAAacnbndntgggg-3' degen=144 temp=-53.8 Extend clamp
E T C W G N P
oligo:5'-GAAACCTGntggggnhnrc-3' degen=384 temp=0.3 Extend clamp
E T C W G N P
oligo:5'-GAAACCTGCTggggnhncc-3' degen=96 temp=50.4 Extend clamp
A M F D F I K A A G F N
oligo:5'-GCGATGTTGATTTATTAAAGCGrmngnntyaa-3' degen=128 temp=61.1
D F I K A A G F N T
oligo:5'-GATTTATTAAAGCGGCGGCGggnntyaaanrc-3' degen=64 temp=60.7
K A A G F N T V
oligo:5'-TTAAAGCGGGCGGGCttyaanrcnrt-3' degen=128 temp=60.4

Complement of Block unknown_B

T C W G N P E
tgnvhnaccccGTTAGGCCTT oligo:5'-TTCCGGATTGccccanhvngt-3' degen=144
temp=60.5
W G N P E T T Q A
accncndynggCCTTGGTGGTCC oligo:5'-CCTGGGTGGTTCCGgnydnccccca-3'
degen=96 temp=60.9
G F N T V R I P C
ccnaartnnygGCACGCATAAGGCACG oligo:5'-GCACGGAATACGCACGgynttraancc-3'
degen=64 temp=62.3
F N T V R I P C T
aartrnnygnyaCGCATAAGGCACGTGG oligo:5'-GGTGCACGGAATACGCayngyntraa-3'
degen=128 temp=60.2

Block unknown_C

M M R V K T V V D Y
oligo:5'-GGATGATGCGTGTGAAAACCrtngtnranta-3' degen=256 temp=61.3
V D Y C M N N N D M Y V I
oligo:5'-GGTGGATTATTGCATGAATAATGATHtntayrynat-3' degen=384 temp=60.2
V D Y C M N N D M Y V I V
oligo:5'-GTGGATTATTGCATGAATAATGATATGtayrynahnt-3' degen=384 temp=60.4
M N N D M Y V I V N I H H
oligo:5'-CATGAATAATGATATGTATGTGATTGTGaaynbncayca-3' degen=192 temp=61.2
M N N D M Y V I V N I H H E
oligo:5'-CATGAATAATGATATGTATGTGATTGTGAATnbncaycayra-3' degen=384
temp=61.3

Complement of Block unknown_C

V D Y C M N N D M Y V I V N
 canytnatrmgsGTACTTATTACTATACATACACTAACACT oligo:5'-
 TCACAATCACATACATATCATTATTGsmrtantynac-3' degen=256 temp=60.2
 Y V I V N I H H E
 atryrntadnaCTTATAAGTAGTACTT oligo:5'-TTCATGATGAATATTGandatnryrta-3'
 degen=384 temp=41.4 Extend clamp
 N I H H E
 ttrnvngtrgtACTT oligo:5'-TTCAgtrgnvnrtt-3' degen=192 temp=-34.6
Extend clamp

Block unknown_D

T Y W T Q	
oligo:5'-ACCnwntggacnca-3'	dgen=128 temp=-102.1
T Y W T Q I	<u>Extend clamp</u>
oligo:5'-ACCTAntggacncara-3'	dgen=32 temp=-51.3
T Y W T Q I	<u>Extend clamp</u>
oligo:5'-ACCTATTggacncarat-3'	dgen=8 temp=20.9
	<u>Extend clamp</u>

Complement of Block unknown_D

W T Q I A N H F K D Y D Q
 acctgngtytaACGCTTAGTAAAATTCTAATACTAG oligo:5'-
 GATCATATACTTAAAATGATTGCGAatytgngtcca-3' degen=8 temp=61.0
 T Q I A N H F K D Y D Q H
 cctgngtytadhGCTTAGTAAAATTCTAATACTAGTCG oligo:5'-
 GCTGATCATAATCTTAAAATGATTGCGhdatytgngtcc-3' degen=72 temp=60.5
 T Q I A N H F K D Y D Q H L
 ctgngtytadhCTTAGTAAAATTCTAATACTAGTCGTAG oligo:5'-
 GATGCTGATCATAATCTTAAAATGATTGshdatytgngtc-3' degen=144 temp=60.7
 T Q I A N H F K D Y D Q H L
 tgngtytadhCTTAGTAAAATTCTAATACTAGTCGTAG oligo:5'-
 GATGCTGATCATAATCTTAAAATGATTGshdatytgngt-3' degen=144 temp=60.7

Block unknown_E

I P V I I G E	
oligo:5'-ATTCCGGTGrtnrnggnga-3'	dgen=256 temp=21.8
	<u>Extend clamp</u>

cel5_392F

Fibrobacter succinogenes (*celG*)
Ruminococcus flavefaciens (*endA*)
Butyrivibrio fibrisolvens (*end1*)
Bacteroides ruminicola (*eng1*)
Clostridium cellulovorans (*engE*)
Clostridium longisporum (*celA*)
Clostridium cellulolyticum (*celA*)
Ruminococcus albus (*celB*)
Clostridium cellulovorans (*engD*)
Ruminococcus albus (*celA*)
Clostridium thermocellum (*celE*)

-CGCCCATGGCGTGGGAATHTGGGNAA
 TGCCCATGGCGCTTCACATGGCTAA
 TGCAGATGGCGTGGAAATCTGGCTAA
 TGCAAGTGGCTGGAAATCTGGCTAA
 TGCGATGGCTGGAAATCTGGCTAA
 TGCAAGATGGCTGGAACTTGGAAAT
 TGGCGCTTGGCTGGAAATCTGGCTAA
 TAAACGGATGGCGTGGAAATCTGGCTAA
 TGCTGCAATGGCGTGGAAATCTGGCTAA
 TGCAAGCTTGGCTGGAAATCTGGCTAA
 TGAAACACACGGCTGGAAATCTGGCTAA
 TAAACATGGCGTGGAAATCTGGCTAA

cel5_754R (reverse complement)

Fibrobacter succinogenes (*celG*)
Ruminococcus flavefaciens (*endA*)
Butyrivibrio fibrisolvens (*end1*)
Bacteroides ruminicola (*eng1*)
Clostridium cellulovorans (*engE*)
Clostridium longisporum (*celA*)
Clostridium cellulolyticum (*celA*)
Ruminococcus albus (*celB*)
Clostridium cellulovorans (*engD*)
Ruminococcus albus (*celA*)
Clostridium thermocellum (*celE*)

GGGIMNCRATTGCGAACCCACITCAAGATATCGTG
 TGGACCCATATTCGGACAACTTACGGATACACCG
 TGGACCTGATTAACGAGATTCAGGTTACGGTATACGAG
 TGGACACGATTCGGACAGGCGTGGACGAACTATACGAG
 TGGMTCTATGCGGCGCTTGGCTGAACTATACGAG
 TGGACGATTCGGACAGGCGTGGACGAACTATACGAG
 TGGACGATTCGGACAGGCGTGGACGAACTATACGAG
 TGGACGATTCGGACAGGCGTGGACGAACTATACGAG
 TGGACTCTGAAATTCGAAATATTCGAAATATTCGAG
 TGGACGATTCGGACAGGCGTGGACGAACTATACGAG
 TGGACGATTCGGACAGGCGTGGACGAACTATACGAG
 TGGACGATTCGGACAGGCGTGGACGAACTATACGAG

Figure B. 4: Multiple DNA alignment of the reference glycoside hydrolase genes of the family 5 and the primers selected for their amplification. Other family 5 glycoside hydrolase genes that were not used for the primer design were also included in the alignment. The alignment was constructed with ClustalX.

B.3. Design of *hydA* primers

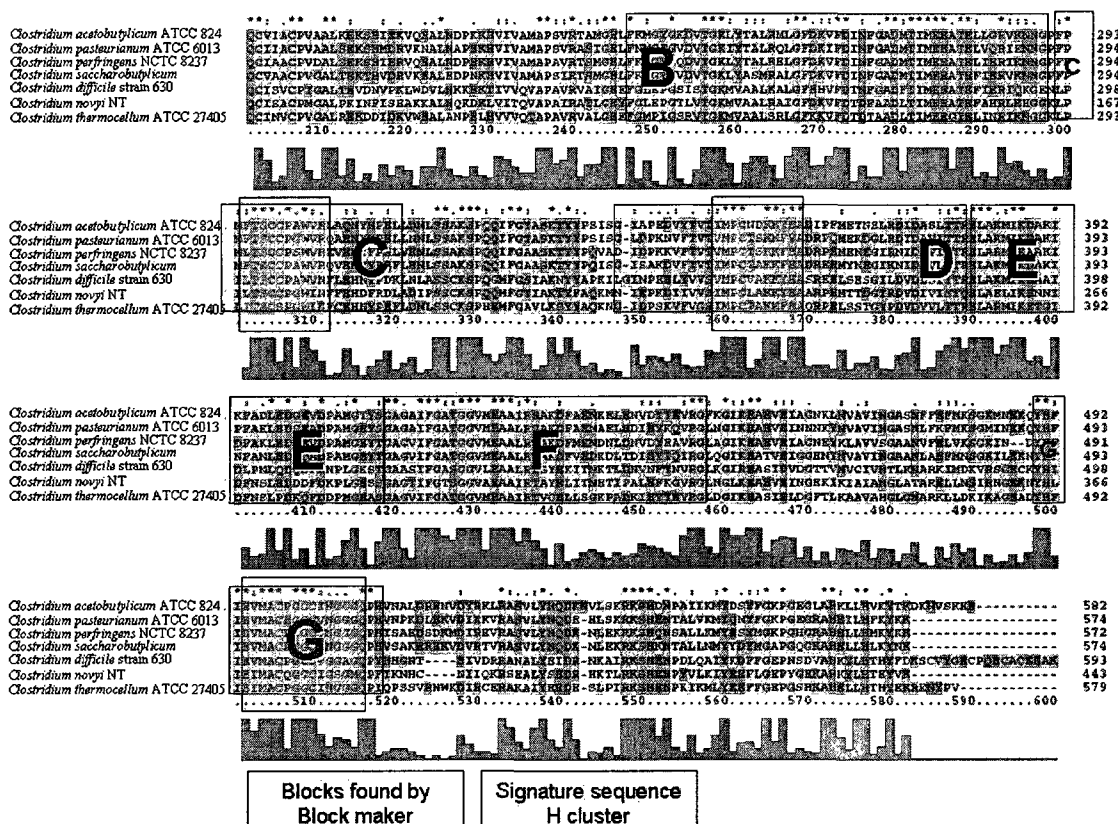


Figure B. 5: Multiple protein alignment of seven glycoside iron hydrogenase sequences and the blocks of conserved protein sequence (indicated with clear boxes) identified by the Blocksmaker program. The signature sequence of the H cluster of iron hydrogenases is indicated with orange boxes. The alignment was constructed using ClustalX.

Primers found with the CODEHOP algorithm in each block of conserved protein sequence. The degeneracy (degen) of the 3' core and the melting temperature of the primer (temp) are indicated. When the melting temperature is too low, the message 'Extend clamp' appears next to the primer:

Block unknown_A

```
D R T K C V
oligo:5'-GATCGTwvnaartgynt-3' degen=384 temp=-27.5 Extend clamp
R T K C V L C G R C
```

```
oligo:5'-CGTACCAAATGCGTGCTGtgvygnmrntg-3' degen=384 temp=63.6
```

Complement of Block unknown_A

```
K C V L C G R C V
ttyacrnnandwCACGCCGGCAACGC oligo:5'-CGAACGGCCGCACwdnanrcaytt-3'
degen=384 temp=63.5
C G R C V S A C
```

acrbcnkynacGCACTCGCGCACG oligo:5'-GCACGCGCTCACGcanyknbrca-3' degen=384
temp=64.6

Block unknown_B

Y G S D V T G K M
oligo:5'-GCTATGGCAGCGATGTGacnggnaarht-3' degen=96 temp=60.4
L R A L G F D K
oligo:5'-CTGCGTGCCTGggnttyranma-3' degen=128 temp=60.9
A L G F D K V F D
oligo:5'-TGCCTGGGCTTGATmanrnttyga-3' degen=128 temp=60.0
A L G F D K V F D I
oligo:5'-TGCCTGGGCTTGATAAnrnttygaya-3' degen=128 temp=61.4
L G F D K V F D I N
oligo:5'-CGCTGGGCTTGATAAAAGTGtgyayaynra-3' degen=64 temp=62.6
F G A D M T I M E
oligo:5'-TTTGGCGCGGATATGacnathatgga-3' degen=12 temp=60.6
G A D M T I M E E
oligo:5'-GGCGCGGATATGACCAtatggarg-3' degen=6 temp=60.4
G A D M T I M E E A
oligo:5'-GGCGCGGATATGACCAAtatggargarg-3' degen=12 temp=60.4

Complement of Block unknown_B

T G K M Y A A L R
tgnccttydaCATACGCCGCGACG oligo:5'-GCAGCGCCGCATAcadyttnccngt-3'
degen=96 temp=60.2
G K M Y A A L R
ccnttydanmwACGCCGCGACGC oligo:5'-CGCAGCGCCGCAwmnadyytncc-3' degen=384
temp=61.3
G F D K V F D I N F G A
ccnaarytnktTCACAAACTATAATTAAAACCGCG oligo:5'-
GCGCCAAAATTAAATATCAAACACTtkntyraancc-3' degen=128 temp=61.6
V F D I N F G A D M
tnyanaarctrtaATTAAAACCGCGCCTATAC oligo:5'-
CATATCCGCGCCAAAATTAAtrtcraanaynt-3' degen=128 temp=61.0
F D I N F G A D M T
aarctrtrnytAAAACCGCGCCTATACTG oligo:5'-GTCATATCCGCGCCAAAAtynrtrtcraa-3'
degen=64 temp=60.8
T I M E E A T E F
tgntadtaacctCTTCGCTGGCTTAA oligo:5'-AATTGGTCGCTTCTtccatdatngt-3'
degen=12 temp=61.0
I M E E A T E F I H R
tadtacctyctTCGCTGGCTTAAATAAGTAGC oligo:5'-
CGATGAATAAATTGGTCGCTcytccatdat-3' degen=6 temp=63.9
M E E A T E F I H R
adtacctyctyGCTGGCTTAAATAAGTAGC oligo:5'-
CGATGAATAAATTGGTCGCTcytccatda-3' degen=12 temp=60.4
M E E A T E F I H R I K N
tacctyctycsCTGGCTTAAATAAGTAGCATAATTTTA oligo:5'-
ATTTTAATACGATGAATAATTGGTCscytccat-3' degen=8 temp=60.1

Block unknown_C

F T S C C P G W V
oligo:5'-TGTTTACCAAGCTGCTGCcndsntggrt-3' degen=192 temp=62.3

Complement of Block unknown_C

P G W V R F C E H Y Y
ggnhsnacccyaCGCAAAACGCTTGTAAATA oligo:5'-
AATAATGTTCGCAAAACGCaayccanshngg-3' degen=192 temp=60.5

Block unknown_D

P K D V F T V T I M P

oligo:5'-CCGAAAGATGTGTTACCGTGwsnrtnatgcc-3' degen=128 temp=60.4
 P K D V F T V T I M P C
 oligo:5'-CCGAAAGATGTGTTACCGTGACnrtnatgccnt-3' degen=128 temp=62.8
 K D V F T V T I M P C
 oligo:5'-CCTAAAGATGTGTTACCGTGACCrtnatgccntg-3' degen=32 temp=62.8
 P C T A K K Y E
 oligo:5'-CCGTGCACCGCGAaraartwyga-3' degen=16 temp=61.2
 P C T A K K Y E A
 oligo:5'-CCGTGCACCGCGAAraartwygarg-3' degen=32 temp=61.2
 C T A K K Y E A
 oligo:5'-CGTGCACCGCGAAGaartwygargc-3' degen=16 temp=61.8
Complement of Block unknown_D
 M P C T A K K Y E A
 antacgggnacrncGGCGCTTTTCATACTTCGC oligo:5'-
 CGCTTCATACTTTTCGCGGnrcanggcatna-3' degen=128 temp=62.9
 M P C T A K K Y E A D
 tacgggnacrndGCGCTTTTCATACTTCGCC oligo:5'-
 CCGCTTCATACTTTTCGCGDnrcanggcat-3' degen=96 temp=62.9
 K K Y E A D R P E
 ttytattyawrctTCGCCTAGCAGGCC oligo:5'-CCGGACGATCCGCTcrwaytattytt-3'
 degen=16 temp=61.4
 K Y E A D R P E
 tytattyawrctycGCCTAGCAGGCCCTT oligo:5'-TTCCGGACGATCCGcytcrrwaytaty-3'
 degen=32 temp=60.3
 K Y E A D R P E
 ttyawrctycgcCTAGCAGGCCCTT oligo:5'-TTCCGGACGATCCGcytcrrwaytt-3' degen=16
 temp=60.3

Block unknown_E
 E L A K M I K E
 oligo:5'-GAACTGGCGAnhtnathaarg-3' degen=288 temp=33.9 Extend clamp
Complement of Block unknown_E
 E L A K M I K E A K I D F
 ctyrancgnbyTTACTAATTCTCGCTTTAACAAA oligo:5'-
 AAATCAATTTCGCTTCTTAATCATTybngcnarytc-3' degen=384 temp=60.8
 I K E A K I D F N N L E D
 antadattycknyGCTTTAACAAAAATTATTAGACCTCT oligo:5'-
 TCTTCCAGATTATTAAAATCAATTTCGynkcytdatna-3' degen=384 temp=61.1
 I K E A K I D F N N L E D Q
 tadattycknykCTTTAACAAAAATTATTAGACCTCTAGT oligo:5'-
 TGATCTCCAGATTATTAAAATCAATTTCkynkcytdat-3' degen=192 temp=61.2

Block unknown_F
 G A G V I F G
 oligo:5'-GGCGCGGGCdbnathettygg-3' degen=216 temp=48.5 Extend clamp
 G A G V I F G A
 oligo:5'-GGCGCGGGCGTGathttyggnc-3' degen=48 temp=64.3
 V I F G A T G G V
 oligo:5'-CGTGATTTGGCGCGwsngngngt-3' degen=256 temp=60.9
 T G G V M E A
 oligo:5'-CGACCGGGCGGCgttnnyngargc-3' degen=256 temp=62.9
 T G G V M E A A
 oligo:5'-GACCGGGCGGCgtGnyngargcngc-3' degen=256 temp=60.5
 G G V M E A A I
 oligo:5'-CGGCGGCGTGATGgargcngcnht-3' degen=96 temp=65.5
Complement of Block unknown_F
 I F G A T G G V

tadaarccnygCTGGCCGCCGC oligo:5'-CGCCGCCGGTCgyncraadat-3' degen=48
 temp=61.9
 F G A T G G V M
 adaarccnygnwGGCCGCCGCACTAC oligo:5'-CATCACGCCGCCGwngyncraada-3'
 degen=384 temp=63.3
 F G A T G G V M E
 aarccnygnwsGCCGCCGCACTACC oligo:5'-CCATCACGCCGCCGswngyncraa-3'
 degen=256 temp=63.3
 V M E A A I R T A
 cannrnctycgCCGTAAGCATGGC oligo:5'-CGGTACGAATGCCgcyclcnrnnac-3'
 degen=256 temp=62.4
 E A A I R T A Y D F I E
 ctycgncndaaGCATGGCGCATACTAAATAAC oligo:5'-
 CAATAAAATCATACGGTACGAadngcngcytc-3' degen=96 temp=62.1
 A A I R T A Y D F I E N
 cgncgndankcATGGCGCATACTAAATAACTTT oligo:5'-
 TTTCAATAAAATCATACGGTACKnadngcngc-3' degen=384 temp=60.5
Block unknown_G
 Y H F I E V M A
 oligo:5'-TATCATTATTgarrtnatggc-3' degen=16 temp=27.2 Extend clamp
 Y H F I E V M A C
 oligo:5'-TATCATTATTGAAGTnatggcntg-3' degen=32 temp=31.5 Extend clamp
 Y H F I E V M A C P
 oligo:5'-TATCATTATTGAAGTnatggcntgyc-3' degen=32 temp=36.6 Extend clamp
 G C I N G G G Q P
 oligo:5'-CGGCTGCATTAATGGCgsnrkncarcc-3' degen=256 temp=62.3
Complement of Block unknown_G
 E V M A C P G
 cttyantaccgCACGGGCC oligo:5'-CCCAGGCACGCCatnayytc-3' degen=16
 temp=64.0
 M A C P G G C
 antaccgnacrgGCCGCCGACG oligo:5'-GCAGCCGCCGgrcangccatna-3' degen=32
 temp=60.6
 M A C P G G C I N G
 taccgnacrgkCCCGCCGACGTAATTAC oligo:5'-CATTAATGCAGCCGCCkgrcangccat-3'
 degen=16 temp=61.2
 G G Q P H
 csnymngtggCGTA oligo:5'-ATGCggytgnmynsc-3' degen=256 temp=-1.2
Extend clamp

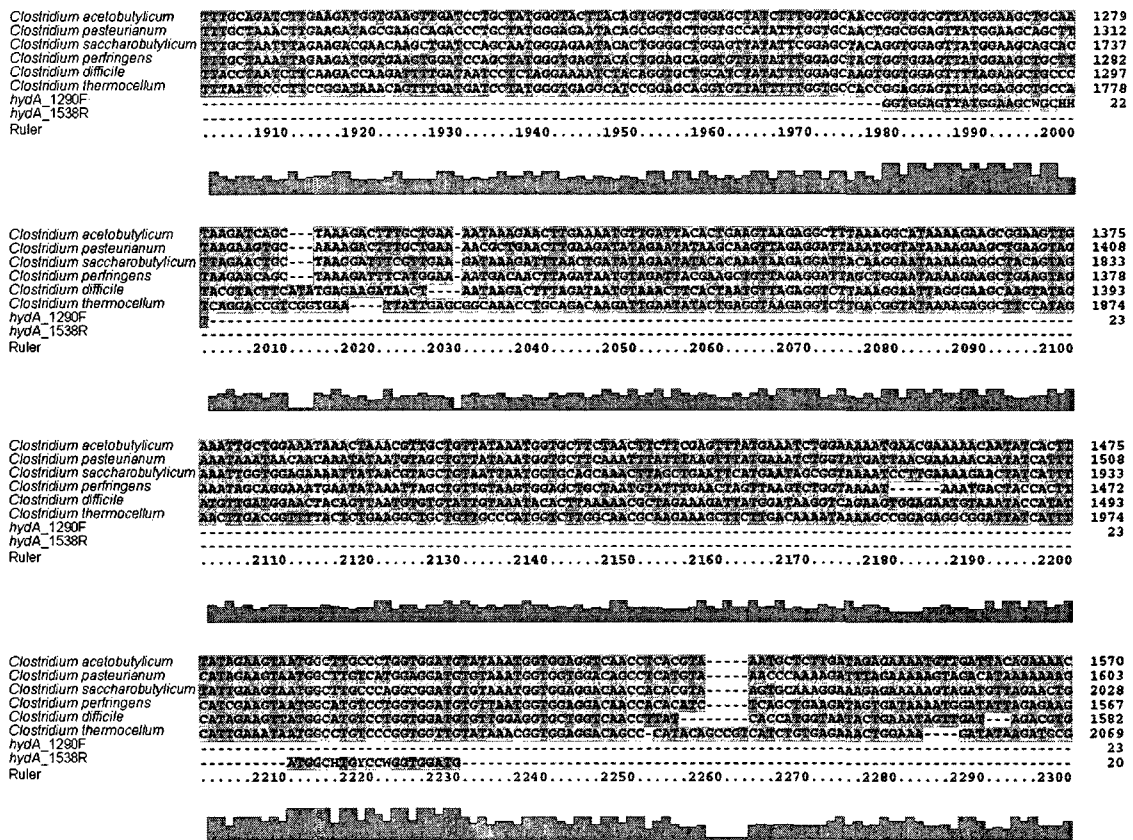


Figure B. 6: Multiple DNA alignment of the reference iron hydrogenase genes and the primers selected for their amplification. The alignment was constructed with ClustalX.

B.4. Design of *dsrA* primers

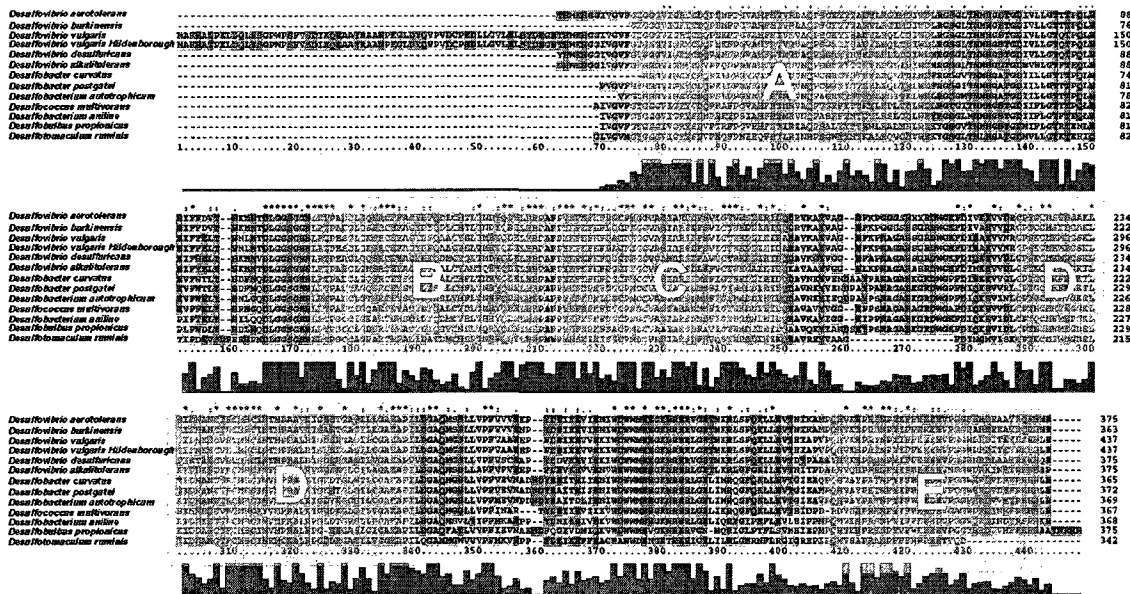


Figure B. 7: Multiple protein alignment of dissimilatory sulfite reductase genes and the blocks of conserved protein sequence (indicated with green boxes) identified by the Blocksmaker program. The alignment was constructed using ClustalX.

Primers found with the CODEHOP algorithm in each block of conserved protein sequence. The degeneracy (degen) of the 3' core and the melting temperature of the primer (temp) are indicated. When the melting temperature is too low, the message 'Extend clamp' appears next to the primer:

Block unknown_A

```

G Y G G G
oligo:5'-GGntayggngng-3' degen=128 temp=-145.2 Extend clamp
G Y G G G
oligo:5'-GGCtayggngngg-3' degen=32 temp=-34.5 Extend clamp
G Y G G G V
oligo:5'-GGCTATggngnggnrt-3' degen=128 temp=9.7 Extend clamp
F P G V A H F H
oligo:5'-TGTTTCCGGGCGTGgmncanttyca-3' degen=64 temp=61.3
F P G V A H F H T
oligo:5'-TTTCCGGGCGTGCGCncanttycaya-3' degen=64 temp=61.4
G V A H F H T
oligo:5'-CGGGCGTGGCGcanttycayac-3' degen=16 temp=65.5
G V A H F H T M
oligo:5'-GGCGTGGCGCATttycayacnnt-3' degen=64 temp=62.9
E Y L R Q L C D I W D
oligo:5'-GAATATCTGCGTCAGCTGTGCrannnttgga-3' degen=128 temp=61.0

```

Complement of Block unknown_A

G Y G G G V I G
ccnatrccnccGCCGCACTAACCG oligo:5'-GCCAATCACGCCGccncrtancc-3' degen=32
temp=63.6
Y G G G V I G R
cnatrcnccnccCGCACTAACCGGCA oligo:5'-ACGGCCAATCACGCCnccnccrtanc-3'
degen=128 temp=60.2
Y G G G V I G R
atrcnccnccGCACTAACCGGCA oligo:5'-ACGGCCAATCACGCCnccnccrtac-3' degen=32
temp=60.2
G G G V I G R Y C D
ccnccnccnyaCTAACCGGCAATAACGC oligo:5'-CGCAATAACGGCAATCayncnccncc-3'
degen=128 temp=61.6
A H F H T M R V N Q
ckngtnaargtATGGTACGCACACTTAGTC oligo:5'-CTGATTACACGCATGGTAtgraantgnkc-
3' degen=64 temp=60.0
H F H T M R V N Q P
gtnaargtrtgGTACGCACACTTAGTCG oligo:5'-GCTGATTACACGCATGgtrtgraantg-3'
degen=16 temp=60.7
F H T M R V N Q P
aargtrtgnaCGCACACTTAGTCGGC oligo:5'-CGGCTGATTACACGCAnngtrtgraa-3'
degen=64 temp=61.7

Block unknown_B

C L G Q S R C E W
oligo:5'-GCTGCCTGGGCCAGAGNmgnagygart-3' degen=128 temp=61.8
H F L T M E Y Q D E
oligo:5'-GCCATTTCTGACCATGGAAAtwyccargayka-3' degen=32 temp=61.1
H F L T M E Y Q D E L
oligo:5'-CCATTTCTGACCATGGAAATATcargaykanht-3' degen=96 temp=62.1

Complement of Block unknown_B

Y Q D E L H R P A
awrgtyctrmtTGACGTAGCAGGCCGC oligo:5'-CGCCGGACGATGCAGTmrtcytgrwa-3'
degen=32 temp=64.5
Q D E L H R P A
gtyctrmtndaCGTAGCAGGCCGC oligo:5'-CGCCGGACGATGCadntmrctytg-3' degen=96
temp=61.2

Block unknown_C

F P Y K F K
oligo:5'-TTCCGtayaarwbnna-3' degen=96 temp=5.7 Extend clamp
F P Y K F K F K F
oligo:5'-TTCCGTATAAATTTaarwthaarht-3' degen=72 temp=41.1 Extend
clamp
F P Y K F K F K F D G C P N
oligo:5'-TTCCGTATAAATTAAATTGATGsntgyccnaa-3' degen=64
temp=60.3
F K F D G C P N C C
oligo:5'-ATTTAAATTGATGGCTGCccnaaykrntg-3' degen=128 temp=60.2
D G C P N C C V
oligo:5'-TTGATGGCTGCCGAaykrntgygt-3' degen=64 temp=60.9

Complement of Block unknown_C

F P Y K F K F D G C
amvgnatrttAAATTAAACTACCGACG oligo:5'-
GCAGCCATCAAATTAAATTAAATTtrtanggvma-3' degen=48 temp=61.0
P Y K F K F K F D G C P
ggnatrttywvATTAAATTAAACTACCGACGGG oligo:5'-
GGGCAGCCATCAAATTAAATTAvwytrtang-3' degen=96 temp=62.3

```

Y K F K F K F D G C P
atrrtywvnttAAATTAAACTACCGACGGG oligo:5'-
GGGCAGCCATCAAATTAAATtnwyttta-3' degen=96 temp=62.3
K F K F D G C P N
ttywadddydaACTACCGACGGGCTT oligo:5'-TTCGGGCAGCCATCAadyttawytt-3'
degen=72 temp=60.9
G C P N C C V A S
csnacrggnnttAACGACGCACCGCT oligo:5'-TCGCCACGCAGCAAtnggrcansc-3'
degen=64 temp=61.1
C P N C C V A S I
acrggntrmyGACGCACCGCTCGTAA oligo:5'-AATGCTGCCACGCAGymrttnggrca-3'
degen=64 temp=60.7
N C C V A S I A R
ttrmynacrcacCGCTCGTAACGCG oligo:5'-GCGCAATGCTGCCacrcanymrta-3'
degen=64 temp=63.9
G T W K D D I K I D Q
ccntgnacckyTCTACTATAATTAACTAGTC oligo:5'-
CTGATCAATTAAATATCATCTykcangtncc-3' degen=64 temp=48.2 Extend clamp
Block unknown_D
A N C T R C M H C
oligo:5'-GCGAATTGCACCCGTTgyatgcaytg-3' degen=4 temp=62.3
A N C T R C M H C I
oligo:5'-GCGAATTGCACCCGTTGyatgcaytgya-3' degen=8 temp=62.3
T R C M H C I
oligo:5'-GCACCCGTTGCatgcaytgyat-3' degen=4 temp=62.7
Complement of Block unknown_D
C M H C I N V M P R
acrtacgtracGTAATTACACTACGGCG oligo:5'-GCGGCATCACATTAAATGcartgcatrca-3'
degen=4 temp=61.6
M H C I N V M P R A
crtacgtracrtAATTACACTACGGCGCAC oligo:5'-CACGCGGCATCACATTAAtrcattgcacrtc-
3' degen=8 temp=60.5
M H C I N V M P R A
tagtracrttaATTACACTACGGCGCAC oligo:5'-CACGCGGCATCACATTAAtrcattgcacrt-3'
degen=4 temp=60.5
Block unknown_E
K E P R S N P Y I
oligo:5'-TGAAAGAACCGCGTAGCaayccntwydt-3' degen=96 temp=60.5
Complement of Block unknown_E
N P Y I F W K E E E V P
ttrggnawrhaGAAAACCTTCTTCTTCACG oligo:5'-
GCACTTCTTCTTCTTCAAAAGahrwanggrtt-3' degen=96 temp=60.4

```

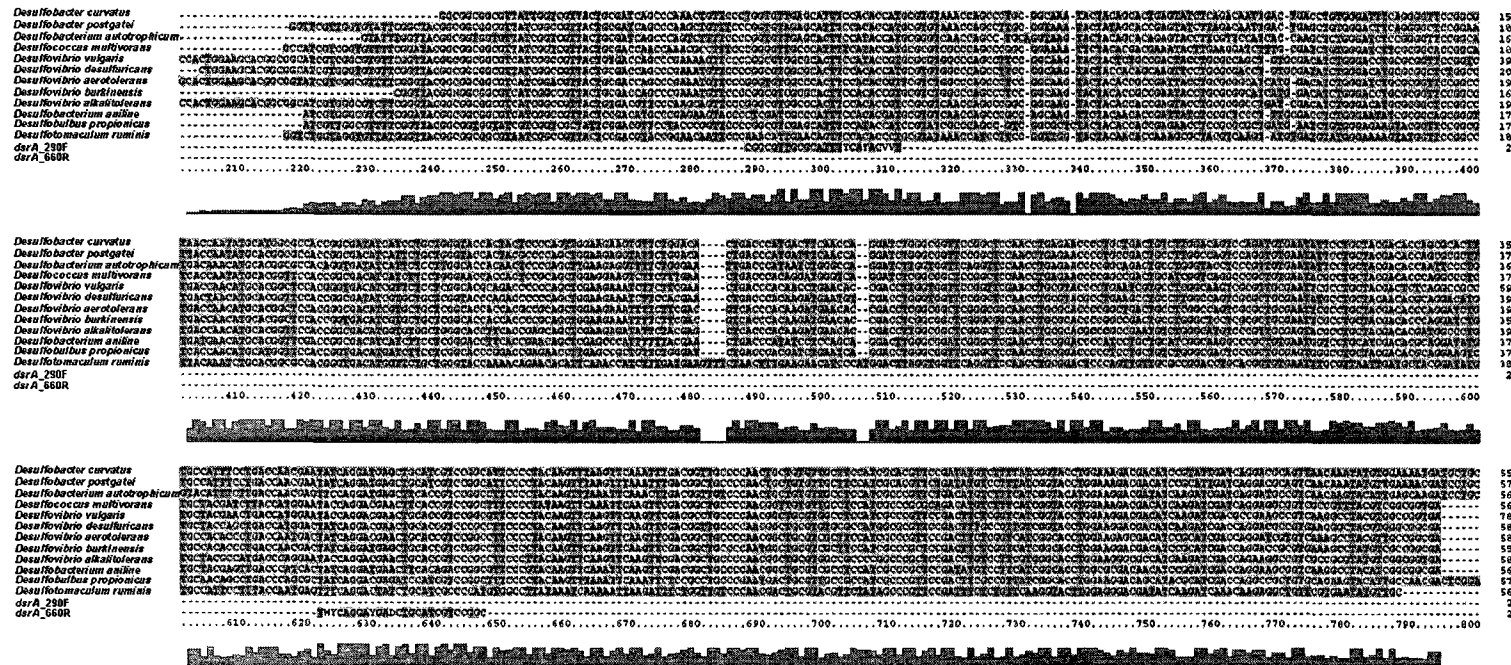


Figure B.8: Multiple DNA alignment of the reference dissimilatory sulfite reductase genes and the primers selected for their amplification. The alignment was constructed with ClustalX.

Appendix C Chapter 7 – Supplementary Material

C.1. Tracer Test

The hydraulic residence time was determined by a tracer test with 10 g/L NaBr in two test columns. The columns were fed deionized water until the conductivity of the effluent was constant and then they were switched to the NaBr solution. The test columns had the same composition and dimensions as the columns used in the experiment. The test was performed at a flow rate (Q) of 24 mL/min and the operational volume (V) of the columns was 2,370 mL.

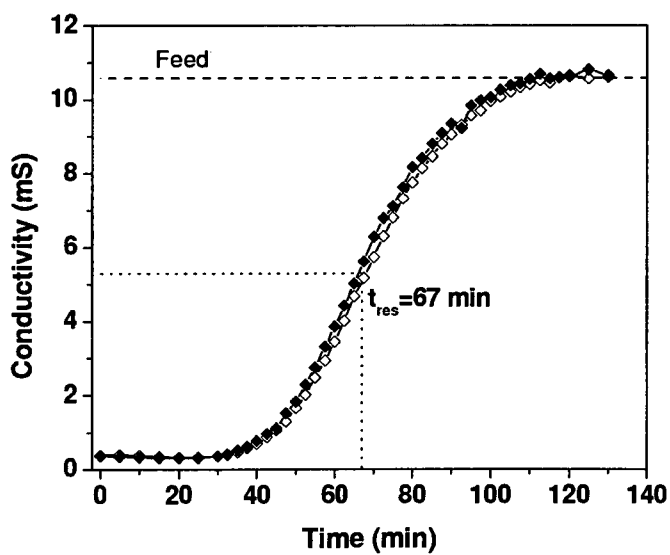


Figure C. 1: Conductivity in the effluent of two replicate columns after the feed was switched from DI water to a 10 g/L NaBr solution.

From the data in Figure C.1, the residence time (t_{res}) in the columns was estimated to be 67 min. The porosity (n) in the columns was estimated as:

$$n = \frac{Q \cdot t_{res}}{V} = 0.68$$

Using this value of porosity, the residence time was estimated for the flow rate used in the experimental columns (250 mL/d):

$$t_{res} = \frac{V \cdot n}{Q} = 6.4d$$

C.2. Gelcompar Analysis

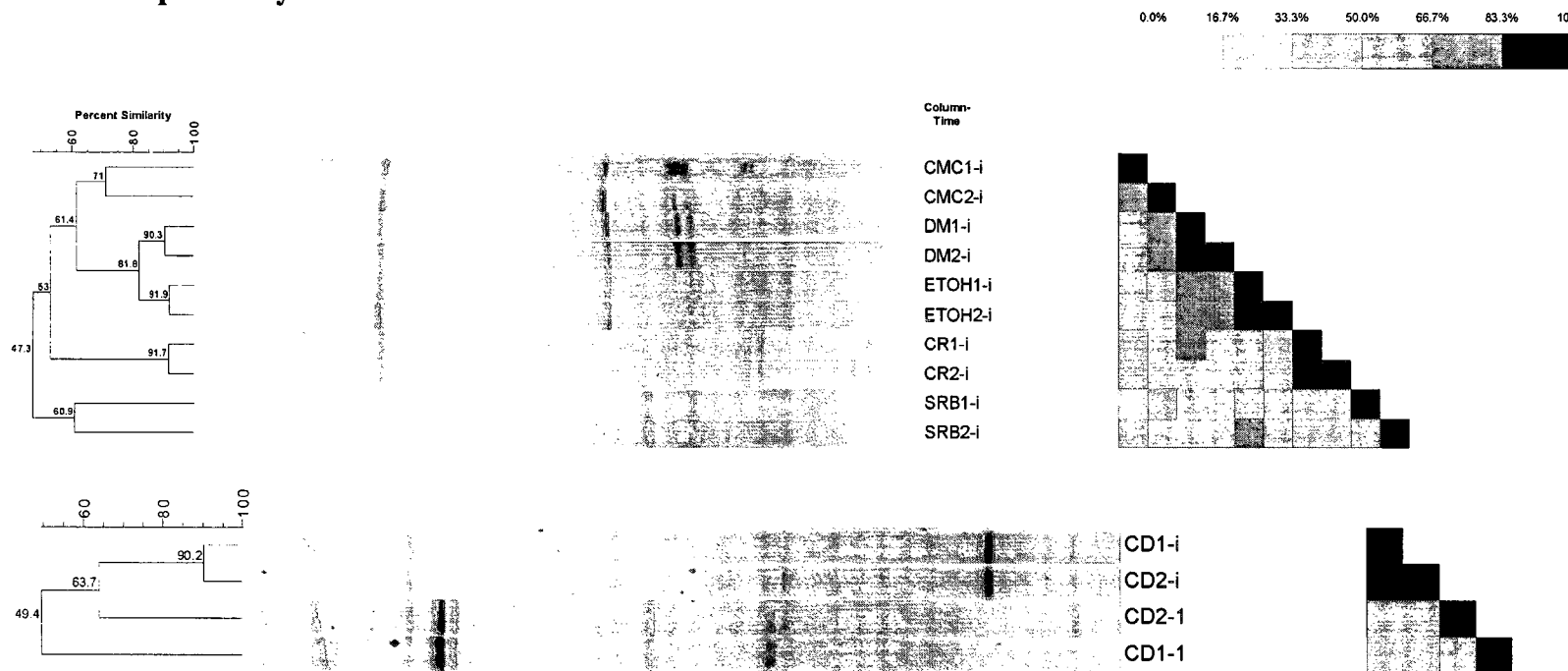


Figure C. 2: Cluster analysis of DGGE fingerprints of I341F/I533R PCR products of DNA extracted from the columns at the beginning of the experiment (-i), and during the pseudo-steady state (-1) for the columns inoculated with dairy manure only (DM), dairy manure and an enrichment of SRB (SRB), dairy manure and an enrichment of cellulose degraders (CD), inoculated with dairy manure alone and supplemented with carboxymethyl cellulose (CMC) or ethanol (EtOH). 1 and 2 after the column name indicate the replicate number.

Table C. 1: Similarity matrix constructed from using the Dice coefficient for pairwise comparisons for the DGGE fingerprints of I341F/I533R PCR products of DNA extracted from the columns at the beginning of the experiment (-i), and during the pseudo-steady state (-1) for the columns inoculated with dairy manure only (DM), dairy manure and an enrichment of SRB (SRB), dairy manure and an enrichment of cellulose degraders (CD), inoculated with dairy manure alone and supplemented with carboxymethyl cellulose (CMC) or ethanol (EtOH). 1 and 2 after the column name indicate the replicate number.

CMC1-i	100															
CMC2-i	71.0	100														
DM1-i	64.7	71.0	100													
DM2-i	62.5	69.0	90.3	100												
ETOH1-i	54.1	47.1	81.1	82.4	100											
ETOH2-i	64.7	58.1	82.4	81.3	91.9	100										
CR1-i	48.3	61.5	69.0	53.8	58.1	48.3	100			CD1-i		100				
CR2-i	33.3	50.0	58.1	50.0	58.8	46.7	91.7	100		CD2-i		90.2	100			
SRB1-i	28.6	33.3	51.9	56.0	46.7	56.0	34.8	33.3	100	CD2-1		65.2	62.2	100		
SRB2-i	40.0	53.8	53.3	57.1	68.8	64.3	41.7	37.0	60.9	100	CD1-1		46.5	42.9	58.8	100

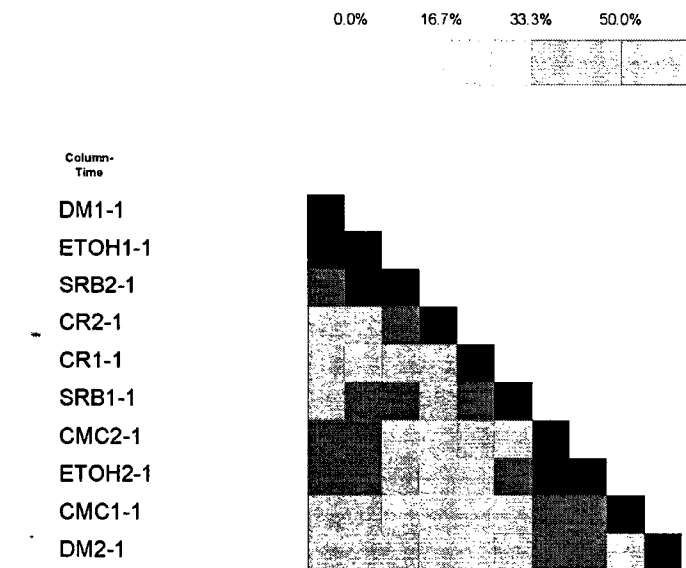
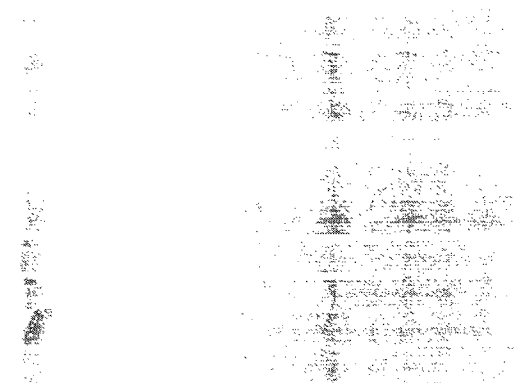
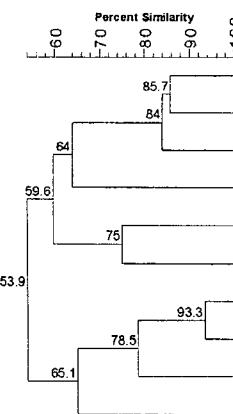


Figure C. 3: Cluster analysis of DGGE fingerprints of I341F/I533R PCR products of DNA extracted from the columns during the pseudo-steady state (-1) for the columns inoculated with dairy manure only (DM), dairy manure and an enrichment of SRB (SRB), inoculated with dairy manure alone and supplemented with carboxymethyl cellulose (CMC) or ethanol (EtOH). 1 and 2 after the column name indicate the replicate number.

Table C. 2: Similarity matrix constructed from using the Dice coefficient for pairwise comparisons for the DGGE fingerprints of I341F/I533R PCR products of DNA extracted from the columns during the pseudo-steady state (-1) for the columns inoculated with dairy manure only (DM), dairy manure and an enrichment of SRB (SRB), inoculated with dairy manure alone and supplemented with carboxymethyl cellulose (CMC) or ethanol (EtOH). 1 and 2 after the column name indicate the replicate number.

DM1-1		100									
ETOH1-1		85.7	100								
SRB2-1		82.4	85.7	100							
CR2-1		63.2	58.8	70.0	100						
CR1-1		50.0	42.9	58.8	63.2	100					
SRB1-1		50.0	66.7	82.4	63.2	75.0	100				
CMC2-1		80.0	71.4	47.1	44.4	53.3	47.1	100			
ETOH2-1		80.0	76.9	62.5	44.4	42.9	66.7	93.3	100		
CMC1-1		53.3	61.5	37.5	33.3	40.0	37.5	80.0	76.9	100	
DM2-1		61.5	54.5	53.3	37.5	42.9	62.5	66.7	71.4	57.1	100

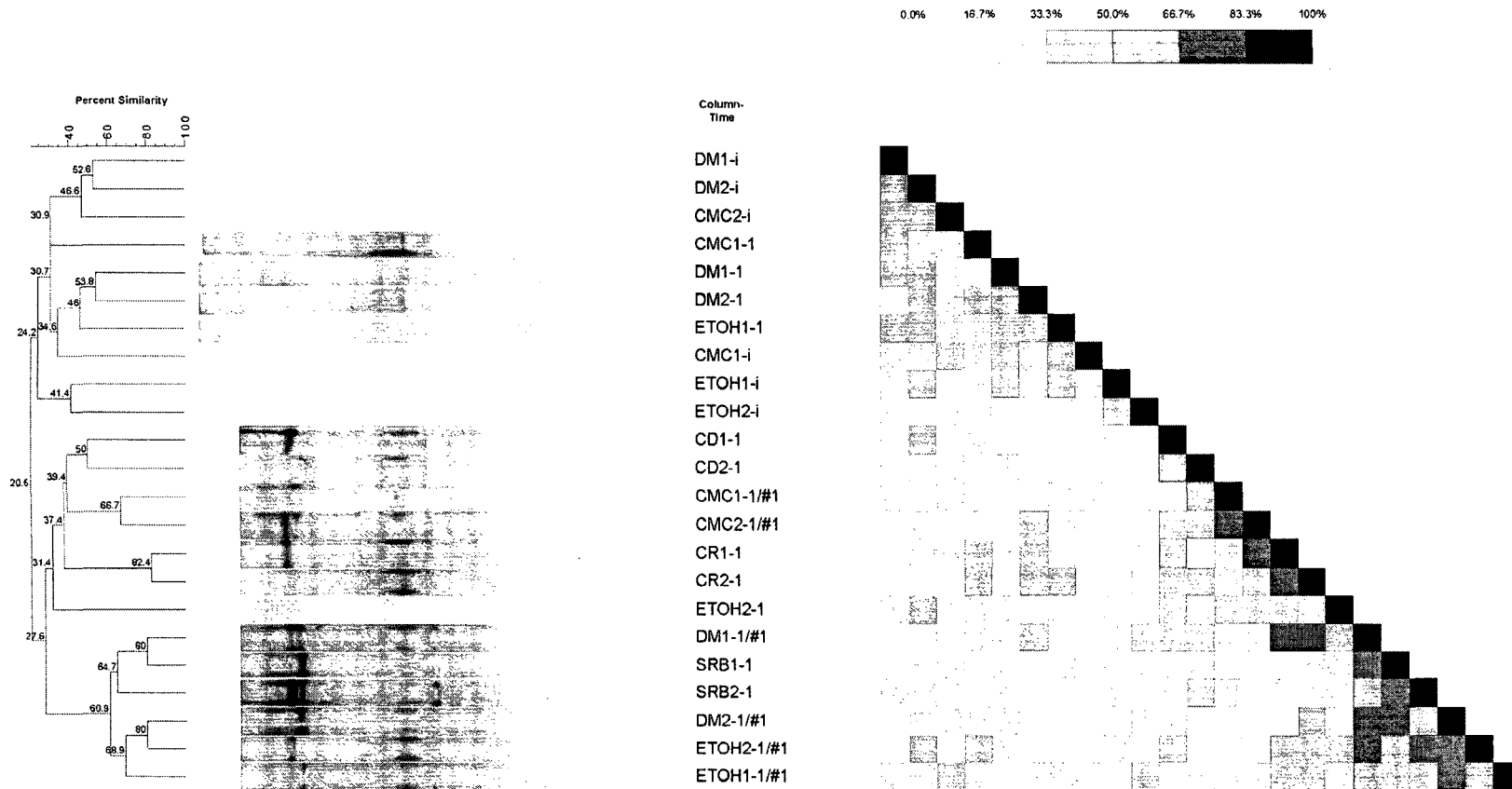


Figure C. 4: Cluster analysis of DGGE fingerprints of GCcel48_490F/cel48_920R PCR products of DNA extracted from the columns at the beginning of the experiment (-i), and during the pseudo-steady state (-1) for the columns inoculated with dairy manure only (DM), dairy manure and an enrichment of SRB (SRB), dairy manure and an enrichment of cellulose degraders (CD), inoculated with dairy manure alone and supplemented with carboxymethyl cellulose (CMC) or ethanol (EtOH). 1 and 2 indicate the replicate number. Samples with a '#' in their label were used as reference to compare different gels.

Table C. 3: Similarity matrix constructed from using the Dice coefficient for pairwise comparisons for the DGGE fingerprints of GCcel48_490F/cel48_920R PCR products of DNA extracted from the columns at the beginning of the experiment (-i), and during the pseudo-steady state (-1) for the columns inoculated with dairy manure only (DM), dairy manure and an enrichment of SRB (SRB), dairy manure and an enrichment of cellulose degraders (CD), inoculated with dairy manure alone and supplemented with carboxymethyl cellulose (CMC) or ethanol (EtOH). 1 and 2 indicate the replicate number. Samples with a '#' in their label were used as reference to compare different gels.

DM1-i	100													
DM2-i	52.6 100													
CMC2-i	48.8 44.4 100													
CMC1-1	40.0 21.4 31.3 100													
DM1-1	34.3 41.0 24.4 24.0 100													
DM2-1	24.0 34.5 18.2 47.1 53.8 100													
ETOH1-1	43.8 33.3 20.5 27.3 48.5 43.5 100													
CMC1-i	29.4 31.6 34.1 24.0 34.3 32.0 37.5 100													
ETOH1-i	29.4 47.4 19.5 16.7 34.3 23.1 37.5 23.5 100													
ETOH2-i	20.7 30.3 16.7 21.1 13.3 9.5 29.6 13.8 41.4 100													
CD1-1	30.8 33.3 18.2 23.5 14.8 11.1 8.3 15.4 23.1 19.1 100													
CD2-1	26.1 29.6 19.4 0.0 16.7 0.0 9.5 8.7 25.0 21.1 50.0 100													
CMC1-1/#1	16.7 14.3 19.4 13.3 24.0 0.0 18.2 25.0 16.7 21.1 25.0 57.1 100													
CMC2-1/#1	16.0 20.7 18.8 25.0 23.1 35.3 26.1 16.0 16.0 0.0 35.3 40.0 66.7 100													
CR1-1	16.0 27.6 18.8 37.5 30.8 35.3 26.1 16.0 24.0 20.0 50.0 13.3 26.7 66.7 100													
CR2-1	16.0 27.6 25.0 35.3 14.8 33.3 33.3 15.4 15.4 19.1 44.4 37.5 25.0 35.3 82.4 100													
ETOH2-1	30.8 34.5 18.8 25.0 23.1 25.0 26.1 15.4 23.1 19.1 33.3 25.0 37.5 35.3 35.3 22.2 100													
DM1-1/#1	16.0 27.6 12.1 23.5 29.6 33.3 26.1 8.0 16.7 38.1 44.4 37.5 26.7 23.5 70.6 66.7 35.3 100													
SRB1-1	8.3 21.4 25.8 13.3 24.0 12.5 18.2 8.3 16.7 21.1 25.0 28.6 15.4 0.0 13.3 25.0 25.0 80.0 100													
SRB2-1	22.2 32.3 29.4 11.8 28.6 10.5 16.0 15.4 22.2 18.2 22.2 35.3 23.5 11.1 22.2 21.1 31.6 58.8 70.6 100													
DM2-1/#1	8.3 21.4 20.0 26.7 24.0 12.5 9.1 8.3 8.7 31.6 25.0 15.4 15.4 13.3 13.3 37.5 25.0 75.0 71.4 47.1 100													
ETOH2-1/#1	16.0 34.5 25.0 37.5 30.8 11.8 8.7 8.0 16.7 20.0 35.3 28.6 28.6 12.5 37.5 35.3 35.3 70.6 53.3 75.0 80.0 100													
ETOH1-1/#1	20.7 24.2 38.9 30.0 13.3 19.1 22.2 20.7 6.9 33.3 28.6 21.1 21.1 20.0 40.0 38.1 28.6 57.1 52.6 45.5 77.8 60.0 100													

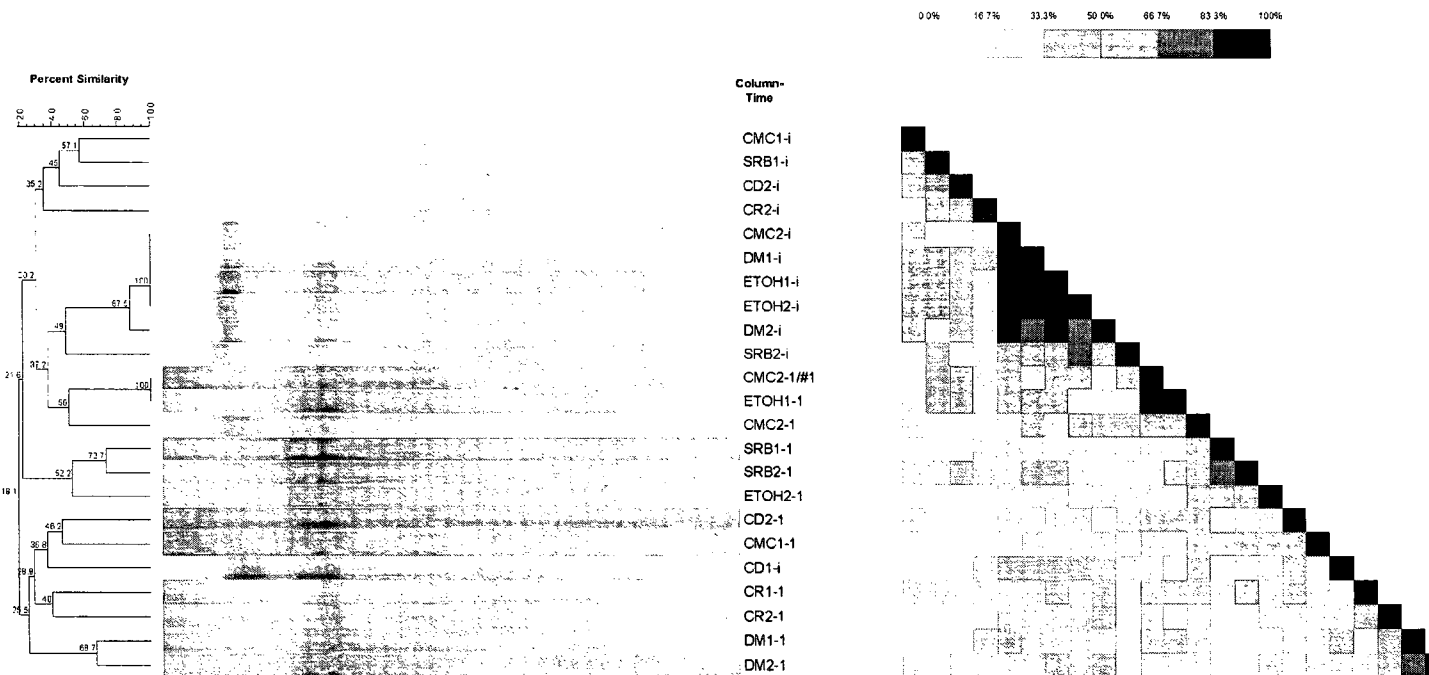


Figure C. 5: Cluster analysis of DGGE fingerprints of *Gc cel5_392F/cel5_754R* PCR products of DNA extracted from the columns at the beginning of the experiment (-i), and during the pseudo-steady state (-1) for the columns inoculated with dairy manure only (DM), dairy manure and an enrichment of SRB (SRB), dairy manure and an enrichment of cellulose degraders (CD), inoculated with dairy manure alone and supplemented with carboxymethyl cellulose (CMC) or ethanol (EtOH). 1 and 2 indicate the replicate number. Samples with a '#' in their label were used as reference to compare different gels.

Table C. 4: Similarity matrix constructed from using the Dice coefficient for pairwise comparisons for the DGGE fingerprints of GCcel5_392F/cel5_754R PCR products of DNA extracted from the columns at the beginning of the experiment (-i), and during the pseudo-steady state (-1) for the columns inoculated with dairy manure only (DM), dairy manure and an enrichment of SRB (SRB), dairy manure and an enrichment of cellulose degraders (CD), inoculated with dairy manure alone and supplemented with carboxymethyl cellulose (CMC) or ethanol (EtOH). 1 and 2 indicate the replicate number. Samples with a '#' in their label were used as reference to compare different gels.

Table C. 5: Similarity matrix constructed from using the Dice coefficient for pairwise comparisons for the DGGE fingerprints of GChydA_1290F/hydA_1538R PCR products of DNA extracted from the columns at the beginning of the experiment (-i), and during the pseudo-steady state (-1) for the columns inoculated with dairy manure only (DM), dairy manure and an enrichment of SRB (SRB), dairy manure and an enrichment of cellulose degraders (CD), inoculated with dairy manure alone and supplemented with carboxymethyl cellulose (CMC) or ethanol (EtOH). 1 and 2 indicate the replicate number. Samples with a '#' in their label were used as reference to compare different gels.

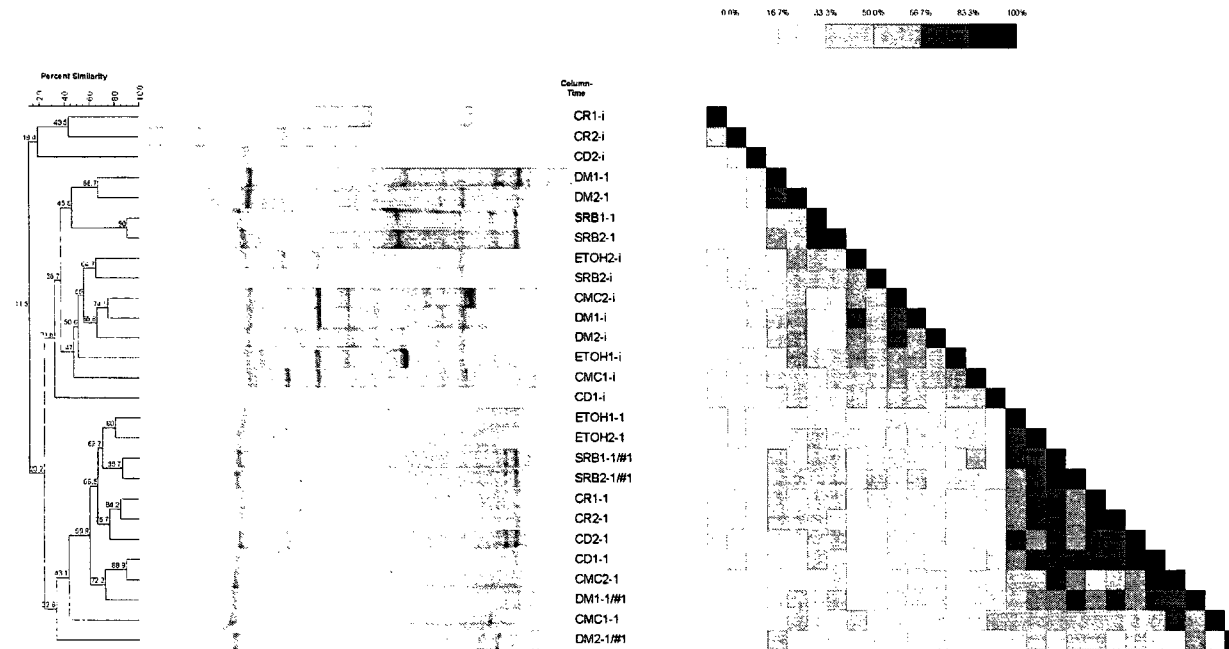


Figure C. 6: Cluster analysis of DGGE fingerprints of GC*dsrA_290F/dsrA_660R* PCR products of DNA extracted from the columns at the beginning of the experiment (-i), and during the pseudo-steady state (-1) for the columns inoculated with dairy manure only (DM), dairy manure and an enrichment of SRB (SRB), dairy manure and an enrichment of cellulose degraders (CD), inoculated with dairy manure alone and supplemented with carboxymethyl cellulose (CMC) or ethanol (EtOH). 1 and 2 indicate the replicate number. Samples with a '#' in their label were used as reference to compare different gels.

Table C. 6: Similarity matrix constructed from using the Dice coefficient for pairwise comparisons for the DGGE fingerprints of GC_{dsrA_290F/dsrA_660R} PCR products of DNA extracted from the columns at the beginning of the experiment (-i), and during the pseudo-steady state (-1) for the columns inoculated with dairy manure only (DM), dairy manure and an enrichment of SRB (SRB), dairy manure and an enrichment of cellulose degraders (CD), inoculated with dairy manure alone and supplemented with carboxymethyl cellulose (CMC) or ethanol (EtOH). 1 and 2 indicate the replicate number. Samples with a '#' in their label were used as reference to compare different gels.

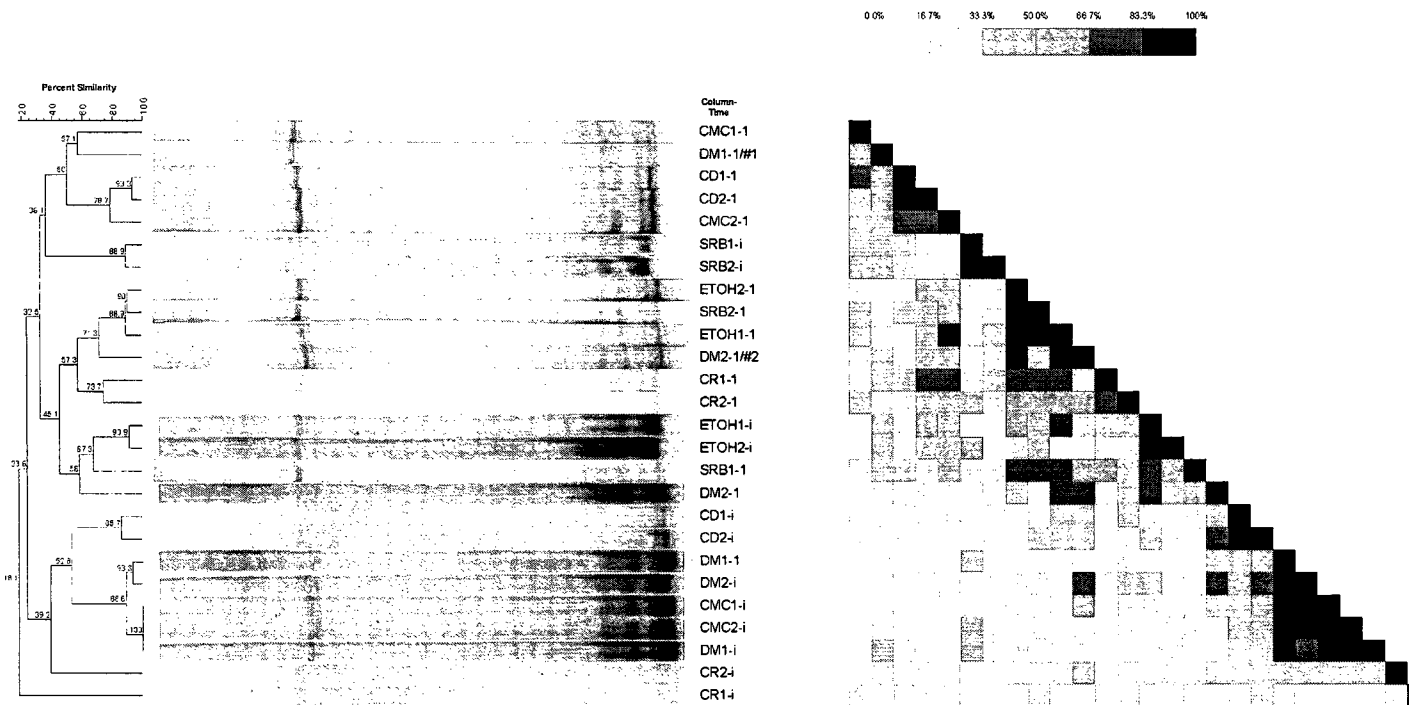


Figure C. 7: Cluster analysis of DGGE fingerprints of GC*mcrA*_1035F/*mcrA*_1530R PCR products of DNA extracted from the columns at the beginning of the experiment (-i), and during pseudo-steady state (-1) for the columns inoculated with dairy manure only (DM), dairy manure and an enrichment of SRB (SRB), dairy manure and an enrichment of cellulose degraders (CD), inoculated with dairy manure alone and supplemented with carboxymethyl cellulose (CMC) or ethanol (EtOH). 1 and 2 indicate the replicate number. Samples with a '#' in their label were used as reference to compare different gels.

Table C. 7: Similarity matrix constructed from using the Dice coefficient for pairwise comparisons for the DGGE fingerprints of GC_{mcrA_1035F/mcrA_1530R} PCR products of DNA extracted from the columns at the beginning of the experiment (-i), and during pseudo-steady state (-1) for the columns inoculated with dairy manure only (DM), dairy manure and an enrichment of SRB (SRB), dairy manure and an enrichment of cellulose degraders (CD), inoculated with dairy manure alone and supplemented with carboxymethyl cellulose (CMC) or ethanol (EtOH). 1 and 2 indicate the replicate number. Samples with a '#' in their label were used as reference to compare different gels.

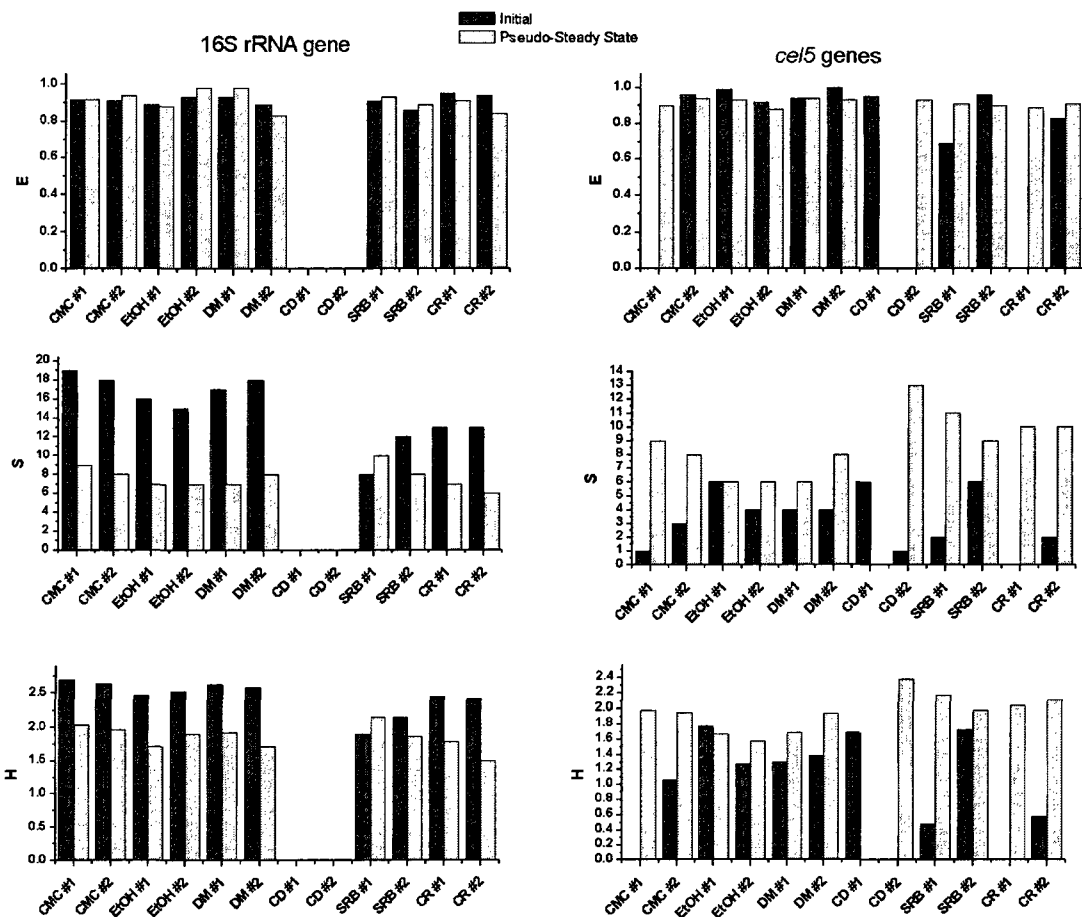


Figure C. 8: Microbial community evenness (E), species richness (S), and Shannon diversity index (H) based on DGGE patterns of PCR products obtained with the I341F/I533R and GCcel5_392F/cel5_754R primers on the substrate samples collected at the beginning of the experiment and during the pseudo-steady state from the columns inoculated with dairy manure only (DM), dairy manure and an enrichment of SRB (SRB), dairy manure and an enrichment of cellulose degraders (CD), inoculated with dairy manure alone and supplemented with carboxymethyl cellulose (CMC) or ethanol (EtOH).

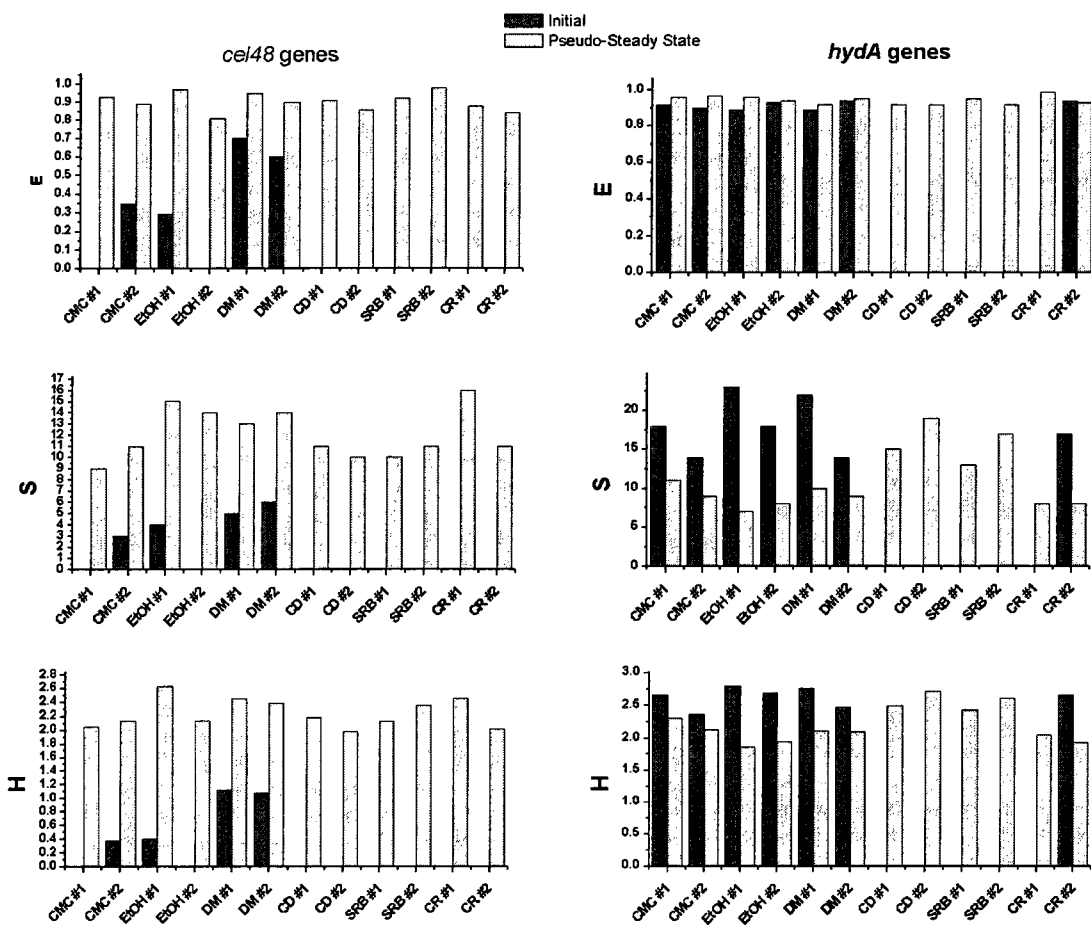


Figure C. 9: Microbial community evenness (E), species richness (S), and Shannon diversity index (H) based on DGGE patterns of PCR products obtained with the GC*cel48_490F/cel48_920R* and GC*hydA_1290F/hydA_1538R* primers on the substrate samples collected at the beginning of the experiment and during the pseudo-steady state from the columns inoculated with dairy manure only (DM), dairy manure and an enrichment of SRB (SRB), dairy manure and an enrichment of cellulose degraders (CD), inoculated with dairy manure alone and supplemented with carboxymethyl cellulose (CMC) or ethanol (EtOH).

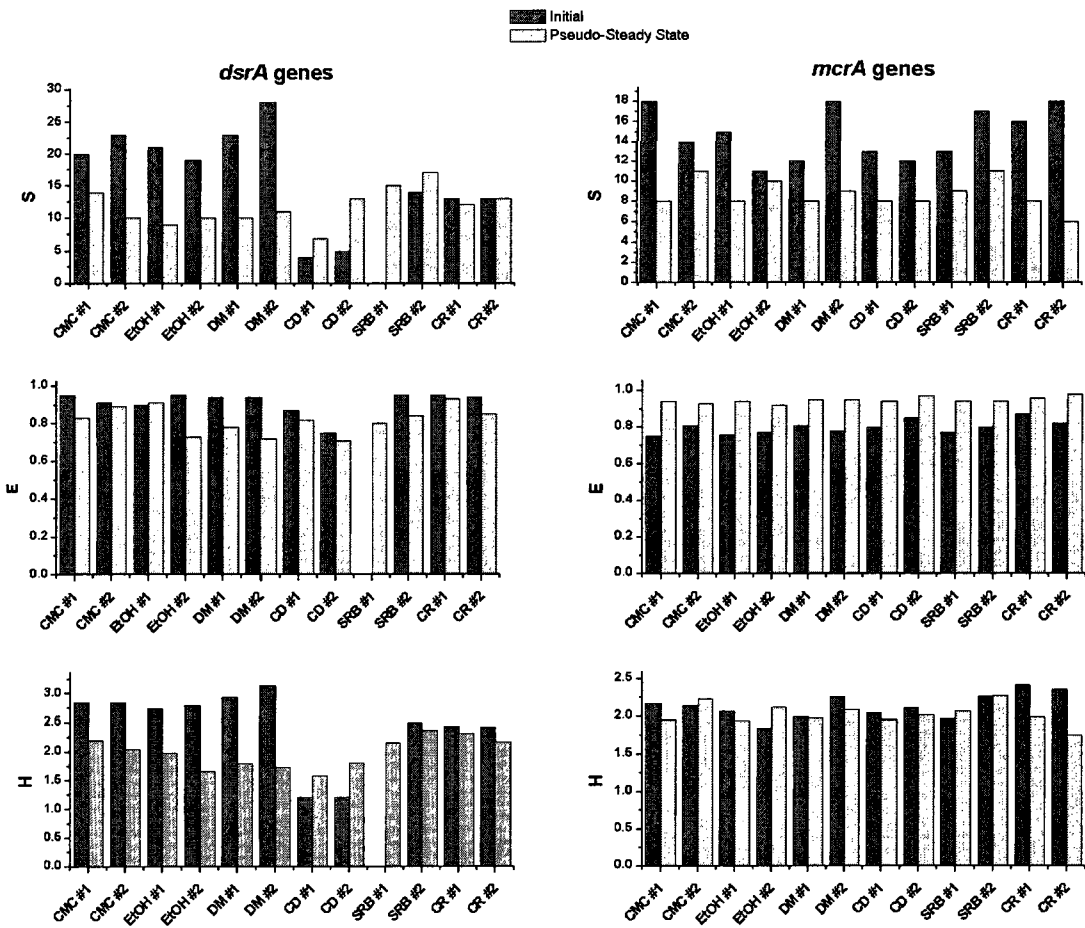


Figure C. 10: Microbial community evenness (E), species richness (S), and Shannon diversity index (H) based on DGGE patterns of PCR products obtained with the GC_{dsrA}_290F/*dsrA*_660R and GC_{mcrA}_1035F/*mcrA*_1530R primers on the substrate samples collected at the beginning of the experiment and during the pseudo-steady state from the columns inoculated with dairy manure only (DM), dairy manure and an enrichment of SRB (SRB), dairy manure and an enrichment of cellulose degraders (CD), inoculated with dairy manure alone and supplemented with carboxymethyl cellulose (CMC) or ethanol (EtOH).

Appendix D Detailed Protocols and Methods

D.1. DNA Extraction

D.1.1. PowerMax™ Soil DNA Isolation Kit (MoBio cat # 12988-10)

1. Add 15 ml of PowerBead Solution to a PowerBead Tube. These tubes will now be referred to as PowerMax™ Bead Solution Tubes.
2. Add approximately 5 g of sample to PowerMax™ Bead Solution Tube. Vortex vigorously for 1 minute. **Note:** Write down how much sample is added to each tube
3. Check Solution C1. If Solution C1 is precipitated, heat the solution at 60°C until the precipitate has dissolved. Add 1.2 mL of Solution C1 to the PowerMax™ Bead Solution Tube and vortex vigorously for 30 seconds.
4. Place PowerMax™ Bead Solution Tubes on the MO BIO Laboratories, Inc. Vortex Adapter and vortex for 5 minutes at the highest speed (10 in our vortex).
5. Centrifuge tubes at 2500 x g for 3 minutes at room temperature.
6. Transfer supernatant to a clean collection tube. The supernatant may still contain some soil particles and color.
7. Add 5 mL of Solution C2 and invert twice to mix. Incubate at 4°C (fridge) for 10 minutes.

8. Centrifuge tubes at 2500 x g for 4 minutes at room temperature. If needed, centrifuge longer.
9. Avoiding pellet, transfer supernatant to a clean collection tube.
10. Add 4 mL of Solution C3 and invert twice to mix. Incubate at 4°C (fridge) for 10 minutes.
11. Centrifuge tubes at 2500 x g for 4 minutes at room temperature. If needed, centrifuge longer.
12. Avoiding pellet, transfer supernatant to a clean collection tube.
13. Add 30 mL of Solution C4 to supernatant and invert twice.
14. Fill Spin Filter with solution from Step 13. Centrifuge at 2500 x g for 2 minutes at room temperature. Discard flow through and add second volume of supernatant to same Spin Filter and centrifuge at 2500 x g for 2 minutes at room temperature. Discard flow through. Repeat until entire volume has been processed.
15. Add 10 mL of Solution C5 to Spin Filter and centrifuge at 2500 x g for 3 minutes at room temperature. Discard flow through.
16. Centrifuge Spin Filter at 2500 x g for 5 minutes at room temperature.
17. Carefully place Spin Filter in a new collection tube. Avoid splashing Solution C5 onto Spin Filter.
18. Add 5 mL of Solution C6 to the center of Spin Filter membrane. Let sit at room temperature for 2 minutes. Centrifuge at 2500 x g for 3 minutes at room temperature.
19. Discard Spin Filter. The DNA in the tube is now ready for any downstream

application.

20. Using filter tips in the laminar-flow hood, aliquot out the DNA extract into five 2-mL O-ring tubes. Also transfer 100 µL aliquots into two 0.5-mL O-ring tubes.
21. Store in -80 °C freezer.

D.1.2. UltraClean™ Soil DNA Isolation Kit (MoBio cat#12800-50 or 12800-100)

1. To the 2-mL Bead Solution tubes provided, add 0.25 - 1gm of soil sample.
NOTE: We generally add ~ 0.5 g or mL. Make sure you write down the volume/mass that you add to each tube.
2. Gently vortex to mix.
3. Check Solution S1. If Solution S1 is precipitated, heat solution to 60°C until dissolved before use. Add 60 µL of Solution S1 and invert several times or vortex briefly.
4. Add 200 µL of Solution IRS (Inhibitor Removal Solution).
5. Bead beat for 3 minutes at HOMOGENIZE
6. Centrifuge tubes at 10,000 x g for 30 seconds.
CAUTION: Be sure not to exceed 10,000 x g or tubes may break.
7. Transfer the supernatant to a clean microcentrifuge tube (provided).
8. Add 250 µL of Solution S2 and vortex for 5 sec. Incubate 4 °C (fridge) for 5 min.
9. Centrifuge the tubes for 1 minute at 10,000 x g.
10. Avoiding the pellet, transfer entire volume of supernatant to a clean microcentrifuge tube (provided).

11. Add 1.3 mL of Solution S3 to the supernatant (careful, volume touches rim of tube) and vortex for 5 seconds.

NOTE: If tube is too full or if there is not enough room for all the liquid, use 15-mL conical tubes.

12. Load approximately 700 μ L onto a spin filter and centrifuge at 10,000 $\times g$ for 1 minute. Discard the flow through, add the remaining supernatant to the spin filter, and centrifuge at 10,000 $\times g$ for 1 minute. Repeat until all supernatant has passed through the spin filter.

13. Add 300 μ L of Solution S4 and centrifuge for 30 seconds at 10,000 $\times g$. Discard the flow through.

14. Centrifuge again for 1 minute.

15. Carefully place spin filter in a new clean tube. Avoid splashing any Solution S4 onto the spin filter.

16. Add 50 μ L of Solution S5 to the center of the white filter membrane.

17. Centrifuge for 30 seconds.

18. Discard the spin filter. DNA in the tube is now application ready.

19. Using filter tips in the laminar-flow hood, combine the three extracts in one 0.5-mL O_ring tube. From there, transfer two 20-uL aliquots to two 0.5-mL O-ring tubes

20. Store in -80 °C freezer.

D.1.3. UltraClean™ Microbial DNA Isolation Kit (MoBio cat # 12224-50 or 12224-250)

1. Using filter tips in the laminar flow hood, add 1.8 mL of culture to a 2 mL Collection Tube (provided). **NOTE:** Make sure you write down the volume of culture you add to each tube. Also make sure that the cultures are well mixed before you take the sample.
2. Centrifuge at 10,000 x g for 5 minutes at room temperature. Decant the supernatant and spin the tubes at 10,000 x g for 1 minute at room temperature and completely remove the media supernatant with a pipette tip.
NOTE: Based on the type of microbial culture, it may be necessary to centrifuge longer than 30 seconds.
3. Resuspend the cell pellet in 300 µL of MicroBead Solution and gently vortex to mix. Transfer resuspended cells to MicroBead Tube.
4. Add 50 µL of Solution MD1 to the MicroBead Tube.
5. Place the tubes in the bead beater and bead beat for 3 minutes at HOMOGENIZE.
6. Centrifuge the tubes at 10,000 x g for 30 seconds at room temperature.
CAUTION: Be sure not to exceed 10,000 x g or tubes may break.
7. Transfer all the supernatant to a clean 2 mL collection tube.
8. Add 100 µL of Solution MD2 to the supernatant. Vortex 5 seconds. Then incubate at 4°C (fridge) for 5 minutes.
9. Centrifuge the tubes at room temperature for 1 minute at 10,000 x g.

10. Avoiding the pellet, transfer the entire volume of supernatant to a clean 2 mL collection tube.
11. Add 900 μ L of Solution MD3 to the supernatant and vortex 5 seconds.
12. Load about 700 μ L into the Spin Filter and centrifuge at 10,000 $\times g$ for 30 seconds at room temperature. Discard the flow through, add the remaining supernatant to the Spin Filter, and centrifuge at 10,000 $\times g$ for 30 seconds at room temperature.

NOTE: A total of 2 to 3 loads for each sample processed are required. Discard all flow through liquid.
13. Add 300 μ L of Solution MD4 and centrifuge at room temperature for 30 seconds at 10,000 $\times g$. Discard the flow through.
14. Centrifuge at room temperature for 1 minute at 10,000 $\times g$.
15. Being careful not to splash liquid on the spin filter basket, place Spin Filter in a new 2 mL collection tube.
16. Add 50 μ L of Solution MD5 to the center of the white filter membrane.
17. Centrifuge at room temperature for 30 seconds at 10,000 $\times g$.
18. Discard Spin Filter.
21. Using filter tips in the laminar-flow hood, combine the three extracts in one 0.5-mL O-ring tube. From there, transfer two 20- μ L aliquots to two 0.5-mL O-ring tubes
22. Store in -80 °C freezer.

D.2. Purification of DNA Extracts

This is the procedure for the GENECLEAN® SPIN Kit (MP Biomedicals cat # 1101-200)

D.2.1. Important Considerations before Use

- Before first use, add the correct volume of **200 proof** (100% ethanol) to the GENECLEAN® SPIN NEW Wash. Remember to label the bottle so everyone knows that ethanol was added. **DO NOT USE 98% ETHANOL.**
- Shake GENECLEAN® SPIN GLASSMILK® to suspend.
- Particles of silica matrix on the cap of the GENECLEAN® SPIN GLASSMILK® container can prevent an airtight seal that will result in the evaporation of the liquid. To reconstitute the GENECLEAN® SPIN GLASSMILK®, add sterile, distilled water to the container so that the amount of liquid and solid is approximately equal and mix well to fully activate.

D.2.2. Purification of DNA from Solutions

1. Shake GENECLEAN® SPIN GLASSMILK® to suspend.
2. Add 400 µl of GENECLEAN® SPIN GLASSMILK® to SPIN Filter.
3. Add DNA solution to GENECLEAN® SPIN GLASSMILK® in SPIN Filter. A maximum volume of 300 µl of DNA solution can be added per filter.

IMPORTANT: GENECLEAN® SPIN can bind up to 5 µg pf DNA/prep. If isolating more than 5 µg of DNA, divide sample into multiple preps.

4. Incubate at room temperature for 5 minutes. Mix every 1-2 minutes to bind the DNA to the silica matrix. Mix by tapping the side of the tube with a finger to ensure that the GENECLAN® SPIN GLASSMILK® stays in suspension.
5. Centrifuge at 14,000 x g for 1 minute or until liquid has emptied into the Catch Tube.
Empty Catch Tube as needed.
6. Add 500 µL of prepared GENECLAN® SPIN NEW Wash to the filter and centrifuge at 14,000 x g for 30 seconds (or until SPIN Filter is emptied of wash).
Empty Catch Tube as needed.
7. Optional: Repeat wash procedure as detailed in Step 6.
8. Centrifuge at 14,000 x g for 2 minutes to dry pellet and transfer SPIN Filter to fresh Catch Tube.
9. Open the tubes and let them air dry for 1 minute.
10. Add 15 to 30 µL GENECLAN® SPIN Elution Solution to SPIN Filter or sterile Tris-HCl buffer pH 8.
11. Vortex the tubes to resuspend GENECLAN® SPIN GLASSMILK®.
12. Incubate the tubes at room temperature for 2 minutes.
13. Centrifuge at 14,000 x g for 30 seconds to transfer eluted DNA to Catch Tube.
14. Discard SPIN Filter and cap the tube. DNA in solution is now ready to use without further manipulation.

D.3. Cloning

Using TOPO TA Cloning Kit for Sequencing (Invitrogen Catalog # K4575-01) with pCR 4-TOPO vector and One Shot TOP 10 chemically competent cells

D.3.1. Preparation pf LB Agar Plates

- Autoclave LB agar mixture
 - o 250 mL DI water with 10.0 grams of LB agar
- Cool until bottle can comfortably be held against your cheek (50-55 °C)
- In the laminar hood:
 - o Add 250 µL of fresh kanamycin 50mg/mL
 - Final concentration in agar should be 50 µg/mL
 - Kanamycin can be stored in the -20 °C freezer for *up to 1 month*
 - o Swirl gently to mix
- Pour plates and allow to cool in a stack until agar solidifies
 - o Should have 10 to 12 plates from 250 mL of agar
- Move to incubator, 37 °C, and place them upside down with so that any condensation is removed
- Store in refrigerator in a sealed plastic bag

D.3.2. Cloning

- Pre-warm plates and incubator before starting
- Remove tube of competent cells from -80 °C freezer and place on/in ice immediately
 - o The competent cells are very sensitive

- Try to have as much of the tube touching an ice cube as possible so that the thawing process is slow
 - Never hold the tube by the bottom as your body heat will affect their transformation efficiency
- Ligation recipe (in a PCR tube)
 - 0.5 – 4.0 μ L PCR product (Do not clean the PCR product)
 - Amount to add is dependent on strength of original PCR product band
 - Typical volume is 2-3 μ L
 - 1 μ L Salt Solution
 - Sterile water to a total of 5 μ L
 - 1 μ L PCR 4-TOPO vector
- Gently flick the tube to mix the components, then tap to get all liquid to the bottom
- Let stand at room temperature for 20-25 minutes
- Add 2 μ L of ligation product to thawed competent cells
 - Retain remaining ligation product
 - Store at -4 °C until cloning reaction verified
 - Ligation product can be used for troubleshooting if cloning fails
- Incubate on ice for 25-30 minutes
- Shock at 42 °C for 30 seconds in a hot water bath
- Add 250 μ L S.O.C. medium *gently* to the side of the tube and *gently* mix by swirling

- Incubate horizontally at 37 °C for 1 hour at 225 rpm
 - o Alternatively, you can rotate by hand every 10 minutes
- Plate approximately 75 µL of cells per plate
- Incubate plates at 37 °C for 16-18 hours
 - o Colonies should be clearly visible and large enough to harvest with pipette tip

D.3.3. M13 PCR

M13 master mix (per reaction, all units are µL)

- o Sterile DI water 15.9
- o 5X Buffer 5.0
- o *GenScript* 10X Buffer 2.5
- o dNTPs (10mM) 0.5
- o M13f (20µM) 0.25
- o M13r (20µM) 0.25
- o Formamide 0.25
- o *GenScript* Taq 0.35
- o Colony 1 per rxn
- M13 PCR thermalcycler program (Typically 35 cycles)
 - o 94 °C – 3 min
 - o 94 °C – 20 sec
 - o 55 °C – 30 sec
 - o 72 °C – 60 sec/1000 bp

- 72 °C – 7 min
 - 4 °C - hold
- Run 1.2% agarose gel on PCR products
- Discard PCR products that do not have a band of the appropriate size

D.4. Preparation of Samples for DNA Sequencing

D.4.1. Preparing a 96-well Plate

1. Quantify M13 PCR products in agarose gel using the Low DNA Mass ladder.
2. Purify samples – Do this in a PCR tube
 - a. For a 96-well plate you have to provide 11 µL of sample at 10 ng per 100 bp
 - i. Example 1 – sample is 30 ng/µL of 1500 bp
 1. Purify 150 ng (5 µL of sample)
 2. Add ExoSAP-IT (2 µL per every 5 µL of sample) ➔ add 2 µL of ExoSAP-IT
 3. Incubate at 37 °C for 15 min to degrade remaining primers and nucleotides and then incubate at 80 °C for 15 min to inactivate ExoSAP-IT
 4. Add 4 µL of water to have a final volume of 11 µL (4 µL H₂O + 2 µL ExoSAP-IT + 5 µL sample)
 - ii. Example 2 – sample is too concentrated, for example 150 ng/µL of 500 bp ➔ 50 ng are required. This means that you have to purify

0.33 μL of sample with 0.13 μL of ExoSAP-IT but we don't have a pipette to handle these small volumes → purify more than 50 ng

1. Purify 2.5 μL of sample (in this case that is 375 ng)
2. Add 1 μL of ExoSAP-IT
3. Incubate at 37 °C for 15 min to degrade remaining primers and nucleotides and then incubate at 80 °C for 15 min to inactivate ExoSAP-IT
4. Calculate how much water to add for the required final concentration. Use the following formulas:

$$C_f = \frac{10\text{ng}}{100\text{bp}} \cdot \text{size(bp)} \cdot \frac{1}{11\mu\text{L}} \quad \text{Eq [A.1]}$$

$$C_f = \frac{10\text{ng}}{100\text{bp}} \cdot 500 \cdot \frac{1}{11\mu\text{L}} = 4.54 \frac{\text{ng}}{\mu\text{L}}$$

$$H = \frac{C_i \cdot V_i}{C_f} - V_i - V_{\text{ExoSAP}} \quad \text{Eq [A.2]}$$

$$H = \frac{150 \frac{\text{ng}}{\mu\text{L}} \cdot 2.5\mu\text{L}}{4.54} - 2.5\mu\text{L} - 1\mu\text{L} = 79.1\mu\text{L}$$

C_f = concentration required by sequencing facility [$\text{ng}/\mu\text{L}$]

H = amount of water to add to ExoSAPed sample to obtain C_f [μL]

C_i = concentration of sample determined by gel quantification [$\text{ng}/\mu\text{L}$]

V_i = volume of sample used for purification [μL]

V_{ExoSAP} = volume of ExoSAP-IT used [μL]

3. Transfer the purified solutions to the 96-well plate.
 - a. In the case of Example 1, you will transfer the whole volume (11 μ L), in the case of Example 2 you will transfer 11 μ L of the 82.6 μ L that you have.
 - b. Samples should be entered numerically (1 through X) according to list below. Example, sample 9 on list should be in the A2 position in the plate

A1

B1

...

G1

H1

A2

B2

C2

Etc

Note: Use the multipipette for this step (two transfers of 5.5 μ L)

4. Add 1 μ L of 3.2 μ M primer (this applies to ALL primers)

Note: Use the multipipette for this step

5. Seal the plate with adhesive film (do not use the Q-PCR optical covers!)

- a. Supplier: GeneMate (www.bioexpress.com or 800-999-2901), catalog #: 100-SEAL-PLT, description: Sealplate adhesive sealing films for microplates sterile

D.4.2. Placing Sequencing Requests

1. Go to <http://dnalims.colostate.edu>
 - a. If you already have an account in the DNAtools lims database, log in
 - b. If you don't have an account, create one by clicking on Create Login Account for dnaLIMS. Complete the registration form. Your account is created right away and you can start submitting sequencing requests if you wish.
2. After you log in the main screen looks like this :

The screenshot shows the dnaLIMS User Tools interface. At the top, there is a decorative banner with a starry background and the text "Macromolecular Resources Research Core Laboratory Fort Collins, CO 80523-2121". Below the banner, the title "dnaLIMS User Tools" is centered. The interface is divided into three columns:

Sequencing Requests & Results	User Profile	Sequencing Resources
Enter DNA Sequencing Requests View Your Requests Download DNA Results You have 96 Well Plate Sequencing Requests Upload and Import File	Change Your Password Change Your Profile Logout	Contact Info. Support Tools Supported Browsers Learn More

At the bottom of the interface, there are links for "Home Page" and "User Help", and a copyright notice: "Copyright © The Regents of the University of Colorado. All Rights Reserved."

3. If you are using the Premium, Standard or Economy levels click on *Enter DNA Sequencing Requests*

4. If you are submitting a 96-well plate click on *96 Well Plate Sequencing Requests*
5. After selecting the sequencing service enter the number of reactions to create sequencing requests for.
6. The next screen looks like this:

Standard DNA Sequencing Request Form

Sequencing Request	View or Delete Request	Retrieve Results	Change Password	Menus	Login Page																																																
<table border="1" style="width: 100%; border-collapse: collapse;"> <tr> <td style="width: 15%;">Payment Type:</td> <td style="width: 85%;">- Select -</td> </tr> <tr> <td colspan="2">Principal Investigator: Pruden Amy</td> </tr> <tr> <td colspan="2">Comments:</td> </tr> <tr> <td colspan="2" style="text-align: center; padding-top: 5px;"> <input type="button" value="Clear"/> <input type="button" value="Validate Table"/> <input type="button" value="Submit"/> </td> </tr> </table>						Payment Type:	- Select -	Principal Investigator: Pruden Amy		Comments:		<input type="button" value="Clear"/> <input type="button" value="Validate Table"/> <input type="button" value="Submit"/>																																									
Payment Type:	- Select -																																																				
Principal Investigator: Pruden Amy																																																					
Comments:																																																					
<input type="button" value="Clear"/> <input type="button" value="Validate Table"/> <input type="button" value="Submit"/>																																																					
No Validation response means all required fields are filled in.																																																					
<table border="1" style="width: 100%; border-collapse: collapse;"> <thead> <tr> <th colspan="2" style="text-align: left; padding-left: 10px;">Template</th> <th colspan="2" style="text-align: center;">DNA Type</th> <th colspan="2" style="text-align: left; padding-left: 10px;">Primer</th> </tr> <tr> <th>Name</th> <th>Conc. ng/<i>ul</i></th> <th>Size bp</th> <th>GC Rich</th> <th>Name</th> <th>Conc. pmol/<i>ul</i></th> </tr> <tr> <th><small>Index</small></th> <th><small>Fill</small> <small>2X</small> <small>Clear</small></th> <th><small>Fill</small> <small>Clear</small></th> <th><small>Fill</small> <small>Clear</small></th> <th><small>Fill</small> <small>Alternate</small> <small>Clear</small></th> <th><small>Fill</small> <small>Clear</small></th> </tr> </thead> <tbody> <tr> <td>1</td> <td></td> <td></td> <td>no</td> <td>- Select -</td> <td>3.2</td> </tr> <tr> <td>2</td> <td></td> <td></td> <td>no</td> <td>- Select -</td> <td>3.2</td> </tr> <tr> <td>3</td> <td></td> <td></td> <td>no</td> <td>- Select -</td> <td>3.2</td> </tr> <tr> <td>4</td> <td></td> <td></td> <td>no</td> <td>- Select -</td> <td>3.2</td> </tr> <tr> <td>5</td> <td></td> <td></td> <td>no</td> <td>- Select -</td> <td>3.2</td> </tr> </tbody> </table>						Template		DNA Type		Primer		Name	Conc. ng/ <i>ul</i>	Size bp	GC Rich	Name	Conc. pmol/ <i>ul</i>	<small>Index</small>	<small>Fill</small> <small>2X</small> <small>Clear</small>	<small>Fill</small> <small>Clear</small>	<small>Fill</small> <small>Clear</small>	<small>Fill</small> <small>Alternate</small> <small>Clear</small>	<small>Fill</small> <small>Clear</small>	1			no	- Select -	3.2	2			no	- Select -	3.2	3			no	- Select -	3.2	4			no	- Select -	3.2	5			no	- Select -	3.2
Template		DNA Type		Primer																																																	
Name	Conc. ng/ <i>ul</i>	Size bp	GC Rich	Name	Conc. pmol/ <i>ul</i>																																																
<small>Index</small>	<small>Fill</small> <small>2X</small> <small>Clear</small>	<small>Fill</small> <small>Clear</small>	<small>Fill</small> <small>Clear</small>	<small>Fill</small> <small>Alternate</small> <small>Clear</small>	<small>Fill</small> <small>Clear</small>																																																
1			no	- Select -	3.2																																																
2			no	- Select -	3.2																																																
3			no	- Select -	3.2																																																
4			no	- Select -	3.2																																																
5			no	- Select -	3.2																																																

Copyright © 2007 Agilent Technologies, All Rights Reserved.

7. Select a payment type (usually Grant) and provide an account number (if using more than one account number use the comments section)
 - a. Complete the table with the name of your samples, concentration, size, whether they are GC rich or not, type of sequence (usually PCR product), primer to use for sequencing, primer concentration, and primer Tm (not necessary for M13r, M13f, Sp6, T3, T7 or if Tm <50 or Tm >70 °C)
8. Click Submit

9. Print two copies of the order confirmation (one for you and one for Macromolecular resources). Place the plate in a Ziplock bag (or similar) and write your name and the order number on it.
10. Take samples to the Proteomics and Metabolomics Facility (C-121 Microbiology Building). Leave samples in the fridge outside C-121 and place the copy of the order in the folder on top of the fridge

Note: If you leave your samples before 10 am they will typically be sequenced the same day

D.5. Denaturing Gradient Gel Electrophoresis (DGGE)

Equipment: DCode Universal Mutation Detection System (Biorad # 170-9103)

D.5.1. Setting up the Glass Plates

- Coat the two glass plates with SigmaCote or RainX using a Kimwipe.

Warning: SigmaCote is volatile and it is dangerous to inhale the fumes- we will do this in the fume hood.

- Place the spacers along the short edges of the large rectangular plate.
- Place the short glass plate on top of the spacers so that it is flush with the bottom edge of the long plate.
- Clamp the glass plate assembly and place the sandwich assembly in the alignment slot.

D.5.2. Preparing the Stacking Gel

- In a 2-mL tube prepare a 100 mg/mL solution of ammonium persulfate (APS) in DI water (0.1 g APS in 1 mL H₂O).

Polyacrylamide gels are formed by copolymerization of acrylamide and bis-acrylamide. The polymerization process is initiated by ammonium persulfate and TEMED (tetramethylethylenediamine): TEMED accelerates the rate of formation of free radicals from persulfate and these, in turn, catalyze the polymerization.

- Add about 2.5 mL (can be approx) of 100% denaturing solution to a 15-mL tube. Add 7.5 μ L of the APS solution and 5 μ L of TEMED to this tube- vortex- and immediately fill a 10-mL syringe with the solution.

The 100% denaturing solution contains 7M urea and 40% vol./vol. formamide in 1X TAE buffer and 8% acrylamide/bis solution (the main component of the gel).

Danger! Acrylamide is a neurotoxin, and should not be allowed to come into contact with the skin!

Once APS and TEMED are added, you only have about 10 minutes to pour the gel before it begins solidifying.

- Dispense enough of the gel solution between the plates to form a thin layer at the bottom of the glass plates. This will be used to form a seal at the bottom of the gel. Rinse the syringe out when done.

D.5.3. Mixing the Gel Solutions

- Label one 50-mL centrifuge tube “H” (for high-density solution) and another “L” (low density solution).
- Add the following solutions to the corresponding tube:

30% to 50% Denaturing Gradient		
	H	L
100% denaturing solution	9 mL	5.4 mL
0% denaturing solution	9 mL	12.6 mL
Blue dye	320 μ L	-----

The 0% solution contains acrylamide/bis in 1X TAE. The blue dye serves as a marker to distinguish the tubes and also so that the gradient can be visualized when it is poured.

- Add 18 μ L of APS (100 mg/mL) and 18 μ L of TEMED to each of the tubes labeled “H” and “L”.
- Fill one 30-mL syringe with the H solution and another 30-mL syringe with the L solution.
- Remove air bubbles from the syringes by turning them upside down and pushing the gel solution to the end of the tubing.
- Attach the syringes to the gradient pourer (H syringe on the right side).
- Connect the syringes to the Y-fitting.
- Attach an 18 gauge needle to the third end of the Y-fitting and hold the beveled side of the needle at the top-center of the gel sandwich.
- Rotate the cam wheel slowly (to avoid formation of bubbles) and steadily to deliver the gel solution

You will notice that the blue solution pours faster at the beginning than the clear solution- this is how the gradient is formed.

- Once the gel solution reaches the top of the plates, insert a 1 inch spacer in between the two glass plates
- Place the gel in a warm place to aid solidification.

D.5.4. Preparing the Second Stacking Gel

- Remove the spacer and pour off any residual unsolidified gel.
- Insert a 16-well comb in between the two glass plates

- To a 15-mL tube add 5 ml of 0% denaturing solution, 10 μ L of TEMED and 15 μ L of APS (100 mg/mL).
- Vortex and quickly add the stacking gel solution to the top of the gel with a 10-mL
- Let solidify for about an hour.

D.5.5. Running the Gel

- Rinse the wells in order to flush out any residual unsolidified gel which may be present in the wells. Wash the wells by filling a 10-mL syringe with the heated buffer and flushing each well individually. Flush each well each well 3 times.

Washing the wells is a critical step for preventing the samples from degrading inside the wells.

- Add 10 μ L of blue loading dye directly to the PCR tubes with the PCR product and mix by pipetting up and down.
- Turn off the pump that recirculates the buffer in the gel chamber and rinse the wells one final time.
- Load your samples. Use extra small-bore pipette tips which allow you to reach the bottom of the well with the sample. If there are clean wells left after all the groups have loaded their samples, load your negative control.

Make sure when you take the sample into the pipette tip that there is a bubble of air beneath the sample (by setting the pipette volume higher than the actual sample volume)- otherwise capillary action will pull your sample out of the tip before you are able to position it in the well.

- Use this formula: $900 / V = t$ (V = volts, t = time in hours) to calculate for how long to run the gel

D.5.6. Preparing the Gel Stain

- Prepare a 1:10,000 dilution (20 µL in 200 mL) of SybrGold in 1X TAE buffer. Keep this solution away from light until ready for use (SybrGold is photosensitive).
- Remove the gel from the DGGE unit.
- Cut off the wells and notch the top right corner (for orientation).
- Place the gel in a tray with the staining solution.
- Place the tray on an orbital shaker (covered) for 15 minutes.
- Label five 0.5-mL microcentrifuge tubes. We will put the gel slices in these tubes when we cut the gel.

D.5.7. Imaging the DGGE Gel

- Carefully transfer the gel from the stain solution to the imager.

The gel is very fragile and can easily tear if mishandled.

- Take a digital image of the gel.
- Transfer the gel onto the cutting tray (this is to avoid damaging the surface of the UV table with the razor blades when we cut the bands).
- Each group will then take turns cutting dominant bands from the gel.

The key to cutting the bands is to avoid the edges and only cut the central 1 mm square portion of the band.

Caution! Make sure to wear the UV shield and protect all exposed skin from the UV light

- Cut the DGGE bands with a fresh razor blade. Transfer the bands to the 0.5-mL microcentrifuge tubes.

- Add 36 µL of sterile water to each microcentrifuge tube and make sure that the gel piece is pushed all the way to the bottom of the tube and submerged in the water.
- Store the gel slices in the freezer for PCR amplification of the DNA in the bands

D.6. Setting up a Quantitative-PCR Run

This is the procedure for setting up Q-PCR runs in the ABI 7300 Real-time PCR cycler (Applied Biosystems)

D.6.1. Creating a Plate Document

1. On the desktop: click on the 7300 System Software icon
2. Select **File > New** (the new document wizard window will open)
 - In Assay drop down menu select **Absolute Quantification (Standard Curve)**
 - Container: **96-well plate**
 - Template: **blank document**
 - Plate name: leave as default or enter plate name
 - Click **NEXT** (the select detectors window opens)
3. Click to select a detector and then press **Add>>**
4. Click **Next**
5. Highlight the wells that you will be using and click **use** to assign the detector to the highlighted wells
6. Click **Finish**
7. In the **Plate** tab: to name the samples highlight the well/s and go to **View > Well inspector**

- Enter the sample name
- In the **task** drop down list select the corresponding task (**unknown** for samples, **standard**, or **NTC** for the blanks)
- For the standards enter the number of gene copies in the **Quantity** column

8. **Close** the Well inspector

9. In the **Instrument** tab:

- Enter the appropriate temperature program
- Enter sample volume in μL
- Data collection = always during the extension step at 72°C

10. Select **File > Save as**, enter a name for the file and click **Save**.

D.6.2. Preparation of Master Mix and 96-well Plate

1. Prepare master mix in PCR workstation and transfer $24 \mu\text{L}$ aliquots to the 96-well plate.
2. Place the 96-well plate on the plate holder and then the plate+holder on ice
3. Add $1 \mu\text{L}$ of the corresponding template (sample, sample + standard, or standard). Try to avoid leaving bubbles in the solution.
Note: It helps to have a diagram of the plate with the samples that go in each well and make a check mark as you add the sample to the wells
4. Seal the reaction with an optical adhesive cover
5. Use the salad spinner to centrifuge the plate briefly (place the plate at a 45° angle)
6. Keep the reaction plate on ice until you are ready to load it into the instrument
7. Load plate into plate holder (the A1 position is in the top-left of the instrument tray)

8. Click Start

D.7. Ion Chromatography

Instrument: Metrohm 861 Advanced Compact IC with MSM and CO₂ Suppressor

Column: Metrospec A Supp 5 High Resolution Anion Column, 250 mm (6.1006.530)

Software: IC NET Chromatography Control and Data Acquisition System

Flow: 0.7 mL/min

Minimum/maximum Pressure: 0 MPa / 20 MPa

D.7.1. Startup Procedure

1. Write name, date, and project number in log book
2. Turn on machines
3. **Very important-** Check that there will be enough eluent, DI water, suppressor regenerant solution, and autosampler rinse water for the number of samples in question (note: the rate at which the eluent is consumed is about 20 mL per sample).
 - a. Eluent - we typically use bagged eluent. If making from scratch, the eluent consists of 3.2 mM Na₂CO₃ and 1 mM NaHCO₃. To make this add 0.678 g Na₂CO₃ and 0.168 g NaHCO₃ to two liters of deaired DI water
 - b. The suppressor regenerant solution is 100 mM H₂SO₄. To make this, add 5.6 mL of concentrated sulfuric acid to 1L of ultrapure water
4. Open program IC Net 2.3. It will require a user name which is CSU (all capital), the password should be left blank, then click on LOG IN

5. Press icon in the upper right of the toolbar. A new window will open displaying the three components of the IC
6. From this window, select “Startup Hardware (measure baseline)” from the Control menu. Immediately proceed to step 7.
7. Double click the middle machine (resembling IC unit) from the warm-up window to open the instrument control window. Click the “Step” button. The suppressor should be stepped three times with 10 minute delays (or until baseline is stable) (note: a timer is displayed next to the “Step” button). (Note: the stepping checks the three channels and gives you a real-time graph of the conductivity. Wait until the baseline is stable before clicking STEP)

**a good rule of thumb is to step the instrument once the conductivity is 1-3 $\mu\text{S}/\text{cm}$ and pressure between 10-13 MPa (Both readings should be fairly stable before stepping). If the *conductivity is high*, make sure that all the components are on (ie. pump, CO₂ suppressor, etc.). If the *pressure is too high* you should refer to the manual for troubleshooting (ie. a filter may need to be replaced).

8. During the stepping, load sample vials into sampler tray and set up sample queue (see below).
9. When the warm-up is complete, it should have reached a steady state and the pressure should read about 10 MPa (10-12 MPa) and the conductivity should read about 1.0 $\mu\text{S}/\text{cm}$, record these values in log book (Note: the baseline conductivity is usually less than 3.5 $\mu\text{S}/\text{cm}$).

Note: Make sure that the System State (on the lower left corner of the screen) says **ONLINE**. If not, turn everything off (computer, IC, autosampler) and then ON again.

D.7.2. Starting up a Sample Queue

1. Select “Sample Queue” from the System menu. Create a file name for which the list will be stored
2. Check the “**Shut down system after the queue finishes**” option (especially on Fridays). Then click on the “Edit” option.
3. A Queue editor window will open. To duplicate the lines click the seventh icon from the right.
4. For samples, standards, and blanks, the “System” column should read anions (note: a different columns is required for cations)
5. Add the identity of the samples, standards, and blanks to be tested in the Ident column. It is recommended that the order be blank →standards→samples→blank, however this is not the required order: the ultimate order is determined by the user.
6. Add the vial number associated to the identity of the vial to the “Vial” column. This can be made easy if the vials are arranged in order, the location of the first vial may be entered into the “Vial” column, then the “Vial” column should be highlighted, and the sixth icon from the right should be clicked
7. If a dilution was performed the program will account for this if a number is placed in the “Dilution” column (e.g., 100 is entered for a 1:100 dilution)

8. In the “Level” column, the blank and samples should read 0. The standards should be numbered sequentially from smallest to largest (the levels for the sulfate standards are : 1(1 mg/L) , 2 (5 mg/L), 3 (10 mg/L),4 (50 mg/L) ,5 (100 mg/L)). (Note: leave 0 in this column for samples, standards, and blanks. The levels for the standards will be added later during data processing).
9. This queue should be saved by clicking on the second icon from the left
10. Click the check mark icon (second from the right) and the Queue editor window will close
11. Click “Start” to begin the run.

**the sample queue can be edited once the run is going (ie. adding/deleting samples in the edit forum is allowed)

D.7.3. Preparation of Standards

- Use a commercial standard solution of 1000 ppm sulfate
- Prepare a 100 ppm stock solution in a 50-mL volumetric flask (add 5 mL of the multi-ion solution and fill with DI water to the 50-mL mark)
- Standard dilutions (Note: these are not serial dilutions, all the dilution are made from the 100 ppm solution):

Final concentration [ppm]	Volume of 100 ppm solution [mL]	Volume of DI water [mL]
50	5	5
10	1	9
5	0.5	9.5
1	0.1	9.9

D.7.4. Processing the Data

1. Look at the files of each of the calibration points and choose the points that you want to use for integration:
 - a. In the IC Net screen go to File →Open→Chromatograms (or you can click the “Open” icon on the toolbar)
 - b. A new window with the samples ID will open
 - c. Select the files corresponding to the standards (keep the CRTL key pressed) and click OK
 - d. Look at the chromatograms. Compare expected and observed values and the shape of the chromatogram. Use this information to determine which points you want to use for the calibration.
 2. Select all calibration points and reprocess:
 - a. File →Open→Chromatograms
 - b. Select all the files corresponding to the calibration points
 - c. Click “To Batch” →OK →yes
 - d. From the drop-down list, select one of the points to use for integration
 - i. Check the Update, Reintegrate, and Recalibrate options
 - ii. Click the Edit sample Table button and add the corresponding calibration levels. Save and close.
 - e. Click Reprocess
 3. Apply the new calibration to the samples:

- a. File → Open → Chromatograms
- b. Choose the files corresponding to the samples and calibration points
- c. Click “To Batch” → OK → yes
- d. From the drop-down list, select one the points of the calibration
 - i. Check the Update, Reintegrate, Recalibrate, and Make report options
- e. Click Reprocess
- f. An Excel file will open with the processed data. **DO NOT MODIFY THIS FILE.**
- g. To save the file, click on the Clear Table button on the upper left corner. A new window will open where you can choose where to save the file. Save it on Sage’s folder on the Desktop. After saving the file, the spreadsheet will be blank.

D.7.5. Purging the IC

When the eluent bag is replaced, air can get in the line. You will know if this happens because the pressure won’t go up. When this happens, the system has to be purged:

1. Open bypass valve (1/4 turn to the left)
2. In the IC Net screen, click on the icon on the right of the tool bar. A new window with the three components of the IC will open.

3. Double click on the IC icon. A new window will open that contains the IC parameters. Turn the IC pump ON.
4. Increase the flow to 2 mL/min (Note: it is VERY important that you open the valve BEFORE increasing the flow) (Note2: the default flow is 0.7 mL/min)
5. Syringe on the front of the IC unit: pull the plunger. Eluent and air will start coming out (Note: you can push the plunger and then release it to see if there is liquid flowing)
6. Once all the air has come out, decrease the flow to 0.7 mL/min and close the valve
7. Let run for a couple of minutes. The pressure should start to go up. If it doesn't, repeat the procedure.
8. After pressure is back to normal, you may turn off the IC pump and all the hardware (from the System menu) or start a new run.

D.8. Microwave Digestion for Inductively Coupled Plasma Atomic Emission

Spectroscopy (from EPA method SW-3015)

Instrument: CEM Microwave digester model MS-2000

1. Open the serum bottle were the effluent is stored and measure the pH
2. Filter ~ 15 mL of effluent through a 0.2 um filter (Fisher # 09-719-2B)
3. In a graduated cylinder, measure 10 mL of the filtered effluent (a smaller or bigger sample size can be used but the final volume prior to addition of nitric acid has to be 45 mL)

4. Add DI water to 45 mL
5. Transfer the solution to a digestion vessel
6. In the fume hood:
 - a) Add 5 mL of nitric acid
 - b) Insert the pressure relief disks in the orange caps (if the disks are not broken during the digestion, they can be re-used)
 - c) Place each digestion vessel into a microwave vessel and close them tightly. Also tighten the orange caps with the pressure relief disks
7. Turn on the microwave digester
8. Press F3 to disable temperature unit
9. On the outside of the unit, back left, turn the valve counterclockwise to the horizontal (open) position and remove the syringe.
10. Place an empty beaker in the microwave cavity and place the open end of the pressure sensing line in the beaker
11. Fill the syringe with DI water and remove the air
12. Attach the syringe back to the open end of the fill tubing
13. Push the plunger on the syringe to force water into the pressure control system until water begins to come out of the pressure tubing into the beaker. As soon as this happens, turn the valve to the vertical (closed) position.

14. Remove the beaker from the microwave cavity and discard the water.
15. Press F1 System Setup
16. Press F4 Temp options
17. Press F2 disable temp unit ("off" on top of panel)
18. Press "O" to exit
19. Press F1 System Setup
20. Press F2 calibrate
21. Press F2 pressure calibrate
22. Press F2 Zero transducer
23. Press Enter
24. Distribute the vessels evenly in the carrousel. When less than 8 samples are digested, fill the remaining vessels with 45 mL of water and 5 mL of nitric acid.
25. Connect pressure line to control vessel
26. Press "0"
27. Press F4 to use EPA methods
28. Press 3 (liquids) or 5 (solids) for EPA 3015 or EPA 3051, respectively
29. Press F1 to start
30. Press F1 for "yes" correct vessels

31. After done, wait until pressure drops to at least to 20 psi
32. Vent the orange caps slowly
33. Allow vessels to reach 0 psig
34. Transfer from microwave to fume hood
35. Open slowly (orangish/yellow vapor comes out)
36. Allow to cool in hood ~15 minutes or until comfortable temperature to handle.
37. If the digested sample contains particulates which may clog nebulizers or interfere with the injection of the sample into the instrument, the sample may be centrifuged, allowed to settle or filtered.
38. Store ~30 mL of the digested sample in glass containers that have been acid-wash and rinsed in DI water three times.